INFORMATION TO USERS

This manuscript has been reproduced from the microfilm master. UMI films the text directly from the original or copy submitted. Thus, some thesis and dissertation copies are in typewriter face, while others may be from any type of computer printer.

The quality of this reproduction is dependent upon the quality of the copy submitted. Broken or indistinct print, colored or poor quality illustrations and photographs, print bleedthrough, substandard margins, and improper alignment can adversely affect reproduction.

In the unlikely event that the author did not send UMI a complete manuscript and there are missing pages, these will be noted. Also, if unauthorized copyright material had to be removed, a note will indicate the deletion.

Oversize materials (e.g., maps, drawings, charts) are reproduced by sectioning the original, beginning at the upper left-hand corner and continuing from left to right in equal sections with small overlaps.

Photographs included in the original manuscript have been reproduced xerographically in this copy. Higher quality 6" x 9" black and white photographic prints are available for any photographs or illustrations appearing in this copy for an additional charge. Contact UMI directly to order.

Bell & Howell Information and Learning
300 North Zeeb Road, Ann Arbor, MI 48106-1346 USA

UMI®
800-521-0600

MODEL INITIATOR NITROXIDE ADDUCTS FOR SFRP

To my husband, Mark

and our two wonderful children,

Heather and Andrew.

SYNTHESIS AND EVALUATION OF MODEL INITIATOR / REVERSIBLE TERMINATING ADDUCTS FOR THE STABLE FREE RADICAL POLYMERIZATION PROCESS

By

KAREN ANN MOFFAT, M. Sc.

A Thesis

Submitted to the School of Graduate Studies

in Partial Fulfillment of the Requirements

for the Degree

Doctor of Philosophy

McMaster University

DOCTOR OF PHILOSOPHY (1998)
(Chemistry)

McMASTER UNIVERSITY
Hamilton, Ontario

TITLE: Synthesis and Evaluation of Model Initiator / Reversible Terminating Adducts for the Stable Free Radical Polymerization Process

AUTHOR: Karen Ann Moffat, M. Sc. (McMaster University)

SUPERVISOR: Professor Harald D. H. Stöver

NUMBER OF PAGES: xxiii, 196

Abstract

This thesis describes the synthesis, characterization and evaluation of model initiator / reversible terminating agents, to enhance the fundamental understanding of the stable free radical polymerization process. One portion of this research, involved AM1 and PM3 semi-empirical molecular orbital calculations on a model SFR reaction. The aim of this work was to identify new nitroxyl radicals with a labile C-O bond, but it became apparent that semi-empirical MO calculations were not accurate enough to differentiate between various nitroxyl radicals. To calibrate the MO calculations and determine where the deficiencies in the methods were, the single crystal X-ray structure of MB-TMP was obtained.

A series of alkoxy and aryloxy-tetramethylpiperidine compounds, RO-TMP were prepared by the reaction of tri-*n*-butyl tin hydride with various alkyl or aryl halides and TEMPO. Using the same synthetic route, the 1-phenylethyl carbon radical fragment was trapped by 1,1,3,3-tetramethyl- and 1,1,3,3-tetraethylisoindoline nitroxide to form MB-TMI and MB-TEI. All compounds were isolated, purified and characterized by ^{1}H and ^{13}C NMR spectroscopy. Using ESR spectroscopy, the enthalpy of activation to homolytically cleave the C-O bond in ten of the nitroxide adducts was measured. In the adduct series, MB-TMP, MiP-TMP and EiB-TMP which mimic the styrene, acrylate and methacrylate monomers respectively, the enthalpy of activation decreased from 131.2 ± 7.2, 125.3 ± 5.4

to 119.2 ± 3.4 kJ/mol, respectively. This indicated that the C-O bond strength between the propagating polymer chain end and TEMPO is the weakest for a methacrylate monomer with increasing C-O bond strength for acrylate and styrene monomers. Steric bulk of the tertiary methacrylate radical carbon contributed to a weaker and more labile C-O bond. In the series of initiating carbon radicals bonded to TEMPO, it was demonstrated that increasing the steric crowding about the carbon radical decreased the enthalpy of activation to break the C-O bond. Also, when steric bulk was increased on the alpha carbons to the nitroxyl functional group in the tetraethylisoindoline nitroxide, the C-O bond in 1-phenylethyl-tetraethylisoindoline adduct, MB-TEI was 4.7 kJ/mol weaker than in MB-TMI.

The thermal decomposition of nitroxide adduct MB-TMP was measured as a function of time at 125°C by ESR and ^{1}H NMR spectroscopy. As a result of this kinetic study, an alternative mechanism to that of Li *et al.* was proposed for possible polymer chain termination when the excess nitroxide in the polymerization system builds up. All major products from the thermal decomposition of MB-TMP were identified and the effect of oxygen in the polymerization via autoxidation mechanism was observed. This study has identified that hydrogen radical abstraction by a significant excess of TEMPO can produce a terminal vinyl group at the end of a polystyrene chain. In the presence of oxygen and excess TEMPO, a phenyl ketone functional group can also be produced to terminate a polystyrene chain end.

Two nitroxide adducts, MB-TMP and B-TMP and the unimer BST were evaluated as initiators and as the only source of nitroxyl radical in the bulk polymerization of styrene by the stable free radical polymerization process. The C-O bond in B-TMP did not cleave at a fast enough rate to enable a controlled SFR polymerization. Instead, polystyrene chains were self-initiated by the Mayo mechanism resulting in a conventional free radical polymerization process. The initiating efficiency of MB-TMP was found to be equivalent to BST and a controlled "living" stable free radical polymerization with narrow polydispersities was demonstrated. The alpha-methyl group on the benzylic carbon in MB-TMP was responsible for increasing the steric bulk around the C-O bond and making the bond more labile. The addition of excess nitroxide decreased the rate constant of propagation and lowered MWD during the initiation period of polymerization.

Acknowledgements

I would like to thank all of my family for their love and support and for taking an interest in this endeavor. My greatest appreciation goes to my husband Mark, and our two wonderful children; Heather and Andrew, for without them I would not have been able to do this. Their love, support, and encouragement never faltered throughout this time as I juggled the responsibilities of a part-time student, employee, mother and wife. Dinner conversations at home always included the question from the kids "So how was school today, Mommy?"

I would also like to thank Professor Harald Stöver for taking me on as a part-time graduate student. His encouragement and inquisitive nature always questioned and pushed my level of knowledge and understanding in many different subject areas. Your patience, enthusiasm and high standards of excellence are greatly appreciated.

To Dr. Michael Georges, my manager, mentor and friend, I will be forever grateful to you for volunteering to be my Xerox supervisor. Your dedication, commitment, never wavering support and encouragement over the past 4 years have helped me reach my goal. It was Michael that first seeded the idea of working on a SFRP project and this has been a very stimulating and rewarding area to study.

I would like to thank Dr. Peter Kazmaier for sharing his knowledge in the area of molecular modelling, Dr. Gord Hamer for his help and NMR expertise and Dr. Rick Veregin for teaching me how to run the old ESR spectrometer.

I would also like to thank Dr. Jim Britten for measuring the X-ray crystal structure of MB-TMP and Dr. Richard Smith for the mass spectroscopy results.

To the members of our NMD area at XRCC and to the many other colleagues at the Xerox Research Center of Canada, I thank you for your words of encouragement and support.

A special thank you is due to the management team at the Xerox Research Center of Canada, for providing me the opportunity to return to graduate school on a part-time basis and still remain employed. They provided a working arrangement that accommodated my professional and personal responsibilities. Even though the members of the team have changed somewhat since I started, their support, patience and encouragement never did.

Publications Based on This Research

In Journals:

Georges, M. K.; Moffat, K. A.; Veregin, R. P. N.; Kazmaier, P. M.; Hamer, G. K. *Polym. Mater. Sci. Eng.* **1993**, *69*, 305.

Kazmaier, P. K.; Moffat, K. A.; Georges, M. K.; Veregin, R. P. N.; Hamer, G. K. *Macromolecules* **1995**, *28*, 1841.

Moffat, K. A.; Britten, J. F.; Hamer, G. K.; Kazmaier, P. K.; Georges, M. K.; Stöver, H. D. H. Deficiencies of Semi-Empirical Molecular Orbital Calculations and the Implications to the Stable Free Radical Polymerization Process, Manuscript in preparation.

Moffat, K. A.; Hamer, G. K.; Georges, M. K.; Stöver, H. D. H. Stable Free Radical Polymerization of Styrene Using a Combined Initiator Reversible Terminating Agent, MB-TMP, Manuscript in preparation.

Moffat, K. A.; Hamer, G. K.; Georges, M. K. Stable Free Radical Polymerization Process: A Thermal Decomposition Study of Nitroxide Adducts That Mimic the Propagating Chain End, Manuscript in preparation.

In Conference Proceedings:

Moffat, K. A.; Hamer, G. K.; Georges, M. K.; Kazmaier, P. K.; Stöver, H. D. H. *Polym. Prepr. Am. Chem. Soc. Div. Polym. Chem.* **1996**, *37(2)*, 509.

MacLeod, P. J.; Georges, M. K.; Quinlan, M.; Moffat, K. A.; Listigovers, N. A. *Polym. Prepr. Am. Chem. Soc. Div. Polym. Chem.* **1997**, *38(1)*, 459.

Odell, P. G.; Rabien, A.; Michalak, L. M.; Veregin, R. P. N.; Quinlan, M. H.; Moffat, K. A.; MacLeod, P. J.; Listigovers, N. A.; Honeyman, C. H.; Georges, M. K. *Polym. Prepr. Am. Chem. Soc. Div. Polym. Chem.* **1997**, *38(2)*, 414.

At Conferences:

Moffat, K. A.; Hamer, G. K.; Georges, M. K.; Stöver, H. D. H. Synthesis and Characterization of Styrenic Model Compounds for Polymerization by a Stable Free Radical Mediated Polymerization Process, *New Organic Chemistry for Polymer Synthesis*, Santa Fe, New Mexico, May 21-24, 1995.

Kazmaier, P. K.; Moffat, K. A.; Georges, M. K.; Veregin, R. P. N.; Hamer, G. K. "Living" Free Radical Polymerization. Molecular Orbital Calculations as a Criterion for Selecting Reversible Terminators, *New Organic Chemistry for Polymer Synthesis*, Santa Fe, New Mexico, May 21-24, 1995.

Moffat, K. A.; Hamer, G. K.; Georges, M. K.; Stöver, H. D. H. Synthesis and Characterization of Model Compounds for Styrene Polymerization by a Stable Free Radical Mediated Polymerization Process, *78th Canadian Society of Chemistry Conference*, Guelph, Ontario, May 31, 1995.

Hazendonk, P.; Bain, A. D.; Moffat, K. A.; Georges, M. K.; Hamer, G. K. New NMR Methods Applied to the Study of the Dynamics of a Saturated Six-Membered Nitrogen-Containing Ring, *37th Experimental Nuclear Magnetic Resonance Conference*, March 17-22, 1996.

Moffat, K. A.; Keoshkerian, B.; Quinlan, M.H.; Georges, M. K. The Stable Free Radical Polymerization Process: Scope of Application, *Canadian High Polymer Forum*, Sarnia Ont., August, 7-9, 1996.

Moffat, K. A.; Hamer, G. K.; Georges, M. K.; Kazmaier, P. M.; Stöver, H. D. H. Stable Free Radical Polymerization of Styrene Using a Combined Initiator Reversible Terminating agent, *American Chemical Society National Meeting*, Orlando Florida, August 26, 1996.

Moffat, K. A.; Hamer, G. K.; Georges, M. K. Stable Free Radical Polymerization Process: A Thermal Decomposition Study of Nitroxide Adducts That Mimic the Propagating Chain End, *81th Canadian Society of Chemistry Conference*, Whistler, B.C., May, 31- June 4, 1998.

U. S. Patents:

5,723,511 Kazmaier, P. M.; Keoshkerian, B.; Moffat, K. A.; Georges, M. K.; Hamer, G. K.; Veregin, R. P. N. Processes for Preparing Telechelic, Branched and Star Thermoplastic Resin Polymers, March 3, 1998.

5,412,047 Georges, M. K.; Saban, M. D.; Kazmaier, P. M.; Veregin, R. P. N.; Hamer, G. K.; Moffat, K. A. Homoacrylate Polymerization Processes with Oxonitroxides, May 2, 1995.

5,449,724 Moffat, K. A.; Saban, M. D.; Veregin, R. P. N.; Georges, M. K.; Hamer, G. K.; Kazmaier, P. M. Stable Free Radical Polymerization Process and Thermoplastic Materials Produced Therefrom, September 12, 1995.

5,498,679 Kazmaier, P. M.; Keoshkerian, B.; Moffat, K. A.; Georges, M. K.; Hamer, G. K.; Veregin, R. P. N. Processes for Preparing Telechelic, Branched and Star Thermoplastic Resin Polymers, March 12, 1996.

European Patents:

Appl. # **95119727.6** Moffat, K. A.; Saban, M. D.; Veregin, R. P. N.; Georges, M. K.; Hamer, G. K.; Kazmaier, P. M. Stable Free Radical Polymerization Process and Thermoplastic Materials Produced Thereform, February 13, 1996.

Appl. # **95120296.9** Moffat, K. A.; Kazmaier, P. M.; Georges, M. K.; Hamer, G. K.; Veregin, R. P. N.; Saban, M. D. Polymerization Multiblock Copolymer Process and Compositions Thereof, February 27, 1996.

Appl. # **96101775.3** Kazmaier, P. M.; Veregin, R. P. N.; Moffat, K. A.; Georges, M. K.; Saban, M. D.; Hamer, G. K. Process for the Preparation of Branched Polymers, April 23, 1996.

Appl. # **97303948.0** Kazmaier, P. M.; Keoshkerian, B.; Moffat, K. A.; Georges, M. K.; Hamer, G. K.; Veregin, R. P. N. Processes for Preparing Telechelic, Branched and Star Thermoplastic Resin Polymers, June 6, 1997.

Table of Contents

List of Figures

Page

Page

List of Schemes

Page

List of Tables

List of Abbreviations

The following abbreviations are found throughout the thesis. They are defined below;

AM1	Austin model 1, semi-empirical molecular orbital calculation method
AIBN	azobisisobutyronitrile
ATRP	atom transfer radical polymerization
BPO	benzoyl peroxide
ESR	electron spin resonance
FRP	free radical polymerization
GTP	group transfer polymerization
MO	molecular orbital
NMR	nuclear magnetic resonance
PDI	polydispersity index
PM3	parametric model 3, semi-empirical molecular orbital calculation method
SFRP	stable free radical polymerization
TEMPO	2,2,6,6-tetramethylpiperidine-1-oxyl

Chapter 1

Introduction

The plastics industry today is a multi-billion dollar industry with over 50 % of its products produced by polymerizing vinyl monomers. In 1993 alone, the Dow Chemical Company generated sales in the thermoplastics business of 3.2 billion dollars. Many of the large corporate players are developing new methods to prepare polymeric materials having enhanced mechanical properties, heat resistance and heat stability. At the same time, manufacturing costs must decrease due to the competitiveness of the industry. Through controlled polymer synthesis, the molecular properties of the polymer can be tailored to provide the enhanced material performance that is required. This is done by controlling the molecular architecture of the polymer (linear, branched, star-shaped, multi-branched) and composition of the polymers in order to fine-tune the physical and mechanical properties of the materials. There is a wide choice of vinyl monomers and methods available to prepare homopolymers, random copolymers, block copolymers and branched polymers with controlled molecular weights and controlled molecular weight distributions. Elaborate polymeric structures such as star-shaped, ladder, and dendrimeric polymers can also be synthesized and will have different physical and mechanical properties compared to their linear analogs.

This thesis introduction will compare conventional free radical polymerization with living and controlled polymerization processes, both ionic and radical. Living and controlled polymerization processes allow the chemist to specially design numerous polymers for specific applications. Emphasis will be placed on the advantages and disadvantages of ionic and radical polymerization.

1.1 Conventional Free Radical Polymerization

Free radical polymerization (FRP) is the most common route to prepare commercial vinyl polymers. More than 50% of all plastics and more than 70% of all vinyl polymers are prepared by conventional free radical polymerization, including low-density polyethylene, acrylic and methacrylate polymers, polystyrene, polyacrylonitrile, poly(vinyl chloride) and many others. FRP can be carried out in bulk monomer or in solution (monomer plus solvent) employing dispersion, suspension and emulsion polymerization methods. This polymerization process consists of three distinct phases: initiation, propagation and chain transfer / termination. The mechanism of FRP can be represented by the series of reactions 1-7 shown in Scheme 1. M represents a molecule of monomer; I• is an initiating radical from the initiator; P_n• is the propagating free radical with a degree of polymerization, *n*; YZ is the chain transfer agent which may be solvent, monomer, initiator, specific chain transfer reagents or others; and P_{n+m} , P_n and P_m are the final terminated polymer chains.

Initiation of free radical polymerization (Scheme 1 equations 1 & 2) can be triggered thermally, photolytically, by redox reactions or with ultrasonic waves resulting in

homolytic cleavage of the initiator in the presence of monomer. Thermal decomposition of initiators such as organic peroxides, i.e. benzoyl peroxide (BPO) or azo compounds, i.e.

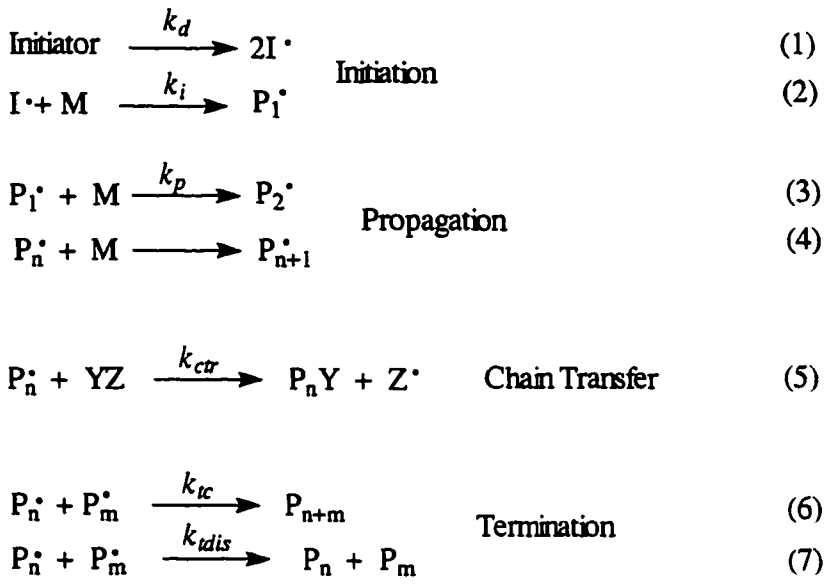

Scheme 1: Mechanism of free radical polymerization.

azobisisobutyronitrile (AIBN) is the most common initiation method used. The thermal decomposition of these initiators is a slow first order reaction ($k_d \approx 10^{-4}$ to 10^{-6} s^{-1}), with half-life times usually in the range of a few hours at 60-80°C. The polymerization rate, R_p is proportional to the square root of the rate of initiation, R_i. The decomposition of one molecule of initiator generates two initiating radicals, but only a fraction of these radicals actually initiates a polymer chain. The efficiency of initiation, or the fraction of initiating radicals f, lies most often between 0.1 and 0.8 due to many competing side reactions for the initiating radical. Generally, the rate of initiation, R_i is written in terms of the rate constant for initiator decomposition, k_d and the initiator efficiency, f.

$$R_i = 2fk_d[I] \tag{8}$$

Once the polymer chains are initiated, chain propagation (Scheme 1 equations 3 & 4) continues by monomer "head-to-tail" addition. The rate constant of propagation is slower for most ionic reactions with $k_p \approx 10^{3\pm1}$ $M^{-1}s^{-1}$ at ≈ 70°C. The activation energies of propagation are in the range of $E_p \approx 6 \pm 2$ kcal/mol. The chains continue to grow until they terminate. A competing reaction with propagation is chain transfer (Scheme 1 equation 5) which involves abstraction of a radical from another monomer molecule, solvent, initiator or polymer chain to terminate one chain and initiate another. When chain transfer competes with propagation, the overall result is a decrease in the average chain length of the polymer produced, or branching if the second molecule is a polymer molecule. The steady-state rate of polymerization, R_p, at a given temperature, is proportional to the square root of the initiator concentration and to the first power of the monomer concentration.

$$R_p = k_p[M]\left(\frac{fk_d[I]}{k_t}\right)^{1/2} \tag{9}$$

Termination in free radical polymerization is a very rapid bimolecular process. It involves either coupling (Scheme 1 equation 6) of two growing polymer chains, or disproportionation (Scheme 1 equation 7) producing one chain with a vinyl terminus and the other chain with a saturated end. The rate constant of termination, $k_t \approx 10^{8\pm1}$ $M^{-1}s^{-1}$ at 70°C, is nearly diffusion controlled with accordingly small activation energies $E_t \approx 3 \pm 2$ kcal/mol. The preference of one type of termination over the other depends on the monomer and the polymerization temperature. Termination by combination has a lower

activation energy over disproportionation which requires breaking a bond; therefore, at low polymerization temperatures, termination by combination dominates. At 60°C, acrylonitrile[1] terminates completely by combination, methyl methacrylate[2] terminates to 79 % by disproportionation and to 21 % by combination, styrene[3] shows 23 % disproportionation and 77 % combination and vinyl acetate[4] at 90°C terminates completely by disproportionation. The total rate of termination, R_t is given by

$$R_t = 2k_t[\mathrm{M}\cdot]^2 \tag{10}$$

where the rate constant of termination, k_t is a summation of the rate constants of termination by chain coupling, k_{tc} and disproportionation, k_{td}.

To understand the relationship between structure and properties of polymers, the molecular weight and the distribution of molecular weights of the material are determined. There are two fundamentally different classes of methods used to measure molecular weights, absolute methods and secondary methods. Absolute methods give a direct estimate of the molecular weights. Secondary methods determine molecular weights by comparison with a series of calibrated polymers of known molecular weight. In this thesis, all molecular weight data were determined by size exclusion chromatography (SEC also called gel permeation chromatography GPC). The calibration curve was generated from a series of narrow molecular weight linear polystyrene standards. The average degree of

---

[1] Bamford, C. H.; Jenkins, A. D.; Johnston, R. *Trans. Faraday Soc.* **1959**, *55*, 179.

[2] Bevington, J. C.; Melville, H. W.; Taylor, R. P. *J. Polymer Sci.* **1954**, *12*, 449; *14*, 463.

[3] Berger, K. C. *Makromol. Chem.* **1975**, *176*, 3575.

[4] Bamford, C. H.; Jenkins, A. D. *Nature* **1955**, *176*, 78.

polymerization, DP, is defined as the average number of monomer molecules per polymer chain. The number-average molecular weight, Mn, is defined as the total weight w of all the molecules in a polymer sample divided by the total number of moles present.

$$Mn = \frac{w}{\sum N_x} = \frac{\sum N_x M_x}{\sum N_x} \tag{11}$$

The weight-average molecular weight, Mw, of a polymer is the weight-fraction of molecules whose weight is Mx. Mw can also be defined as

$$Mw = \frac{\sum c_x M_x}{\sum c_x} = \frac{\sum N_x M_x^2}{\sum N_x M_x} \tag{12}$$

where c_x is the weight concentration of M_x molecules and c is the total weight concentration of all the polymer molecules. The molecular weight distribution, MWD, also called polydispersity, PD, is defined as the weight-average molecular weight divided by the number-average molecular weight, Mw/ Mn. For a perfectly monodispersed polymer sample, Mw/Mn would be 1.0. Only living ionic polymerization and a few living free radical polymerization methods can synthesize polymers that approach the ideal PD of 1.0, but generally, PDs are in the range of 1.1 to 1.3.

Both the mechanism and kinetics of free radical polymerization are well understood. There is a wide range in reaction conditions and media for polymerization along with a large choice in polymerizable monomers that do not have to be rigorously purified. This makes FRP the preferred method for producing commercial polymers. The major drawback of FRP is the lack of control over the chain architecture and chain length.

If control over the propagating chain end could be obtained, then narrow molecular weight polymers with specific architectures such as block copolymers, telechelics, stars, etc. could be prepared. This would be a tremendous technological advancement for the polymer industry. Living ionic polymerization methods can provide the architectural control during the polymerization process. Three types of ionic polymerizations are discussed in the following section.

1.2 Living Ionic Polymerization

The development of living polymerization processes began with the discovery of living anionic polymerization by Szwarc[5,6] in 1956. The ability to prepare living polymer chains via anionic polymerization came about by controlling the reactivity of the end of the polymer chain. The control over the chain terminus allows polymers of specific structure, monomer sequence, end group functionality, molecular weight and narrow molecular weight distributions to be prepared. Over the years, many new living polymerization processes have been invented. This section will review the advantages and limitations in three living ionic polymerization techniques; anionic, group transfer and carbocationic polymerization. Other types of polymerization that will not be discussed include ring-

[5] Szwarc, M. *Nature* **1956**, *178*, 1168.

[6] Szwarc, M.; Levy, M.; Milkovich, R. *J. Am. Chem. Soc.* **1956**, *78*, 2656.

opening metathesis (ROMP)[7], [8], [9], [10] and coordination polymerizations such as Ziegler-Natta[11] polymerization.

Anionic polymerization is widely applied to conjugated π–electron systems such as styrenes, methacrylates, 1,3-butadienes and acrylonitrile, to produce polymers with precisely controlled chain structures.[12] Certain functional monomers containing reactive polar groups or labile acidic protons, for example; hydroxy[13], mercapto[14], amino[15], formyl[16], carbonyl[17], ethynyl[18] or carboxy[19] groups can not be polymerized by anionic methods unless these reactive groups are protected. One family of protecting groups are trimethylsilyl or *tert*-butyldimethylsilyloxy groups. Monomers with electron withdrawing groups such as amido, imino and cyano at the *para*-position of the phenyl ring[12] in styrene,

---

[7] Gilliom, L. R.; Grubbs, R. H. *J. Am. Chem. Soc.* **1986**, *108*, 733.

[8] Schrock, R. R.; Feldman, J.; Cannizzo, L. F.; Grubbs, R. H. *Macromolecules* **1987**, *20*, 1169.

[9] Wallace, K. C.; Liu, A. H.; Dewan, J. C.; Schrock, R. R.; *J. Am. Chem. Soc.* **1988**. *110*, 4964.

[10] Novak, B. M.; Risse, W.; Grubbs, R. H. *Adv. Polym. Sci.* **1992**, *102*, 47.

[11] Odian, G. Principles of Polymerization, 2nd ed. J. Wiley & Sons, Toronto, 1981, pp. 591.

[12] Allcock, H. R.; Lampe, F. W. Contemporary Polymer Chemistry, 2nd ed. Prentice Hall Canada, 1990.

[13] Hirao, A.; Yamaguchi, K.; Takenaka, K.; Suzuki, K.; Nakahama, S.; Yamazaki, N. *Makromol. Chem. Rapid Commun.* **1982**, *3*, 941.

[14] Hirao, A.; Shione, H.; Wakabayashi, S.; Nakahama, S.; Yamaguchi, K. *Macromolecules* **1994**, *27*, 1835.

[15] Yamaguchi, K.; Hirao, A.; Suzuki, K.; Takenaka, K.; Nakahama, S.; Yamazaki *J. Polym. Sci.; Polym. Lett. Ed.*, **1983**, *21*, 395.

[16] Ishizone, T.; Kato, R.; Ishino, Y.; Hirao, A.; Nakahama, S. *Macromolecules* **1991**, *24*, 1449.

[17] Hirao, A.; Kato, K.; Nakahama, S. *Macromolecules* **1992**, *25*, 535.

[18] Tsuda, K.; Ishizone, T.; Hirao, A.; Nakahama, S.; Kakuchi, T.; Yokota, K. *Macromolecules* **1993**, *26*, 6985.

[19] Hirao, A.; Ishino, Y.; Nakahama, S. *Macromolecules* **1988**, *21*, 561.

polymerize very nicely without any functional group protection due to the stabilization of the anionic charge.

Typical initiating systems used in living anionic polymerization include alkali metal suspensions such as Na in THF, organolithium reagents prepared by reaction of lithium metal with organic halides such as *sec*-BuLi, *n*-BuLi; or Grignard reagents. These initiating systems are very flammable and / or explosive requiring absolutely anhydrous conditions under an inert atmosphere of dried N_2, Ar or He. Moisture and CO_2 must be rigorously removed from solvent, monomer, and the reaction apparatus. Monomers are usually purified by reaction with NaH or CaH_2 followed by distillation to remove inhibitors. Since the propagation rate in anionic polymerization is very fast, the reaction temperature is lowered to slow the polymerization. Reaction temperatures are usually around –78°C. After all the monomer is consumed, the living anionic chain ends are terminated with a terminating agent such as water, CO_2 or methanol. Once terminated, the chains are "dead" and rejuvenation of livingness is impossible without a subsequent chemical reaction. The concentration of initiator determines the number of polymer chains produced with all of the chains initiating at the same time. The monomer / initiator ratio controls the chain length, assuming all chains grow at the same rate until all the monomer is consumed. Consequently, DP can be accurately predicted by the following equation, $DP_n = \Delta[M]/[I]_o$ where Δ [M] is defined as the change in monomer concentration and $[I]_o$ is the initial initiator concentration.

In a typical living anionic polymerization as shown in Scheme 2, the initiator, *n*-BuLi, begins the polymerization by addition across the double bond of a vinyl monomer, i.e., styrene. All the polymer chains are initiated at the same time and the rate of initiation is very fast. This produces an ion pair consisting of a propagating anionic chain end together with the lithium countercation. Propagation proceeds by addition of monomer molecules into the terminal ionic bond. Propagation continues until all the monomer is consumed

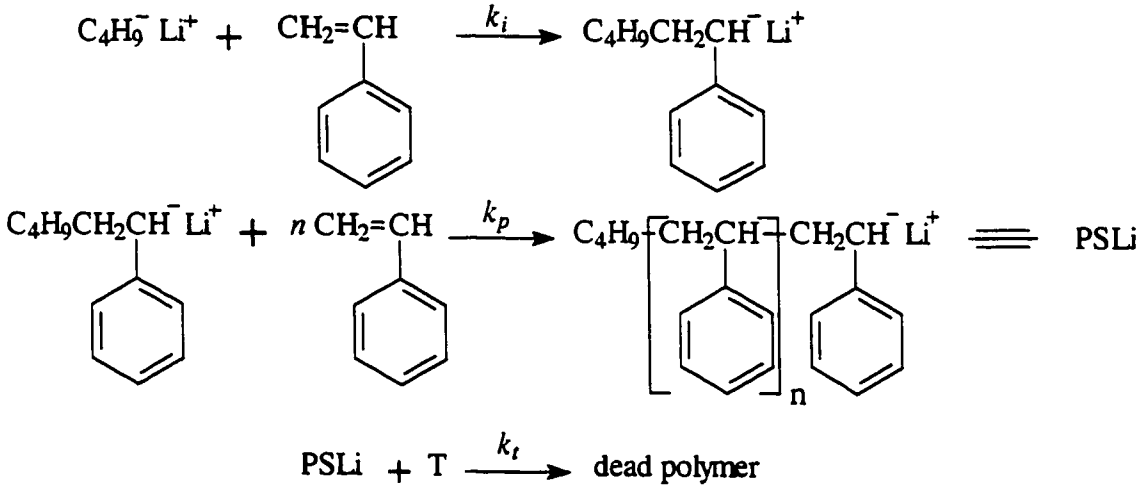

Scheme 2: Living anionic polymerization of styrene initiated with *n*-butyl lithium.

or the reaction is terminated. Due to the electronic and steric environment of the ion pair at the chain end and choice of solvent, chain transfer is minimized. If a second quantity of a different monomer is added prior to chain termination, the polymer chains will continue to grow producing a block copolymer. When preparing block copolymers, the sequence of addition of monomers is important. If monomer B, such as methyl methacrylate, has a

more electron withdrawing substituent than monomer A (styrene), then monomer B will polymerize onto polymer A, but not vice versa. Another example is that acrylonitrile can be polymerized onto a MMA polymer chain block which was added onto a styrenic polymer segment.

Anionic polymerization is an example of a living polymerization process and the product of the reaction is a polymer chain, which retains the reactive carbanionic chain end when all the monomer has been consumed. Molecular weights increase linearly with conversion and the number of polymer molecules remains constant and independent of conversion. Mn is a function of the degree of conversion of the monomer and the stoichiometry of the reaction. Narrow molecular weight distributions MWD $\leq$ 1.1 polymers are possible.

There is a long list of complex architectural polymers which may be prepared by living anionic polymerization including blocks[20], block-grafts[21], telechelics, stars, combs, ladders and many others. Living anionic polymerization provides tremendous control and design flexibility over the polymer composition but it comes at a price. Very strict reaction conditions are required such as cryogenic reaction temperatures, pure monomers, solvent and initiators, a solvent medium and some restriction on monomer choice. This makes living anionic polymerization difficult to scale-up and commercialize.

---

[20] Rempp, P.; Franta, E. *Polym. Prepr. (Am. Chem. Soc. Div. Polym. Chem.)* **1993**, *34(2)*, 658.

[21] Yamazaki, H.; Shibamoto, T.; Takano, A.; Fujimoto, T. *Macromolecules* **1997**, *30*, 1570.

The second method of ionic polymerization to be discussed is group transfer polymerization, which is a catalyzed Michael-type addition reaction. In the early 1980s, Sogah and Webster[22], [23] at DuPont, did the pioneering work in the area of group transfer polymerization (GTP). The applicability of the GTP process to prepare narrow polydispersed polymers is restricted to a small set of polar monomers such as acrylic and methacrylic esters, acrylonitrile and *N,N*-dimethylacrylamide. GTP offers equivalent polymerization control to anionic polymerization, with the advantages of operating at and above room temperature, and is applicable to acrylate and methacrylate monomers. One of the three proposed mechanisms[24] for GTP; the associative mechanism, is illustrated in Scheme 3a to polymerize MMA. The reaction involves the use of silyl ketene acetal, (**1**), 1-methoxy-2-methyl-1-trimethylsiloxypropene (MTS), as initiator in the presence of suitable catalysts which may be either a nucleophile (e. g., HF_2^- CN^-, F^-, N_3^-) or a Lewis acid. The catalysts of choice (typically 0.12 mol %) are tetrabutylammonium biacetate or bibenzoate. In another possible mechanism for GTP, the silyl group (10^{-3} M), which protects the chain end from termination, does not directly transfer to the incoming monomer. It rapidly exchanges with a small amount of enolate ended polymer, (10^{-5} M) generated by the catalyst. This produces polymers with protected terminal functional

---

[22] Webster, O. W.; Hertler, W. R.; Sogah, D. Y.; Farnham, W. B.; RajanBabu, T. V. *J. Am. Chem. Soc.* **1983**, *105*, 5706.

[23] Sogah, D. Y.; Webster, O. W. *J. Polym. Sci., Polym. Lett. Ed.* **1983**, *21*, 927.

[24] Webster, O. W. *Macromol. Eng. (Proc. Int. Conf. Adv. Polym. Macromol. Eng.)* **1995**, 1 Ed. by Munmaya, M. K., Plenum, New York. Mijs, W. J.; Addink, R Rec. *Trav. Chim. Pays-Bas.* **1991**, *110*, 526. Davis, T. P.; Haddleton, D. M.; Richards, S. N. *J. M. S.-Rev. Macromol. Chem. Phys.* **1994**, *C34*, 243.

groups which minimize termination by backbiting reactions. Dry monomers with pendent functional groups free of active hydrogen are required for GTP. The silyl ketene acetal initiator is very expensive and, as a consequence, polymers prepared by GTP cannot compete economically with free radical initiated products. Molecular weights over 50,000 are difficult to obtain. DuPont used the GTP process to prepare block copolymer dispersing agents for pigments.

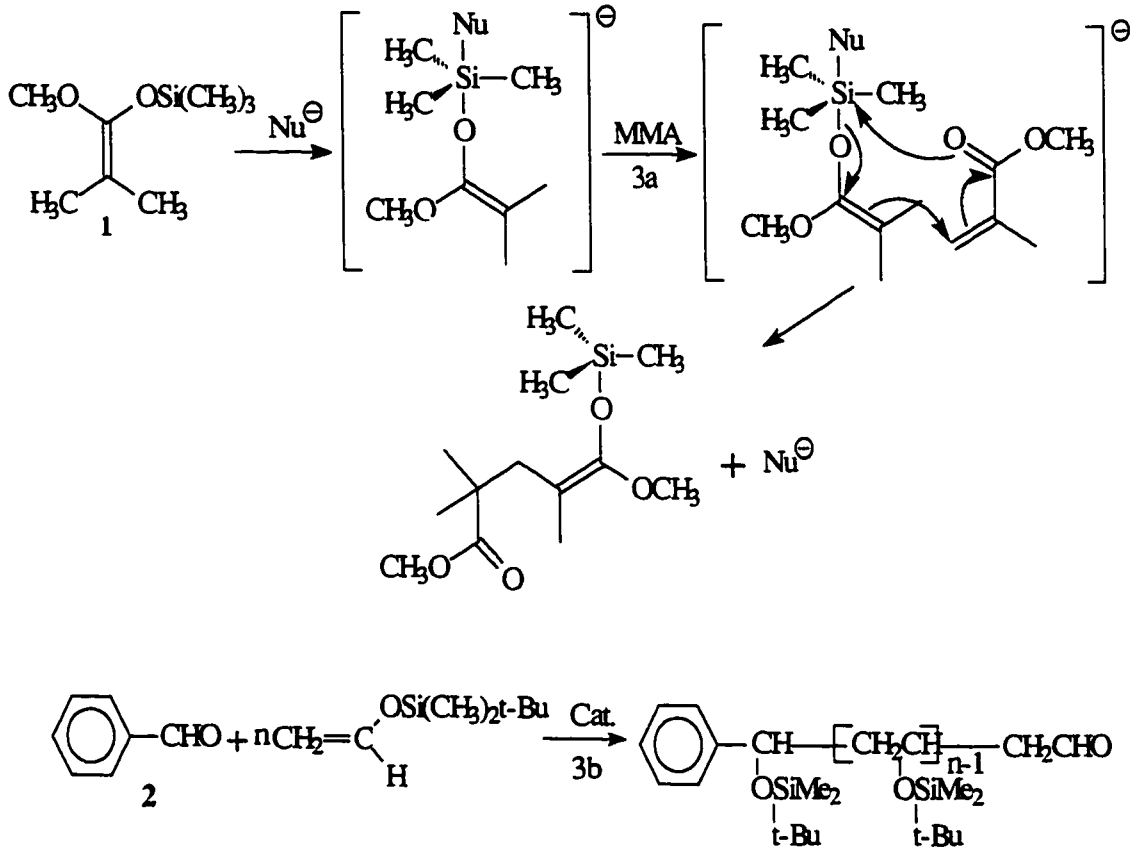

Scheme 3: Group transfer polymerization (3a) of MMA and Aldol-GTP (3b) of *tert*-butyldimethylsilyloxyacrylate initiated by benzaldehyde (2).

In a similar process, called Aldol-GTP[25],[26],[27] (Scheme 3b) aldehydes (2) initiate the polymerization of silyl vinyl ethers to give poly(vinyl alcohol). In both types of GTP, the reactive silyl functional group originally from the initiator is regenerated at the terminal end of the chain upon each reaction in such a manner that undesirable chain transfer and chain termination reactions are minimized.

DP is controlled by the molar ratio of monomer to silyl ketene acetal. Advantages of the GTP process include that the polymerization proceeds quickly at room temperature, and that monomers containing functional pendent groups can be used that would otherwise crosslink in a conventional free radical polymerization process. Many complex architectures including ladder, star-shaped and comb copolymers have been made by the living GTP process.[25]

The third approach to make controlled or living ionic polymers is by cationic polymerization. It was not until 1984 that the first well-defined cationic polymerization system was established for vinyl ethers by Sawamoto *et al.*[28] Suitable monomers for this process include vinyl ethers, styrene, *p*-substituted styrenes and 1,3-butadiene. Monomers that contain electron-donating groups attached to the cationic center help stabilize the charge.

---

[25] Sogah, D. Y. *Polym. Prepr. (Am. Chem. Soc. Div. Polym. Chem.)* **1988**, *29*, 3.

[26] Sogah, D. Y.; Webster, O. W. *Macromolecules* **1986**, *19*, 1775.

[27] Sogah, D. Y.; Hertler, W. R.; Dicker, I. B.; DePra, P. A.; Butera, J. R. *Makromol. Chem., Macromol. Symp.* **1990**, *32*, 75.

[28] Miyamoto, M.; Sawamoto, M.; Higashimura, T. *Macromolecules* **1984**, *17*, 265.

Cationic polymerization is performed in an inert atmosphere of nitrogen or helium. To make the process living, a suitable initiating system consisting of an initiator and an activator must be chosen. A variety of Lewis acids can be used to initiate cationic polymerization at low temperatures to yield high molecular weight polymers. These include metal halides (e.g., $AlCl_3$, BF_3, $SnCl_4$, $SbCl_5$, $ZnCl_2$, $TiCl_4$, PCl_5)[29] organometallic derivatives (e.g., $RAlCl_2$, R_2AlCl, R_3Al)[30] and oxyhalides (e.g., $POCl_3$, CrO_2Cl, $SOCl_2$, $VOCl_3$).[31] Initiation by Lewis acids proceeds faster in the presence of either a proton donor (protogen) such as water, alcohol and organic acids or a cation donor (cationogen) such as *tert*-butyl chloride or triphenylmethyl fluoride. Odian[32] adopted the terminology of Kennedy[29] that the protogen or cationogen are referred to as the initiator, while the Lewis acid is the coinitiator or activator. Initiation must be equal to or faster than propagation to ensure that all polymer chains start out at the same time. The most studied initating system is hydrogen iodide and iodine, HI/I_2 to polymerize a variety of vinyl ethers.[33, 34, 35, 36] The

---

[29] Kennedy, J. P.; Feinburg, S. C. *J. Polym. Sci. Polym. Chem. Ed.* **1978**, *16*, 2191. Kennedy, J. P.; Huang, S. Y.; Feinberg, S. C. *J. Polym. Sci. Polym. Chem. Ed.* **1977**, *2801*, 2869.

[30] DiMaina, M.; Cesca, S.; Giusti, P.; Ferraris, G.; Magagnini, P. L. *Makromol. Chem.* **1977**, *178*, 2223. Reibel, L.; Kennedy, J. P.; Chung, D. Y. L. *J. Polym. Sci. Polym. Chem. Ed.* **1979**, *17*, 2757.

[31] Biswas, M.; Kabir, G. M. A. *J. Polym. Sci. Polym. Chem. Ed.* **1979**, *17*, 673; *Eur. Polym. J.* **1978**, *14*, 861. Taninaka, T.; Uemura, H.; Minouri, Y. *Eur. Polym. J.* **1978**, *14*, 199.

[32] Odian, G. Principles of Polymerization 2nd ed. J. Wiley & Sons, Toronto, pg. 343-344.

[33] Sawamoto, M.; Higashimura, T. *Makromol. Chem. Macromol. Symp.* **1986**, *3*, 83.

[34] Higashimura, T.; Aoshima, S.; Sawamoto, M. *Polym. Prepr. (Am. Chem. Soc., Div. Polym. Chem.)* **1988**, *29(2)*, 1.

[35] Sawamoto, M.; Aoshima, S.; Higashimura, T. *Makromol. Chem., Macromol. Symp.* **1988**, *13/14*, 513.

[36] Sawamoto, M. Kamigaito, M. *New Methods Polym. Synth.* **1995**, 37.

strong protonic acid HI, rapidly and quantitatively initiates all the polymer chains to form a stable HI-ether adduct (3) as illustrated in Scheme 4. The carbon-iodine (C-I) bond in this adduct is electrophilically activated by iodine to trigger living propagation. Without the activator a living cationic polymerization is not possible. Scheme 4 illustrates the mechanism of the HI/I_2-initated living cationic[34] polymerization.

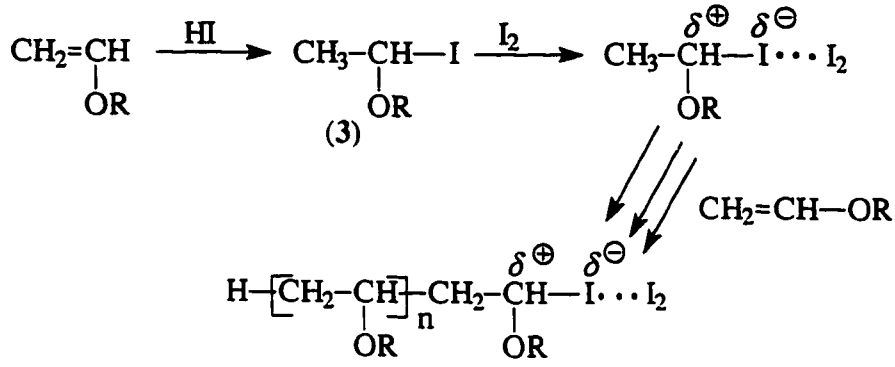

Scheme 4: Mechanism of living cationic polymerization of vinyl ether initiated by HI/I_2 system.

The propagating species consists of a stabilized growing carbocation and a nucleophilic counteranion. The strong ion pair interaction of the cation-anion suppresses chain transfer and minimizes undesirable chain termination. The livingness of the polymerization is illustrated by the linear increase in the number-average molecular weight as a function of monomer conversion and the initial molar ratio of the monomer to initiator. As with anionic polymerization, $DP = \Delta[M]/[I]_o$ there is a change in monomer concentration as a function of the initial initiator concentration. Other activators have been identified such as weak Lewis acids like metal halides[34] ZnX_2 and SnX_2; X=Cl, Br, I for

the HI-mediated polymerization. The Me_3SiI/ZnI_2 system initiated a living polymerization of isobutyl vinyl ether (IBVE)[34] in toluene below 0°C. Also, living polymerization of IBVE was demonstrated with another class of Lewis acid activators, titanium (IV) chlorides $[TiCl_{4-n}(OR)_n]$[37] with various alkoxy or aryloxy groups as ligands on the titanium metal. Stereoregularity of up to 86% isotactic content in poly(IBVE) was obtained with $TiCl_2(OR)_2$ at –78°C when bulky *o*-substituted phenoxy ligands were on the titanium compound. The strength of the Lewis acid must be adjusted for the choice of monomer. More reactive monomers such as vinyl ethers, produce covalent species which are very easily ionized by weak Lewis acids, whereas styrene and isobutene require stronger Lewis acids.

The second type of initiating system involves addition of weak nucleophiles to the reaction mixture. For example, IBVE polymerization by $EtAlCl_2$ in the presence of ethyl acetate[38], [39] or dioxane[40] produced living polymers. The propagating carbocation is stabilized by the added nucleophile through strong ion pair interactions. The solvents that are generally used are nonpolar solvents such as toluene and n-hexane. Unexpectedly, Sawamoto[33] found that more polar solvents such as CH_2Cl_2 provide a faster rate of polymerization. If the solvent polarity is increases too much, as with CH_2Cl_2/nitrobenzene

---

[37] Sawamoto, M.; Kamigaito, M. *Macromol. Symp.* **1996**, *107*, 43.

[38] Aoshima, S.; Higashimura, T. *Polym. Bull.* **1986**, *15*, 417.

[39] Aoshima, S.; Kobayashi, E. *Macromol. Symp.* **1995**, *95*, 91.

[40] Higashimura, T.; Kishimoto, Y.; Aoshima, S. *Polym. Bull.* **1987**, *18*, 111.

mixed solvent (4/1 v/v), a broadening of the polymer MWD appears. Also, in polar solvents the livingness of the system is dependent on the $[HI]_o$. If the initial initiator concentration is too low, then a non-living system results with broad polydispersity. The solvent polarity strongly affects the ionization equilibria. As the solvent polarity increases the dielectric constant also increases which enhances the ionization and reduces the rate of collapse of the ion pair into a covalent species. Thus, it is important to use solvents of low dielectric constants[41] in order to suppress free dissociated ions and increase the rate of the deactivation of the ion pair.

The temperature range for living cationic polymerization depends on the initiating system and monomer, but maintaining a low reaction temperature of –78°C to –40°C suppresses side reactions. For vinyl ethers initiated with HI/I_2 or *p*-methoxystyrene in toluene, living polymers are prepared at –40°C up to +25°C. Switching to HI/MXn systems, higher reaction rates are demonstrated and the polymerization temperature can be up to +40°C but lower molecular weights result. Maintaining a low polymerization temperature minimizes side reactions, like chain transfer via β-hydrogen abstraction. Since the activation energy for chain transfer is higher than propagation, a lower temperature affords higher molecular weight polymers because $k_p/k_{tr,M}$ is larger.

Many different types of functional polymers have been prepared by living cationic polymerization including pendant-functionalized polymers[35], end-functionalized

---

[41] Matyjaszewski, K. *Macromol. Symp.* **1996**, *107*, 53.

polymers[35], [42] amphiphilic[35] block copolymers and graft copolymers.[42] Sawamoto illustrated how complex, well-defined structures can be synthesized by living cationic polymerization. Multi-armed polymers[43] were prepared by linking living polymer chains through divinyl compounds. Amphiphilic star block copolymers were prepared by initiating the block copolymerization of acetoxyethyl vinyl ether (AcOVE) and isobutyl vinyl ether (IBVE) with HI/ZnI_2 in toluene at –15°C. The living block copolymer was then reacted with the linking bifunctional vinyl ether to give star polymers.

The living cationic polymerization system is a very versatile process with a large choice in initiating systems and monomers, but it still has some limitations. The temperatures required for a living cationic system are typically low, i.e. –78°C to 0°C, to reduce chain transfer via β–hydrogen abstraction. This solution polymerization process produces polymer chains with a protected living end, but after all the monomer is consumed, the chains are terminated prior to isolation. Once terminated, the chains are dead. The system must be extremely free of moisture, and impurities in the solvent and monomer cannot be tolerated. The choice of solvent is critical. Generally, nonpolar solvents such as toluene and n-hexane are used, but more polar solvents such as CH_2Cl_2 enable living cationic polymerization under specific conditions. The correct balance of

---

[42] Lu,J.; Kamigaito, M.; Sawamoto, M.; Higashimura, T.; Deng, Y-X. *J. Polym. Sci. A: Polym. Chem.* **1997**, *35*, 1423.

[43] Sawamoto, M.; Kanaoka, S.; Omura, T.; Higashimura, T. *Polym. Prepr. (Am. Chem. Soc. Div. Polym. Chem.)* **1992**, *33*, 148.

solvent polarity is required to achieve reasonable Mn and low polydispersity. Number-average molecular weights typically less than 50,000 are reported.

1.3 Early Attempts at Controlling Free Radical Polymerization

The extension of the living concept to free radical polymerization has taken a much longer time to develop in comparison to anionic and cationic living polymerization. The control of complex polymeric structures by free radical polymerization has been a synthetic goal of polymer chemists for years since there are a variety of monomers that polymerize by FRP that cannot be used in ionic methods.

The earliest work on cleaving hydrocarbons with weak C-C bonds was first applied to thermal initiation of free radical polymerization. This work led into the trapping of the ω-end of an oligomeric chain by a second initiating carbon radical but the concept of reversible termination did not come until much later. Early investigations by Borsig *et al.* reported the thermal decomposition of 3,3,4,4-tetraphenylhexane (TPH) and 1,1,2,2-tetraphenylcyclopentane (TPCP) and used the resultant radicals to initiate free radical polymerization of methyl methacrylate[44] and styrene.[45] Similarly, other groups investigated the use of 1,2-disubstituted symmetric tetraarylethanes, which decompose by thermal cleavage into free radicals. Due to the steric hindrance of the phenyl substituents, the resultant free radicals by homolysis are very stable and in many cases are not reactive

---

[44] Borsig, E.; Lazár, M.; Capla, M. *Makromol. Chem.* **1967**, *105*, 212.

[45] Borsig, E.; Lazár, M.; Capla, M. *Collect. Czech. Chem. Commun.* **1968**, *33*, 4264.

enough to initiate polymerization.[46],[47] In 1967 Faust[48] observed that when benzopinacol (4) was irradiated, the resulting carbon radical (5) was able to initiate vinyl polymerization.

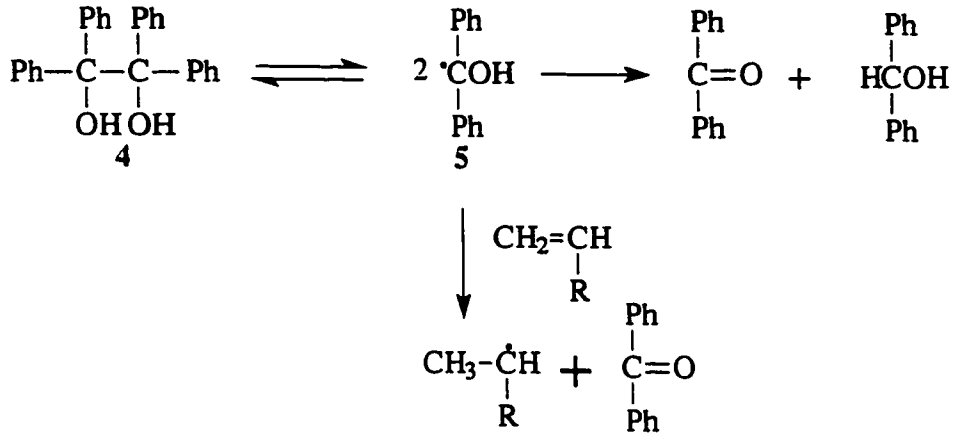

Scheme 5: Thermal dissociation of benzopinacol into the diphenyl methanol radical that initiated vinyl polymerization.

The mechanism of this polymerization as shown in Scheme 5 was investigated by Braun and Becker.[49],[50] The initiating ability of benzopinacol was caused by the hydrogen transfer reaction from the benzyl alcohol radical (5) to monomer. Based on this early work, Braun continued investigating a large number of related disubstituted tetraarylethanes as initiators for free radical polymerizations.

---

[46] Rüchardt, C.; Beckhaus, H.-D. *Angew. Chem.* **1980**, *92*, 417.

[47] Rüchardt, C.; Beckhaus, H.-D. *Top. Curr. Chem.* **1986**, *130*,1.

[48] Faust, R. J. Dissertation TH Darmstadt 1967.

[49] Braun, D.; Becker, K. H. *Makromol. Chem.* **1971**, *147*, 91.

[50] Braun, D.; Becker, K. H. *Ind. Eng. Chem. Prod. Res. Dev.* **1974**, *10*, 386.

One such compound, 1,1,2,2-tetraphenyl-1,2-diphenoxyethane, TPPA (**6**) was used to initiate the free radical polymerization of styrene[51], [52] but only oligomers were formed with low degrees of polymerization (DP $\leq$ 20) and termination of the oligomeric chains occurred by primary radical termination. Braun also expanded the study of tetraarylethanes as free radical initiators to the polymerization of methyl methacrylate[53] as illustrated in Scheme 6. With MMA the polymerization occurred in two steps. In the first step, initiators such as TPPA (**6**), tetraphenylbutanedinitrile (**7**), and 1,1,2,2-tetraphenyl-1,2-bis(trimethylsiloxy)ethane (**8**) produced telechelic oligomers with α, ω-end groups originating from the initiator.

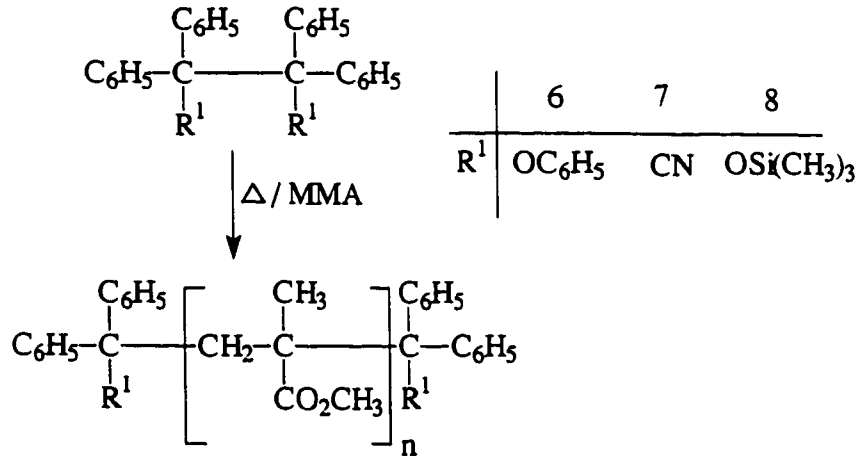

Scheme 6: Initiation of MMA polymerization using tetraarylethanes.

In the second step, when the majority of the initiator TPBD (**7**) was consumed, the oligomeric end groups could reinitiate polymerization by thermal cleavage of the C-C bond

---

[51] Bledzki, A.; Braun, D. *Makromol. Chem.* **1986**, *187*, 2599.

[52] Bledzki, A.; Braun, D.; Titzschkau, K. *Makromol. Chem.* **1987**, *188*, 2061.

between the two sterically hindered carbons. This generated a cyanodiphenylmethyl radical and a growing chain radical.[54] Unfortunately, the growing chain would loose the living ends through termination by disproportionation of two MMA chains and combination of an MMA chain with the *para* position of a phenyl ring of the cyanodiphenylmethyl initiator radical. The homolytic cleavage is a consequence of the steric hindrance between the large substituents on the quaternary carbons.

In a series of papers, Otsu and Yoshida[55], [56] detailed an interesting approach to living free radical polymerization through the use of a series of compounds called *ini*tiator-trans*fer* agent-*ter*minator (*iniferter*). Using tetraethylthiuram disulfide (**9**), and dibenzoyl disulfide (**10**) as iniferters, Otsu[55]polymerized styrene and MMA.

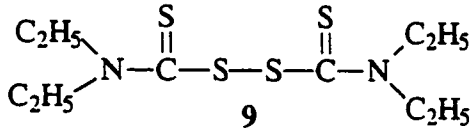

9

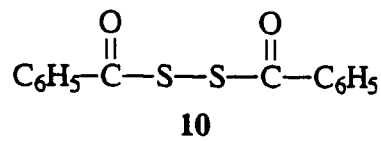

10

Otsu's original concept consisted of an initiator (**I-I′**) that has a high reactivity for chain transfer and/or primary radical termination. Subsequently, during thermolysis or photolysis of the initiator, two nonequivalent radicals, **I** and **I′** are formed. The more reactive radical **I**, initiates the polymer chain and the second radical **I′**, of lower reactivity, terminates the polymer chain. Under thermal or photolytic conditions, the reactive

---

[53] Bledzki, A.; Balard, H.; Braun, D. *Makromol. Chem.* **1988**, *189*, 2807.

[54] Bledzki, A.; Balard, H.; Braun, D. *Makromol. Chem.* **1981**, *182*, 3195.

[55] Otsu, T.; Yoshida, M. *Makromol. Chem., Rapid Commun.* **1982**, *3*, 127.

[56] Ostu, T.; Yoshida, M.; Tazaki,T. *Makromol. Chem., Rapid Commun.* **1982**, *3*, 133.

propagating polymer chain end can dissociate into a reactive propagating radical and a small molecule radical, I′ which was intended to be stable enough not to initiate new polymer chains. However, the initiators that Otsu employed were symmetrical about the thermally labile S-S bond. Consequently, the I′ radical was equivalent to the initiating radical, I, and not of lower reactivity. This resulted in initiating a second population of polymer chains by I′. Four organic sulphide photoiniferters; diphenyl disulphide (DPD), tetraethyl thiuram disulphide (TD), benzyl diethyldithiocarbamate (BDC), and 2-phenylethyl diethyldithiocarbamate (PEDC) were used to initiate the free radical polymerization of styrene.[57] The polymerization data showed an increase in molecular weight and conversion as a function of time, but the molecular weight distribution Mw/Mn was large (>2.0) and increased as the polymerization proceeded. The large molecular weight distribution is attributed to the sulphide or dithiocarbamate end group initiating a second crop of polymer chains which continues throughout the polymerization, increasing MWD.

Otsu *et al.*[58],[59] continued using the iniferter approach to prepare block copolymers by a free radical mechanism. Starting with polymeric photoiniferters; TD-PSt or TD-PMMA, consisting of tetraethyl thiuram disulfide (TD) and styrene or MMA as the A-block, four different monomers, styrene, MMA, vinyl acetate and ethyl acrylate were

---

[57] Otsu, T.; Yoshida, M.; Kuriyama, A. *Polym. Bull.* **1982**, *7*, 45.

[58] Otsu, T.; Yoshida, M. *Polym. Bull.* **1982**, *7*, 197.

[59] Otsu, T.; Kuriyama, A. *J. Macromol. Sci. Chem.* **1984**, *A21*, 961.

polymerized as the B-block. Otsu observed that only 70% of the isolated polymer consisted of pure AB-block copolymer. The rest consisted of homopolymers of monomers A and B. The homopolymers were extracted from the block copolymer by an appropriate choice of solvents. The presence of significant quantities of homopolymers in AB-block copolymer mixtures indicated that not all of the polymeric photoiniferters were telechelic dithiocarbamate-functionalized polymers. In addition, during the polymerization of the second monomer, new polymer chains were initiated by the dithiocarbamate end group radical to produce homopolymers of the B-monomer. Turner and Blevins[60] repeated some of Otsu's work involving photoinitiated block copolymer formation using the iniferter tetraethylthiuram disulfide. In chain extension experiments of the dithiocarbamate-terminated polystyrene with added styrene, Turner observed an increase in Mn as a function of photolysis time and minimal broadening of the molecular weight distribution. The photochemical chain extension of the dithiocarbamate-terminated poly(methyl methacrylate) illustrated a non-linear dependence of Mn on the photolysis time. A side reaction was identified that produced CS_2 gas as a byproduct that increased linearly with photolysis time. The evolution of CS_2 led to the loss of the living nature of the end group producing dead polymer chains.

Otsu had the correct idea in protecting the propagating polymer chain end with a reactive end group such as dithiocarbamate. This reactive small molecule would

---

[60] Turner, A. R.; Blevins, R. W. *Polym. Prepr. (Am. Chem. Soc. Div. Polym. Chem.)* **1988**, *29(2)*, 6; Turner, A. R.; Blevins, R. W. *Macromolecules* **1990**, *23*, 1856.

homolytically cleave from the propagating chain end under specific experimental conditions. However, the shortfall of this approach was that the dithiocarbamate radical also re-initiated new chains and decomposed to liberate CS_2. The re-initiation of new chains resulted in a broadening of the polydispersity, and, in the case of AB-block copolymer, in formation of homopolymers of the second monomer. The liberation of CS_2 changed the reactivity of the capping radical from a sulphur radical to a nitrogen radical which irreversibly terminated the polymer chains.

1.4 Chemistry of Nitroxyl Radicals

Another interesting area of organic chemistry is the study of stable free radicals such as nitroxyl radicals and their applications.[61] Nitroxide radicals are derivatives of nitrogen oxide with a disubstituted nitrogen atom formally containing a mono-valent oxygen atom as the third substituent.[62] They are used as spin labels and spin probes to study the structure and function of active centers of enzymes or properties of biological membranes.[63] As a consequence of nitroxides' paramagnetism, these molecules can affect relaxation times, T_1, and T_2, of the nuclei adjacent to the nitroxyl group. Thus, stable

---

[61] Volodarsky, L. B.; Reznikov, V. A.; Ovcharenko, V. I. Synthetic Chemistry of Stable Nitroxides, CRC Press, Boca Raton, 1994.

[62] Rozantsev, E. G. Free Nitroxyl Radicals, Plenum Press, New York, 1970.

[63] Kuznetsov, A. N. Spin Labeling Method, Nauka, Moscow, 1976, *Chem. Abstr.* **1977**, *86*, 148698e.

nitroxides can be used as contrasting agents in NMR (MRI) tomography.[64] The presence of the unpaired electron makes the molecule paramagnetic, thus observable by electron paramagnetic (spin) resonance spectroscopy (EPR or ESR). The unpaired electron changes its spin state upon absorption of microwave energy in the presence of a magnetic field.[65]

Nitroxide radicals are stable enough to be handled at room temperature. The stability is due to delocalization of three electrons in the N-O bond. The high delocalization energy (~30.4 kcal/mol)[66] provides a greater thermodynamic stability for the radical center[67] and prevents dimerization of most nitroxides. However, adjacent groups attached to nitrogen influence the thermodynamic stability, and it is these substituents, which determines possible degradation pathways. For example;

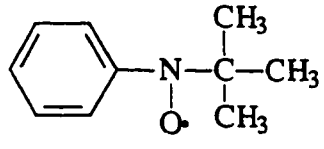

11

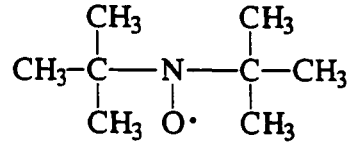

12

conjugation of the radical center with the benzene ring of **11** leads to electron density delocalization into the aromatic ring and thus reduces the stability of the nitroxide radical. This is compared to di-*tert*-butyl nitroxide (**12**) which is very stable due to the two electron donating groups that enhance the unpaired electron density.

---

[64] Keana, J. F. W.; Lex, L.; Mann, J. S.; May, J. M.; Park, J. H.; Pou, S.; Prabhu, V.S.; Rosen, G.M.; Sweetman, B. J.; Wu, Y. *J. Pure Appl. Chem.* **1990**, *62(2)*, 201.

[65] Pool, C. P. Electon Spin Resonance, 2nd ed., Wiley Interscience, New York, 1983.

[66] Rozantsev, E. G.; Sholle, V. D. *Synthesis* **1971**, 401.

[67] Mahoney, L. R.; Mendenhall, G. D.; Ingold, K. U. *J. Am. Chem. Soc.* **1973**, *95*, 8610.

The stability of nitroxides containing two sp^3-carbon atoms adjacent to nitrogen depends on the presence of hydrogen atoms at these carbons. The presence of one β-hydrogen makes disproportionation of the nitroxide[68] (**13**) to nitrone (**14**) and the *N*-hydroxlyamine (**15**) possible (Scheme 7). This disproportionation reaction is the major cause of poor radical stability.

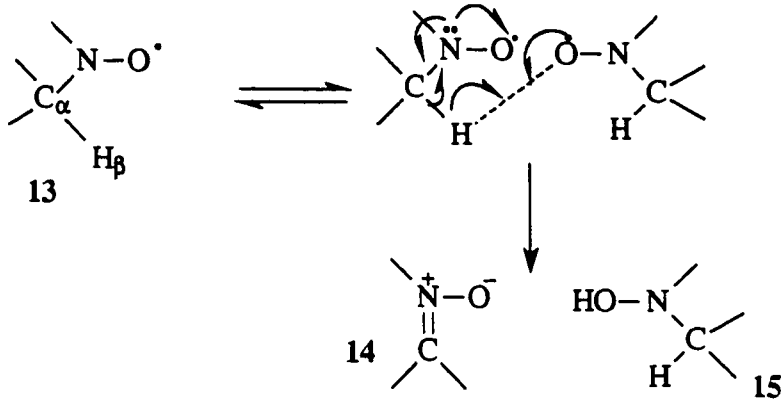

Scheme 7: Mechanism of disproportionation of β-hydrogen nitroxides to nitrone and hydroxylamine.

The first synthetic example of a nitroxide containing two *tert*-alkyl substituents on nitrogen was illustrated in 1959. Even though triacetonamine (**16**) had been known for

[68] Volodarsky, L. B.; Reznikov, V. A.; Ovcharenko, V. I. Synthetic Chemistry of Stable Nitroxides, CRC Press, London, pg. 6.

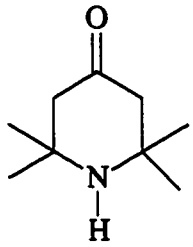

16

almost a century, the oxidation of these sterically hindered amines had not been developed. Very close to this, was the work by Todd *et al.*[69] who developed a synthesis of alkyl nitrones (**19**) via oxidation of hydroxylamine derivatives (**18**) derived from less substituted nitrones (17) and organometallic compounds (Scheme 8). This reaction became the foundation for the oxidation of hydroxylamines to nitroxides (Scheme 9) developed by Keana *et al.*[70]

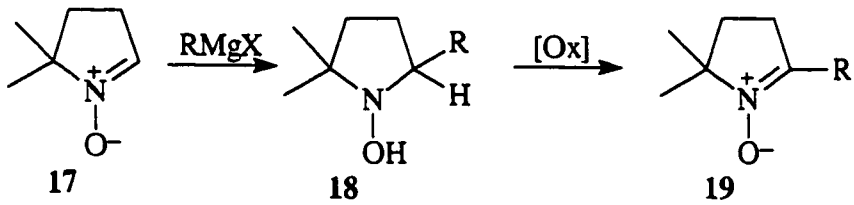

17 18 19

Scheme 8: Oxidation of hydroxylamines to more substituted nitrones.

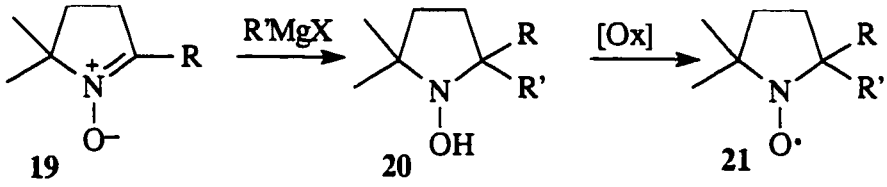

19 20 21

Scheme 9: Oxidation of hydroxylamines to nitroxides.

---

[69] Bonnett, R.; Brown, R. F. C.; Clark, V. M.; Sutherland, I. O.; Todd, A. *J. Chem. Soc.* **1959**, 2094.

[70] Keana, J. F. W. *Chem. Rev.* **1978**, *78*, 37. Keana, J. F. W.; Lee, T. D.; Bernard, E. M.; *J. Am. Chem. Soc.* **1976**, *98*, 3052.

It was not until the 1960s that Lebedev and Kazarnovsky[71] developed the important synthetic route to nitroxides involving oxidation of the hydroxylamine with hydrogen peroxide in the presence of a catalyst. This became the most commonly used route to prepare nitroxides from *N*, *N*-disubstituted hydroxylamines. A number of different oxidizing agents can be used under mild conditions so that other functional groups on the molecule are not affected. The kinetics of the reaction have been studied and the reaction proceeds by the mechanism[72] shown in Scheme 10. A few of the oxidizing agents employed are hydrogen peroxide with sodium tungstate as catalyst[73], metal oxides PbO_2, MnO_2, silver oxide and nitrous acid, HNO_2. In addition, the oxidation of secondary amines

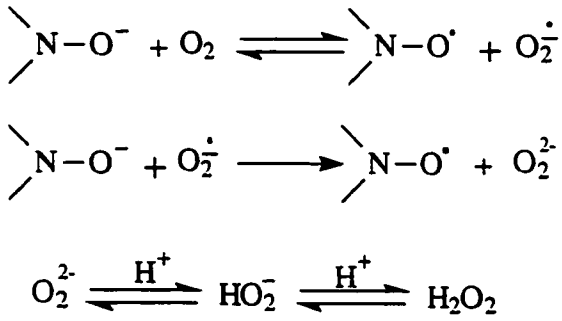

Scheme 10: Oxidation of *N*,*N*-disubstituted hydroxylamines to nitroxides.

such as 2,2,6,6-tetramethylpiperidine to the nitroxide can be performed using H_2O_2 in the presence of Na_2WO_4 and Triton B using H_2O or aqueous methanol[61], [62] or H_2O_2 in aqueous

---

[71] Lebedev, O. L.; Kazarnovsky, S. N. *Treatise on Chemistry and Chemical Technology*, Gorky, **1959**, *3*, 649 (in Russian). Lebedev, O. L.; Khidekel, M. L.; Razuvaev, G. A. *Dokl. Akad. Nauk. S.S.S.R.*, **1961**, *140*, 1327, (in Russian). Rozantsev, E. G.; Sholle, V. D.*Synthesis*, **1971**, 190.

[72] Sen', V. D.; Golubev, V. A.; Rosenburg, A. N.; *Symp. Stable Nitroxide Free Radicals: Synthesis and Application (Abstr.)* Pècs, Hungary, **1979**, 77.

[73] Rauckman, E. J.; Rosen, G. M.; Abou-Donia, M. B. *Syn. Comm.* **1975**, *5(6)*, 409.

acetonitrile with or without a catalyst. The reaction is usually carried out at room temperature. Oxidation of secondary amines to nitroxides can also be achieved with peracids such as *m*-chloro or *m*-nitroperbenzoic acid in an organic solvent, $CHCl_3$ or CH_2Cl_2. The hydroxylamine intermediate is formed as a result of nucleophilic attack by nitrogen on oxygen of the peroxide group of the acid.[74] Care must be taken not to over oxidize the nitroxyl function group to the oxammonium derivative.[75]

In acidic media, or in the presence of strong oxidants, the nitroxyl group has limited stability. The nitroxyl radical reacts[61] with the acid (Scheme 11) to produce the corresponding oxammonium and hydroxylamine which can be oxidized into the oxammonium molecule. In the presence of water the nitroxyl group can be regenerated

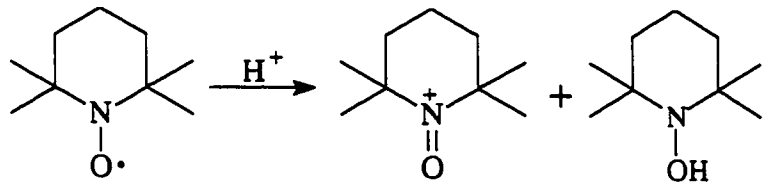

Scheme 11: Reaction of a strong acid with nitroxyl radicals.

by oxidation of the hydroxylamine by oxammonium salt or reduction of the oxammonium group by water.

The ease of reduction of the nitroxyl group depends on its environment. Increasing the electron density on oxygen and its nucleophilicity is illustrated by a greater contribution of the canonical structure B over A.

---

[74] Toda, T.; Mori, E.; Murayama, K. *Bull. Chem. Soc. Jpn.* **1972**, *45*, 1904.

[75] Cella, J. A.; Kelley, J. A.; Kenehan, E. F. *Tet. Lett.* **1975**, 2869.

The hyperfine coupling constant, a_N of the unpaired electron with nitrogen changes in the opposite direction with the ease of nitroxyl group reduction. The contribution of canonical form B decreases on introduction of electron-withdrawing substituents resulting in a decrease of the a_N value. Under identical conditions, the more electon-withdrawing the substituents on nitrogen the lower a_N, favoring canonical form A, and the slower the oxidation reaction of the hydroxylamino group to the nitroxide. For a quantitative estimation of the ease of the one-electron reduction of the nitroxyl group the reduction potential should be used.[76]

The nitroxyl group shows weak basic properties (pK ≈ –5.5) and consequently, it can be protonated by strong acids: H_2SO_4, CF_3COOH / H_2SO_4 and HCl / dried CCl_4. Long storage of 4-oxo-TEMPO (**22**), or heating to above 100°C leads to disproportionation (Scheme 12) because of hydrogen abstraction from another nitroxide molecule. The products of this reaction are the dimer **25** and a small amount of phorone.[77] Above 125°C or when exposed to UV irradiation, di-*tert*-butyl nitroxide undergoes C-N bond cleavage to generate the corresponding O-*tert*-butyl derivative.[78] Dialkylnitroxides in the ground state react very slowly with hydrocarbons, but in the presence of UV irradiation the reaction is

---

[76] Volodarsky, L. B. Ed. Imidazoline Nitroxides, Synthesis and Properties Vol. CRC Press, Boca, Raton, FL. 1988.

[77] Yoshioka, T.; Higashida, S.; Morimura, S.; Murayama, K. *Bull. Chem. Soc. Jpn.* **1971**, *44*, 2207.

[78] Anderson, D. R.; Koch, T. H. *Tet. Lett.* **1977**, 3015.

more pronounced. For example, 4-hydroxy-TEMPO in solution upon irradiation produces the hydroxylamine and the O-benzyl derivative in a 1:1 molar ratio.[79] The hydrogen radical is abstracted from the solvent by the photoexcited nitroxyl group in the n→π* excited state.

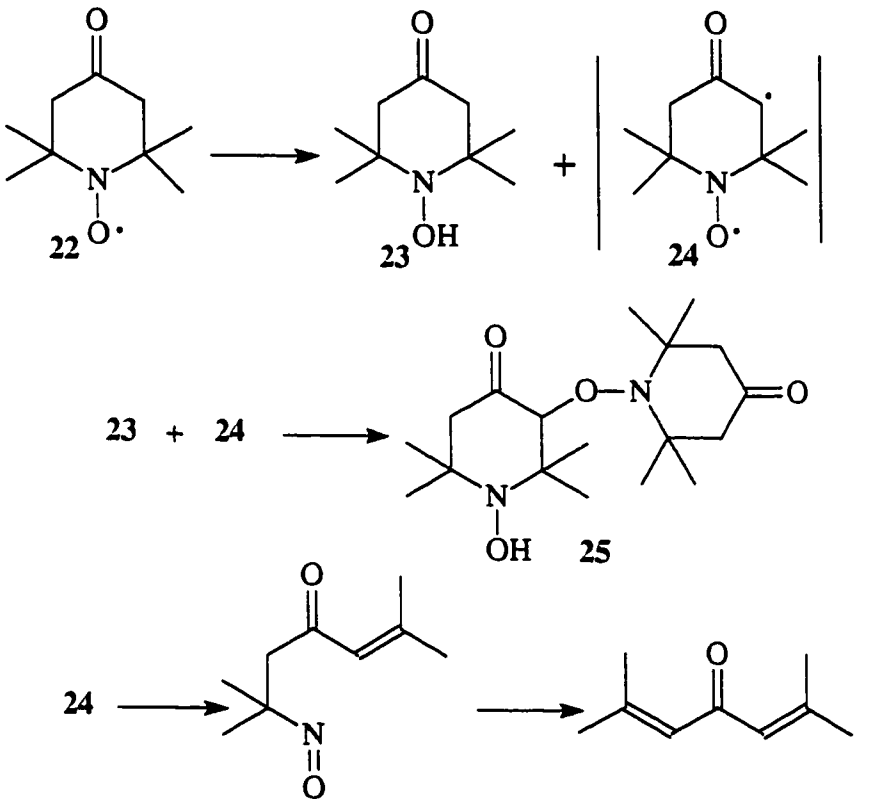

Scheme 12: Disproportionation of 4-oxo-TEMPO.

[79] Keana, J. F. W.; Dinerstein, R. J.; Baitis, F. *J. Org. Chem.* **1971**, *36*, 209.

1.5 Radical Trapping of Initiating Byproducts Using Nitroxyl Radicals

The Australian group under the direction of D. H. Solomon has studied the mechanism of free radical initiation of various vinyl monomers by thermal decomposition of initiators at low temperatures. Using nitroxide radicals, Solomon *et al.* developed a technique for trapping transient radicals. The nitroxyl radicals rapidly and efficiently react with carbon-centered radicals at close to diffusion controlled rates ($k = 10^7 - 10^9\ M^{-1}s^{-1}$)[80] to form stable alkoxyamine products. This completely inhibits the propagation of vinyl monomers ($k = 10^2 - 10^4 M^{-1}s^{-1}$) at these temperatures. These products are subsequently isolated and identified by the usual techniques, HPLC, NMR, FT-IR etc. This section will summarize the different initiating radicals species that are captured by nitroxides as a function of the monomer investigated.

The selectivity of the reaction of benzoyloxy radicals (formed by thermal decomposition of BPO) with styrene in the presence of radical trapping agents TEMPO[81]

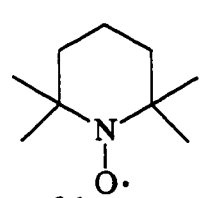

26

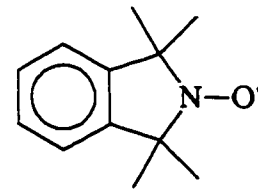

27

(**26**) or the isoindoline nitroxide[82] (**27**) show that the reaction with styrene proceeds with 80% "tail" addition, 5% "head" addition and 15% aromatic substitution.[81] Aromatic

---

[80] Schmid, P.; Ingold, K. U. *J. Am. Chem. Soc.* **1978**, *100*, 2493.

[81] Moad, G.; Rizzardo, E.; Solomon, D. H. *J. Macromol. Sci. Chem.* **1982**, *A17*, 51.

substitution of the benzoyloxy radicals on styrene produce cyclohexadienyl radicals which can be trapped by the nitroxide. This reaction occurs by oxidation (hydrogen abstraction or combination followed by elimination) to produce the corresponding aromatic compound and the hydroxylamine. The hydroxylamine can subsequently be oxidized by benzoyl peroxide to regenerate the nitroxide radical TEMPO (**26**). Moad *et al.*[82] noted that the isoindoline nitroxide (**27**) appears to be a poorer oxidant than TEMPO thus decreasing the

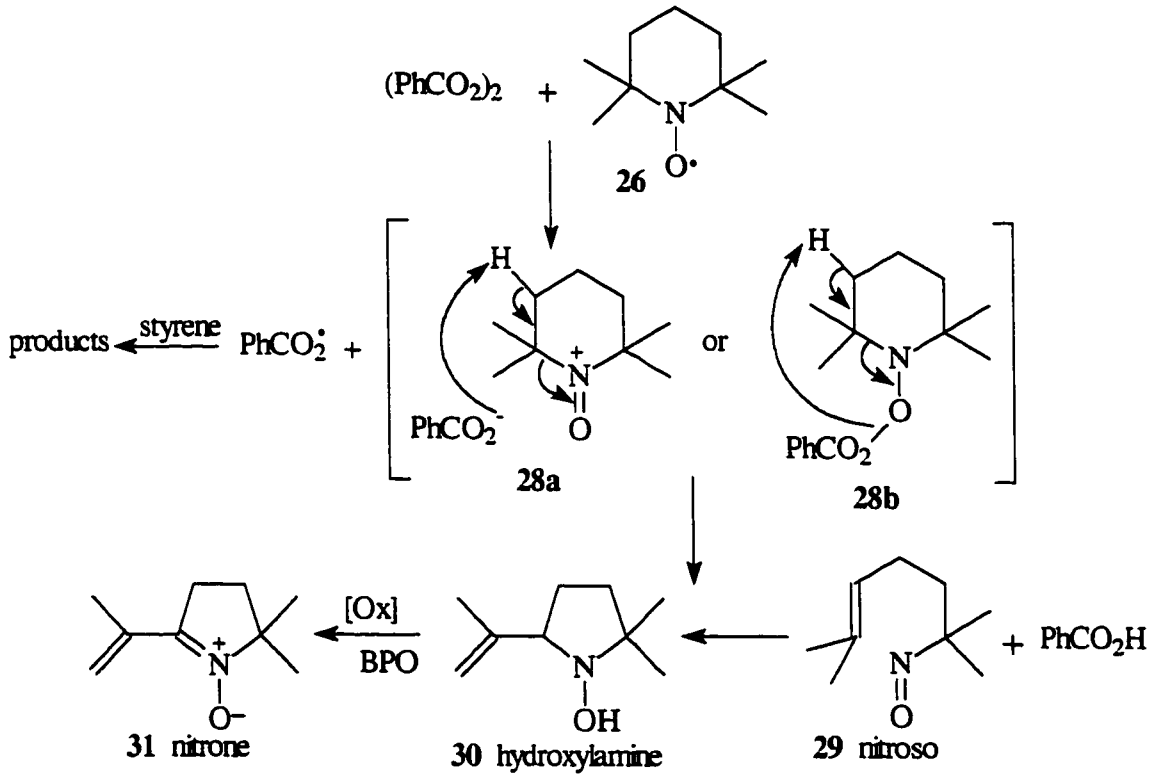

Scheme 13: Promoted decomposition of BPO by nitroxyl radical TEMPO.

[82] Moad, G.; Rizzardo, E.; Solomon, D. H. *Macromolecules* **1982**, *15*, 909. Moad, G.; Solomon, D. H.; Johns, S. R.; Willing, R. I. *Macromolecules* **1982**, *15*, 1188.

amount of hydroxylamine formed. Five percent of the benzoyloxy radicals decarboxylate to form phenyl radicals that also can add to the vinyl group or the aromatic ring of styrene or be trapped by TEMPO.

In the absence of monomer, nitroxide radicals such as TEMPO[83] promote the decomposition of BPO into benzoyloxy radicals and benzoic acid with the transformation of the nitroxide (**26**) to the nitrone (**31**) (Scheme 13).[83] Each equivalent of nitrone (**31**) produced three equivalent of benzoic acid form. This promoted decomposition of BPO was also observed when nitroxide **27** was used[82] but, this only occurs with BPO.

Moad *et al.*[84] applied this nitroxide radical trapping technique to capture the initiating radicals of the spontaneous initiation of styrene polymerization at 100°C. After isolation and identification, the product analysis showed that nitroxyl radicals **26** and **27** react by hydrogen abstraction from a thermally generated styrene dimer (1-phenyl-1,2,3,9-tetrahydronaphthalene) to form the corresponding hydroxylamine and the nitroxide trapped dimer. This study provided additional evidence for the Mayo mechanism[85] being responsible for the self initiated polymerization of styrene.

The radical trapping experiments have been extended to the comonomer system of styrene[86] and acrylonitrile.[87] The *tert*-butoxyl radicals from di-*tert*-butyl peroxyoxalate

---

[83] Moad, G.; Rizzardo, E.; Solomon, D. H. *Tet. Lett.* **1981**, *22*, 1165.

[84] Moad, G.; Rizzardo, E.; Solomon, D. H. *Polym. Bull.* **1982**, *6*, 589.

[85] Mayo, F. R. *J. Am. Chem. Soc.* **1968**, *90*, 1289. Chong, Y. K.; Rizzardo, E.; Solomon, D. H. *J. Am. Chem. Soc.* **1983**, *105*, 7761.

[86] Busfield, W. K.; Jenkins, I. D.; Thang, S. H.; Rizzardo, E.; Solomon, D. H. *Eur. Polym. J.* **1993**, *29*, 397.

(DBPOX) add to styrene five times more rapidly than to acrylonitrile, whereas methyl radicals add to acrylonitrile about four times more rapidly than to styrene.

Using the same initiator at 60°C the *tert*-butoxy radicals react with methyl acrylate monomer by several pathways as evident by the radical trapping with nitroxide **27**.[88] The major pathway is addition of the *tert*-butoxy radical to the "tail" of MA (62.9%). In addition, other competing reactions occurred including "head" addition (0.9%), hydrogen abstraction from the methyl ester group of the monomer (8.8%) and fragmentation of the *tert*-butoxy radical to methyl radicals and acetone. Similar product ratios were obtained when the trapping radical was TEMPO.[89]

Griffith, Rizzardo, Solomon,[90] and others extensively investigated the thermal decomposition of different initiators and their reaction with methyl methacrylate. The resulting carbon-centered radicals were trapped with 1,1,3,3-tetramethylisoindoline-2-oxyl (**27**). The di-*tert*-butyl peroxalate initiator thermally decomposed to *tert*-butoxy radicals and methyl radicals. The following products of the initiation of MMA were trapped by nitroxide **27** (Scheme 14). The majority of the *tert*-butoxy radical adds via "tail" addition to MMA accounting for only 63% of the total products. With MMA there is a significant

---

[87] Busfield, W. K.; Jenkins, I. D.; Monteiro, M. J. *Polymer* **1997**, *38*, 165.

[88] Griffiths, P. G.; Rizzardo, E.; Solomon, D. H. *Tet. Lett.* **1982**, *23*, 1309.

[89] Rizzardo, E.; Solomon, D. H. *Polym. Bull.* **1979**, *1*, 529.

[90] Griffiths, P. G.; Rizzardo, E.; Solomon, D. H. *J. Macromol. Sci. Chem.* **1982**, *A17*, 45. Rizzardo, E.; Serelis, A. K.; Solomon, D. H. *Aust. J. Chem.* 1982, *35*, 2013. Cuthbertson, M. J.; Moad, G.; Rizzardo, E.; Solomon, D. H. *Polym. Bull.* **1982**, *6*, 647. Busfield, W. K.; Jenkins, I. D.; Rizzardo, E.; Solomon, D. H. *J. Chem. Soc. Perkin Trans.* **1991**, *1*, 1351.

contribution of hydrogen abstraction from monomer, both from the allylic position of MMA (29%) and the ester methyl group, the latter accounting for 4% of the total alkoxyamines produced. This implies that a large portion of polymer chains will have unsaturated terminal end groups and some chains could contain chain branching points. Steric hindrance of the initiating radical has the greatest influence on the orientation of addition to the olefin.

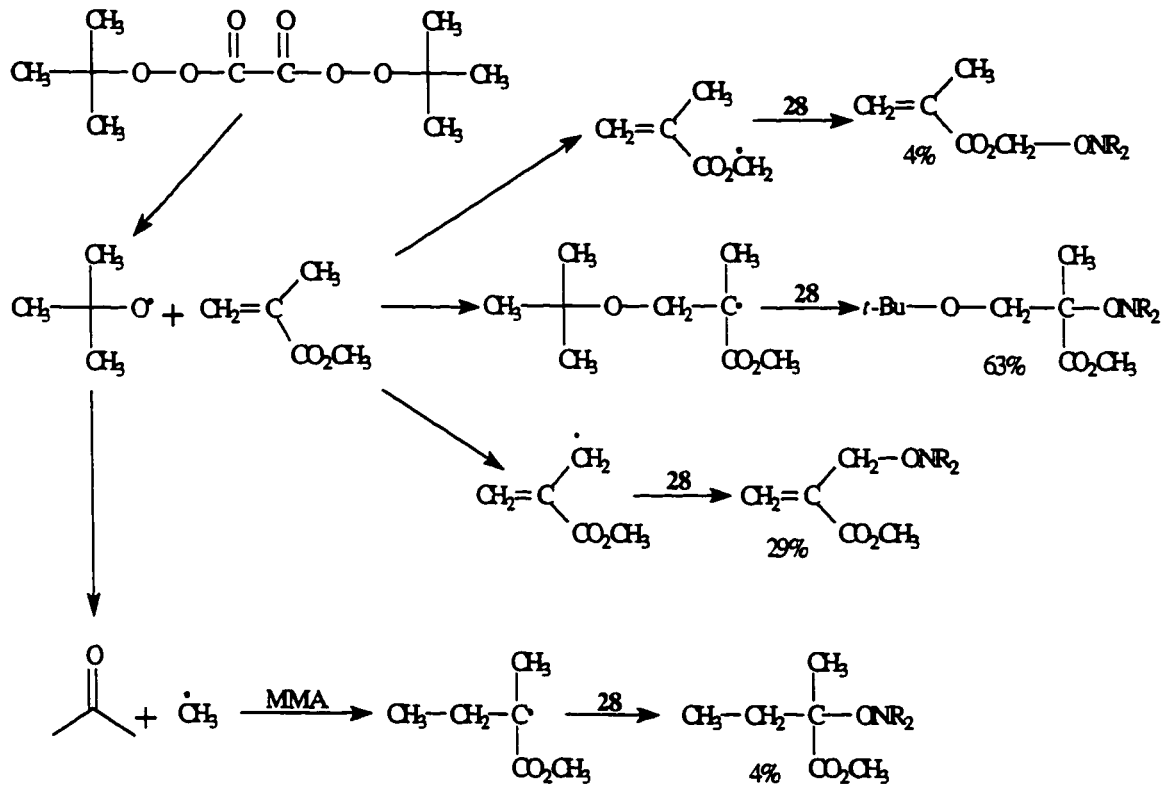

Scheme 14: Radical trapping of initiating radical from thermal decomposition of DBPOX and attack on MMA.

This technique has also been employed to study stable alkoxylamines formed when a nitroxide is used to scavenge various radicals. The alkoxylamines are produced by reaction of initiator-derived radicals with monomers such as allyl acrylate and diallyl ether[91], and other vinyl monomers.[92] Solomon extended this trapping study with nitroxides to determine absolute rate constants for the first few propagation steps of methyl acrylate initiated with BPO or DBPOX.[93] By decreasing the nitroxide concentration, one, two and three monomer units could add to the initiating radical before the carbon-centered radical was captured by the nitroxide.

1.6 Stable Free Radical Polymerization (SFRP)

Solomon and colleagues continued on with the nitroxide radical trapping study at 60°C with alkoxyamines to initiate polymerization. This early work[94] was very sketchy with few details and almost no experimental data. This concept was derived from the fact that alkoxyamines are thermally labile. Upon heating, they decompose reversibly to a stable nitroxide radical and a reactive carbon-centered radical that can attack a vinyl monomer. The resultant carbon radical is trapped by the nitroxide. At that time, the

---

[91] Busfield, W. K.; Jenkins, I. D.; Thang, S. H.; Rizzardo, E.; Solomon, D. H. *J. Chem. Soc. Perkin Trans.* **1988**, *1*, 485.

[92] Bottle, S.; Busfield, W. K.; Jenkins, I. D.; Thang, S.; Rizzardo, E.; Solomon, D. H. *Eur. Polym. J.* **1989**, *25*, 671. Bottle, S.; Busfield, W. K.; Jenkins, I. D.; Skelton, B. W.; White, A. H.; Rizzardo, E.; Solomon, D. H. *J. Chem.Soc. Perkin Trans.* **1991**, *2*, 1001. Busfield, W. K.; Jenkins, I. D.; Van Le, P. *Polym. Bull.* **1996**, *36*, 435.

[93] Moad, G.; Rizzardo, E.; Solomon, D. H.; Beckwith, A. L. J. *Polym. Bull.* **1992**, *29*, 647.

[94] Rizzardo, E. *Chem Aust.* **1987**, *54*, 32. Moad, G.; Rizzardo, E. *Pacific Polymer Conf. Prepr.* **1993**, *3*, 651.

process only worked for alkyl acrylates producing oligomers of low molecular weights (Mn<10,000) and broad polydisperties (PD = 1.5-2.0)[95] at polymerization temperatures of 100°C. This did not demonstrate a controlled or living free radical polymerization.

Independently, the group at the Xerox Research Center of Canada was trying to make narrow molecular weight resins by a free radical mechanism in a similar manner to the iniferter work by Otsu.[96] Initial molecular orbital calculations[97] indicated that stable nitroxyl radicals would yield weaker C-O bonds with a propagating styrene chain than a C-S bond formed with a sulphur radical from an iniferter. This led to the first publication by Georges *et al.*[98] demonstrating that the stable free radical polymerization (SFRP) of styrene initiated with BPO and reversibly terminated with 2,2,6,6-tetramethyl-1-piperidinyloxy (TEMPO) at 123°C, produced a linear increase in Mn with conversion and polydispersities of 1.2 to 1.3.

For a conventional free radical polymerization, the theoretical lower limit for polymer molecular weight distribution, Mw/Mn is 1.5[99] and in practice on the lab scale, polydispersities are generally between 2.0 to 2.4 for styrene polymerization. This value

---

[95] Solomon, D. H.; Rizzardo, E.; Cacioli, P. U. S. Pat. **4,581,429**, April 8, 1986.

[96] Otsu, T.; Yoshida, M. *Makromol. Chem., Rapid Commun.* **1982**, *3*, 127. Otsu, T.; Yoshida, M.; Tazaki, T. *Makromol. Chem., Rapid Commun.* **1982**, *3*, 133.

[97] Georges, M. K.; Veregin, R. P. N.; Kazmaier, P. M.; Hamer, G. K. *TRIP*, **1994**, *2*, 66.

[98] Georges, M. K.; Veregin, R. P. N.; Kazmaier, P. M.; Hamer, G. K. *Macromolecules*. **1993**, *26*, 2987.

[99] Odian, G. G. *Principles of Polymerization*, 2nd ed., **1981**, John Wiley & Sons, pp. 280-281. The limiting value of 1.5 for Mw/Mn was obtained with assumptions of 100% termination by coupling and conversion.

increases to 3 or greater on the industrial scale.[100] Based on theory, synthetic chemists believed that polymers produced by a free radical mechanism could not have narrow molecular weight distributions less than 1.5 and this hampered chemists from pushing the limit. The SFRP process was not operating by a truly conventional free radical mechanism.

The concepts of living anionic polymerization were applied to designing a process for obtaining living polymers by a free radical mechanism. Narrow polydisperse polymers in principle can be obtained by a free radical mechanism. This is possible if the initiation of all the polymer chains occurs over a very short time; analogous to anionic initiation, and the process proceeds with no premature chain termination by coupling, disproportionation or chain transfer. Also, the steady-state concentration of propagating radicals must be very low. Fast initiation was accomplished by promoted decomposition of peroxide initiator BPO by TEMPO[83] and increasing the polymerization temperature so that the half-life, $t_{½}$ for BPO[101] was less than a few minutes. The activation energy determined by ESR[97], [102], [103] for SFR promoted BPO decomposition is 40 ± 5 kJ/mol as compared to 120 kJ/mol for BPO thermal decomposition. After thermal decomposition of BPO, the initiating radicals add to the vinyl monomer and then these carbon-centered radicals are reversibly terminated by the nitroxide radicals at close to diffusion controlled rates. The oxygen-centered

---

[100] Rudin, A. *Comprehensive Polymer Science* Vol . 3 Part 1, **1989**, pp. 239, Pergamon Press.

[101] Odian, G. G. *Principles of Polymerization*, 2nd ed. **1981**, John Wiley, & Sons, pp.196.

[102] Veregin, R. P. N.; Georges, M. K.; Kazmaier, P. M.; Hamer, G. K. *Proc. Am. Chem. Soc., Div. Polym. Mater: Sci. Eng.* **1993**, *68*, 8.

[103] Veregin, R. P. N.; Georges, M. K.; Kazmaier, P. M.; Hamer, G. K. *Macromolecules*, **1993**, *26*, 5316.

radicals from the initiator are not captured by nitroxides. This labile C-O bond at temperatures >120°C undergoes homolytic cleavage for additional chain growth followed by reversible termination with the nitroxyl. This controlled reversible chain capping by the nitroxide substantially reduces the irreversible termination reactions that prematurely stop propagation of the polymer chains. At this point in the development of the SFRP process, chain termination is not completely removed. As a consequence, this author will designate the SFRP process as a "living" radical or controlled polymerization as defined by Matyjaszewski and Müller[104] versus a living polymerization like the anionic variety where chain termination can be almost completely eliminated.

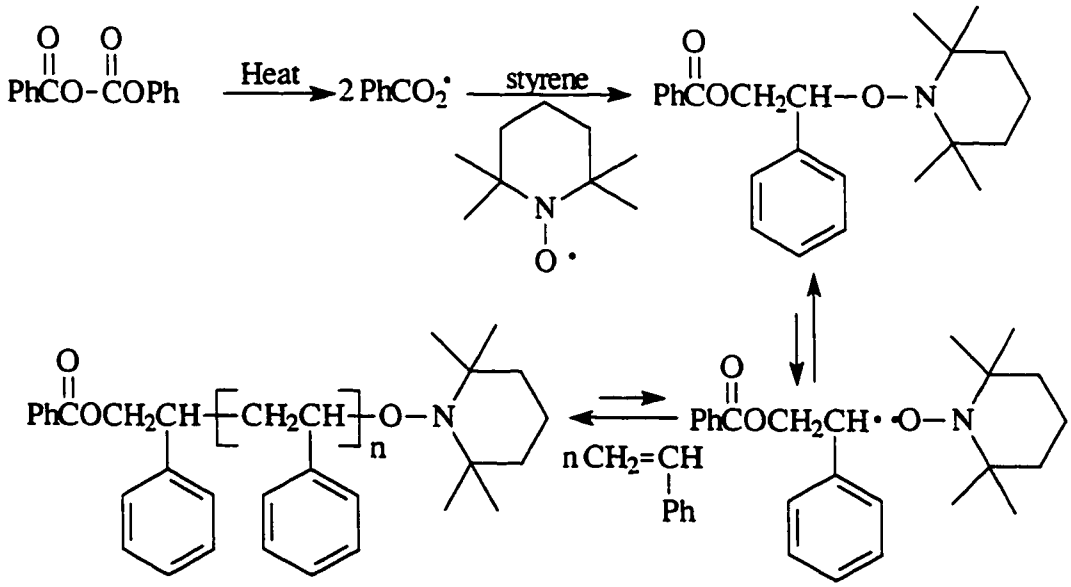

Figure 1: Stable Free Radical Polymerization of Styrene

[104] Matyjaszewski, K.; Müller, A. H. E. *Polym. Prepr. (Am. Chem. Soc. Div. Polym. Chem.)* **1997**, *38(1)*, 6.

Number-average molecular weights (Mn) increase linearly with conversion and time while maintaining MWD between 1.15 and 1.3. The mechanism of the stable free radical polymerization process is illustrated in Figure 1.

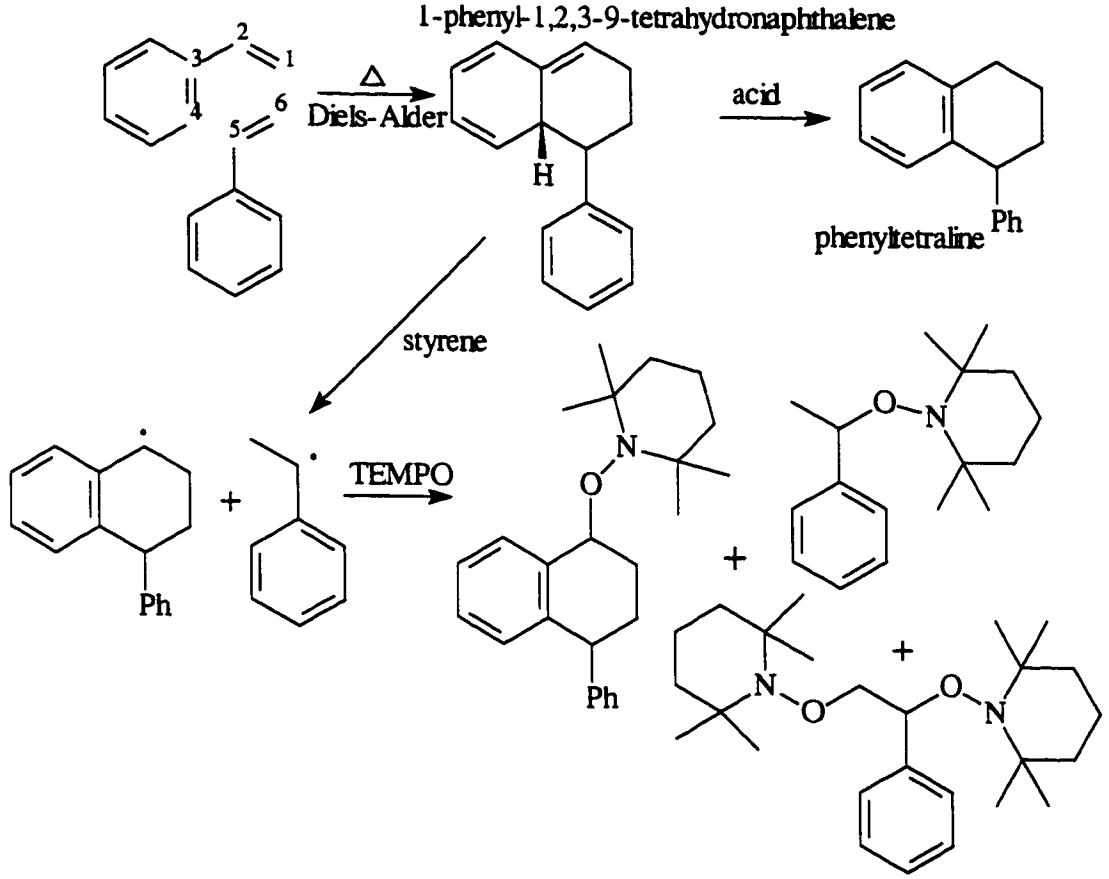

Scheme 15: Mechanism of autopolymerization of styrene via Diels-Alder mechanism and radical trapping of initiating radicals with TEMPO.

Priddy *et al.*[105] have studied the autopolymerization of styrene in the presence of different acids without added nitroxide. The net result is that the rate of spontaneous initiation is suppressed allowing the polymerization to be conducted at higher temperatures than normal where propagation rates are faster. There is an increase in the amount of protonated Diels-Alder dimer, 1-phenyltetraline produced as shown in Scheme 15. Hawker *et al.*[106] and Matyjaszewski *et al.*[107] also explored the autopolymerization of styrene in the presence of the nitroxyl radical TEMPO and found molecular weight control during the thermal self initiation of styrene. The ethylbenzene-nitroxide adduct *N*-(1′-methylbenzyloxy)-2,2,6,6-tetramethylpiperidine, MB-TMP, **32** and the dintroxide-styrene adduct are formed at close to diffusion controlled rates due to the fast trapping by the nitroxide. The ethylbenzene-TEMPO adduct, MB-TMP is itself an initiator for SFR polymerization and thus initiates an *in situ* controlled polymerization of styrene. Since propagation is first order in monomer and spontaneous initiation of styrene is second order in monomer, the contribution of autopolymerization of styrene decreases with conversion in a reversibly terminated system.[108]

---

[105] Buzanowski, W. C.; Graham, J. D.; Priddy, D. B.; Shero, E. *Polymer* **1992**, *33*, 3055. Li, I.; Howell, B. A.; Priddy, D. B. *Polym. Prepr. (Am. Chem. Soc. Div. Polym. Chem.)* **1996**, *37(2)*, 511.

[106] Michalak, L.; Malmström, E.; Devonport, W.; Mate, M.; Hawker, C. J. *Polym. Prepr. (Am. Chem. Soc. Div. Polym. Chem.)* **1997**, *38(1)*, 727. Devonport, W.; Michalak, L.; Malmström, E.; Mate, M.; Kurdi, B.; Hawker, C. J. *Macromolecules* **1997**, *30*, 1929.

[107] Gaynor, S.; Greszta, D.; Mardare, D.; Teodorescu, M.; Matyjaszewski, K. *J. M. S. Pure Appl. Chem.* **1994**, *A31*, 1561. Mardare, D.; Shigemoto, T.; Matyjaszewski, K. *Polym. Prepr. (Am. Chem. Soc. Div. Polym. Chem.)* **1994**, *35(2)*, 557.

[108] Matyjaszewski, K.; Gaynor, S.; Greszta, D.; Mardare, D.; Shigemoto, T. *Macromol.* Symp. **1995**, *98*, 73.

The rate of polymerization of styrene by SFRP was initially very slow. Sixty-nine hours were required to achieve 90% conversion. In the SFRP of styrene, acids such as camphorsulfonic acid (CSA),[105b, 109] *in situ* generated benzoic acid and 2-fluoro-1-methylpyridinium *para*-toluenesulfonate (FMPTS)[110] have been identified and used to increase the rate of polymerization and decrease the amount of autoinitiation[111] of styrene. It was later found that thermal initiation of styrene in the presence of CSA[112] and FMPTS[113] also decreased the concentration of excess nitroxide which had a profound effect on increasing the polymerization rate. Increased propagation rates were also demonstrated when the initial ratio of [TEMPO]/[BPO] was reduced from 1.3:1 to 1.1:1.[114] This shifts the equilibrium between the capped or dormant chains [P_i–T] over to the exposed or active propagating chain end radical [P_i•] and free nitroxide [T•].

Control of the SFR polymerization is achieved by homolytic cleavage of the dormant alkoxyamine that reversibly produces propagating radicals according to the

---

[109] Georges, M. K.; Moffat, K. A.; Veregin, R. P. N.; Kazmaier, P. M.; Hamer, G. K. *Polym. Mater. Sci. Eng.* **1993**, *69*, 305. Georges, M. K.; Veregin, R. P. N.; Kazmaier, P. M.; Hamer, G. K. *Polym. Prepr. (Am. Chem. Soc. Div. Polym. Chem.)* **1994**, *35(2)*, 870. Georges, M. K.; Veregin, R. P. N.; Kazmaier, P. M.; Hamer, G. K.; Saban, M. *Macromolecules* **1994**, *27*, 7228.

[110] Odell, P.G.; Veregin, R. P. N.; Michalak, L. M.; Brousmiche, D.; Geroges, M. K. *Macromolecules* **1995**, *28*, 8453.

[111] Georges, M. K.; Kee, R. A.; Veregin, R. P. N.; Hamer, G. K.; Kazmaier, P. M. *J. Phy. Org. Chem.* **1995**, *8*, 301.

[112] Veregin, R. P. N.; Odell, P. G.; Michalak, L. M.; Geroges, M. K. *Macromolecules* **1996**, *29*, 4161. Veregin, R. P. N.; Odell, P. G.; Michalak, L. M.; Georges, M. K. *Macromolecules* **1996**, *29*, 2746.

[113] Odell, P.G.; Veregin, R. P. N.; Michalak, L. M.; Georges, M. K. *Macromolecules* **1997**, *30*, 2232.

[114] MacLeod, P. J.; Veregin, R. P. N.; Odell, P. G.; Georges, M. K. *Macromolecules* **1997**, *30*, 2207.

following equilibrium:

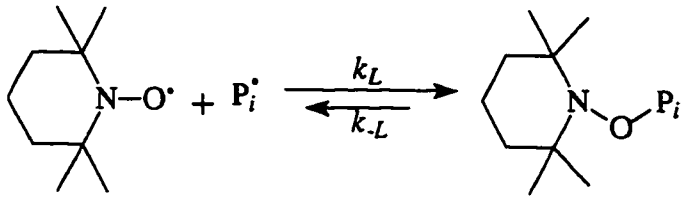

(13)

which can also be written as:

$$T^{\bullet} + P_i^{\bullet} \underset{k_{-L}}{\overset{k_L}{\rightleftharpoons}} P_i\text{-}T \qquad K_L = \frac{k_L}{k_{-L}} = \frac{[P_i\text{-}T]}{[T^{\bullet}][P_i^{\bullet}]} \tag{14}$$

$$P_i^{\bullet} + M \xrightarrow{k_p} P_{i+1}^{\bullet} \tag{15}$$

Here k_L and k_{-L} or k_c and k_d as reported by Fukuda *et al.*[115] are the rate constants for trapping the propagating polymer chain by a nitroxide (combination) and release of the propagating radical (dissociation), respectively. The trapping of carbon-centered radicals is close to a diffusion-controlled reaction with a rate constant k_L that approximately equals 10^9 $M^{-1}s^{-1}$. Here P_i-T [116] denotes a dormant polymer chain that is capable of reversible homolytic cleavage. The rate constant for the bond breaking reaction k_{-L} (rate of homolytic cleavage) is determined by the strength of the NO-C bond between the nitroxide TEMPO, and the propagating polymer chain. If this bond does not break then polymerization does not occur. As the free nitroxide concentration is reduced the equilibrium is shifted to the

---

[115] Fukuda, T.; Terauchi, T. *Chem. Lett.* **1996**, *4*, 293. Goto, A.; Fukuda, T. *Macromolecules* **1997**, *30*, 4272. Goto, A.; Fukuda, T. *Macromolecules* **1997**, *30*, 5183.

[116] Veregin R. P. N.; Georges, M. K.; Hamer, G. K.; Kazmaier, P. M. *Polym. Prepr. (Am. Chem. Soc. Div. Polym. Chem.)* **1994**, *35(1)*, 797. Veregin, R. P. N.; Georges, M. K.; Hamer, G. K.; Kazmaier, P. M. *Macromolecules* **1995**, *28*, 4391.

left increasing the concentration of propagating radicals and thus the rate of polymerization.

At temperatures >120°C polymerization occurs with a rate that is proportional to the propagation rate constant k_p, the concentration of monomer M, the concentration of living polymer chains, L_N and to $1/K_L$ and $1/T_{free}$ where T_{free} denotes free TEMPO concentration.

$$-\frac{dM}{dt} = k_p[M]L_N\left(\frac{1}{K_L T_{free}}\right) \qquad (16)$$

After a period of time, the rate of polymerization becomes constant and is given by the integration of equation 16 with T_{free} and L as constants.

$$-\ln\left(\frac{[M]}{[M_o]}\right) = k_p\left(\frac{L_N}{K_L T_{free}}\right)t \quad \text{where} \quad k_{obs} = \frac{k_p L_N}{K_L T_{free}} \qquad (17)$$

A plot of equation 17 of $-ln([M]/[M_o])$ vs time[116] gives the slope equal to k_{obs}. While k_p is fixed by the choice of monomer and T_{free} is fixed by the initial conditions, K_L can be changed by varying k_L which depends on the strength of NO-C bond. To study the strength of the NO-C bond, unimers BST, **33** and BSP, **34** were heated *in situ* in an ESR cavity, to liberate free TEMPO. The concentration of free TEMPO was followed as a function of time using ESR to determine the rate of bond breaking for the NO-C bond. By systematically varying temperature, the activation energy ($\Delta H^{\neq}$) for this C-O bond breaking was calculated. From this, it was possible to measure activation energies with different nitroxides.

$$\frac{k}{T} = \frac{\Delta S^{\ddagger}}{R} \exp \frac{-\Delta H^{\ddagger}}{RT} \qquad (18)$$

The measured activation energies ($\Delta H^{\ddagger}$) correlate with the rate of polymerization. The weaker the NO-C bond the faster the polymerization rate. The observed $\Delta H^{\ddagger}$ is given by

$$\Delta H^{\ddagger} = \Delta H^{\ddagger}_{k\text{-}L} + \Delta H^{\ddagger}_{kt} - \Delta H^{\ddagger}_{kL} \qquad (19)$$

where $\Delta H^{\ddagger}_{k\text{-}L}$, $\Delta H^{\ddagger}_{kt}$ and $\Delta H^{\ddagger}_{kL}$ are the activation energies and where k_{-L} is the measured rate constant of NO-C bond breaking reaction, k_L is essentially diffusion controlled and the activation energies in free radical polymerization are very small, $\Delta H^{\ddagger}_{kL} \approx 4$ kJ/mol. The maximum value of $\Delta H^{\ddagger}_{kt}$ is equal to the activation energy for k_{to} or $\Delta H^{\ddagger}_{kt} = 14.5$ kJ/mol which is reasonably low and can be ignored. As a consequence, $\Delta H^{\ddagger} \approx \Delta H^{\ddagger}_{k\text{-}L}$. The enthalpy of activation for the C-O bond breaking reaction in BST was $\Delta H^{\ddagger} = 130 \pm 4$ kJ/mol and in BSP the $\Delta H^{\ddagger} = 113 \pm 4$ kJ/mol. Following the kinetic and mechanistic study of Veregin *et al.*[116], Fukuda *et al.*[117] measured the dissociation rate constant k_d, which is related to the homolytic cleavage of the NO-C bond in polystyrene-TEMPO terminated polymer. This was accomplished by adopting a GPC method using BST as a probe and *tert*-butyl peroxide as an initiator. The result was given by the Arrhenius equation where $k_d = A \exp(-E/RT)$ with $A = 3.0 \times 10^{13}$ s^{-1} and E = 124 kJ/mol. The value of E for the polymer is very close to the activation enthalpy ($\Delta H^{\ddagger}$) for BST of 130 ± 4 kJ/mol reported by Veregin *et al.*[116] This approach to determine the strength of the NO-C bond is extended

[117] Goto, A.; Terauchi, T.; Fukuda, T.; Miyamoto, T. *Macromolecules* **1997**, *18*, 673.

to various alkyl or aryl groups on TEMPO to mimic vinyl monomers such as styrenics, acrylates and methacrylates and various alkoxyamine initiators in Chapter 4.

Others have investigated the kinetics of the SFRP process including Catala[118] and Matyjaszewski.[119] Catala claims that the rate of styrene polymerization is independent of the ethylbenzene-di-*tert*-butyl nitroxide adduct (A-T) initiator but the molecular weight of the polymers formed was controlled by the A-T concentration. He concludes, that the adduct does not undergo rapid homolytic cleavage in the temperature range explored (80-100°C).

Other areas where the SFRP process has been applied is the synthesis of water soluble polymers[120] and complex architectural polymers such as block copolymers.[121] To synthesize block copolymers, the A block polymer is prepared which can then be used directly or isolated and put on the shelf until required. When preparing A-B block copolymers, the homopolymer of monomer A capped with the nitroxyl radical is dissolved

---

[118] Catala, J. M.; Bubel, F.; Hammouch, S. O. *Macromolecules* **1995** *28*, 8441. Hammouch, S. O.; Catala, J. M. *Macromol. Rapid Commun.* **1996**, *17*, 149. Hammouch, S. O.; Catala, J. M. *Macromol. Rapid Commun.* **1996**, *17*, 683.

[119] Greszta, D.; Matyjaszewski, K. *Macromolecules* **1996**, *29*, 7661. Greszta, D.; Matyjaszewski, K. *J. Polym. Sci. A. Polym. Chem.* **1997**, *35*, 1857.

[120] Keoshkerian, B.; Georges, M. K.; Boils-Boissier, D. *Macromolecules* **1995**, *28*, 6381. Gabaston, L. I.; Armes, S. P.; Jackson, R. A. *Polym. Prepr. (Am. Chem. Soc. Div. Polym. Chem.)* **1997**, *38(1)*, 719.

[121] Georges, M. K.; Veregin, R. P. N.; Kazmaier, P. M.; Hamer, G. K. *Polym. Prepr. (Am. Chem. Soc. Div. Polym. Chem.)* **1994**, *35(2)*, 582. Keoshkerian, B.; Georges, M. K.; Listigovers, N. *Polym. Prepr. (Am. Chem. Soc. Div. Polym. Chem.)* **1996**, *37(2)*, 406. Listigovers, N. A.; Georges, M. K.; Odell, P. G.; Keoshkerian, B. *Macromolecules* **1996**, *29*, 8992. Kazmaier, P. M.; Daimon, K.; Georges, M. K.; Hamer, G. K.; Veregin, R. P. N. *Macromolecules* **1997**, *30*, 2228. MacLeod, P. J.; Georges, M. K.; Hamer, G. K. Polym. *Mater. Sci. Eng.* **1997**, *76*, 150. Georges, M. K.; Listigovers, N. A. *Polym. Mater. Sci. Eng.* **1997**, *76*, 149. Listigovers, N. A.; Georges, M. K.; Honeyman, C. H. *Polym. Prepr. (Am. Chem. Soc. Div. Polym. Chem.)* **1997**, *38(2)*, 410.

in monomer B. At elevated temperatures of >120°C, the SFRP of monomer B is added onto the A block to produce the desired A-B block copolymer. This is a unique capability of the SFRP process in that homopolymers can be isolated and stored at room temperature without polymer degradation and without loss of macromolecular control that is later required at elevated temperatures to add the second block. The "livingness" or control is rejuvenated at the polymerization temperatures. With ionic polymerizations polymer chain livingness can not be rejuvenated. ^{1}H NMR studies of block copolymers such as polystyrene-*b*-poly(1,3-butadiene)[121] clearly show the transfer of the nitroxide radical from the styryl chain end to the butadiene chain end.

Initiation of the SFRP process can be accomplished by either employing conventional thermally labile initiators such as BPO and AIBN which decompose in the presence of stable nitroxides, or alkoxyamines which are synthesized and isolated prior to polymerization. To control the number of initiating species for the SFR polymerization, nitroxide adducts are used to provide a cleaner and simplified initiating system. Numerous groups have used the alkoxyamine approach. Veregin *et al.*[122] reported the isolation of unimers prepared by radical attack of the benzoyloxy radical on the "tail" of styrene and then trapped by 2,2,6,6-tetramethyl-1-piperidinyloxy or 3-carboxy-2,2,5,5-tetramethyl-2-pyrrolidinyloxy to give the unimers; benzoyloxy-styrene-TEMPO, BST (structure **33**) and

---

[122] Veregin, R. P. N.; Georges, M. K.; Hamer, G. K.; Kazmaier, P. M. *Macromolecules* **1995**, *28*, 4391.

benzoyloxy-styrene-3-carboxy-PROXYL, BSP (structure **34**) respectively. Solomon *et al.*[123] prepared "one-pot" microgels using the initiating adduct **35** to polymerize *tert*-butylstyrene and divinylbenzene at 130°C for 72 hours.

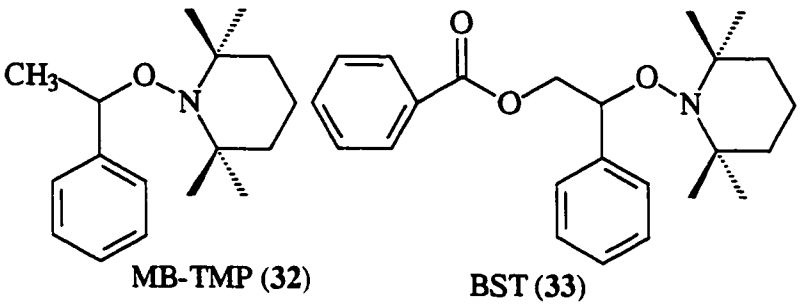

MB-TMP (32)

BST (33)

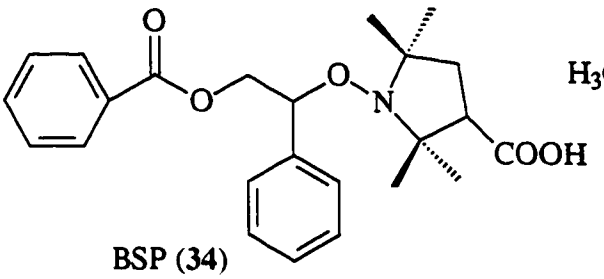

BSP (34)

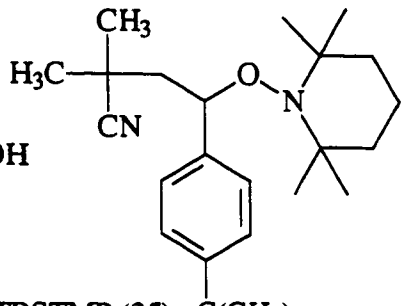

ATBSTMP (35)

Hawker isolated the TEMPO-based initiator BST and used it to initiate an SFR polymerization of styrene and form block copolymers with *p*-acetoxymethylstyrene.[124] Hawker also prepared telechelic polymers[125] and random copolymers[126] of styrene with

---

[123] Abrol, S.; Kambouris, P. A.; Looney, M. G.; Solomon, D. H. *Macromol. Rapid. Commun.* **1997**, *18*, 755.

[124] Hawker, C. J. *J. Am. Chem. Soc.* **1994**, *116*, 11185.

[125] Hawker, C. J.; Carter, K. R.; Hedrick, J. L.; Volksen, W. *Polym. Prepr. (Am. Chem. Soc. Div. Polym. Chem.)* **1995**, *36(2)*, 110. Hawker, C. J.; Hedrick, J. L. *Macromolecules* **1995**, *28*, 2993.

MMA or butyl acrylate by hydrolyzing the benzoyloxy group of **33** with KOH to give the hydroxyl derivative as the initiator prior to polymerization. Priddy *et al.* also used the hydroxyl derivative of **33** to initiate block copolymer[127] synthesis via the SFRP polymerization process. The hydroxyl derivative of BST was also reacted with dendritic fragments having a bromobenzyl group to form an initiating macromolecule for synthesis of dendritic-linear block copolymers of styrene.[128] Three-armed polystyrene star polymers[129], hyperbranched polymers[130] and block copolymers[131] have also been prepared, starting with derivatives of **33**. In each of these applications, BST is isolated and purified from the oligomeric reaction mixture of BPO, styrene and TEMPO at low temperatures to minimize the degree of polymerization. BST is then used as the initiator / reversible terminating agent or further derivatized prior to SFR polymerization.

A third approach to initiating SFR polymerization is to prepare unimolecular nitroxide adducts, alkoxyamines, by a separate synthetic step. Various routes have been

---

[126] Barclay, G. G.; Orellana, A.; Hawker, C. J.; Elce, E.; Dao, J *Polym. Mater. Sci. Eng.* **1996**, *74*, 311. Hawker, C. J.; Elce, E.; Dao, J.; Volksen, W.; Russell, T. P.; Barclay, G. G. *Macromolecules* **1996**, *29*, 2686.

[127] Kobatake, S.; Harwood, H. J.; Quirk, R. P.; Priddy, D. B. *Polym. Prepr. (Am. Chem. Soc. Div. Polym. Chem.)* **1996**, *38(2)*, 664. Kobatake, S.; Harwood, H. J.; Quirk, R. P.; Priddy, D. B. *Macromolecules* **1997**, *30*, 4238. Li, I. Q.; Howell, B. A.; Dineen, M. T.; Priddy, D. B. *Polym. Prepr. (Am. Chem. Soc. Div. Polym. Chem.)* **1997**, *38(1)*, 762. Li. I. Q.; Howell, B. A.; Dineen, M. T.; Kastl, P. E.; Lyons, J. W.; Meunier, D. M.; Smith, P. B.; Priddy, D. B. *Macromolecules* **1997**, *30*, 5195.

[128] Leduc, M. R.; Hawker, C. J.; Dao, J.; Fréchet, J. M. J. *J. Am. Chem. Soc.* **1996**, *118*, 11111.

[129] Hawker, C. J. *Angew. Chem. Int. Ed. Engl.* **1995**, *34*, 1456.

[130] Hawker, C. J.; Fréchet, J. M. J.; Grubbs, R. B.; Dao, J. *J. Am. Chem. Soc.* **1995**, *117*, 10763.

[131] Hawker, C. J.; Hedrick, J. L.; Malmström, E.; Trollsås, M.; Waymouth, R. M.; Stehling, U. M. *Polym. Prepr. (Am. Chem. Soc. Div. Polym. Chem.)* **1997**, *38(2)*, 412.

utilized to do this. Moffat *et al.*[132] have used a low temperature reaction procedure to prepare MB-TMP, **32** and other adducts from the reaction of *tri*-n-butyl tin hydride with alkyl or aryl halides and nitroxides. This work will be discussed in detail in Chapters 4 and 6 of this thesis. Another low temperature procedure was reported by Braslau *et al.*[133] She reported on different synthetic routes to produce carbon radicals that were subsequently trapped by TEMPO, which included PbO_2 with benzylic radicals and alkyl or phenylhydrazines. Also lithium enolates were produced followed by oxidation with $CuCl_2$ and subsequent radical trapping with TEMPO. Hawker has also prepared unimolecular initiators[134] by two other routes. Firstly, benzyl radicals of organometallic reagents were trapped with TEMPO at –78°C. This reaction required 5 molar equivalents of TEMPO at –78°C to obtain reasonable reaction yields of 86%. If the temperature was increased, the yield of the nitroxide adduct decreased significantly. The second route to adduct **32**, first reported by Priddy and Howell,[135] involved the reaction of ethylbenzene with *tert*-butyl peroxide in the presence of TEMPO at the refluxing temperature of ethylbenzene (136°C).

---

[132] Moffat, K. A.; Hamer, G. K.; Georges, M. K.; Kazmaier, P. K.; Stöver, H. D. H. *Polym. Prepr. (Am. Chem. Soc. Div. Polym. Chem.)* **1996**, *37(2)*, 509. MacLeod, P. J.; Georges, M. K.; Quinlan, M.; Moffat, K. A.; Listigovers, N. A. *Polym. Prepr. (Am. Chem. Soc. Div. Polym. Chem.)* **1997**, *38(1)*, 459.

[133] Braslau, R.; Burrill, L. C.; Siano, M.; Naik, N.; Howden, R. K.; Mahal, L. K. *Macromolecules* **1997**, *30*, 6445. Braslau, R.; Burrill, L. C.; Mahal, L. K.; Wedeking, T. *Angew. Chem. Int. Ed. Engl.* **1997**, *36(3)*, 237.

[134] Hawker, C. J.; Barclay, G. G.; Orellana, A.; Dao, J.; Devonport, W. *Macromolecules* **1996**, *29*, 5245.

[135] Li, I.; Howell, B. A.; Ellaboudy, A.; Kastl, P. E.; Priddy, D. B. *Polym. Prepr. (Am. Chem. Soc. Div. Polym. Chem.)* **1995**, *36(1)*, 469. Li, I.; Howell, B. A.; Matyjaszewski, K.; Shigemoto, T.; Smith, P. B.; Priddy, D. B. *Macromolecules* **1995**, *28*, 6692. Howell, B. A.; Priddy, D. B.; Li, I. Q.; Smith, P. B.; Kastl, P. E. *Polym. Bull.* **1996**, *37*, 451.

This unimolecular initiator **32** was used to initiate novel styrenic graft copolymers[136] and block copolymers.[137]

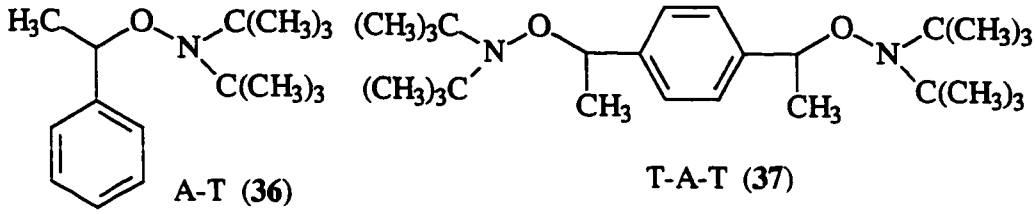

A-T (**36**) T-A-T (**37**)

Catala *et al.*[138] prepared a different adduct (A-T) consisting of ethylbenzene-di-*tert*-butyl nitroxide **36** which was used in their kinetic studies of the SFRP of styrene at 80-100°C. This nitroxide adduct, **36** was prepared[138] in THF by reacting under argon, (1-bromoethyl)benzene with the sodium salt of di-*tert*-butyl nitroxide. Catala *et al.*[139] also prepared the di-initiating nitroxide adduct, T-A-T (**37**) in the same manner and used it to initiate the controlled SFRP of styrene in two directions.

Various small molecule organic synthetic routes have been described to prepare nitroxide adducts. Scaiano[140] has taken a different route and used a photochemical reaction

---

[136] Hawker, C. J.; Barclay, G. G.; Grubbs, R. B.; Fréchet, J. M. J. *Polym. Prepr. (Am. Chem. Soc. Div. Polym. Chem.)* **1996**, *37(2)*, 515. Grubbs, R. B.; Hawker, C. J.; Dao, J.; Fréchet, J. M. J. *Angew. Chem. Int. Ed. Eng.* **1997**, *36*, 270. Mecerreyes, D.; Dubois, P.; Jérôme, R.; Hedrick, J. L.; Hawker, C. J.; Beinat, S.; Schappacher, M.; Deffieux, A. *Polym. Mat. Sci. Eng.* **1997**, *77*, 189. Hawker, C. J.; Mecerreyes, D.; Elce, E.; Dao, J.; Hedrick, J. L.; Barakat, I.; Dubois, P. Jérôme, R.; Volksen, W. *Macromol. Chem. Phys.* **1997**, *198*, 155.

[137] Li, I.; Howell, B. A.; Priddy, D. B.; Smith, P. B. *Polym. Prepr. (Am. Chem. Soc. Div. Polym. Chem.)* **1996**, *37(1)*, 612. Li, I. Q.; Howell, B. A.; Koster, R. A.; Priddy, D. B. *Macromolecules* **1996**, *29*, 8554.

[138] Catala, J.M.; Bubel, F.; Hammouch, S.O. *Macromolecules* **1995**, *28*, 8441. Hammouch, S. O.; Catala, J. M. *Macromol. Rapid Commun.* **1996**, *17*, 683.

[139] Hammouch, S. O.; Catala, J. M. *Macromol. Rapid Commun.* **1996**, *17*, 149.

[140] Connolly, T. J.; Baldoví, M. V.; Mohtat, N.; Scaiano, J. C. *Tet. Lett.* **1996**, *37*, 4919. Baldoví, M. V.; Mohtat, N. Scaiano, J. C. *Macromolecules* **1996**, *29*, 5497.

to synthesize similar nitroxide adducts. In the presence of light (300 nm), *tert*-butyloxy radicals were generated from the di-*tert*-butyl peroxide initiator that abstracts a hydrogen radical from the solvent (toluene, ethylbenzene, propylbenzene or cumene) to produce carbon-centered radicals that are trapped by TEMPO. The nitroxide adducts are produced in very high yield >90%. This synthetic approach works well to prepare aryloxy-nitroxide adducts of TEMPO but extending this route to the synthesis of acrylate or methacrylate ester derivatives of MB-TMP such as *N*-(methyl-iso-propionate-2-oxy)-2,2,6,6-tetramethylpiperidine, MiP-TMP and *N*-(ethyl-iso-butyrate-2-oxy)-2,2,6,6-piperidine, EiB-TMP is more challenging and has not been demonstrated.

Since the invention of stable free radical polymerization using TEMPO as the reversible terminating agent, others working in this field have been actively searching for better nitroxides that enable faster polymerizations at lower temperatures. Puts and Sogah[141] synthesized an asymmetric nitroxide, 2,5-dimethyl-2,5-diphenylpyrrolidin-1-oxyl (DDPO) and evaluated it in the bulk SFRP of styrene. At 130°C the bulk polymerization of styrene with [nitroxide]/[BPO] of 1.3 was evaluated. DDPO gave a faster polymerization compared to TEMPO with observed rate constants of $k_{obs} = 4.6 \times 10^{-3}$ and 2.4×10^{-3} s^{-1} for DDPO and TEMPO respectively but the polydispersity index (PDI) was lower with TEMPO. At a lower polymerization temperature of 90°C, molecular weights were low (Mn=9500), polydispersity broader (DPS= 1.95) and monomer conversion to polymer was only 32%. These polymerization data at 90°C do not illustrate a controlled "living" SFR

polymerization. The linear increase in Mn as a function of monomer conversion to an appreciable molecular weight value was not demonstrated at 90°C. The polydispersity of 1.95 is quite high for a "living" radical polymerization. These molecular properties have yet to be illustrated to prove that this asymmetric nitroxide (DDPO) is a significantly better nitroxide than TEMPO.

Matyjaszewski *et al.*[105b, 108] studied the effect of adding a phosphonic acid group to the 4-position of TEMPO and observed a faster rate of polymerization when compared to TEMPO and 4-hydroxy-TEMPO. They hypothesized that hydrogen bonding of the acidic proton to the nucleophilic oxygen of the nitroxyl group aided in promoting homolytic cleavage of the C-O bond. Other groups interpret these results as follows. The acid group can reacted with free nitroxide to keep the amount of excess nitroxide low by decomposing the free nitroxide. By maintaining a low level of free nitroxide, this enables a faster rate of polymerization.

Other nitroxide radicals have recently been prepared and evaluated in the SFRP of styrene that contained phosphonyl groups. Nitroxyl radicals **38** to **40** which contain a hydrogen atom on the α–carbon to the nitroxyl group were synthesized by Grimaldi, Finet *et al.*[142]. Employing AIBN as the initiator, molar ratios of [nitroxide]/[AIBN] of 2.5 to 5.0 were required to demonstrate linear kinetic plots of ln([M]o/[M]) vs time and a linear

---

[141] Puts, R. D.; Sogah, D. Y. *Macromolecules* **1996**, *29*, 3323.

[142] Grimaldi, S.; Finet, J-P.; Zeghdaoui, A.; Tordo, P.; Benoit, D.; Gnanou, Y.; Fontanille, M.; Nicol, P.; Pierson, J-F. *Polym. Prepr. (Am. Chem. Soc. Div. Polym. Chem.)* **1997**, *38(1)*, 651. Benoit, D.; Grimaldi, S.; Finet, J-P.; Tordo, P.; Fontanille, M.; Gnanou, Y. *Polym. Prepr. (Am. Chem. Soc. Div. Polym. Chem.)* **1997**, *38(1)*, 729.

increase in Mn as a function of monomer conversion. The molar ratio of nitroxide to initiator is very high, which is indicative of nitroxide decomposition at elevated temperatures due to the hydrogen atom present on the α-carbon to the nitroxyl group. The other possible explanation for why such a large excess of nitroxide is required to demonstrate a controlled polymerization, is that the initiator is extremely efficient but this does not seem too likely. These results are somewhat inconclusive and require further study.

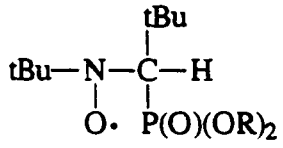

38 R = Et
39 R = $CH_2C_6H_5$

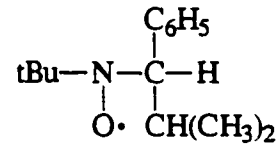

40

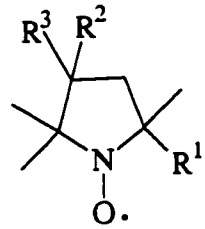

41 $R^1 = CH_3$, $R^2 = R^3 = H$
42 $R^1 = C_6H_5$, $R^2 = R^3 = H$
43 $R^1 = C_6H_5$, $R^2 = H$, $R^3 = CH_3$
44 $R^2 = C_6H_5$, $R^2 = R^3 = CH_3$

Yoshida *et al.* have employed 4-methoxy-TEMPO and 4-hydroxyl-TEMPO as the reversible capping agents in the SFR polymerization of styrene[143], *p*-bromostyrene[144] and chlorostyrenes[145] initiated with BPO. In addition, five-membered pyrrolidinyloxyl nitroxides (**41-44**) were synthesized and evaluated in the SFRP of styrene at 110°C and

---

[143] Yoshida, E.; Okada, Y. *Bull. Chem. Soc. Jpn.* **1997**, *70*, 275. Yoshida, E.; Okada, Y. *J. Polym. Sci. Part A: Polym. Chem.* **1996**, *34*, 3631. Yoshida, E.; Tanimoto, S. *Macromolecules* **1997**, *30*, 4018. Yoshida, E.; Sugita, A. *Macromolecules* **1996**, *29*, 6422.

[144] Yoshida, E. *J. Polym. Sci. Part A: Polym. Chem.* **1996**, *34*, 2937.

compared to TEMPO.[146] Increasing the steric hindrance at the α-carbon to the nitroxyl group from 5,5-dimethyl to 5-methyl-5-phenyl, produced broader molecular weight distributions in the 1.73-1.79 range. One explanation for this broader MWD is that radical trapping by the more hindered nitroxide **42** is slower, rendering higher concentrations of propagating radicals that can prematurely terminate bimolecularly. Slower trapping rates of propagating radicals inherently give broader PD values because PD is determined by the rate constant of termination relative to the rate constant of propagation.

The stable free radical polymerization process was applied to radical ring-opening polymerization of a cyclic ketene acetal.[147] This is an interesting area of study because functional groups such as esters, amides and carbonates can be incorporated into the polymer backbone. Wei *et al.* demonstrated the SFRP of 2-methylene-1,3-dioxepane in the presence of TEMPO and di-*tert*-butyl peroxide (DTBP) as initiator. The optimum molar ratio of [TEMPO]/[DTBP] was 1.6 to give polydispersity as low as 1.2 but Mn values were <10,000.

1.7 Atom Transfer Radical Polymerization (ATRP)

Matyjaszewski's initial system employed to prepare living polymers via a radical mechanism was the polymerization of vinyl acetate (Vac) initiated by triisobutylaluminum

---

[145] Yoshida, E.; Fujii, T. *J. Polym. Sci. Part A: Polym. Chem.* **1997**, *35*, 2371.

[146] Yamada, B.; Miura, Y.; Nobukane, Y.; Aota, M. *Polym. Prepr. (Am. Chem. Soc. Div. Polym. Chem.)* **1997**, *38(1)*, 725.

($Al(iBu)_3$) complexed with a bidentate nitrogen ligand, 2,2'-bipyridyl (bpy) and activated with a stable nitroxyl radical, 2,2,6,6-tetramethylpiperidin-1-oxyl (TEMPO).[107], [148] Typical composition of the initiating system was 1:1:2 of Al:bpy:TEMPO. This process was difficult to control and the polymerization process was not always reproducible. This was partially due to the aging factor of the initiator and sensitivity of the initiating system to O_2 and moisture.

In 1995 Matyjaszewski reported[149] a second living radical polymerization process, atom transfer radical polymerization, ATRP, based on the organic reaction of atom transfer radical addition. ATRP has its roots in organic chemistry's atom transfer radical addition[150] (ATRA), which is also called Kharasch addition.[151] The ATRP process involves the reaction of an alkyl halide such as 1-phenylethyl chloride, 1-PECl, as the initiator, with monomer and a transition-metal halide, CuCl, which complexes with 2,2-bipyridine (bpy). Bpy behaves as the chlorine atom transfer promoter to enable initiation of the polymerization of styrene at 130°C. The reported Mn (8,000) increased linearly with monomer conversion to 95% and the molecular weight distribution was reasonably narrow (Mw/Mn = 1.30-1.45). The mechanism of the ATRP[149] process is illustrated in Scheme 16. This process involves the activation and deactivation of a propagating chain end as a result

---

[147] Wei, Y.; Connors, E. J.; Jia, X.; Wang, B.; Deng, C. *Polym. Prepr. (Am. Chem. Soc. Div. Polym. Chem.)* **1995**, *36(2)*, 241. Wei, Y.; Connors, E. J.; Jia, X.; Wang, B. *Chem. Mater.* 1996, *8*, 604.

[148] Mardare, D.; Matyjaszewski, K. *Macromolecules* **1994**, *27*, 645.

[149] Wang, J-S.; Matyjaszewski, K. *J. Am. Chem. Soc.* **1995**, *117*, 5614.

[150] Curran, D. P. *Synthesis* **1988**, 489. Bellus, D. *Pure Appl. Chem.* **1985**, *57*, 1827.

[151] Kharasch, M. S.; Jensen, E. V.; Urry, W. H. *Science* **1944**, *102*, 128.

of the reversible atom transfer reaction between a $Cu^{I}X/Cu^{II}X_2$ metal salt and alkyl halide promoted by a solubilizing ligand, 2,2′-bipyridyl.

Initiation:

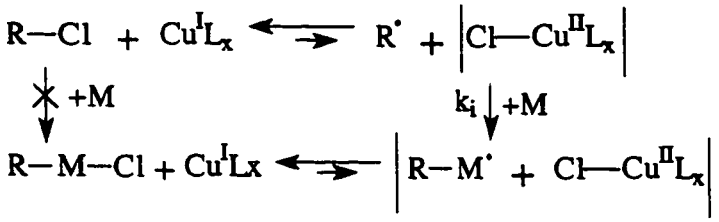

Propagation:

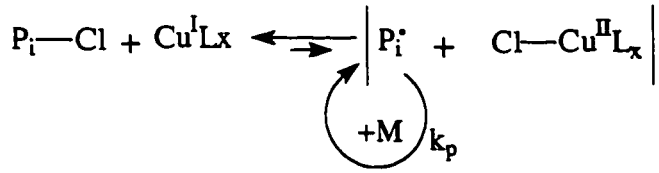

Scheme 16: Atom Transfer Radical Polymerization, ATRP

The process was extended to polymerize styrene, MA, BuA and MMA[152] using different alkyl halides[153] combined with $Cu^{I}X$/bpy, X = Cl or Br. In this particular system, the Cu-bpy complex was only slightly soluble in the reaction medium. Thus, ATRP proceeded in a heterogeneous system, limiting the polydispersity. The polymerization temperatures generally used for bulk and solution ATRP ranged from 90 to 130°C. In an attempt to make ATRP a homogeneous polymerization, longer aliphatic solubilizing chains: 4,4′-di-*t*-butyl, 4,4′-di-*n*-heptyl and 4,4′-di-(5-nonyl)-2,2'-dipyridyl were added as

---

[152] Grimaud, T.; Matyjaszewski, K. *Macromolecules* **1997**, *30*, 2216.

[153] Wang, J-S.; Matyjaszewski, K. *Macromolecules* **1995**, *28*, 7901.

bipyridyl ligands to enhance the solubility of the Cu-bpy complex.[154] This decreased the polydispersity of the resulting polymers while maintaining the linear increase in Mn as a function of monomer conversion. This process has been used to prepare hyperbranched polymers[155] of chloromethylstyrene (CMS) in the presence of Cu^{I} and 2,2′-bipyridyl and branched copolymers of CMS with styrene.

Prior to Matyjaszewski's first report on ATRP[149], Sawamoto *et al.*[156] published a paper on the new living polymerization of methyl methacrylate with CCl_4 / dichlorotris(triphenylphosphine)ruthenium (II) $[RuCl_2(PPh)_3]_3$ and methylaluminum bis(2,6-di-*tert*-butylphenoxide) $[MeAl(ODBP)_2]$as a new initiating system for a novel living radical polymerization. This is similar to the ATRP process except ruthenium was used instead of copper. Sawamoto called this process transition metal-catalyzed radical polymerization. Other initiators[157] such as 1,1,1-trichloroacetone (CCl_3COCH_3), α,α-dichloroacetophenone ($CHCl_2COC_6H_5$)[157, 158] and ethyl 2-bromoisobutyrate $[(CH_3)_2CBrCO_2C_2H_5]$ and aluminum compounds[157] such as aluminum triisopropoxide $[Al(OiPr)_3]$ were also evaluated to polymerize MMA. The polymerization reactions were carried out in toluene at 80°C but 60-80 hours were required for 90% conversion. This radical process involves a reversible homolytic cleavage of the carbon-halide bond

---

[154] Patten, T. E.; Xia, J.; Abernathy, T.; Matyjaszewski, K. *Science* **1996**, *272*, 866.

[155] Gaynor, S. G.; Edelman, S.; Matyjaszewski, K. *Macromolecules* **1996**, *29*, 1079.

[156] Kato, M.; Kamigaito, M.; Sawamoto, M.; Higashimura, T. *Macromolecules* **1995**, *28*, 1721.

[157] Ando, T.; Kato, M.; Kamigaito, M.; Sawamoto, M. *Macromolecules* **1996**, *29*, 1070.

[158] Nishikawa, T.; Ando, T.; Kamigaito, M.; Sawamoto, M. *Macromolecules* **1997**, *30*, 2244.

activated by $RuCl_2(PPh_3)_3$ as a redox activator. In a similar manner to the ATRP process, controlled molecular weights with narrow polydispersities were obtained.

Both Sawamoto[159] and Percec[160], [161] have employed sulfonyl chlorides (RSO_2Cl) as new initiators for the living radical polymerization of MMA[159] in solution with $RuCl_2(PPh_3)_3$ or bulk polymerization of styrene[160], [161] with Cu^ICl/bipy. With sulfonyl chlorides as initiators, the polymers produced have slightly broader polydispersities of 1.3 to 1.5 and the rate of initiation was slower, but the α-end of the polymers were functionalized. More recently Sawamoto[162] employed an iron(II)chloride complex $FeCl_2(PPh_3)_3$, without the aluminum accelerator compound $Al(O\textit{i}Pr)_3$, in the presence of an initiator to polymerize MMA in a controlled fashion.

Similar to the stable free radical polymerization process, both ATRP and transition metal-catalyzed radical polymerization require a low stationary concentration of propagating radicals, $M_n\bullet$. These propagating radicals are in a fast equilibrium with the dormant species Mn-X, where X is a radical molecule. This also provides a sufficiently high overall concentration of growing chains, both active and dormant, and minimizes the rate of bimolecular termination.

---

[159] Matsuyama, M.; Kamigaito, M.; Sawamoto, M. *J. Polym. Sci. Part A: Polym. Chem.* **1996**, *34*, 3585.

[160] Percec, V.; Barboiu, B. *Macromolecules* **1995**, *28*, 7970.

[161] Percec, V.; Barboiu, B.; Neumann, A.; Ronda, J. C.; Zhao, M. *Macromolecules* **1996**, *29*, 3665.

[162] Ando, T.; Kamigaito, M.; Sawamoto, M. *Macromolecules* **1997**, *30*, 4507.

1.8 Objectives of This Research

With the development of the SFRP process and later the ATRP process, controlled molecular weight polymers with narrow molecular weight distributions are now a reality. Utilizing these free radical polymerization processes has enabled advanced architectural polymers such as blocks, grafts, hyperbranched, multi-armed stars and dendritic copolymers to be prepared. In both systems, control over the polymerization requires a rapid initiation of all the propagating chains and a low stationary concentration of growing radicals, $P_n^{\bullet}$, which are in a fast dynamic equilibrium with the dormant species, P_n-T (X). Under these conditions, the contribution of bimolecular termination is dramatically reduced. In addition, radical processes offer the advantages of being applicable to polymerize a wide variety of commercial monomers that can not be polymerized by living ionic methods.

To understand the fundamental chemistry of the SFRP process and, more specifically, the reactivity of the key C-O bond has been the goal of this research project. To achieve this goal, this research has focused on utilizing model initiator / reversible terminating agents to probe into the C-O bond. The objectives are summarized below:

1. To investigate the usefulness of semi-empirical molecular orbital calculations to identify stable nitroxyl radicals for the SFRP process which will have a weaker C-ON bond. If these methods are not appropriate, then determine where these methods breakdown and what parameters in the Hamiltonian equations (AM1 and PM3) are faulty.

2. To synthesize, characterize and evaluate a series of model initiator / reversible terminating agents that mimic both polymerizable monomers and different carbon-centered initiating radicals. In this series of nitroxide adducts, determine what effect changing the alkyloxy or aryloxy group has on the strength of the C-ON bond.
3. Since the SFRP process is not completely void of bimolecular termination reactions, using the nitoxide adducts identify the possible termination reactions for this process.
4. To evaluate some of the model initiator / reversible terminating agents to initiate a stable free radical polymerization which included demonstrating narrow polydispersity and a linear increase in Mn as a function of monomer conversion and time.

Chapter 2

Experimental Methods and Synthesis

2.1 Experimental Methods and Instrumentation

Analytical TLC was performed on commercially available 1 inch x 3 inch Whatman TLC plates coated with MK6F silica gel 60Å (250 µm thick). Detection of the components was done using a Spectroline Model CM-10 Fluorescence Analysis Cabinet at 254 nm. The silica gel used for flash chromatography was Merck silica gel grade 9385, 230-400 mesh, 60Å. Size exclusion chromatography (SEC) also called gel permeation chromatography (GPC) was performed on a Hewlett Packard 1090 LC equipped with HP 1047A refractive index detector and a series of PLgel 5 μm columns; (Mixed-C, 10^4Å, 10^3Å, 500Å and 100 Å). The GPC system was calibrated with a series of narrow polystyrene standards ranging in molecular weight from 2.1 million to 517 daltons. The solvent used was tetrahydrofuran. The conversion of monomer to polymer was determined by gas chromatography (GC) from the eluted peak areas and referenced internally to acetone. This was performed on a Hewlett Packard Gas Chromatograph 5890 equipped with a packed Carbowax column.

Transmission infrared spectra were recorded at 4 cm^{-1} resolution on a Nicolet Magna Series II 550 FT-IR using a CsI beamsplitter and DTGS detector. The nitroxides were dispersed in KBr powder and pressed into standard infrared discs for analysis.

^1H NMR spectra were recorded in $CDCl_3$ solution on either a 400 MHz Bruker AMX400 or a 300 MHz Bruker Avance DPX300 spectrometer. The ^1H NMR spectra were referenced internally to tetramethylsilane at 0.0 ppm. The sample temperature was controlled using a Bruker BVT-1000 temperature controller. ^{13}C NMR J-modulated spin-echo spectra were also recorded at either 100.6 MHz or 75.4 MHz using the 400 MHz or 300 MHz Bruker spectrometers and internally referenced to $CDCl_3$ at 77.0 ppm.

ESR spectra were collected using a Bruker ESP300 spectrometer and ER4111 variable temperature accessory. The spin purity and hyperfine coupling constant, a_N of each synthesized nitroxide was measured on the ESR spectrometer. Preparation of nitroxide samples for this evaluation involved dissolving a known weight of nitroxide (<10 mg) in 10 mL of toluene in a 10 mL volumetric flask. Then 80-85 mg of the nitroxide solution was added into a thin walled ESR tube. The ESR spectrometer was calibrated with strong pitch green reference at 300K. The ESR tube containing the sample was inserted into the cavity at 300K and the concentration of the nitroxide in toluene was measured from the double integrated area of the ESR spectrum. After correcting for changes in the green pitch reference, volume differences between the synthesized nitroxide in solution and the external standard of TEMPO (100% spin purity) and mass of nitroxide, the spin purity and a_N was determined. The hyperfine coupling constant, a_N was measured directly from the

spectrum. The difference, in Gauss, between the peak maximum position or peak minimum of two adjacent peaks was measured. A total of six values were obtained. The numbers were averaged and errors determined to give the reported values.

Chemical ionization (CI) mass spectrometry utilizing ammonia (NH_3) as the reagent gas and electron impact ionization (EI) mass spectra were recorded on a Finnigan 4500 quadrupole mass spectrometer. Typical source conditions for electron impact ionization include: source temperature of 190°C, source pressure of 1 x 10^{-7} mbar, unit mass resolution across the whole mass range (1000 daltons) and electron energy = 70 eV. All parameters are the same for CI except for the source pressure, which is normally in the range of 2-4x10^{-5} mbar of NH_3. Mass spectra were recorded as percent intensity versus mass/charge ratio.

2.2 Synthesis of Nitroxide Radicals

2.2.1 4-Benzoyloxy-2,2,6,6-tetramethylpiperidinyl-1-oxyl (**45**)

The synthetic procedure reported by Rozantsev *et al.*[1] was used as a starting point to prepare **45**.

4-Hydroxy-TEMPO (5.0 g, 0.029 mol) and 4-dimethylaminopyridine (4-DMAP, 4.0 g, 0.033 mol) were dissolved in 80 mL CH_2Cl_2 in a 250 mL beaker. The beaker was cooled in an ice water bath and benzoic anhydride (6.78 g, 0.03 mol) dissolved in 60 mL

[1] Rozantsev, E. G., Free Nitroxyl Radicals., Hazzard, B. J. (Ed.), Plenum Press, New York, 1970, pg.216.

CH_2Cl_2 was added dropwise with agitation over a 15 minute period. The reaction mixture was gradually warmed to room temperature and stirred for 8 hours. The reaction was monitored by FT-IR with an ATR deep immersion probe in the reaction mixture. After the reaction was complete, the majority of the CH_2Cl_2 was removed using a rotary-evaporator. The concentrated 4-benzoyloxy-TEMPO nitroxide mixture was dissolved in diethyl ether resulting in precipitation of the 4-DMAP benzoate salt. The salt was removed by filtration. The Et_2O layer was washed with water (3 X 300 mL) to remove any residual salt and then dried over $MgSO_4$. During slow evaporation of diethyl ether in the fumehood, red needle-like crystals formed. The crystals, 4-benzoyloxy-TEMPO were dried *in vacuo*. Yield: 5.92 g (0.021 mol, 74%); mp: 105-108°C (lit.[1] 105°C); spin purity of 4-benzoyloxy-TEMPO was measured by ESR using the procedure outlined in Section 2.1 to give a spin purity of 94%; hyperfine coupling constant, a_N = 15.36 G; υ_{max} (KBr) 2980, 2939, 1715, 1317, 1282, 1242, 1178, 1117, 1071 and 713 cm^{-1}.

2.2.2 1,1,3,3-Tetraalkylisoindolin-2-yloxyl

A four step synthesis similar to that given in the literature[2] was used to prepare 1,1,3,3-tetramethyl- and 1,1,3,3-tetraethylisoindolin-2-yloxyl.

---

[2] Griffiths, P. G.; Moad, G.; Rizzardo, E.; Solomon, D. H. *Aust. J. Chem.* **1983**, *36*, 397.

2.2.2.1 N-Benzylphthalimide[3] (**46**)

Into a 500 mL three neck round bottom flask equipped with a reflux condenser and magnetic stirrer were added glacial acetic acid (250 mL), benzylamine (69.0 g, 0.644 mol) and phthalic anhydride (60.2 g, 0.406 mol). The mixture was heated at reflux for 4 hours. The reaction mixture was cooled to room temperature and added to near boiling distilled water (2.5 L) to crystallize the *N*-benzylphthalimide. The solution was cooled, washed and compound **46** was isolated by vacuum filtration. The crude product, **46** was subsequently dissolved in hot glacial acetic acid (200 mL) and crystallized from hot distilled water (3 L). The slurry was stirred overnight at room temperature, filtered and dried overnight *in vacuo* at 60°C. Yield: 89.9%; mp: 114-116°C (literature[3], 116°C); ^{1}H NMR ($CDCl_3$/TMS) [400 MHz]: δ 4.85 (s, 2H, CH_2 of N-benzyl), 7.26-7.44 (m, 5H, H-aryl of N-benzyl), 7.68-7.85 (2 dd, 4H, ArH of phthalimide); ^{13}C NMR [100.6 MHz] ($CDCl_3$): δ 41.58 (CH_2), 127.79 (benzyl C4), 123.31, 128.58, 128.65, 133.95 (4 peaks 8C, 4 aromatic C of phthalimide and 4 aromatic C of benzyl), 132.11 (quaternary C of benzyl), 136.34 (2 quaternary C of phthalimide), 168.0 (C(O)).

2.2.2.1 N-Benzyl-1,1,3,3-tetramethylisoindoline (**47**)

Slight modifications to the Grignard reaction were made to the procedure reported by Griffiths *et al.*[2]

---

[3] Vanags, G. *Latv. Univ. Rakstim Kim. Fak. Ser.* **1939**, *4*, 405; *Chem. Abstr.* **1940**, *34*, 1982.

A solution of methyl Grignard reagent was prepared under an argon atmosphere from methyl iodide (114.58 g, 0.807 mol) and activated magnesium turnings (20.65 g, 0.85 mol) in diethyl ether (300 mL) at 10°C. The magnesium surface was cleaned using 1N aqueous HCl (70 mL), rinsed with water, methanol and diethyl ether. Diethyl ether was placed over 4Å molecular sieves. The reaction vessel, 500 mL 3 neck round bottom flask was equipped with a magnetic stirrer, reflux condenser, argon inlet and a 60 mL dropping funnel containing methyl iodide. The methyl iodide was added dropwise into the magnesium turnings in Et_2O. After the formation of the methyl Grignard reagent was complete, the condenser was replaced with a distillation apparatus containing a thermometer. The solution was concentrated by slow distillation of ether until the internal vapour temperature reached 70°C. A solution of *N*-benzylphthalimide (20 g, 84.9 mmol) dissolved in 300 mL of toluene (dried over NaH and distilled) was added dropwise at such a rate as to maintain the internal temperature between 60°C and 70°C. After the addition was complete, the temperature was slowly increased to distill off the remaining diethyl ether. Once the internal reaction temperature reached approximately 110°C, the distillation apparatus was changed to the reflux set-up and the reaction was left to reflux overnight (13 hours). The final volume of the reaction mixture was 350 mL.

The solution was further concentrated by distillation to approximately 200 mL and cooled. Hexane (300 mL) was added to the mixture. The yellow solution was filtered through Celite under reduced pressure and rinsed with hexane (3 X 300 mL). Upon exposure to air the solution turned purple. It was left to stir in a wide mouth flask for 2

hours. The solution was filtered again through Celite under reduced pressure to yield a clear yellow filtrate. It was concentrated on a rotary evaporator to produce a dark brown oil. The brown oil was purified on a column of basic alumina (activity 1, 70 g) using CH_2Cl_2 as the eluting solvent. The product was subsequently loaded onto a silica gel column (8 cm by 45 cm) using silica gel (Merck, grade 9385, 230-400 mesh, 60Å, 200 g) and eluting with a hexane / CH_2Cl_2 (4%/96%) solvent system. A yellow oil was collected which crystallized out of methanol to yield white crystals, 5.3 g at a 24% yield, mp: 62-64°C. This was identified as pure *N*-benzyl-1,1,3,3-tetramethylisoindoline, **47** by ^1H NMR ($CDCl_3$/TMS) [400 MHz]: δ 1.30 (s, 12H, CH_3), 3.97 (s, 2H, CH_2), 7.11-7.45 (m, 9H, ArH); ^{13}C NMR ($CDCl_3$) [100.6 MHz]: δ 28.39 (CH_3), 46.23 (CH_2), 65.18 ($C(CH_3)_2$), 121.30, 126.75, 127.90, 128.31 (4 peaks 8C, 4 aromatic C of isoindoline and 4 aromatic C of benzyl), 126.39 (*p*-benzyl C), 143.44 (quaternary C of benzyl), 147.86 (2 quaternary C of isoindoline).

2.2.2.3 1,1,3,3-Tetramethylisoindoline[2] (**48**)

A solution of *N*-benzyl-1,1,3,3-tetramethylisoindoline (1.55 g, 5.85 mmol) in 200 mL of glacial acetic acid and 1.0 g of 5% Pd/C was added into a stainless steel 2L Buchi reactor equipped with a mechanical stirrer. The reactor was pressurized with H_2 gas to 60 psi for 4 hours at an internal temperature of 29°C. The suspension was filtered under reduced pressure through a packed layer of Celite. The filtrate was diluted with 100 mL H_2O, neutralized with 10% NaOH and then made basic to pH 9. Using Et_2O, the product

was extracted into the organic layer from the basic solution (3 X 150 mL). The organic phase was washed 3X with brine solution and H_2O, dried over $MgSO_4$ and concentrated using a rotary evaporator to produce a pale yellow oil, compound **48** (1.02 g, 5.83 mmol, 99%). This compound showed ^1H NMR ($CDCl_3$/TMS) [300 MHz]: δ 1.45 (s, 12H,CH_3), 4.80 (s, 1H, NH), 7.09-7.25 (2 dd, 4H, ArH of isoindoline); ^{13}C NMR ($CDCl_3$) [75 MHz]: δ 31.72 (CH_3), 62.60 ($C(CH_3)_2$), 121.23, 126.93 (aromatic CH), 148.48 (quaternary aromatic C).

2.2.2.4 1,1,3,3-Tetramethylisoindoline-2-oxyl (**49**)

The oxidation of **48** was followed according to the procedure developed by Rauckman *et al.*[4] and also used by Griffiths *et al.*[2]

To a solution of 1,1,3,3-tetramethylisoindoline (1.02 g, 5.83 mmol) in methanol (30 mL) and acetonitrile (25 mL) was added sodium hydrogen carbonate (1.26 g, 15 mmol), sodium tungstate dihydrate (0.18 g, 0.55 mmol) and 30% aqueous hydrogen peroxide (7 mL, 62 mmol). The suspension was stirred at room temperature for 43 hours producing a bright yellow solution. The solution was diluted with distilled water and extracted into hexane (3 X 50 mL), which was washed with brine and water. The solvent was removed by rotary evaporation to produce yellow crystals. Yield was 1.01 g, 5.3 mmol, 91%, mp: 127-128°C, (lit.[2], mp: 128-129°C). Spin purity of this nitroxide as measured by ESR was 94%; a_N = 13.98G: υ_{max} (KBr) 2976, 2928, 1484, 1452, 1374, 1357,1168, 1121, 762 cm^{-1}.

---

[4] Rauckman, E. J.; Rosen, G. M.; Abou-Donia, M. B. *Syn. Comm.* **1975**, *5(6)*, 409.

2.2.2.5 N-Benzyl-1,1,3,3-tetraethylisoindoline (**50**)

The synthetic procedure used to prepare compound **50** was similar to the procedure used to prepare compound **47** except the alkyl halide used was iodoethane (40 mL, 0.5 mol). Iodoethane was added dropwise to a solution of activated Mg (9.75 g, 0.4 mol) in dried Et_2O to form the ethyl Grignard reagent. After concentration of the Grignard reagent, *N*-benzylphthalimide (19.0 g, 0.08 mol) dissolved in dried toluene (200 mL) was added dropwise. The remaining portion of the synthesis as outlined in section 2.2.2.2 was followed. A total of 2.7 g, 8.4 mmol, of compound **50** was isolated with 10.5 % yield. This compound showed: ^{1}H NMR ($CDCl_3$/TMS) [300 MHz]: δ 0.76 (triplet, J = 7 Hz, 12H, CH_3), 1.46-1.58, 1.85-1.97 (dm, 8H, CH_2CH_3), 4.00 (s, 2H, CH_2Ph), 7.02-7.20 (2 dd, 4H, ArH of isoindoline), 7.22-7.45 (m, 5H, ArH of phenyl): ^{13}C NMR ($CDCl_3$) [75 HMz]: δ 9.57 (CH_2CH_3), 30.32 (CH_2CH_3), 46.71 (CH_2Ph), 71.26 ($C(CH_2CH_3)_2$), 123.38-127.30 (9C, aromatic CH), 142.37 (quaternary phenyl C), 144.53 (2 quaternary C of isoindoline).

2.2.2.6 1,1,3,3-Tetraethylisoindoline (**51**)

The synthetic procedure used to perform the hydrogenolysis reaction of compound **50** to yield 1,1,3,3-tetraethylisoindoline was identical to the reaction used to prepare the tetramethyl derivative, compound **48**, see section 2.2.2.3. Starting with 2.7 g, 8.4 mmol of N-benzyl-1,1,3,3-tetraethylisoindoline yielded 1.66 g, 7.2 mmol of 1,1,3,3-tetraethylisoindoline, a reaction yield of 85%. This compound showed: ^{1}H NMR

($CDCl_3$/TMS) [300 MHz]: δ 0.87 (triplet, J = 7 Hz, 12H, CH_3), 1.61-1.81 (m, 8H, CH_2CH_3), 2.24 (s, NH), 7.04-7.22 (2 dd, ArH of isoindoline); ^{13}C NMR ($CDCl_3$) [75 MHz]: 8.85 (CH_2CH_3), 33.67 (CH_2CH_3), 68.34 ($C(CH_2CH_3)_2$), 122.41, 126.50 (aromatic CH), 147.30 (fused ring aromatic C).

2.2.2.7 1,1,3,3-Tetraethylisoindoline-2-oxyl (**52**)

The oxidation reaction of **51** was performed following the general literature[2, 4] procedure given for the oxidation of the analogous tetramethylisoindoline nitroxide, compound **49** reported in section 2.2.2.4. Oxidation of compound **51** (1.65 g, 7.2 mmol) produced 1.7 g, 6.9 mmol of the corresponding nitroxide **52** with a yield of 96%. The spin purity of nitroxide **52** was 90% and a_N = 13.73 G; υ_{max} (KBr) 2968, 2937, 1755, 1668, 1461, 1378, 756 cm^{-1}.

2.3 Synthesis and Isolation of Benzoyloxy-Styrene-TEMPO, **33**, *(BST)*

Into a 1 litre three neck round bottom flask equipped with a mechanical stirrer were added styrene monomer (600 mL, 5.24 mol), benzoyl peroxide (10 g, 0.041 mol) and 2,2,6,6-tetramethylpiperidine-1-oxyl, TEMPO (6.75 g, 0.043 mol). All of the reagents were added at room temperature and then the flask was placed into a preheated oil bath set to 135°C for five to seven minutes. The excess styrene monomer was evaporated off in the fumehood followed by passing the concentrated mixture through a silica gel column eluting with 10% hexane / 90% CH_2Cl_2. The BST containing fractions were combined and passed

through a second column eluting with pure CH_2Cl_2. The yield of BST was 3.7 g, 23.7 %. This compound showed: ^{1}H NMR ($CDCl_3$/TMS) [300 MHz]: δ 0.67, 0.98, 1.12, 1.29 (4s, 12H, CH_3), 1.18-1.42 (m, 6H, CH_2), 4.44, (dd, 1H, $CH_2CH(C_6H_5)$), 4.75, (dd, 1H, $OCH_aH_bCH(C_6H_5)$), 4.98 (overlapping dd, 1H, $OCH_aH_bCH(C_6H_5)$), 7.17-7.52 (m, 8H, ArH), 7.83-7.86 (m, 2H, *ortho*-ArH of benzoyloxy); ^{13}C NMR ($CDCl_3$) [100.6 MHz]: δ 17.10 (CH_2 at C4 of piperidine ring), 20.35 (2C, *anti* CH_3 to N lone pair), 34.00 (2C, *syn* CH_3 to N lone pair), 40.36 (2C, CH_2 at C3 and C5 of piperidine ring), 60.06 (2C, quaternary C2 and C6 of piperidine ring), 66.73 (OCH_2-$CH(C_6H_5)$), 83.90 (OCH_2-$CH(C_6H_5)$), 126.70-132.78 (aromatic CH), 140.64 (aromatic quaternary C), 166.29 ($C(O)OCH_2$).

2.4 Synthesis of Model Initiator Reversible Terminating Adducts

2.4.1 General Synthetic Procedure for TMP Adducts

The synthetic method outlined by Anderson *et al.*[5] was used as a guide to prepare all alkyl and aryl nitroxide adducts. Into a 250 mL 3 neck RB flask, cooled in an ice bath equipped with an argon purge, reflux condenser, $CaCl_2$ drying tube, a dropping funnel and stirring bar, were added 2,2,6,6-tetramethyl-1-piperidinyloxy, TEMPO dissolved in dried diethyl ether and a molar excess of the appropriate alkyl halide or aryl halide. Using a dropping funnel, *tri*-butyltin hydride was added to the TEMPO/halide solution at a rate to maintain the reaction temperature below 10°C. The mixture was stirred for 4 hours and

[5] Anderson, J. E.; Tocher, D. A.; Corrie, J. E. T.; Lunazzi, L. *J. Am. Chem. Soc.* **1993**, *115*, 3494.

then allowed to warm to room temperature. The solution was concentrated using a rotary evaporator and then passed through a column of silica gel using flash chromatography techniques[6] with the appropriate solvent combination based on CH_2Cl_2, hexane and ethyl actetate. The yields of each nitroxide adduct are based on one molar equivalent of TEMPO. Identification of the adducts was performed using TLC and NMR techniques.

2.4.2 N-(1´-Methylbenzyloxy)-2,2,6,6-tetramethylpiperidine, **32**, *(MB-TMP)*

N-(1´-methylbenzyloxy)-2,2,6,6-tetramethylpiperidine, (MB-TMP) was prepared according to the general procedure[5] outlined in section 2.3.1. The reagents used were TEMPO (3.84 g, 0.025 mol), (1-bromoethyl)benzene (2.3 g, 12.5 mmol) and *tri*-butyltin hydride (5.3 g, 18 mmol). Isolation of MB-TMP by flash chromatography[6] involved CH_2Cl_2 as the eluting solvent for the first column and 2% ethyl actetate / 98% CH_2Cl_2 for the second column. Pure crystalline MB-TMP (2.0 g, 62.4%) was obtained. This compound showed: mp: 48-50°C (lit.[7], 44.5-45.0°C, lit.[8], 46-47°C): MS (CI) m/z (RI%): 262 (38%), 157 (47%), 142 (100%), 105 (45%): ^{1}H NMR ($CDCl_3$/TMS) [400 MHz] at 243K: δ 0.635, 1.016, 1.166, 1.308 (each as sharp s, 12H, CH_3), 1.36-1.38 (m, 6H, CH_2), 1.48 (d, J = 7 Hz, 3H, $CH(CH_3)$), 4.75 (quartet, J = 7 Hz, 1H, $CH(CH_3)$), 6.21-7.20 (m, 5H, ArH); ^{13}C NMR ($CDCl_3$) [100.6 MHz] at 243K: δ 16.88 (CH_2 at C4 of piperidine ring),

---

[6] Still, W. C.; Kahn, M.; Mitra, A. *J. Org. Chem.* **1978**, *43*, 2923.

[7] Howell, B. A.; Priddy, D. B.; Li, I. Q.; Smith, P. B.; Kastl, P. E. *Polymer Bulletin* **1996**, *37*, 451.

[8] Hawker, C. J.; Barclay, G. G.; Orellana, A.; Dao, J.; Devonport, W. *Macromolecules* **1996**, *29(16)*, 5245.

20.11 (2C, *anti* CH_3 to N lone pair), 23.97 ($CH(CH_3)$), 33.83, 34.21 (2C, *syn* CH_3 to N lone pair), 39.75, 39.78 (2C, CH_2 at C3 and C5 of piperidine ring), 59.37, 59.52 (2C, quaternary C2 and C6 of piperidine ring), 83.08 ($CH(CH_3)$), 126.32, 126.65, 127.91 (5C, aromatic CH), 145.58 (aromatic quaternary C).

2.4.3 N-(Benzyloxy)-2,2,6,6-tetramethylpiperidine, **53**, *(B-TMP)*

The synthesis of *N*-(benzyloxy)-2,2,6,6-tetramethylpiperidine, (B-TMP) was carried out according to the general procedure[5] outlined in section 2.3.1. The reagents used were TEMPO (3.84 g, 0.025 mol), benzyl bromide (2.2 g, 12.5 mmol) and *tri*-butyltin hydride (5.3 g, 18 mmol). Isolation of B-TMP by flash chromatography[6] employed 2% hexane / 98% CH_2Cl_2 gradually changing to pure CH_2Cl_2 as the nitroxide was eluted. Pure B-TMP (2.2 g) was isolated with yield of 72.6%. This compound showed: ^{1}H NMR ($CDCl_3$/TMS) [400 MHz]: δ 1.15, 1.26 (2s, 12H, CH_3), 1.49-1.51 (m, 6H, CH_2), 4.82 (s, 2H, CH_2), 7.25-7.38 (m, 5H, ArH); ^{13}C NMR ($CDCl_3$) [75 MHz]: δ 17.10 (CH_2 at C4 of piperidine ring), 20.27 (2C, *anti* CH_3 to N lone pair), 33.07 (2C, *syn* CH_3 to N lone pair), 39.69 (2C, CH_2 at C3 and C5 of piperidine ring), 59.97 (2C, quaternary C2 and C6 of piperidine ring), 78.70 (CH_2Ph), 127.27, 127.42, 128.19 (5C, aromatic CH), 138.27 (aromatic quaternary C).

2.4.4 N-(tert-Amyloxy)-2,2,6,6-tetramethylpiperidine, **54**, *(tA-TMP)*

N-(*tert*-amyloxy)-2,2,6,6-tetramethylpiperidine, (*t*A-TMP) was prepared according to the general procedure[5] outlined in section 2.3.1. The reagents used were TEMPO (5.0 g, 0.032 mol), 2-bromo-2-methylbutane (2.4 g, 16 mmol) and *tri*-butyltin hydride (4.7 g, 16 mmol). Isolation of *t*A-TMP by flash chromatography[6] employed hexane and ethyl acetate as the eluting solvent beginning with pure hexane and gradually changing to 5% ethyl acetate / 95% hexane. Only 0.31 g, 8.5% yield of pure *t*A-TMP was isolated. This compound showed: ^{1}H NMR ($CDCl_3$/TMS) [400 MHz]: δ 0.93 (triplet, J=7.5 Hz, 3H, $C(CH_3)_2CH_2CH_3$), 1.08, 1.11 (2s, 12H, CH_3), 1.23 (s, 6H, $C(CH_3)_2CH_2CH_3$), 1.42-1.56 (m, 6H, ring CH_2), 1.61 (quartet, J = 7.5 Hz, 2H, $C(CH_3)_2CH_2CH_3$); ^{13}C NMR ($CDCl_3$) [100.6 MHz]: δ 8.70 ($C(CH_3)_2CH_2CH_3$), 17.16 (CH_2 at C4 of piperidine ring), 20.61 (2C, *anti* CH_3 to N lone pair), 26.36 ($C(CH_3)_2CH_2CH_3$), 34.76 (2C, *syn* CH_3 to N lone pair), 35.70 ($C(CH_3)_2CH_2CH_3$), 40.87 (2C, CH_2 at C3 and C5 of piperidine ring), 59.11 (2C, quaternary C2 and C6 of piperidine ring), 78.80 ($C(CH_3)_2CH_2CH_3$).

2.4.5 N-(tert-Butoxy)-2,2,6,6-tetramethylpiperidine, **55**, *(tB-TMP)*

N-(*tert*-butoxy)-2,2,6,6-tetramethylpiperidine, (*t*B-TMP) was prepared according to the general procedure[5] outlined in section 2.3.1. The reagents used were TEMPO (2.9 g, 16.0 mmol), 2-iodo-2-methylpropane (9.4 g, 0.051 mol) and *tri*-butyltin hydride (4.7 g, 0.016 mol). Isolation of *t*B-TMP by flash chromatography[6] employed 2% hexane and 98% CH_2Cl_2 as the initial eluting solvent which was then gradually changed to pure

CH_2Cl_2. Only 1.85 g, a 54.3% yield, of pure *tB*-TMP was isolated. This compound showed: ^{1}H NMR ($CDCl_3$/TMS) [300 MHz]: δ 1.07, 1.12 (2s, 12H, CH_3), 1.28 (s, 9H, $C(CH_3)_3$), 1.41-1.58 (m, 6H, CH_2); ^{13}C NMR ($CDCl_3$) [75MHz]: 17.16 (CH_2 at C4 of piperidine ring), 20.39 (2C, *anti* CH_3 to N lone pair), 29.44 ($C(CH_3)_3$), 34.81 (2C, syn CH_3 to N lone pair), 40.84 (2C, CH_2 at C3 and C5 of piperidine ring), 59.06 (2C, quaternary C2 and C6 of piperidine ring), 77.11 ($C(CH_3)_3$).

2.4.6 N-(Ethyl-iso-butyrate-2′-oxy)-2,2,6,6-tetramethylpiperidine, **56**, *(EiB-TMP)*

N-(ethyl-iso-butyrate-2′-oxy)-2,2,6,6-tetramethylpiperidine, (EiB-TMP) was prepared according to the general procedure[5] outlined in section 2.3.1. The reagents used were TEMPO (5.0 g, 0.032 mol), ethyl 2-bromoisobutyrate (3.1 g, 16.0 mmol) and *tri*-butyltin hydride (4.7 g, 0.016 mol). Isolation of EiB-TMP by flash chromatography[6] employed CH_2Cl_2 as the eluting solvent passing through a column twice. Only 1.69 g, a 39.0% yield of pure EiB-TMP was isolated. This compound showed: ^{1}H NMR ($CDCl_3$/TMS) [300 MHz]: δ 1.00, 1.15 (s, 12H, CH_3), 1.30 (triplet, J = 7.1 Hz, 3H, $C(O)OCH_2CH_3$), 1.47 ($C(CH_3)_2$), 1.41-1.54 (m, 6H, ring CH_2), 4.17 (quartet, J = 7.1 Hz, 2H, $C(O)OCH_2CH_3$); ^{13}C NMR ($CDCl_3$) [75 MHz]: 13.99 ($C(O)OCH_2CH_3$), 16.93 (CH_2 at C4 of piperidine ring), 20.31 (2C, *anti* CH_3 to N lone pair), 24.31 ($C(CH_3)_3$), 33.30 (2C, *syn* CH_3 to N lone pair), 40.48 (2C, CH_2 at C3 and C5 of piperidine ring), 59.39, 60.38 (2C, quaternary C2 and C6 of piperidine ring), 80.95 ($C(CH_3)_2$), 175.85 ($C(O)OCH_2CH_3$).

2.4.7 N-(iso-Propoxy)-2,2,6,6-tetramethylpiperidine, **57**, *(iP-TMP)*

N-(*iso*-propoxy)-2,2,6,6-tetramethylpiperidine, (*i*P-TMP) was prepared according to the general procedure[5] outlined in section 2.3.1. The reagents used were TEMPO (5.0 g, 0.032 mol), 2-bromopropane (2.0 g, 16.0 mmol) and *tri*-butyltin hydride (4.7 g, 16.0 mmol). Isolation of *i*P-TMP by flash chromatography[6] employed 5% hexane / 95% CH_2Cl_2 as the eluting solvent. The isolated yield (3.1%) of *i*P-TMP was 0.1 g. The compound showed: ^{1}H NMR ($CDCl_3$/TMS) [300 MHz]: δ 1.12 (broad shoulder, 12H, ring CH_3), 1.15 (d, J = 6.3 Hz, 6H, $CH(CH_3)_2$), 1.45 (broad m, 6H, CH_2), 3.98 (septet, J = 6.3 Hz, $CH(CH_3)_2$); ^{13}C NMR ($CDCl_3$) [75 MHz]: δ 17.35 (CH_2 at C4 of piperidine ring), 20.24 (broad weak s, 2C, *anti* CH_3 to N lone pair), 22.35 ($CH(CH_3)_2$), 34.45 (broad weak s, 2C, *syn* CH_3 to N lone pair), 40.25 (2C, CH_2 at C3 and C5 of piperidine ring), 59.48 (2C, quaternary C2 and C6 of piperidine ring), 75.06 ($CH(CH_3)_2$).

2.4.8 N-(Cycloheptoxy)-2,2,6,6-tetramethylpiperidine, **58**, *(CH-TMP)*

N-(cycloheptoxy)-2,2,6,6-tetramethylpiperidine, (CH-TMP) was prepared according to the general procedure[5] outlined in section 2.3.1. The reagents used were TEMPO (5.0 g, 0.032 mol), cycloheptyl bromide (2.8 g, 16.0 mmol) and *tri*-butyltin hydride (4.7 g, 16.0 mmol). Isolation of CH-TMP by flash chromatography[6] employed CH_2Cl_2 as the eluting solvent. The isolated yield of CH-TMP was 0.8 g, 19.8%. The compound showed: ^{1}H NMR ($CDCl_3$/TMS) [300 MHz]: δ 1.11 (s, 12H, CH_3), 1.29-2.05

(3m, 18H, CH_2), 3.82 (septet, J = 4.2 Hz, 1H, $NOCHC_6H_{12}$); ^{13}C NMR ($CDCl_3$) [100.6 MHz]: 17.29 (CH_2 at C4 of piperidine ring), 20.34 (broad weak s, 2C, *anti* CH_3 to N lone pair), 23.36, 28.61, 33.41 (3s, 6C, CH_2 of cycloheptyl), 34.35 (broad weak s, 2C, syn CH_3 to N lone pair), 40.28 (2C, CH_2 at C3 and C5 of piperidine ring), 59.60 (2C, quaternary C2 and C6 of piperidine ring), 83.80 ($NOCHC_6H_{12}$).

2.4.9 N-(Methyl-iso-propionate-2'-oxy)-2,2,6,6-tetramethylpiperidine, **59**, *(MiP-TMP)*

N-(methyl-iso-propionate-2'-oxy)-2,2,6,6-tetramethylpiperidine, (MiP-TMP) was prepared according to the general procedure[5] outlined in section 2.3.1. The reagents used were TEMPO (5.0 g, 0.032 mol), methyl-2-bromopropionate (2.7 g, 16.0 mmol) and *tri*-butyltin hydride (4.7 g, 0.016 mol). Isolation of MiP-TMP by flash chromatography[6] employed CH_2Cl_2 as the eluting solvent for the first column. The second time this adduct was passed through a column, 5/2 solvent ratio of CH_2Cl_2/CH_3CN was used. The isolated yield of the white solid MiP-TMP was 2.68g, 69%. The compound showed: mp: 29-33°C: MS (CI) m/z (RI%): 244 (100%), 156 (100%): ^1H NMR ($CDCl_3$/TMS) [300 MHz]: δ 1.02, 1.12, 1.18 (3s but not baseline separated, 12H, CH_3), 1.25-1.44 (m, 6H, CH_2), 1.40 (d, J = 7.0 Hz, $CH(CH_3)$), 3.71 (s, $C(O)OCH_3$), 4.33 (quartet, J = 7.0 $CH(CH_3)$); ^{13}C NMR ($CDCl_3$) [75 MHz]: δ 17.19 (CH_2 at C4 of piperidine ring), 18.02 ($CH(CH_3)$), 19.96, 20.09 (s, 2C, *anti* CH_3 to N lone pair), 32.79, 33.56 (2s, *syn* CH_3 to N lone pair), 40.10, 40.21

(2s, CH_2 at C3 and C5 of piperidine ring), 51.29 ($C(O)COCH_3$), 59.97 (2C, quaternary C2 and C6 of piperidine ring), (81.49 ($CH(CH_3)$), 174.39 ($C(O)COCH_3$).

2.4.10 N-(1′-Methylbenzyloxy)-2,2,6,6-tetramethylisoindoline, **60**, *(MB-TMI)*

N-(1′-methylbenzyloxy)-2,2,6,6-tetramethylisoindoline, (MB-TMI) was prepared according to the general procedure[5] outlined in section 2.4.1. The reagents used were 1,1,3,3-tetramethylisoindolin-2-yloxyl (1.8 g, 9.47 mmol), (1-bromoethyl)benzene (0.92 g, 5.0 mmol) and *tri*-butyltin hydride (1.45 g, 5.0 mmol). Isolation of MB-TMIso by flash chromatography[6] employed 90 % hexane / 10 % CH_2Cl_2 as the eluting solvent. The isolated yield of MB-TMI, a white crystalline solid, was 200 mg, 14.3 %. The compound showed: mp: 69-71°C: MS (CI) m/z (RI%): 296 (26%), 191 (34%), 176 (100%), 105 (50%): ^{1}H NMR ($CDCl_3$/TMS) [300 MHz]: δ 0.92, 1.26, 1.42, 1.60 (4s, baseline separate, 12H, CH_3), 1.57 (d, J = 6.8 Hz, $CH(CH_3)$), 4.86 (quartet, J = 6.8 Hz, $CH(CH_3)$), 7.05-7.07 (m, *ortho*-aryl H of isoindoline ring), 7.14-7.17 (m, *ortho*-aryl H of isoindoline ring), 7.23-7.47 (m, 7H, 5 ArH of phenyl ring and 2 ArH of indoline ring); ^{13}C NMR ($CDCl_3$) [75 MHz]: δ 22.43 ($CH(CH_3)$), 25.23, 25.46 (s, 2C, *anti* CH_3 to N lone pair), 29.66, 30.24 (2s, *syn* CH_3 to N lone pair), 67.11, 67.68 (2C, quaternary alpha C to NO), 83.32 ($CH(CH_3)$), 121.41, 121.60 (2s, aromatic CH of isoindoline ring), 127.13 (s, 2C aromatic CH of isoindoline ring), 127.04, 127.33, 128.08 (3s, 5ArH of phenyl), 145.06, 145.43, 145.85 (3s, quaternary C of phenyl and isoindoline rings).

2.4.11 N-(1´-Methylbenzyloxy)-2,2,6,6-tetraethylisoindoline, **61**, *(MB-TEI)*

N-(1´-methylbenzyloxy)-2,2,6,6-tetraethylisoindoline, (MB-TEI) was prepared according to the general procedure[5] outlined in section 2.4.1. The reagents used were 1,1,3,3-tetraethylisoindolin-2-yloxyl (1.0 g, 4.0 mmol), (1-bromoethyl)benzene (0.4 g, 2.0 mmol) and *tri*-butyltin hydride (0.58 g, 2.0 mmol). Isolation of MB-TMIso by flash chromatography[6] employed 90 % hexane / 10 % CH_2Cl_2 as the eluting solvent. The isolated yield of the clear and colourless oily liquid MB-TEI was 100 mg, 13.6 %. The compound showed: ^{1}H NMR ($CDCl_3$/TMS) [300 MHz]: δ 0.33, 0.78, 0.82, 0.98 (triplets, J = 7.5 Hz, 12H, CH_2CH_3), 1.52 (d, J = 6.8 Hz, $CH(CH_3)$), 1.57-2.27 (overlapping quartets, 8H not equivalent, CH_2CH_3), 4.79 (quartet, J = 6.8 Hz, $CH(CH_3)$), 6.91-6.94 (m, *ortho*-aryl H of isoindoline ring), 7.01-7.05 (m, *ortho*-aryl H of isoindoline ring), 7.13-7.21 (m, 2 *meta*-aryl H of isoindoline ring),7.24-7.40 (m, 5H, ArH of phenyl); ^{13}C NMR ($CDCl_3$) [75 MHz]:8.77, 9.06, 9.44, 9.57 (s, 4C, CH_2CH_3), 23.13 (s, $CH(CH_3)$), 28.47, 29.01, 30.63, 30.72 (4C, CH_2CH_3), 72.90, 73.47 (2C, $C(CH_2CH_3)_2$), 82.53 (s, $CH(CH_3)$), 123.40, 123.61 (2s, aromatic CH of isoindoline ring), 125.96, 126.00 (2s not baseline separated, 2C aromatic CH of isoindoline ring),126.75, 127.26, 127.99 (3s, 5ArH of phenyl),142.24, 142.30 (2s not baseline separated, quaternary C isoindoline rings), 145.30 (s, quaternary C of phenyl ring).

2.4.12 N-(Methyl-iso-propionate-2'-oxy)-2,2,6,6-tetramethyl-4-benzoyloxypiperidine, **62**, *(MiP-4BenTMP)*

N-(methyl-iso-propionate-2'-oxy)-2,2,6,6-tetramethyl-4-benzoyloxypiperidine, (MiP-4BenTMP) was prepared according to the general procedure[5] outlined in section 2.3.1. The reagents used were 4-benzoyloxy-TEMPO (5.0 g, 0.018 mol), methyl-2-bromopropionate (1.5 g, 9.0 mmol) and *tri*-butyltin hydride (2.6 g, 9.0 mmol). Isolation of MiP-4BenTMP by flash chromatography[6] employed a solvent system starting with hexane then 50/50 hexane / CH_2Cl_2 and then gradually switching to pure CH_2Cl_2. The isolated yield of the white solid MiP-4BenTMP was 1.47 g, 45%. The compound showed: mp: 73-76°C: MS (CI) m/z (RI%): 364 (100%), 276 (37%), 154 (22%): ^{1}H NMR ($CDCl_3$/TMS) [300 MHz]: δ 1.12 1.29 (2s, 12H, ring CH_3), 1.44 (d, J = 6.9 Hz, 3H, $CH(CH_3)$), 1.66-2.04 (2m, 4H, CH_2), 3.74 (s, $C(O)OCH_3$), 4.38 (quartet, J = 6.9 Hz, $CH(CH_3)$), 5.21-5.32 (m, ring CH), 7.44 (m, 2H, *meta*-ArH), 7.56 (m, *para*-ArH), 8.02 (m, 2H, *ortho*-ArH); ^{13}C NMR ($CDCl_3$) [75 MHz]: 18.12 ($CH(CH_3)$), 20.89, 21.04 (2s, *anti* CH_3 to N lone pair), 32.85, 33.61 (2s, *syn* CH_3 to N lone pair), 44.38, 44.59 (2s, CH_2 at C3 and C5 of piperidine ring), 51.57 ($C(O)COCH_3$), 59.93, 60.50 (2C, quaternary C2 and C6 of piperidine ring), 67.13 (CH of piperidine ring), 81.731 ($CH(CH_3)$), 128.30, 129.47, 132.86 (5C, aromatic CH), 130.48 (quaternary aromatic C), 166.10 (OC(O)Ph), 174.26 ($CHC(O)OCH_3$).

2.4.13 N-hydroxy-2,2,6,6-tetramethyl-4-benzoyloxypiperidine, **63**, *(4BenTMPOH)*

During the concentration of MiP-4BenTMP, a white precipitate came out of solution. The material was isolated by vacuum filtration and washed with a non-solvent such as hexane. The isolated yield of this white solid was 0.23 g. This compound showed: mp: 146-148°C: MS (EI) m/z : 278: MS (CI) m/z (RI%): 278 (100%): ^{1}H NMR ($CDCl_3$/TMS) [300 MHz]: 1.27 (s, 12H, CH_3), 1.73 (m, 2H, CH_2), 2.04-2.10 (m, 2H, CH_2), 4.25 (broad s, NOH), 5.32 (m, methine H of piperidine ring), 7.46 (m, 2H, *meta*-ArH), 7.58 (m, *para*-ArH), 8.04 (m, 2H, *ortho*-ArH); ^{13}C NMR ($CDCl_3$) [75MHz]: 20.37 (2C, *anti* CH_3 to N lone pair), 31.47 (2C, *syn* CH_3 to N lone pair), 43.56 (CH_2 at C3 and C5 of piperidine ring), 59.24 (2C, quaternary C2 and C6 of piperidine ring), 67.00 ($CH_2CH(OCO)$), 128.02, 129.19, 132.59 (5C, aromatic CH), 130.15 (quaternary aromatic C), 165.80 (OC(O)Ph).

Approximately 3 drops of D_2O was added to the NMR sample of 4BenTMPOH in $CDCl_3$. The solution was shaken to mix the deuterated water into the solution. The labile OH proton of the hydroxylamine was exchanged with deuterium. This was evident by the disappearance of the broad OH singlet at 4.25 ppm.

Chapter 3

Molecular Orbital Calculations

3.1 Introduction and Rationale

With the advent of controlled and living radical polymerization processes, each new method has required an additional reagent to control the reactivity of the propagating radical chain end. In the case of the iniferter polymerization process, sulphur based radicals are used to initiate the polymerization and also to reversibly terminate the propagating chain end. In the case of ATRP, the activation and deactivation of the propagating chain end is a result of the reversible atom transfer reaction between a $Cu^{I}X/Cu^{II}X_2$ metal salt and an alkyl halide. For the stable free radical polymerization process, stable nitroxide radicals reversibly cap the propagating polymer chain end.

The critical selection process used to identify stable nitroxyl radicals as suitable reversible terminating agents for the SFRP process was previously reported by Kazmaier *et al.*[1] At that time, our work illustrated how beneficial semi-empirical molecular orbital calculations AM1 and PM3, were in identifying appropriate nitroxyl radicals. The molecular orbital calculations determined the bond dissociation enthalpies (BDEs) for

systems where the radical fragments were structurally very different, i.e. benzoyloxy, dithiocarbamate and nitroxyl radicals. It was shown that semi-empirical MO calculations can be used to identify initiator / reversible terminating adducts with bond dissociation enthalpies that can lead to controlled radical polymerization systems. Systems with BDEs < 35 kcal mol^{-1} such as alkoxyamines which contain the nitroxyl radical, enable thermal homolytic cleavage of the C-ON bond between the propagating polymer chain end and a nitroxyl capping radical.

Moad *et al.*[2] have performed semi-empirical molecular orbital calculations on a series of alkoxyamines to identify possible correlations between structure and C-ON homolysis rates where the ring size of the nitroxides was varied along with different initiating radical fragments. Sogah *et al.*[3] also employed semi-empirical calculations to determine the ground state enthalpy, $\Delta H°$, for C-ON bond homolysis of the two diastereomers of DDPO-styrene adduct, and the enthalpy of activation $\Delta H^{\ddagger}$ for the DDPO-styrene and TEMPO-styrene adducts.

As our modelling efforts continued, it became apparent that semi-empirical molecular orbital methods were not accurate enough to distinguish among radicals of the same structural family, i.e., nitroxide radicals. Researchers specializing in theoretical MO calculations are very much aware of the shortcomings and pitfalls of semi-empirical

---

[1] Kazmaier, P. M.; Moffat, K. A.; Georges, M. K.; Veregin, R. P. N.; Hamer, G. K. *Macromolecules* **1995**, *28*, 1841.
[2] Moad, *G.;* Rizzardo, E. *Pac. Polym. Conf. Prepr; Polym. Div., Royal Aust. Chem. Inst.*: Brisbane, **1993**, *3*, 651. Moad, G.; Rizzardo, E. *Macromolecules* **1995**, *28*, 8722.

methods when used to calculate BDEs on systems such as the ones proposed for the SFRP process. Dewar *et al.*[4] demonstrated there are some limitations in using semi-empirical molecular orbital calculations. The AM1 method, which is parameterized for C, O, N, and H, is very reliable for calculating heats of formation for hydrocarbons. For example, the ΔH_f for styrene by AM1 is 38.8 kcal mol^{-1} compared to the experimental value of 35.4 kcal mol^{-1}. For systems that contain O and N atoms bonded to each other, the AM1 method is less reliable. The error in ΔH_f values between experimental and AM1 for neutral radicals, such as •NO and $•NO_2$, are 20.2 and 22.6 kcal mol^{-1}, respectively[23]. Kalkanis and Shields[5] compared AM1 and PM3 calculations for neutral radical $•CH_2OH$ reactions with •NO and $•NO_2$. They determined that PM3 and AM1 calculated heats of formation differ from experimental by 8.6 and 18.8 kcal mol^{-1}, respectively. This indicated that the PM3 MO method provides ΔH_f values closer to experimental values for molecules that contain both oxygen and nitrogen atoms than AM1, but the errors are still significant. The number of atoms in these systems are quite small in comparison to the smallest model initiator *N*-(1´-methylbenzyloxy)-2,2,6,6-tetramethylpiperidine, MB-TMP (32) for the SFRP process. In 1992, Crayston *et al.*[6] reported on the EPR study of two nitroxyl radicals; pyrrolyl-1-oxyl and 3-pyrrolinyl-1-oxyl. These very short lived radicals ($< 10^{-2}$ s) were generated by hydrogen abstraction

---

[3] Puts, R. D.; Sogah, D. *Macromolecules* **1996**, *29*, 3323.
[4] Dewar, M. J. S.; Zoebisch, E. G.; Healy, E. F.; Stewart, J. J. P. *J. Am. Chem. Soc.* **1985**, *107*, 3902
[5] Kalkanis, G. H.; Shields, G. C. *J. Phys. Chem.* **1991**, *95*, 5085.
[6] Crayston, J. A.; Kakouris, C.; Walton, J. C. *Magn. Reson. Chem.* **1992**, *30(1)*, 77.

from the corresponding *N*-hydroxypyrroles and observed by EPR. In addition to the hyperfine splittings patterns observed for these radicals, AM1 semi-empirical MO calculations were performed. The bond lengths of the C2-C3, C3-C4 and C4-C5 bonds in the pyrrole ring were calculated inaccurately. The geometry of the N atom was determined to be pyramidal and the calculated spin densities did not correspond to the experimental hyperfine coupling constants observed by EPR. Crayston *et al.*[6] concluded that semi-empirical methods were not accurate enough to give a good description of the molecular orbitals of pyrrolyl-1-oxyl.

It is not clear to synthetic polymer chemists where these methods break down and what parameters in the Hamiltonian equations of AM1 and PM3 are faulty. This chapter will discuss an approach that was used to calibrate semi-empirical MO calculations and identify where the deficiencies lie with these methods.

3.2 Experimental Section

3.2.1 Molecular Orbital Calculations

All calculations were performed on a Silicon Graphics 4D/480 workstation. Semi-empirical AM1 and PM3 molecular orbital calculations were carried out using the program MOPAC (Version 6.0).[7] All starting structures for geometry optimization were drawn using PC Model (Version 4.0). The AM1 and PM3 geometries were optimized until the gradient norm was less than 0.01 kcal mol^{-1} $Å^{-1}$. The keywords PRECISE,

---

[7] Stewart, J. J. P. *J. Computer-Aided Mol. Design* **1990**, *4*, 1.

GNORM=0.01, EF and GRAD in MOPAC were used[8] in the calculations of the heat of formation (ΔH_f) for both radical fragments and the closed shell adduct. The half electron method developed by Dewar *et al.*[9] was used to calculate the open-shell systems. Bond dissociation enthalpies (BDEs) were estimated by adding the product radical ΔH_f energies and subtracting the ΔH_f energy of the closed shell adduct.[1]

A conformational search was performed to determine the lowest energy conformation of MB-TMP on a potential energy surface (PES). This was performed using the PhiPsi Excel 4 for Windows macro and HyperChem for Windows. Two dihedral angles, Φ_1 (∠ C1-C2-O3-N4) and Φ_2 (∠ C2-O3-N4-C11) were chosen as Phi and Psi, respectively. The MB-TMP file with $\Phi_1 = 60.0°$ and $\Phi_2 = -59.3°$ was used by the macro as the starting conformation corresponding to zero. Each PhiPsi point was determined by molecular mechanics with the MM+ force field using HyperChem 4.0 software (Hypercube Inc.). The torsion angles were varied in increments of 10° steps producing a 36 X 36 matrix. Each point was imported into an Excel spreadsheet and plotted using a 3-D plot to produce the potential energy surface. The lowest energy point was identified and the PM3 Hamiltonian method, operating from the MOPAC software program, used this point as the starting input conformation file for full geometry optimization.

---

[8] Masamura, M. *J. Mol. Str. (Theochem)* **1988**, *168*, 227.
[9] Dewar, M. J. S.; Hashmall, J. A.; Venier, C. G. *J. Am. Chem. Soc.* **1968**, *90*, 1953.

3.2.2 Synthesis of MB-TMP

Synthesis of the nitroxide adduct MB-TMP compound **32** was described in Chapter 2 Section 2.4.2. Included in section 2.4.2 are the ^{1}H and ^{13}C solution NMR data for this compound.

3.2.3 X-ray Experiment and Calculations

A single crystal fragment (0.3 x 0.3 x 0.2 mm) of the MB-TMP solid was glued to a fiber and cooled to -63°C on a Siemens P4RA diffractometer. The unit cell is monoclinic, with a = 13.5584(2) Å, b = 7.72710(10) Å, c = 14.9489(2) Å, β = 91.626(10)°. A total of 13,148 reflections in the ranges $-16 \leq h \leq 16$, $-9 \leq k \leq 9$, $-18 \leq l \leq 18$, $4 \leq 2\theta \leq 53°$ were collected using φ and ω scans with a SMART CCD detector and a rotating anode source. Mo-Kα radiation was used, having a linear absorption coefficient of only 0.068/mm.

The MB-TMP molecule crystallized in the space group $P2_1/n$, with one molecule per asymmetric unit. Direct methods revealed all non-hydrogen atoms, with the expected connectivity. Hydrogen atoms were found in the difference map and refined isotropically. Anisotropic refinement (173 parameters) using 3032 unique data with $I \geq -3\sigma I$ and minimizing $|F_o^2 - F_c^2|$ gave a clean difference map (-0.138 to .185 eÅ^{-3}), a goodness of fit of 1.005, and a final agreement factor with wR2 of 0.0969, based on weighted F^2. The traditional R factor, using 2577 $F > 4\sigma F$, is 0.0363. The data

collection software SMART, SAINT and SHELXTL were used for structure solution and refinement, tables and diagrams. All software packages were purchased from Siemens Analytical.

The final structure has normal bond lengths and angles. The full data set for the single crystal X-ray structure of MB-TMP at 27°C and –63°C can be found in Appendix I.

3.3 Results and Discussion

Semi-empirical molecular orbital calculations have been used to determine bond dissociation enthalpies (BDEs)[1] of the C-ON bond in nitroxide adducts. These adducts mimic the C-ON bond between the propagating radical center at the end of the growing

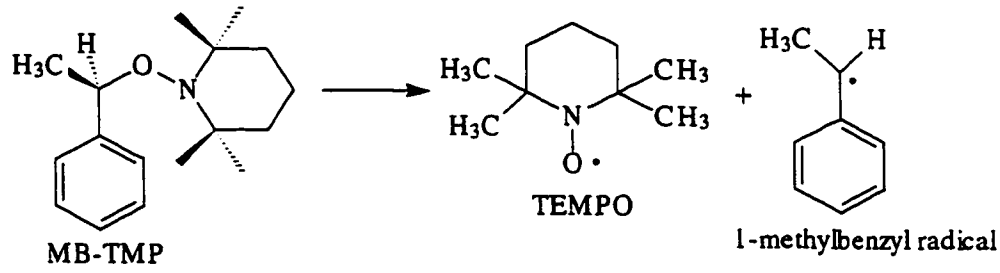

Scheme 17: The reaction scheme used to calculate the bond dissociation enthalpy for the C-O bond cleavage in MB-TMP.

polymer chain and the oxygen atom of the reversible terminating agent, the nitroxide.[1] Shown in Scheme 17, is the reaction used to calculate the BDE for the C-ON bond in the closed shell species MB-TMP. This nitroxide adduct mimics the propagating chain end

of styrene polymerized by the SFRP process, which at elevated temperatures undergoes homolytic cleavage to produce the nitroxyl radical fragment TEMPO and the α-methylbenzyl radical fragment. This α-methylbenzyl radical represents the propagating polystyryl chain end. In addition, MB-TMP has been studied as an initiator / reversible terminating agent in the SFRP of styrene and *n*-butyl acrylate. The polymerization data are presented in Chapter 6. The initiation and reversible terminating properties of MB-TMP have also been compared to BST[10], which is also included in Chapter 6. Understanding how to vary the strength of this C-ON bond is key to enabling good control over the SFRP process and ultimately, to lowering the polymerization temperature of the reaction and influencing the rate constant of polymerization. As illustrated by Kazmaier *et al.*[1] the bond dissociation enthalpy calculations require determining the heats of formation for both radical species and the closed shell system (Scheme 17). Subtraction of the heat of formation of the reactant from the products provided the BDE for this homolytic cleavage reaction. Summarized in Table 1 are the bond dissociation enthalpies for a series of 1-substituted ethylbenzenes where the nitroxide radical TEMPO has been changed to cover a variety of structurally different nitroxide radicals. The BDEs obtained by AM1 and PM3 for these nitroxides are essentially the same with an average value of 23.5 ± 7 kcal mol^{-1} and 27.6 ± 6 kcal mol^{-1}, respectively. Both semi-empirical methods cannot identify any differences in the C-O

[10] Moffat, K. A.; Hamer, G. K.; Georges, M. K.; Kazmaier, P. M.; Stöver, H. D. H. *Polym.Prepr.(Am. Chem. Soc., Div. Polym. Chem.)* **1996**, *37(2)*, 509.

bond strength for these 19 structurally different nitroxides, even though experimental data suggests[1] there are differences in the rate of polymerization.

Table 1. Calculated Bond Dissociation Enthalpies for 1-Substituted Ethylbenzenes

Nitroxide Radicals	AM1 (kcal/mol)	PM3 (kcal/mol)
TEMPO	22.4	27.6
4-hydroxy-TEMPO	21.1	29.0
4-oxo-TEMPO	23.4	28.8
4-chloro-TEMPO	23.1	28.3
4-methoxy-TEMPO	22.5	26.8
4-benzyloxy-TEMPO	22.9	26.7
4-amino-TEMPO	21.9	25.7
4-hydroxylimino-TEMPO	23.1	28.3
PROXYL	23.1	26.6
3-oxo-PROXYL	24.6	28.2
3,4-di-*tert*-butyl-PROXYL	22.5	34.2
3-carbamoyl-PROXYL	23.3	27.8
3-aminomethyl-PROXYL	24.1	25.9
3-methoxy-PROXYL	22.9	25.7
3-carboxyl-PROXYL	29.4	27.7
diphenyl nitroxide	30.1	29.9
di-*tert*-butyl nitroxide	21.3	25.4
tert-butyl-*tert*-amyl nitroxide	21.2	26.7
1,1,3,3-tetramethylisoindolin-2-yloxyl	23.6	25.8

Theoretical chemists[11] are aware that semi-empirical MO calculations are not accurate enough to distinguish between different nitroxyl radicals as in the series of Table 1. What is not clear to synthetic polymer chemists is where these methods break down and what parameters in the Hamiltonian equations are faulty. To

[11] Dewar, M. J. S.; Zoebisch, E. G.; Healy, E. F.; Stewart, J. J. P. *J. Am. Chem. Soc.*, **1985**, *107*, 3902. Kalkanis, G. H.; Shields, G. C. *J. Phys. Chem.*, **1991**, *95*, 5085.

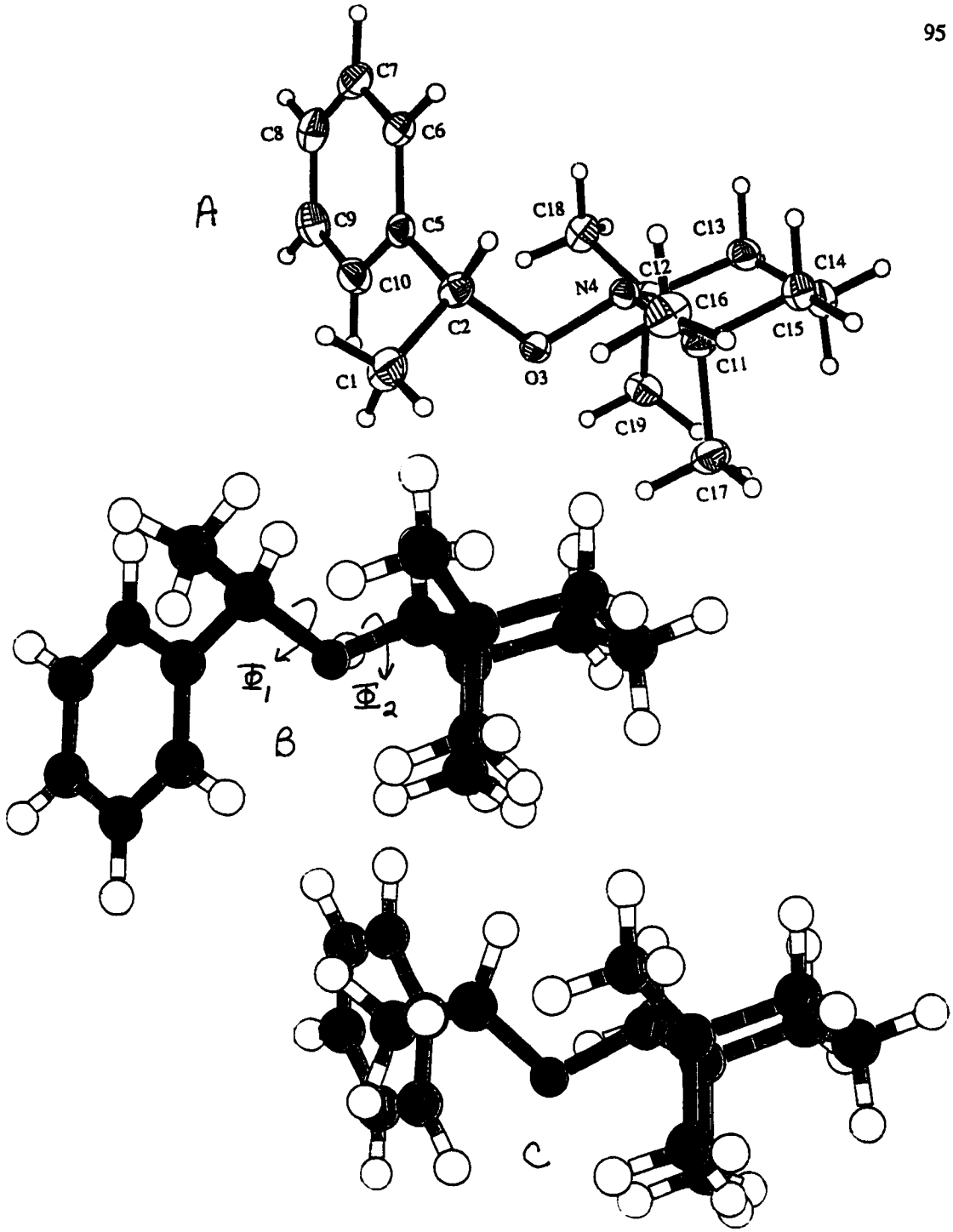

Figure 2: Comparison of a) thirty percent thermal ellipsoid depiction of *N*-(1´-methylbenzyloxy)-2,2,6,6-tetramethylpiperidine as determined by X-ray crystallography (showing the atomic numbering scheme) with optimized geometries calculated by b) AM1 and c) PM3 methods.

Table 2: Comparison of Selected Bond Lengths, Bond Angles and Torsion Angles of MB-TMP Minimzed by AM1 and PM3 Semi-Empirical Methods, *Ab Initio* and X-ray Crystallographic Structure.

Atoms	AM1 ΔH_f= -0.52 kcal mol^{-1}	PM3 ΔH_f=-15.35 kcal mol^{-1}	ROHF/3-21G E=-492208.18	X-ray Structure (27°C)	X-ray Structure (-63°C)
	Bonds (Å)				
C1-C2	1.518	1.532	1.536	1.528(3)	1.518(2)
C2-O3	1.461	1.427	1.456	1.468(2)	1.453(1)
O3-N4	1.354	1.501	1.466	1.470(2)	1.457(1)
N4-C11	1.501	1.515	1.5	1.515(3)	1.502(1)
N4-C12	1.502	1.514	1.502	1.515(3)	1.501(1)
	Bond < (°)				
C1-C2-O3	108.4	107.0	109.8	105.0(2)	105.19(10)
C2-O3-N4	114.3	110.7	113.7	112.58(1)	112.45(8)
O3-N4-C11	107.6	109.0	106.4	106.28(1)	106.27(8)
O3-N4-C12	115.6	118.4	108.5	106.88(1)	107.08(8)
	Torsion < (°)				
C1-C2-O3-N4	-102.5	-127.7	-112.8	-148.37(0.1)	-148.35(0.1)
C2-O3-N4-C11	131.1	110.5	128.2	107.39(0.1)	107.38(0.1)
C2-O3-N4-C12	-102.7	-118.9	-102.6	-126.37(0.1)	-126.38(0.1)

provide some insight into this problem the single crystal X-ray structure of MB-TMP was obtained. The crystal structure provided accurate information about the preferred conformation of MB-TMP in the solid state and also experimental data on the bonding parameters of the atoms in the molecule, especially the critical atoms of interest, C-O-N. The crystal structure was determined at room temperature, 27°C

and -63°C. The structure of MB-TMP as shown in Figure 2a was compared to the optimized geometries of the lowest energy minima (global minimum) calculated by AM1 and PM3. Summarized in Table 2 are the relevant bond lengths, bond angles and torsion angles for the calculated structures along with the X-ray crystal structure at 27°C and –63°C and an *ab initio* calculation at the 3-21G level. The geometry of the crystal structure is comparable to the same rotational conformer calculated by the PM3 semi-empirical method as illustrated by comparing Figure 2a with 2c, but there was a significant difference in the length of the N-O bond and also smaller differences in the adjacent C-O bond.

The N-O bond length determined by the crystal structure was 1.457(1)Å at –63°C. The length of this bond as calculated by AM1 and PM3 was 1.354Å and 1.501Å, respectively. Thus, AM1 underestimates this bond length by 0.103Å and PM3 determines the bond to be longer than experiment by 0.044 Å. The *ab initio* calculation at the 3-21G level determines the N-O bond length to be 1.466 Å which is closer to the experimental value but is still too high by 0.009 Å. When comparing the calculated geometry and bonding parameters of MB-TMP obtained by the AM1 method with the crystal structure data, the shorter N-O bond also effects the bond of interest, the C-O bond. The calculated C-O bond is longer than the experimental value and as a consequence the calculations suggest that the bond will undergo homolytic cleavage more easily, producing a lower BDE value. Similarly, a comparison of the calculated bonding parameters obtained by PM3 predicts the C-O

bond to be shorter than the crystal structure value by 0.026Å. This suggests a stronger bond and a slower homolysis rate. This is reflected in a calculated higher BDE value by PM3. This direct comparison of the experimental bonding parameters of **32** with the calculated values clearly illustrates that semi-empirical methods are deficient in accurately describing the linear combination of atomic orbitals of nitrogen and oxygen and the resulting molecular orbitals when nitrogen is bonded to oxygen. The lone pair of electrons on nitrogen and the two lone pairs of electrons on oxygen are not well described by atomic orbitals p_x, p_y and p_z. d-orbitals are required to provide a more accurate parametization of atoms bonded to each other that contain lone pairs of electrons. The type of calculations where d-orbitals are included in the atom parametization are in the higher order *ab initio* calculations. Unfortunately, the time required to perform such intense calculations becomes prohibitive for systems with a large number of atoms and high degree of conformational flexibility as depicted in Table 1. These deficiencies also spill over into the atomic and molecular orbitals that describe the adjacent C-O bond. The parameters in AM1 and PM3 that describe these critical atoms, the N-O and C-O bond lengths and angles, must be refined and adjusted to improve the accuracy of these semi-empirical methods.

Puts and Sogah[3] also used semi-empirical methods to calculate ground state enthalpies, $\Delta H°$, for C-ON bond homolysis of both diastereomers of DDPO-styryl adduct and TEMPO-styryl adduct, **32**. The BDEs for the two DDPO-styryl adducts,

diastereomers *(R,R)-R* and *(R,R)-S* were 118.5 kJ/mol (28.3 kcal/mol) and 112.9 kJ/mol (26.9 kcal/mol), respectively, which falls within the range of BDE values presented in Table 1. The BDE value calculated by Puts *et al.*[3] for **32** was 122 kJ/mol (29.2 kcal/mol) which compares favourably to the PM3 value of 27.6 kcal/mol reported for **32** in Table 1. The caution that we express from the comparison of the crystal structure data with calculated values is that semi-empirical methods are not accurate enough or sensitive enough to provide any guidance in choosing a better nitroxide. The scatter in the data is too large to be of any benefit and therefore cannot be used to select nitroxyl radicals for the SFRP process. Puts did not rely completely on semi-empirical calculations to select a better nitroxide radical. Experimental data were presented that under identical conditions the stable free radical polymerization of styrene in bulk at 130°C employing the nitroxide DDPO, doubled the rate of polymerization when compared to TEMPO as the reversible capping reagent. Unfortunately, they did not show incremental increases in the number-average molecular weight as a function of monomer conversion, which is necessary to illustrate a living, or controlled polymerization; therefore, the data is inconclusive.

Puts *et al.*[3] also used semi-empirical calculations to locate the transition state for both DDPO-styryl adducts and MB-TMP. From the transition state calculations, the enthalpy of activation $\Delta H^{\neq}$ was found to be 140.9 and 139.3 kJ/mol, respectively for *(R,R)-R* and *(R,R)-S* DDPO-adducts. These values were compared to $\Delta H^{\neq} = 141.2$ kJ/mol calculated for **32**[3] and the experimental enthalpy of activation for **33** of 130 ± 4

kJ/mol reported by Veregin *et al.*[12] More recently the $\Delta H^{\neq} = 131 \pm 7$ kJ/mol was determined for **32** by the ESR method reported by Veregin *et al.*[8] and is included in Chapter 4 of this thesis. The calculated enthalpies of activation reported by Puts *et al.*[3] are approximately 10% higher than the experimental enthalpy of activation data illustrating another deficiency of the semi-empirical methods in locating transition states.

Moad and Rizzardo[2] used semi-empirical molecular orbital calculations on a series of alkoxyamines to establish correlations between structure and C-ON homolysis rates. Various semi-empirical methods were evaluated and this group found that the AM1 method provided the best estimate for calculating heats of formation. As illustrated in Table 1, the BDE values calculated in this work by AM1 are generally lower than the PM3 values and lower when compared to the single crystal data obtained on MB-TMP as discussed previously. Camaioni[13] noted lower calculated AM1 BDE values when compared to experimental data and large errors were apparent between calculated BDEs and experimental H_f for organic nitro compounds.[14]

In addition to obtaining the single crystal X-ray structure of MB-TMP, which was compared to the calculated bonding parameters and geometry obtained by AM1 and PM3, a thorough conformational search was performed on the PM3 calculated geometry

---

[12] Veregin, R. P. N.; Georges, M. K.; Hamer, G. K.; Kazmaier, P. M. *Macromolecules* **1995**, *28*, 4391.
[13] Camaioni, D. M. *J. Am. Chem. Soc.* **1990**, *112*, 9475.
[14] Davis, L. P.; Storch, D. M.; Guidry, R. M. *J. Energ. Mater.* **1987**, *5*, 89. Stewart, J. J. P. *J. Comput. Chem.* **1989**, *10*, 221.

of MB-TMP. This was done to make sure that the minimum chosen was indeed the global or lowest energy minimum. Some of these closed shelled adducts contain 5 or 6 membered aliphatic rings which are very flexible. As a consequence, there are many local minima where the semi-empirical MO calculation could get trapped in a higher energy minimum well and not reach the global minimum.

The conformational search was done using the PhiPsi® macro operating from Excel® which varied two interdependent torsion angles that covered the entire potential energy surface (PES). This search determined all the local energy conformations of MB-TMP, as well as the desired global minimum conformation. The input geometry of MB-TMP was determined by a full geometry optimization using the PM3 Hamiltonian in HyperChem®. The only restrictions made were that the N-O bond was in the equatorial position and the piperidine ring was in the most stable chair conformation. Two dihedral angles Φ_1 ($\angle$ C1-C2-O3-N4) and Φ_2 ($\angle$ C2-O3-N4-C11) were defined as Phi and Psi (see Figure 2) where the starting values of Phi and Psi were 60.0° and –59.4°, respectively. Both angles were varied a full 360 degrees in 10° increments. This input geometry was active in the HyperChem® window and a molecular mechanics MM+ calculation was chosen as the method to compute each point as a function of varying Phi and Psi.

As each point was completed using the MM+ calculation, the potential energy value was tabulated in an Excel® spreadsheet to produce a 36 X 36 chart which was

subsequently plotted in a 3-D plot. Illustrated in Figure 3 is the potential energy surface identifying the global minimum with an energy of 21.02 kcal mol^{-1}, Phi = 150° and Psi = -100°. The lowest energy conformation was then used as the input file for a full geometry optimization using the PM3 Hamiltonian to produce the global

Figure 3: Potential Energy Surface as a Function of Two Torsion Angles: Phi & Psi for MB-TMP

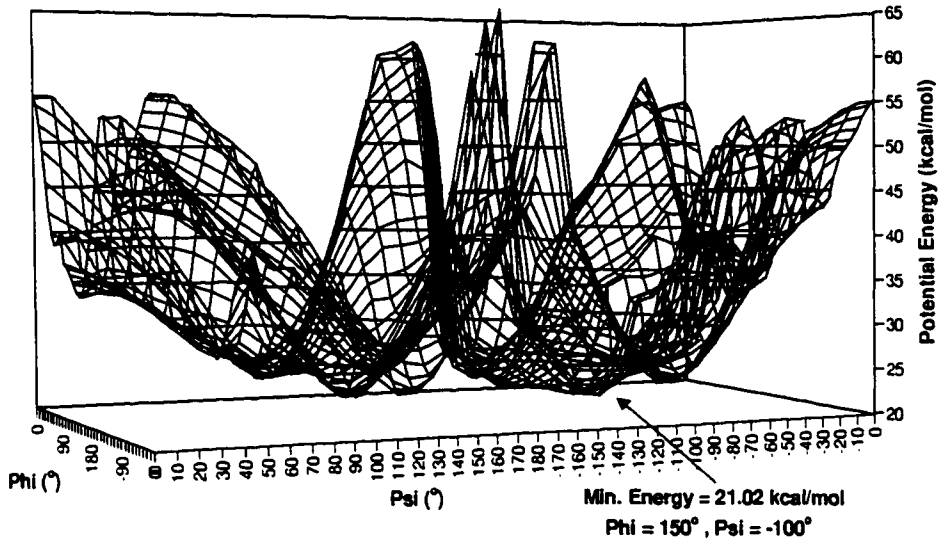

minimum of MB-TMP. The heat of formation of the global conformer was ΔH_f = -15.35 kcal mol^{-1} with Φ_1 = -127.7° and Φ_2 = 110.5°. The PhiPsi® macro was used to perform a conformational search of two interdependent torsion angles followed by a full

geometry optimization to identify the global energy conformer which was necessary for the BDE calculations.

This conformational search confirmed that the geometry that was previously identified was indeed the global energy minimum. This work illustrated that the deficiencies in semi-empirical MO calculations lies in the parameters that describe the N-O bond which is a linear combination of the atomic orbitals; p_x, p_y and p_z for each atom. Using the single crystal X-ray structure for MB-TMP we were able to identify where AM1 and PM3 theoretical calculations break down and why they should not be used in selecting nitroxides for the stable free radical polymerization process.

Chapter 4

NMR and ESR Spectroscopic Evaluation of Nitroxide Adducts

4.1 Introduction and Rationale

As outlined in the introduction (section 1.6), three different approaches have been used to initiate the stable free radical polymerization of vinyl monomers. The most commercially viable route employs conventional free radical initiators such as BPO[1] and AIBN in the presence of vinyl monomers and an excess of the nitroxyl radical. The second method used was to isolate the unimer BST[2, 3] or the like, produced when the initiating benzoyloxy radical from BPO attacks the CH_2 end of a styrene vinyl group, followed by trapping by TEMPO. The third approach was to synthesize alkoxyamine reagents, which are isolated and purified prior to initiating a SFR polymerization. These unimolecular nitroxide adducts contain both the initiating fragment to begin a SFR polymerization and also an equimolar amount of the reversible trapping reagent, the nitroxide, within the same molecule. Various synthetic procedures have been used to

---

[1] Georges, M. K.; Veregin, R. P. N.; Kazmaier, P. M.; Hamer, G. K. *Macromolecules* **1993**, *26*, 2987.

[2] Veregin, R. P. N.; Georges, M. K.; Hamer, G. K.; Kazmaier, P. M. *Macromolecules* **1995**, *28*, 4391.

[3] Hawker, C. J. *J. Am. Chem. Soc.* **1994**, *116*, 11185. Hawker, C. J.; Carter, K. R.; Hedrick, J. L.; Volksen, W. *Polym. Prepr. (Am. Chem. Soc. Div. Polym. Chem.)* **1995**, *36(2)*, 110. Hawker, C. J.; Hedrick, J. L. *Macromolecules* **1995**, *28*, 2993.

prepare nitroxide adducts, including; 1) refluxing ethylbenzene with the initiator *tert*-butyl peroxide in the presence of TEMPO as reported by Priddy *et al.*[4] and Hawker[5] ; 2) trapping benzyl radicals of organometallic reagents with TEMPO at -78°C[5] and 3) utilizing a low temperature procedure reported by Braslau *et al.*[6] involving oxidative routes for producing carbon radicals that are subsequently trapped by TEMPO.

The approach used in this study was to synthesize the initiator / reversible terminating reagents employing the *tri*-n-butyl tin hydride route reported by Anderson *et al.*[7] The reaction conditions include performing the reaction at 5-10°C for 2-4 hours, followed by warming to room temperature, isolation and purification. The low temperature of the reaction enables preparation of a series of alkoxy and aryloxy-tetramethylpiperidine reagents, RO-TMP, where R can include benzyl, tertiary and secondary carbon-centered radicals. Many of these RO-TMP adducts would not have formed if the reaction temperature was above 100°C. The R-groups were chosen to mimic different initiating carbon-centered radicals and different vinyl monomers. In addition, this series of TEMPO-adducts, RO-TMP, was expanded upon by preparing

---

[4] Li, I.; Howell, B. A.; Ellaboudy, A.; Kastl, P. E.; Priddy, D. B. *Polym. Prepr. (Am. Chem. Soc. Div. Polym. Chem.)* **1995**, *36(1)*, 469. Li, I.; Howell, B. A.; Matyjaszewski, K.; Shigemoto, T.; Smith, P. B.; Priddy, D. B. *Macromolecules* **1995**, *28*, 6692. Howell, B. A.; Priddy, D. B.; Li, I. Q.; Smith, P. B.; Kastl, P. E. *Polym. Bull.* **1996**, *37*, 451.

[5] Hawker, C. J.; Barclay, G. G.; Orellana, A.; Dao, J.; Devonport, W. *Macromolecules* **1996**, *29*, 5245.

[6] Braslau, R.; Burrill, L. C.; Siano, M.; Naik, N.; Howden, R. K.; Mahal, L. K. *Macromolecules* **1997**, *30*, 6445. Braslau, R.; Burrill, L. C.; Mahal, L. K.; Wedeking, T. *Angew. Chem. Int. Ed. Engl.* **1997**, *36(3)*, 237.

[7] Anderson, J. E.; Tocher, D. A.; Corrie, J. E. T.; Lunazzi, L. *J. Am. Chem. Soc.* **1993**, *115*, 3494.

adducts based on two other nitroxide radicals; 1,1,3,3-tetraalkylisoindolin-2-yloxyl and 4-benzoyloxy-2,2,6,6-tetramethylpiperidin-1-oxyl.

The nitroxide adduct synthesis will be discussed first in this chapter, followed by a discussion on the ^{1}H and ^{13}C NMR spectra of some of these reversible / terminating reagents. Then the calculated bond dissociation enthalpies (BDE) for breaking the C-O bond in this series of RO-TMP adducts as determined by AM1 and PM3 semi-empirical MO methods will be discussed. The calculated BDE values are compared to the experimental values for the enthalpy of activation ($\Delta H_{k\text{-}L}^{\ddagger}$) for the homolytic C-O bond cleavage reaction as determined by ESR. These nitroxide adducts are model compounds that mimic the dormant propagating polymer chain consisting of the nitroxyl end group. When the temperature of a polymerization is increased above 100°C, and preferably above 120°C, the C-O bond between the propagating polymer chain end and the nitroxide undergoes homolytic cleavage to liberate a free nitroxide and an exposed propagating chain end, which grows in presence of monomer. As discussed in the introduction, there exists an equilibrium between the dormant chain end, and the free nitroxide radical and the propagating carbon-centered radical. When the nitroxyl radical dissociates from the chain end, the chain propagates and then is rapidly captured by the nitroxide radical. This reversible equilibrium of a bond breaking / bond forming reaction continues throughout the polymerization. The homolytic cleavage of the C-O bond in the small molecule nitroxide adducts mimics this reversible termination that is characteristic of the stable free radical polymerization. Using ESR techniques, the enthalpy of activation

required to break this C-O bond in all of the model nitroxide adducts synthesized has been determined. The data can be directly related to the SFR polymerization and provide insight into the main factors controlling the strength of the C-O bond and the reversible capping by the nitroxide. This information will be discussed in the last section of this chapter.

4.2 Experimental Section

The synthesis of all the nitroxide adducts are reported in Chapter 2, section 2.4.

4.2.1 Sample Preparation for Enthalpy of Activation Study by ESR Spectroscopy

Measuring the enthalpy of activation by ESR spectroscopy is illustrated here for the ethylbenzene-tetraethylisoindoline adduct, MB-TEI.

Into a 10 mL volumetric flask was added *N*-(1′-methylbenzyloxy)-1,1,3,3-tetraethylisoindoline (MB-TEI, 10.9 mg, 0.031 mmol) in 10 mL *para*-xylene. The concentration of MB-TEI in *p*-xylene was 3.1×10^{-3} M. Eleven equal aliquots of this solution were weighed into separate thin walled ESR tubes. At the beginning of the experiment the ESR spectrometer was calibrated at 300 K using the strong pitch green reference, which was measured with 20 scans at a receiver gain of 1.0×10^{4}. One of the MB-TEI samples was then inserted into the variable temperature Dewar of the ESR spectrometer which had been previously set at the desired elevated temperature. The temperature range covered in these experiments for the eleven different nitroxide adducts

ranged from 340K to 410K. At each temperature the rate of formation of the nitroxide radical was measured from the double integrated area of the ESR spectrum as a function of time. Typically 8 to 12 scans were obtained for each time point and a total of 12-20 points were collected over 15-20 minutes. Plots of the observed nitroxide concentration as a function of time were linear over most of this time interval. The linear portion of each curve was then used for a linear regression to give the best-fit line representing the rate of nitroxide formation at that temperature. The procedure was repeated using another ESR sample of MB-TEI in *p*-xylene at a different temperature. The experiment was repeated at 3- 5 K intervals depending on the adduct evaluated. For MB-TEI adduct, 11 rates were obtained and these values were then used to calculate the activation enthalpy for the homolysis of the C-ON bond in MB-TEI. In order to obtain accurate activation energies for each adduct, the relative rate measurements were made on identical sample volumes of each adduct solution. This procedure was followed for all the different nitroxide adducts evaluated in this study.

4.3 Results and Discussion

4.3.1 ^{1}H and ^{13}C NMR Spectroscopic Analysis of Nitroxide Adducts

To enhance our understanding of the stable free radical polymerization process, a series of model initiator reversible terminating agents were prepared. This included aryloxy- and alkyloxy-TEMPO adducts denoted as RO-TMP, *N*-(methyl-iso-propionate-2-oxy)-4-benzoate-TEMPO also called MiP-4BenTMP, and other ethylbenzyl-adducts

where the nitroxide radicals employed were 1,1,3,3-tetramethyl- and 1,1,3,3-tetraethylisoindolin-2-yloxyl. All the nitroxide adducts were prepared using the *tri*-n-butyl tin hydride synthetic procedure previously reported by Anderson *et al.*[7] The reaction is shown in Figure 4 for the synthesis of *N*-trialkylhydroxylamines from TEMPO and various alkyl or aryl halides.

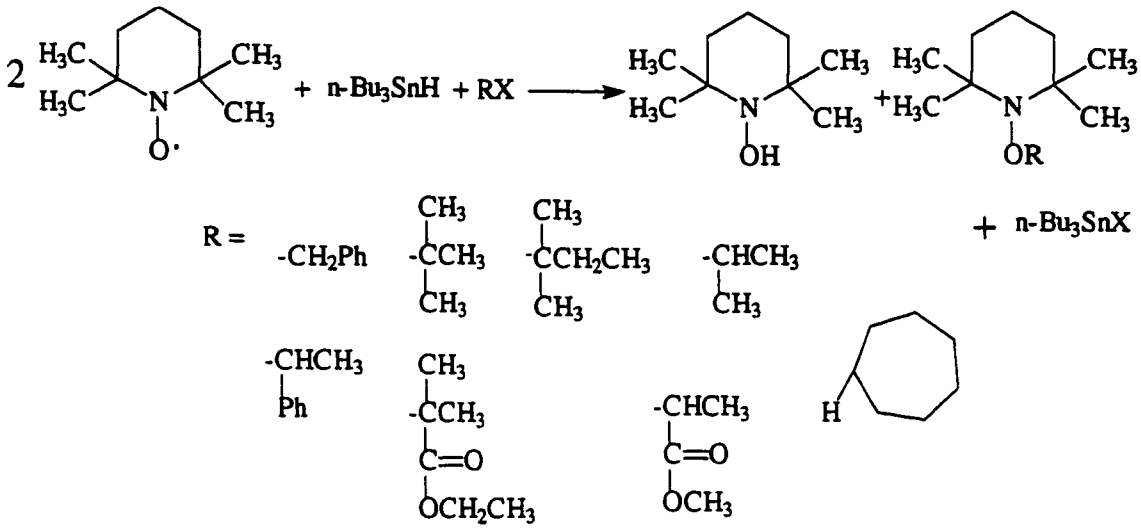

Figure 4: Synthesis of initiator / reversible terminating adducts RO-TMP using TEMPO as the nitroxide.

A series of different alkyl or aryl halides were reacted with four different nitroxides. The yield of the reactions varied due to the instability of the resulting product and difficulty in separating the tin halide byproduct from the nitroxide adduct. For example, the yield of *i*P-TMP was only 3.1 % whereas the yield of MB-TMP was 64%. However, an advantage of this synthetic route over the refluxing solvent procedure used

by Priddy[4] and Hawker[5] or the photochemical route used by Scaiano[8] is that acrylate or methacrylate functional groups can be more easily trapped by the nitroxyl radical without decomposition. For example, the MiP-TMP adduct consisting of a methyl acrylate radical fragment trapped by TEMPO was prepared by the tin hydride route. Thus, MiP-TMP models a propagating acrylate SFRP chain end. Similarly, the EiB-TMP adduct consisting of an ethyl methacrylate radical fragment models a methacrylate propagating SFRP chain end.

Under an inert atmosphere of Ar, two molar equivalents of nitroxide are necessary for the reaction to go to completion. The nitroxide abstracts a hydrogen radical from *tri*-n-butyl tin hydride to generate the *N*-hydroxylamine and the resulting *tri*-n-$Bu_3Sn\bullet$ subsequently reacts with the alkyl halide to form n-Bu_3SnX and a carbon-centered radical. The reactive carbon-centered radical is immediately trapped by a second molecule of nitroxide at close to diffusion controlled rates.[9] The reaction can be followed visually since the characteristic orange-red colour of the unreacted nitroxide in solution fades to produce a clear and almost colourless mixture when the reaction is completed. The resulting product mixture was concentrated by rotor evaporation of the solvent. The products were isolated by flash chromatography.[10] Four of the products, MB-TMP, MiP-TMP, MiP-4BenTMP and MB-TMI were crystalline and the other

---

[8] Connolly, T. J.; Baldovi, M. V.; Mohtat, N.; Scaiano, J. C. *Tet. Lett.* **1996**, *37(28)*, 4919.
[9] Chateauneuf, J.; Lusztyk, J.; Ingold, K. U. *J. Org. Chem.* **1988**, *53*, 1629. Beckwith, A. L. J.; Bowry, V. W.; Moad, G. *J. Org. Chem.* **1988**, *53*, 1632. Beckwith, A. L. J.; Bowry, V. W.; Ingold, K. U. *J. Am. Chem. Soc.* **1992**, *114*, 4983. Bowry, V. W.; Ingold, K. U. *J. Am. Chem. Soc.* **1992**, *114*, 4992.

products, B-TMP, *t*A-TMP, *t*B-TMP, EiB-TMP, iP-TMP, CH-TMP and MB-TEI were liquid.

The ^{1}H and ^{13}C NMR spectra were obtained for each nitroxide adduct. The following adducts, MiP-TMP, MiP-4BenTMP, MB-TMI, *t*A-TMP, EiB-TMP, *i*P-TMP and MB-TEI are new materials and have not been previously reported in the literature. A selected number of these spectra are presented below. The proton NMR spectra for the alkoxy-TMP series of compounds illustrates a dynamic NMR intramolecular exchange process that can be followed by variable temperature NMR. The exchange process previously observed by Anderson *et al.*[11] on different *N*-acyloxy-2,2,6,6-tetramethylpiperidine molecules, consists of a complex combination of ring inversion, nitrogen inversion and rotation about the N-O bond. With the larger less flexible nitroxides, 1,1,3,3-tetramethyl and 1,1,3,3-tetraethylisoindolin-2-yloxyl, the resulting *N*-trialkylhydroxylamines undergo only two intramolecular exchange processes; nitrogen inversion and rotation about the N-O bond as studied by Busfield *et al.*[12] In their short communication, five different nitroxide adducts were prepared employing the nitroxide 1,1,3,3-tetramethylisoindolin-2-yloxyl. The 1-methylbenzyl functional group was not used to prepare their five adducts, therefore, adducts MB-TMI and MB-TEI are new materials.

---

[10] Still, C. W.; Kahn, M. Mitra, A. *J. Org. Chem.* **1978**, *43*, 2923.
[11] Anderson, J. E.; Corrie, J. E. T. *J. Chem. Soc. Perkin Trans.* **1992**, *2*, 1027.
[12] Busfield, W. K.; Jenkins, I. D.; Thang, S. H.; Moad, G.; Rizzardo, E.; Solomon, D. H. *J. Chem. Soc., Chem. Commun.* **1985**, 1249.

In Figure 5, signals due to the four diastereotopic ring methyls are shown as four well separated singlets resonating at δ 0.92, 1.26, 1.42 and 1.60. An expansion of this region is shown as an insert on the full ^{1}H NMR spectrum. The presence of four distinct lines is due to the asymmetric centre in the molecule, and the orientation of the phenyl ring attached to the chiral center also contributes to this large resonance difference between the four lines. The methyl group attached to the asymmetric center of the 1-methylbenzyloxy group also appears in the insert at 1.57 ppm. This signal is a doublet with ^3J = 6.8 Hz due to the methine proton. The characteristic methine proton of the

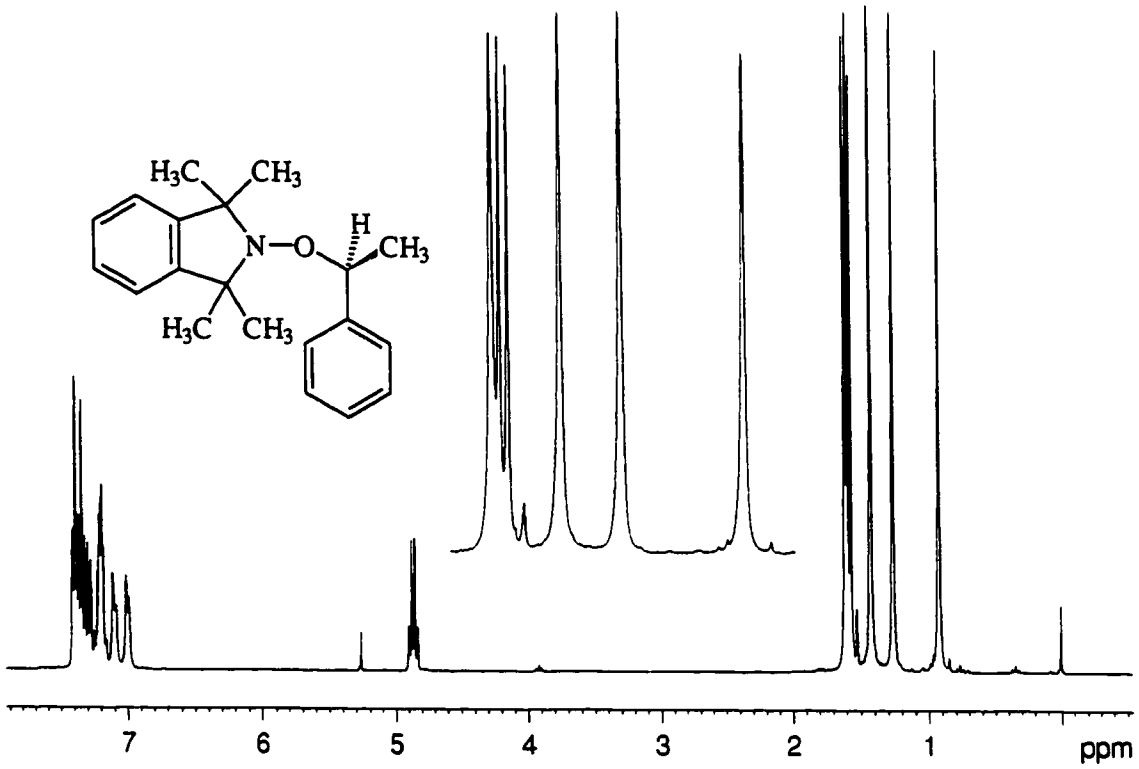

Figure 5: 300 MHz ^{1}H NMR spectrum of nitroxide adduct MB-TMI.

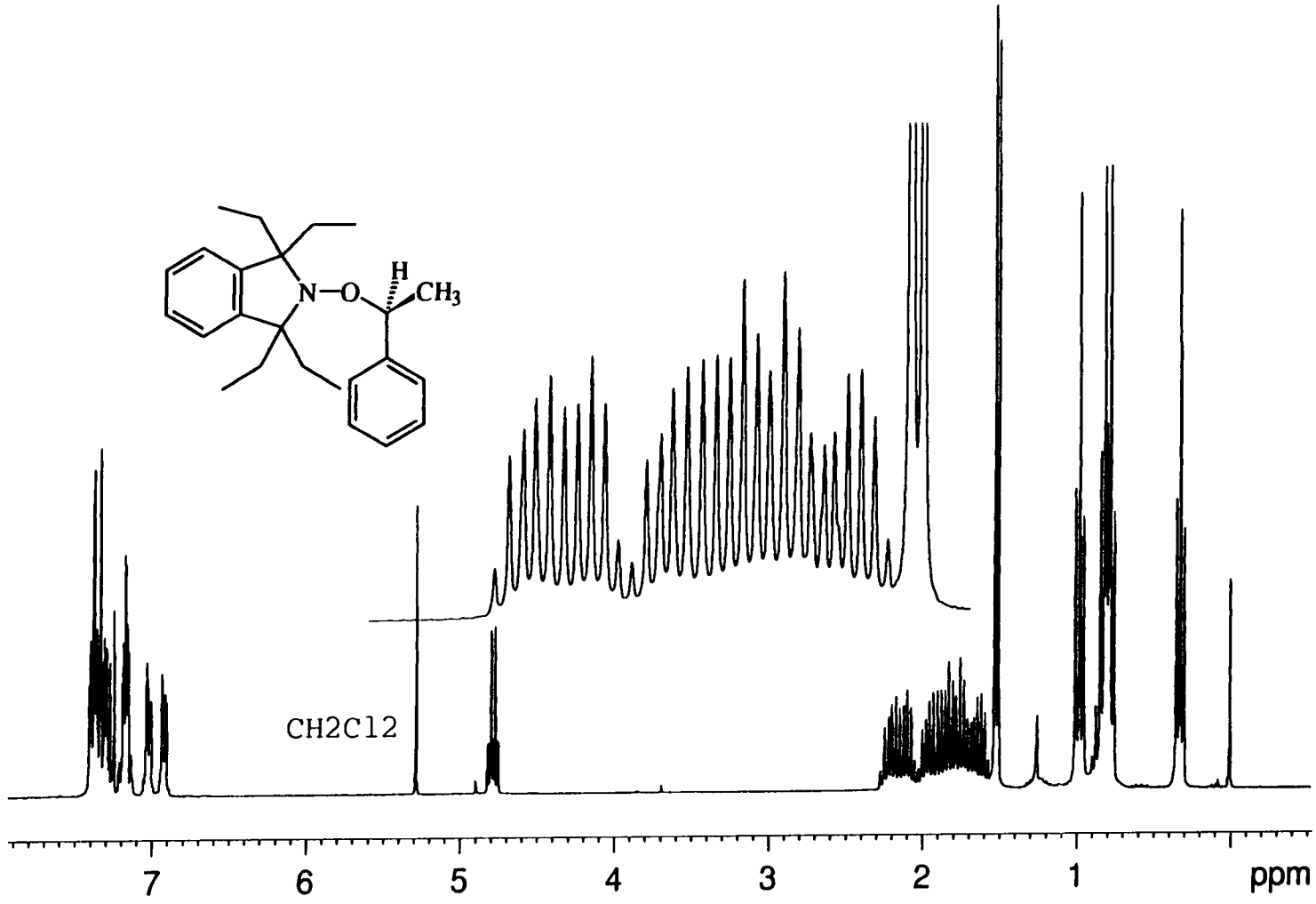

Figure 6: 300 MHz Proton NMR spectrum of nitroxide adduct MB-TEI.

styrene-nitroxide adducts appears at δ 4.86 as a quartet due to coupling to the methyl group (^3J = 6.8 Hz) and some residual methylene choride appears at 5.25 ppm. The four aromatic protons of the isoindoline ring are split showing separate multiplet resonances for two different *ortho*-aryl protons at 7.05-7.07 and 7.14-7.17 ppm. The other two aryl protons of the isoindoline are in the complex resonances at 7.23 to 7.47 ppm along with the 5 aryl protons on the phenyl ring.

Replacing the four methyls with ethyl groups in MB-TEI at the carbons alpha to the N-O bond increases the complexity of the ^1H spectrum as demonstrated in Figure 6. The four CH_3 singlets are replace by four triplets due to the coupling to the methylene protons (^3J = 7.5 Hz). The methylene protons illustrate a complex splitting pattern because all 8 protons are not equivalent as a result of the orientation of the phenyl ring, which shields one side of the molecule more than the other. In fact, one methylene proton resonates upfield in the methyl region at approximately 0.8 ppm. The quartet at δ 4.79 is due to the methine proton on the asymmetric center (^3J = 6.8 Hz) and the single peak at 5.3 ppm is due to residual methylene chloride. The aromatic region is similar to the same region discussed for MB-TMI consisting of four isoindoline methine protons and 5 phenyl methine protons.

The signals of the ^{13}C J-modulated spin-echo NMR spectra for the new compounds MB-TMI and MB-TEI are illustrated in Figure 7 and 8, respectively. All the signals are assigned. Signals with positive amplitudes are assigned to CH or CH_3 groups and those with negative amplitude are assigned to quaternary carbons or CH_2 groups. One

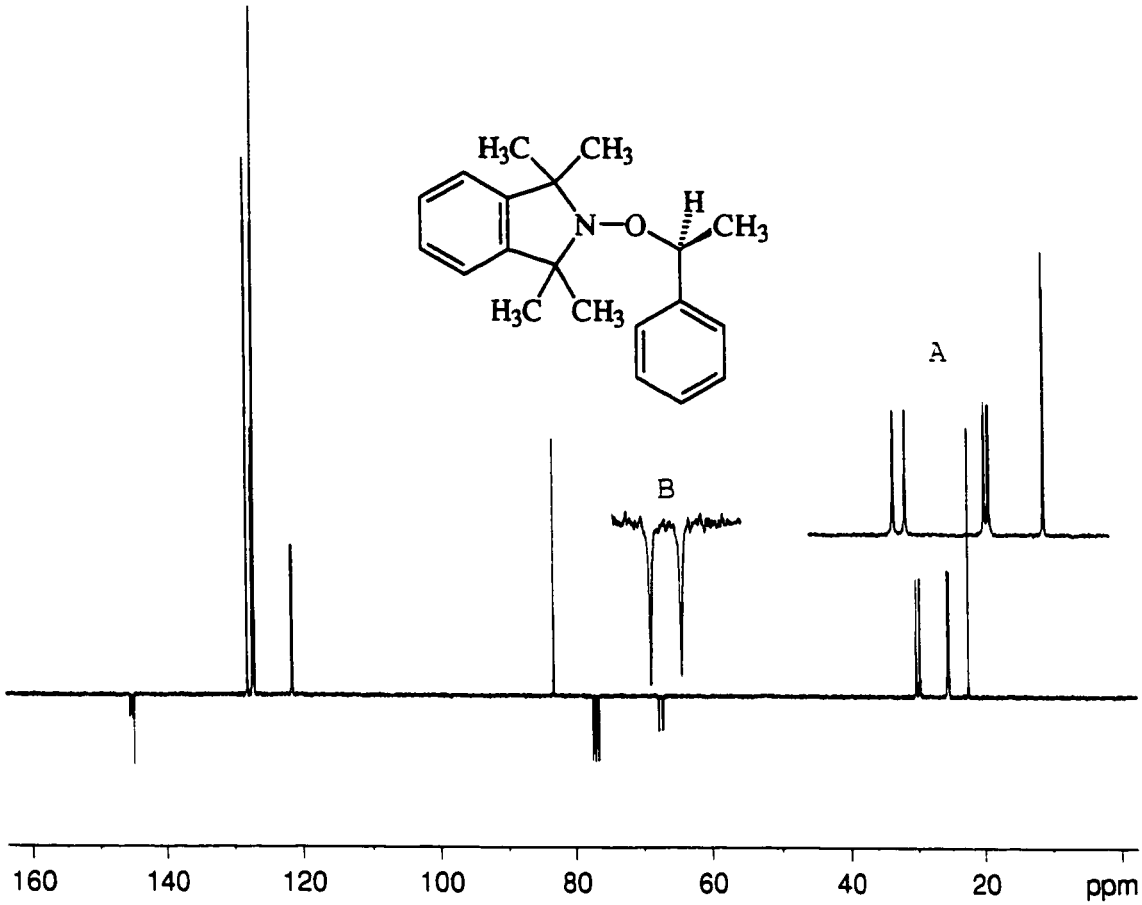

Figure 7: 300 MHz J-modulated spin-echo (J = 140 Hz) ^{13}C NMR spectrum of nitroxide adduct MB-TMI.

of the interesting features in both of these spectra is that the two quaternary carbons of the fused isoindoline ring are not equivalent and the two alpha quaternary carbons next to the nitroxide functional group are also not equivalent. In Figure 7 adduct **60**, MB-TMI, shows two quaternary carbon signals at 67.11 and 67.68 ppm (insert B) and 3 signals

around 145 ppm, corresponding to the quaternary carbon of the phenyl ring (145.06 ppm) and to the two quaternary carbons of the fused rings in the isoindoline portion of the molecule (δ 145.43, 145.85). The four methyls of the nitroxide resonate at δ 25.23, 25.46, 29.66 and 30.24 (see insert A) along with the α-methyl group of ethylbenzyl at 22.5 ppm. The two methyl resonances at δ 25.23 and 25.46 correspond to methyl groups *anti* to the nitrogen lone pair and the two methyl resonances at δ 29.66 and 30.24 are due to the methyl groups *syn* to the nitrogen lone pair.

In the ^{13}C NMR J-modulated spin-echo spectrum of MB-TEI shown in Figure 8, similar splitting of the quaternary carbons are illustrated. The two quaternary carbons alpha to the nitroxide are shifted downfield to δ 72.90 and 73.47 (insert C) which is a large shift of 5 ppm when compared to the same carbons in MB-TMI. The two nonequivalent aromatic quaternary carbons in the isoindoline portion of the molecule resonate at 142.24 and 142.30 ppm. The methylene region is expanded and shown in insert B along with the four separate methyl groups of the ethyl substituents shown in insert A. The exchange process in MB-TMI and MB-TEI is very slow or non-existant since the methyl and ethyl protons are well resolved.

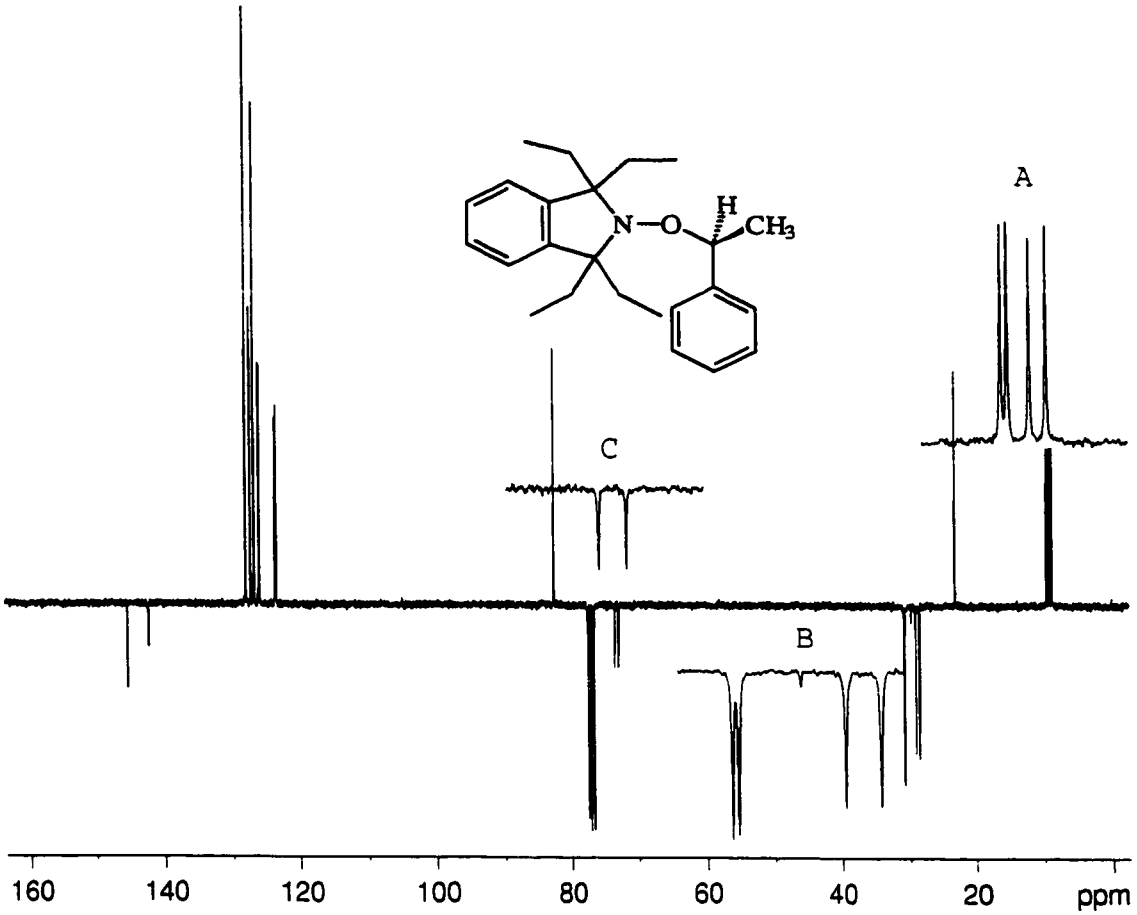

Figure 8: 300 MHz J-modulated spin-echo (J = 145 Hz) ^{13}C NMR spectrum of nitroxide adduct MB-TEI.

In the case of the various aryloxy and alkyoxy-tetramethylpiperidine adducts the dynamic exchange process is even more complex. The dynamic exchange conformation process[11] involves piperidine ring inversion, nitrogen inversion and rotation about the nitrogen-oxygen bond. This exchange process is evident by the number of methyl peaks shown in the ^{1}H NMR spectra, which is a function of the R group and the temperature dependence on the exchange. At room temperature, and in molecules that do not contain

a chiral center, the four ring methyls can appear as a broad hump as in the case of *i*P-TMP (Figure 9), or as a sharp singlet as illustrated for 4BenTMPOH (Figure 10), or as two sharp singlets demonstrated for EiB-TMP (Figure 11) and *t*A-TMP (Figure 12).

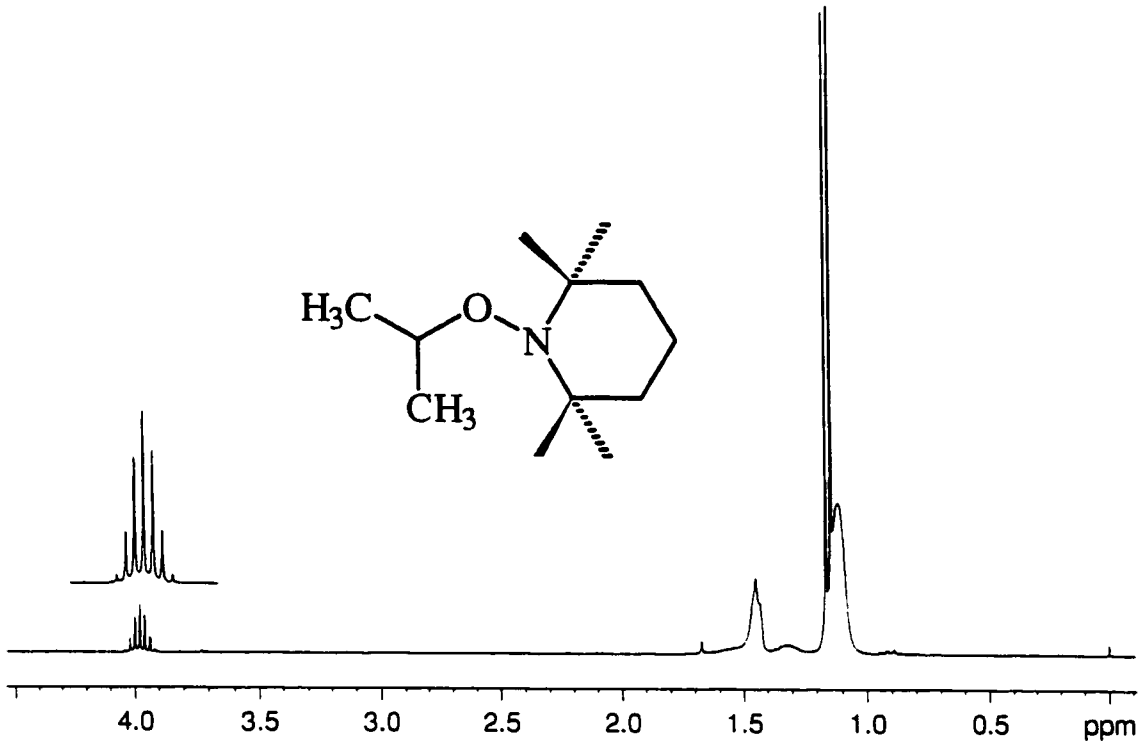

Figure 9: 300 MHz ^{1}H NMR spectrum of nitroxide adduct *i*P-TMP.

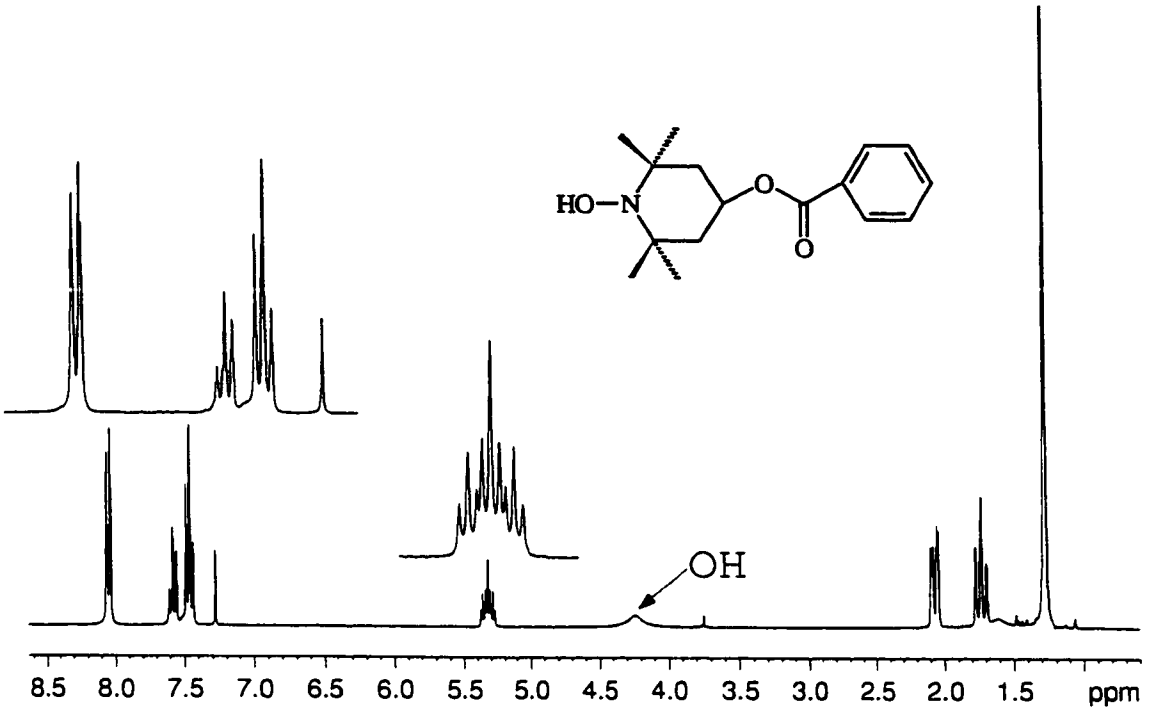

Figure 10: 300 MHz ^{1}H NMR spectrum of the nitroxide derivative 4BenTMPOH.

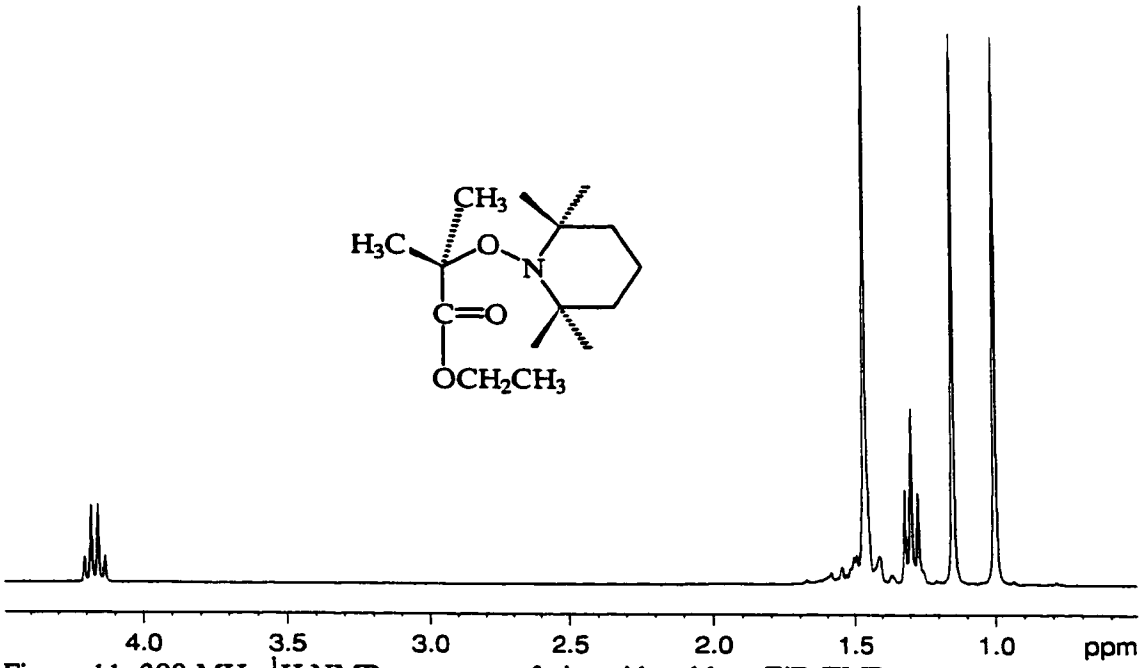

Figure 11: 300 MHz ^{1}H NMR spectrum of nitroxide adduct EiB-TMP.

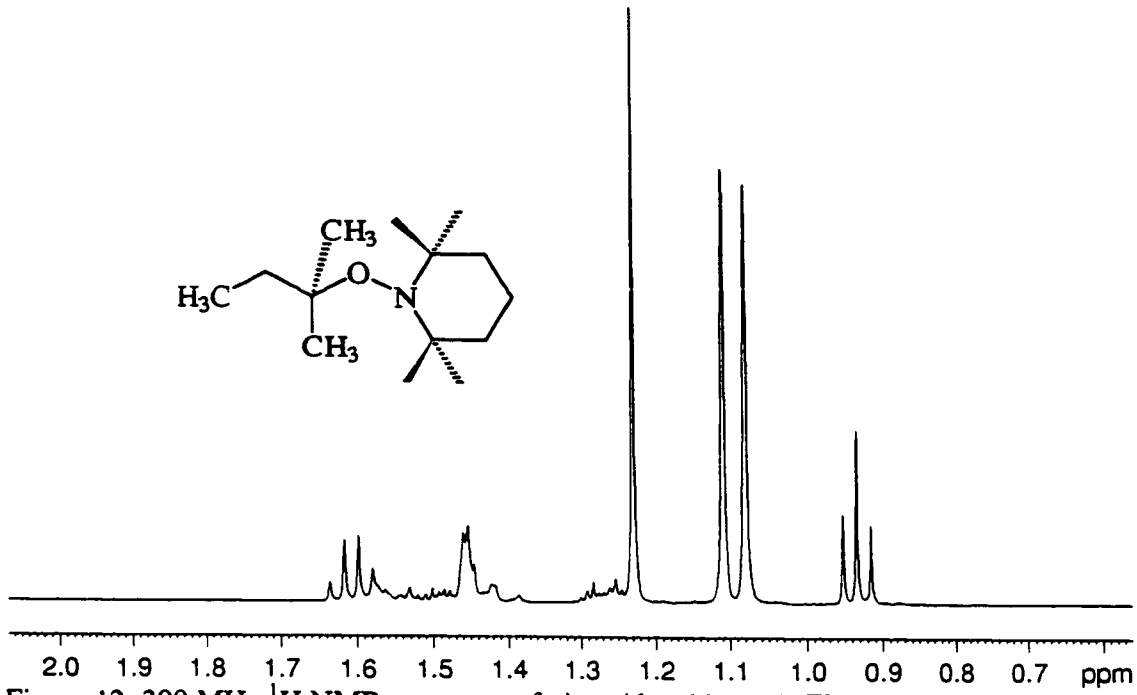

Figure 12: 300 MHz ^{1}H NMR spectrum of nitroxide adduct *t*A-TMP.

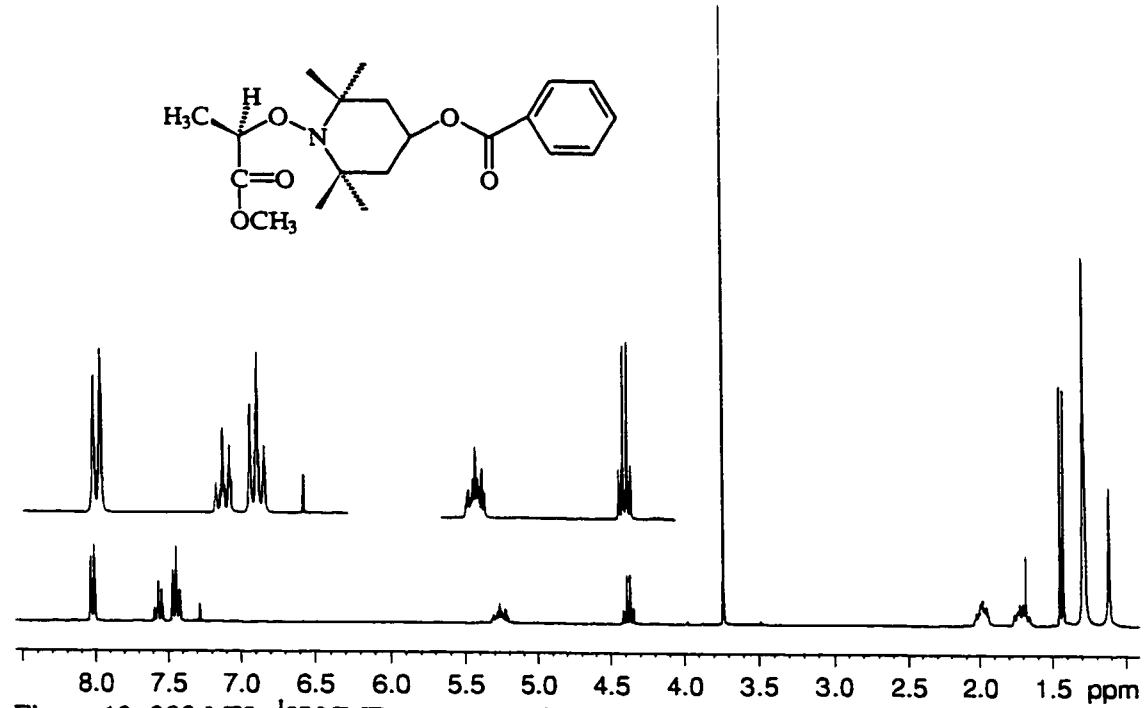

Figure 13: 300 MHz ^{1}H NMR spectrum of nitroxide adduct MiP-4BenTMP.

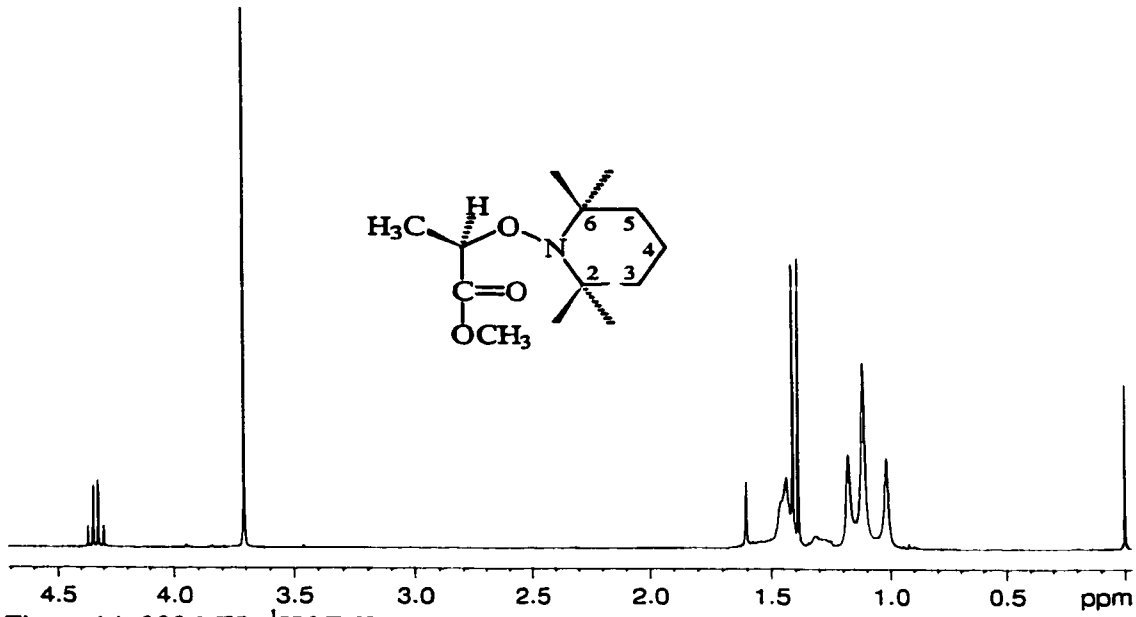

Figure 14: 300 MHz ^{1}H NMR spectrum of nitroxide adduct MiP-TMP.

When the molecule contains a chiral center, the four ring methyl groups may appear as two non-symmetrical singlets as illustrated for MiP-4BenTMP in Figure 13. If the dynamic intramolecular exchange process is faster at room temperature, then the four methyl groups may also appear as three signals as in MiP-TMP (Figure 14). Figure 15 and 16 are 400 MHz variable temperature ^{1}H NMR spectra of MB-TMP and BST, respectively. At a low temperature (243K) the four piperidine methyl protons (denoted as A) in both MB-TMP and BST spectra appear as four sharp singlets. As the temperature is increased to 328 K for MB-TMP and 333 K for BST, coalescence of the four sets of methyl protons occurs producing a broad band. The shielding of the phenyl ring at higher temperatures becomes equivalent, whereas, at room temperature or lower, the methyl protons are in different magnetic environments.

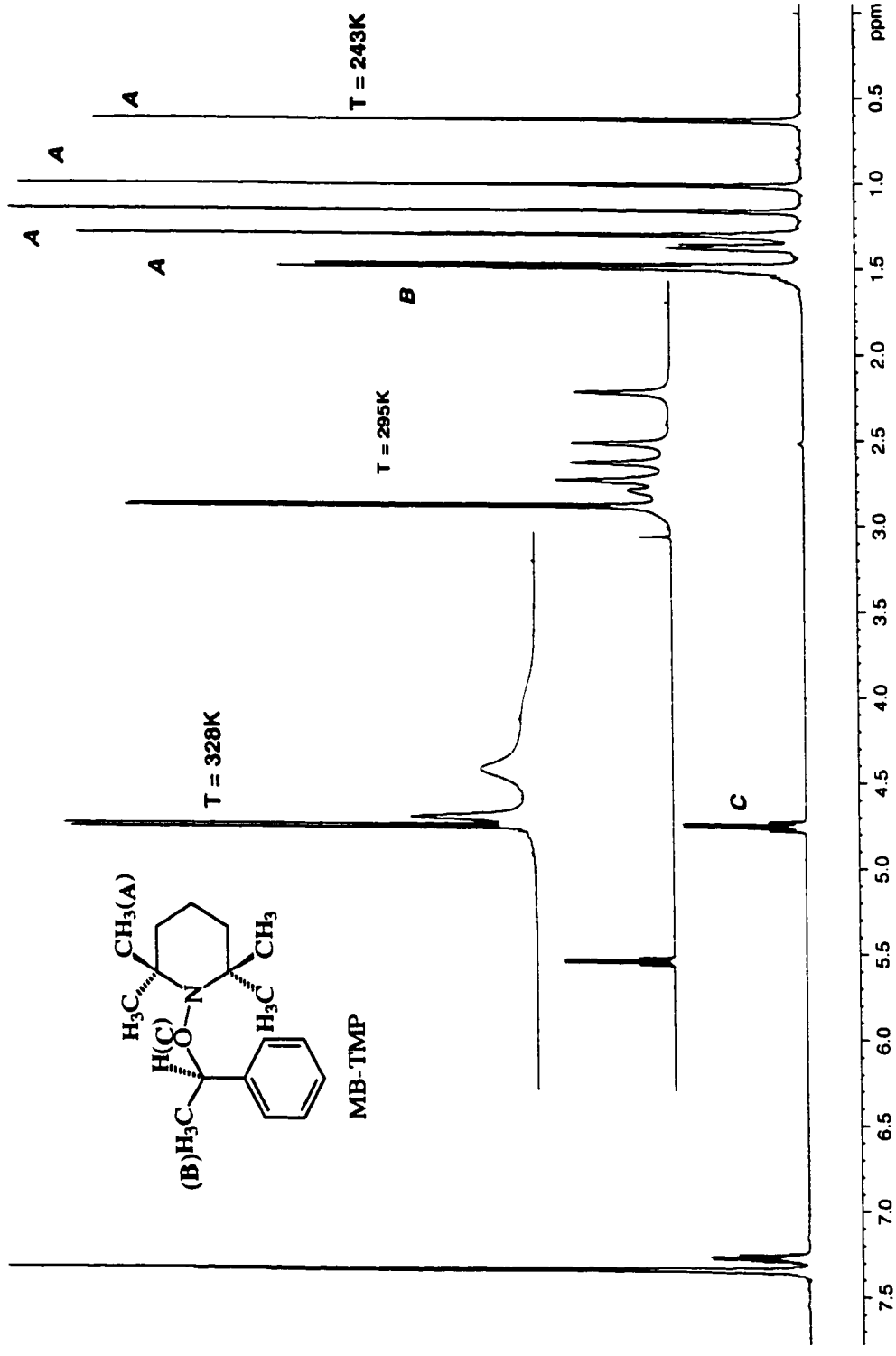

Figure 15: 400 MHz variable temperature ^{1}H NMR spectra of nitroxide adduct MB-TMP

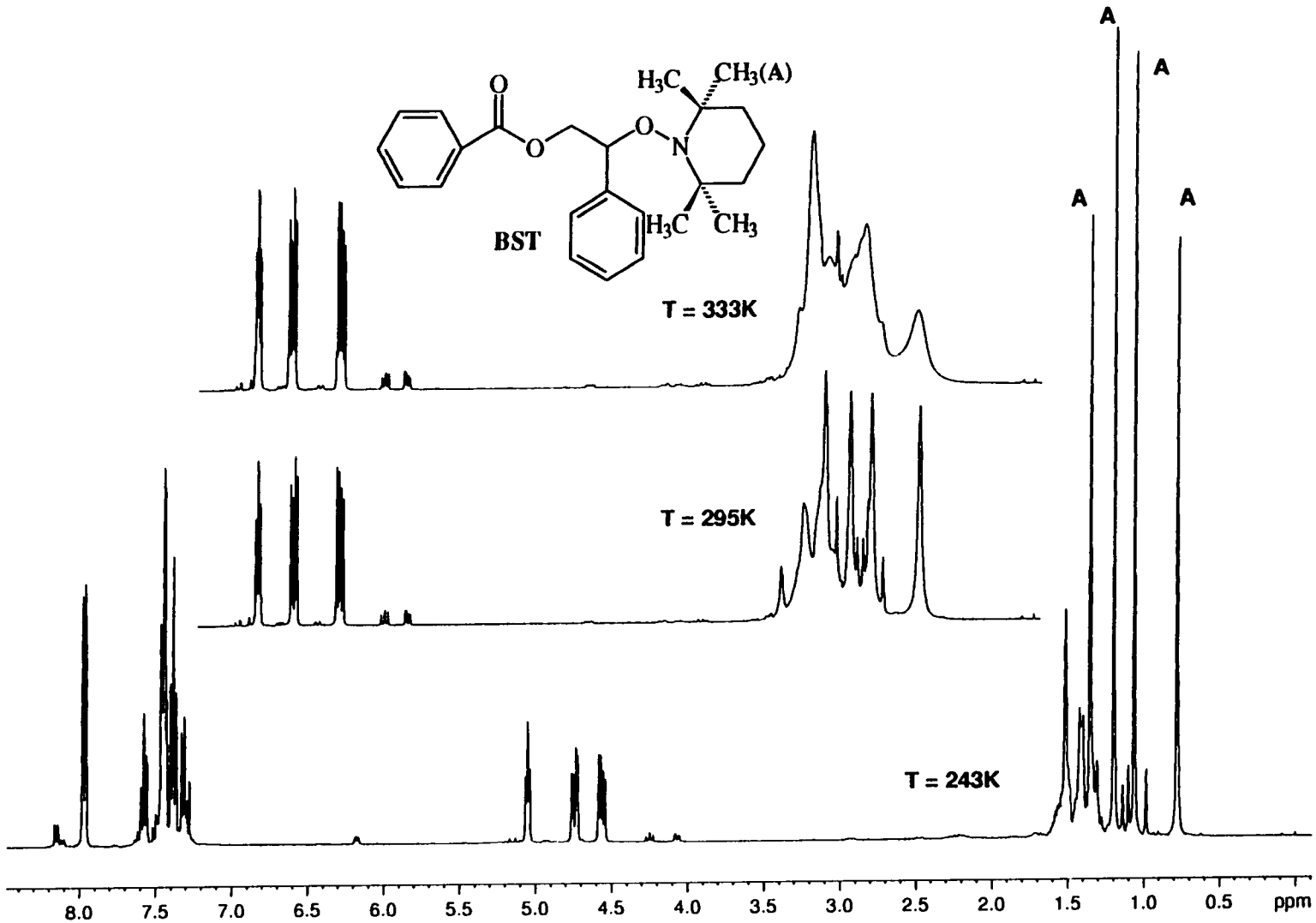

Figure 16: 400 MHz variable temperature ^{1}H NMR spectra of the isolated unimer BST.

During the synthesis of the nitroxide adducts, one molar equivalent of *N*-hydroxylamine is formed relative to the R-nitroxide compounds. In the case of TEMPO, the *N*-hydroxylamine is very sensitive to air and, over a couple of hours, the mixture turns red, due to oxidation of the *N*-hydroxylamine by O_2 to TEMPO. As a consequence, the *N*-hydroxylamine of TEMPO could not be isolated. During the workup of MiP-4BenTMP, which contains a benzoyloxy group at the 4-position on the piperidine ring, a white crystalline material precipitated out of solution. The white product, soluble in Et_2O but insoluble in hexane was purified, isolated and characterized by NMR and mass spectroscopy. Shown in Figure 10 is the ^1H NMR spectrum of 4BenTMPOH with a very distinctive broad OH resonance at 4.25 ppm. To verify that this compound was indeed the *N*-hydroxylamine of 4-benzoxyloxy-2,2,6,6-tetramethylpiperidine, the OH proton was exchanged with deuterium by adding a few drops of D_2O into the NMR tube and shaking it. After a few minutes the ^1H NMR spectrum was taken again and the OH proton resonance disappeared. The mass spectrum was obtained both by chemical ionization (CI) using ammonia as the reagent gas, and by electron impact (EI) ionization. The EI spectrum contained a m/z +1 peak at 278 for the mass of the *N*-hydroxylamine (FW = 277 g/mol). A mass spectrum obtained by CI with NH_3 as illustrated in Figure 17, also confirmed the mass of the *N*-hydroxylamine with an intense peak at m/z of 278.

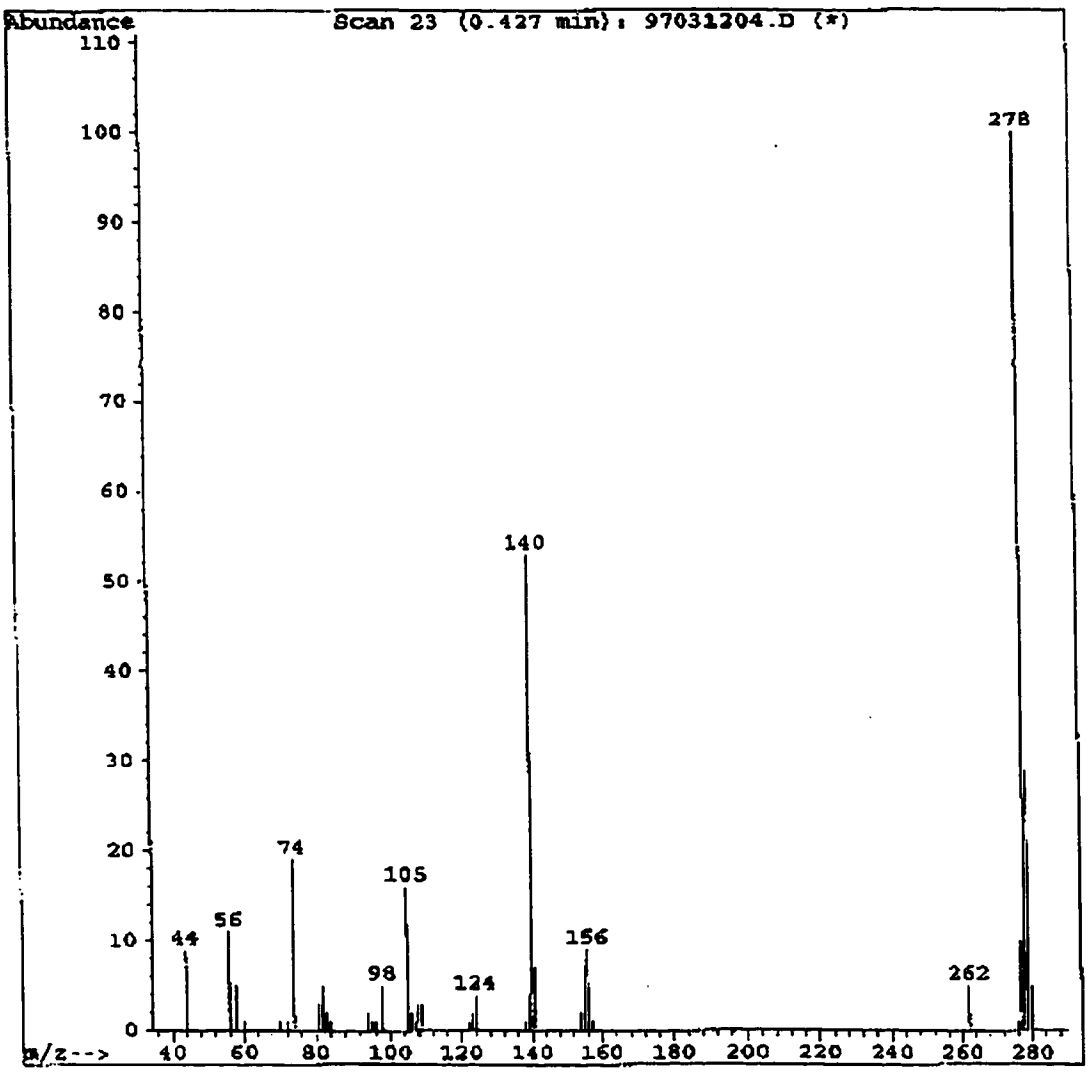

Figure 17: Chemical ionization (CI + NH_3) mass spectrum of *N*-hydroxyl-2,2,6,6-tetramethyl-4-benzoyloxypiperidine, 4BenTMPOH.

4.3.2 Enthalpy of Activation for C-O Bond Breaking in Nitroxide Adducts Activation

This series of model initiator / reversible terminating agents were used to determine the strength of the C-ON bond between different nitroxides and different carbon-centered radicals. As previously mentioned, these carbon-centered radicals were chosen not only to systematically evaluate benzyl, tertiary and secondary carbon-centered radicals which mimic various initiators, but also to evaluate different vinyl monomers such as styrene, acrylates and methacrylates. As described in the introduction section 1.6 on the stable free radical polymerization process, the control of the SFRP is achieved through the equilibrium between the radical capture rate and reversible homolytic cleavage of the capped polymer chain end. The rate of polymerization is controlled by K_L, k_p and the free nitroxide concentration denoted by T•. For a given monomer, the rate constant of propagation, k_p, is fixed but it is possible to change K_L since K_L depends on k_L and k_{-L} as denoted in equation 14 section 1.6. k_L is the rate constant of radical capture by the nitroxide and is close to being diffusion controlled, but k_{-L} depends on the strength of the C-ON bond between the nitroxide and the carbon-centered radical which represents a propagating polymer chain end. The rate constant k_{-L}, is the rate of homolytic cleavage of the C-ON bond to give the propagating polymer chain end and the free liberated nitroxide radical as shown in equation 13 of section 1.6. The strength of the C-ON bond might vary for different nitroxides and for different carbon-centered radicals. Variations in the C-O bond strength will be a function of steric and electronic factors on this bond. The

aim of the ESR study is to identify any changes. Using these small molecules that represent the important chain end of an SFR polymerization, we can isolate and determine what the important factors are that control the bond strength and thus the rate of homolytic cleavage for this C-ON bond.

The initial study of measuring the strength of the C-O bond via a series of ESR measurements to obtain the enthalpy of activation ($\Delta H_{k\text{-}L}^{\ddagger}$) for the C-O bond cleavage reaction was initiated and performed on two model compounds, BST and BSP.[2] The approach developed by Veregin *et al.*[2] was adopted for this more comprehensive study involving the adducts listed in Table 3.

The *para*-xylene solutions were prepared as described in the experimental section

Table 3: Initial Conditions for Enthalpy of Activation Measurements by ESR: Initial Concentration of the Model Nitroxide Adduct Compounds and Free Nitroxide Concentration

Model Compounds	Acronyms	[R-Nitroxide] (mol/L)	[Free Nitroxide] (mol/L)
N-(Benzyloxy-TMP)	B-TMP	2.0×10^{-3} M	6.0×10^{-7} M
N-(1′-Methylbenzyloxy)-TMP	MB-TMP	4.1×10^{-3} M	N/A
N-(t-Amyloxy)-TMP	tA-TMP	1.5×10^{-2} M	5.5×10^{-6} M
N-(t-Butoxy)-TMP	tB-TMP	1.4×10^{-2} M	1.0×10^{-7} M
N-(Ethyl-iso-butyrate-2-oxy)-TMP	EiB-TMP	2.3×10^{-2} M	2.5×10^{-4} M
N-(Cycloheptoxy)-TMP	CH-TMP	1.7×10^{-2} M	4.4×10^{-6} M
N-(Methyl-iso-propionate-2-oxy)-TMP	MiP-TMP	4.8×10^{-2} M	N/A
N-(Methyl-iso-propionate-2-oxy)-4-BenTMP	MiP-4BenTMP	9.1×10^{-3} M	3.0×10^{-7} M
N-(1′-Methylbenzyloxy)-TMI	MB-TMI	8.3×10^{-3} M	3.0×10^{-7} M
N-(1′-Methylbenzyloxy)-TEI	MB-TEI	3.1×10^{-3} M	1.1×10^{-6} M

4.2, and were heated one at a time in the ESR cavity. As shown in Table 3, the concentration of each nitroxide adduct solution in *p*-xylene was kept as constant as possible. The concentrations ranged from 2.0×10^{-3} to 4.8×10^{-2} M. Within one adduct series the concentrations were identical. For each adduct evaluated in these ESR experiments except for MB-TMP and MiP-TMP, the free nitroxide concentration was measured on one of the ESR samples prior to heating at 300 K. In all the measured samples, the concentration of free unbound nitroxide was very low (10^{-6} to 10^{-7} M). Even after extensive purification of the adducts, there was always free unbound nitroxide present, evidence of an equilibrium between the dormant nitroxide adduct and free nitroxyl stable radical in solution.

The concentration of the liberated nitroxide was followed over time using ESR to determine the rate of bond breaking for the C-ON bond. By systematically varying the temperature, the enthalpy of activation, ($\Delta H_{k\text{-}L}^{\ddagger}$) required to break the carbon-oxygen bond was also determined. Figures 18 and 19, for the nitroxide adduct *N*-(*tert*-butoxy)-2,2,6,6-tetramethylpiperidine, *t*B-TMP, represent sets of data and the best-fit linear regression curves for the increase in TEMPO concentration as a function of time at each different temperature. The temperature range covered for this adduct was from 350 K to 380 K. The curves are linear as long as the temperature is kept low and /or the data

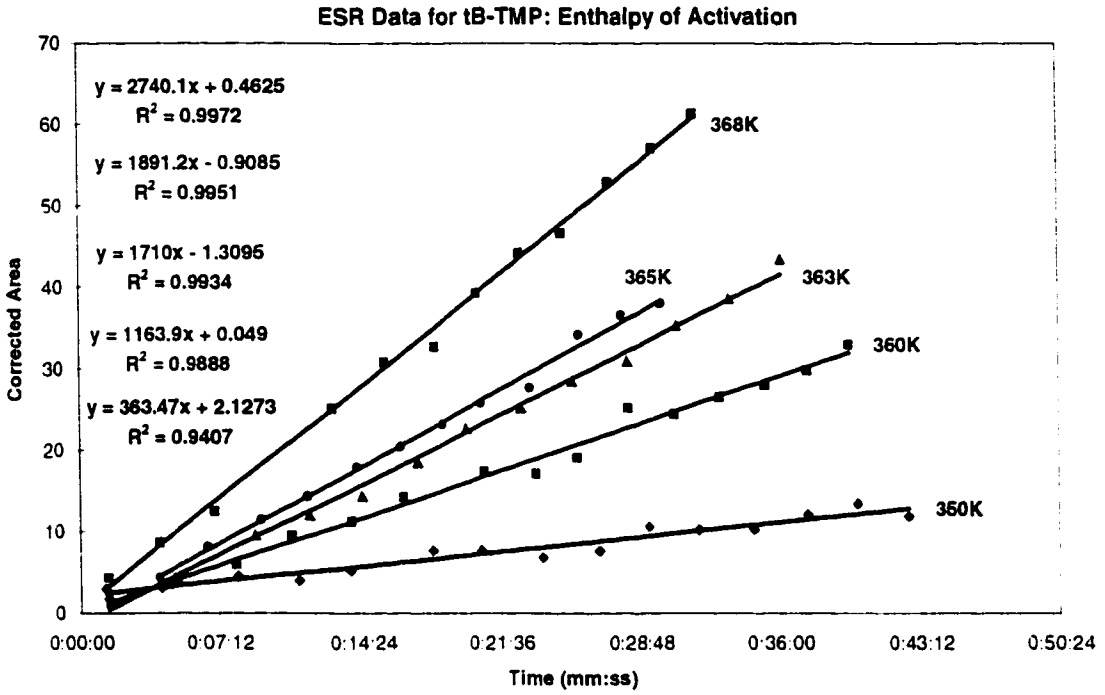

Figure 18: ESR data for *t*B-TMP: Calculation of observed rates for liberating TEMPO at various temperatures (350K to 368K).

collection period is short (< 30 minutes). This is to minimize the various termination reactions that compete with the radical trapping/bond breaking reactions.

Veregin *et al.*[2] showed that to a good first order approximation, the termination reactions can be ignored when analyzing the initial few minutes of the polymerization at each temperature. The adducts evaluated in this study demonstrate that when the temperature is kept low, the reaction profiles are linear over a longer period of time. When the temperature is too high, the reaction profiles show curvature at longer reaction

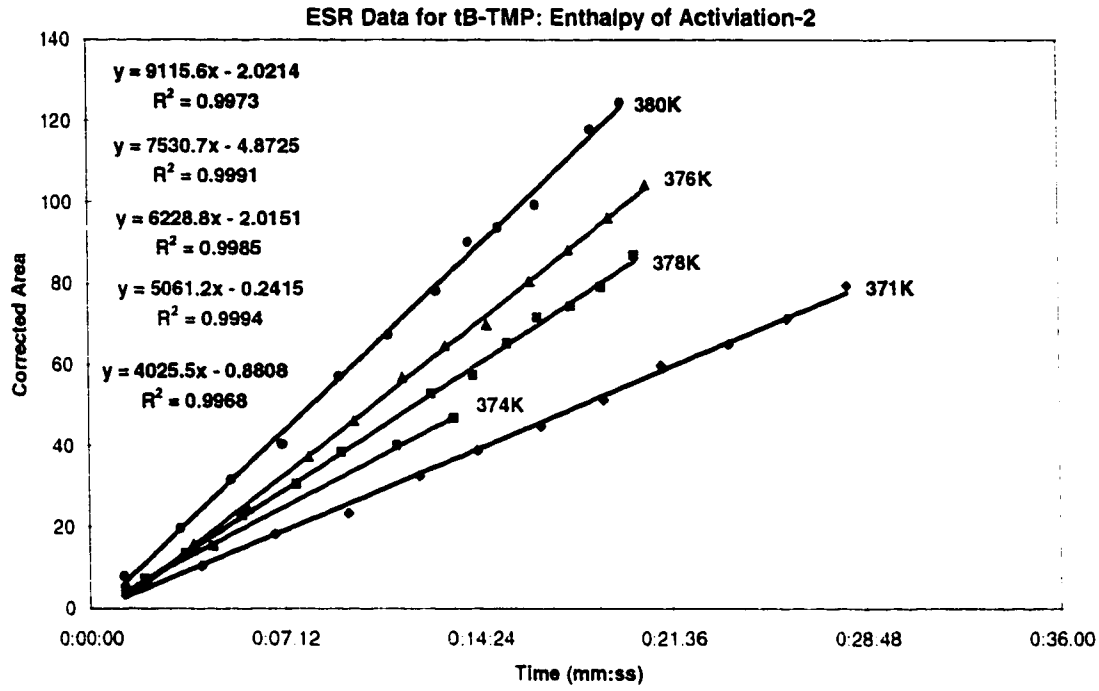

Figure 19: ESR data for *t*B-TMP: Calculation of observed rates for liberating TEMPO at various temperatures (371K to 380K).

times which is evidence of competing termination reactions becoming more pronounced. These termination reactions were previously reported by Veregin *et al.*[2], which include carbon-centered radical termination by coupling or disproportionation, or the involvement of the solvent through chain transfer of a hydrogen radical to the carbon-centered radical and subsequent solvent radical capture by the nitroxide or the carbon-centered radical. As long as the initial reaction profile for each adduct solution is

determined over a relatively short period of time, and the temperature range is minimized, the termination reactions can be neglected.

As shown in the kinetic analysis explicitly developed by Veregin *et al.*[2] and summarized in section 1.6 of the thesis introduction, the initial observed rates, k_{obs} which are a relative value of $k_{-L}k_t / k_L$ can be measured. From the k_{obs}, it is possible to calculate the activation energy ($\Delta H^{\neq}$) as being approximately equal to the enthalpy of activation for breaking the C-ON bond ($\Delta H_{k-L}{}^{\neq}$) in different adducts since $\Delta H_{kL}{}^{\neq} \approx 4$ kJ/mol and $\Delta H_{kt}{}^{\neq}$ = 14.5 kJ/mol which is also small enough to ignore. Summarized in Table 4 are the observed initial rates k_{obs}, for the nitroxide adduct *t*B-TMP. The $\ln(k_{obs}/T)$ vs.1/T plotted

Table 4: Calculation Summary of the Enthalpy of Activation for the C-O Bond Breaking Reaction in the Nitroxide Adduct tB-TMP.

Temp.(K)	1/T	1/Tx10^3	*k*(rate)	R^2	*k*/T	ln(*k*/T)
350	0.002857	2.857	363.47	0.9407	1.038486	0.037764
360	0.002778	2.778	1163.9	0.9888	3.233056	1.173428
363	0.002755	2.755	1710	0.9934	4.710744	1.549846
365	0.00274	2.74	1891.2	0.9951	5.18137	1.645069
368	0.002717	2.717	2740.1	0.9972	7.445924	2.007667
371	0.002695	2.695	4025.5	0.9968	10.8504	2.384202
374	0.002674	2.674	5061.2	0.9994	13.53262	2.605103
376	0.00266	2.66	6228.8	0.9985	16.56596	2.80735
378	0.002646	2.646	7530.7	0.9991	19.92249	2.991849
380	0.002632	2.632	9115.6	0.0073	23.98842	3.177571

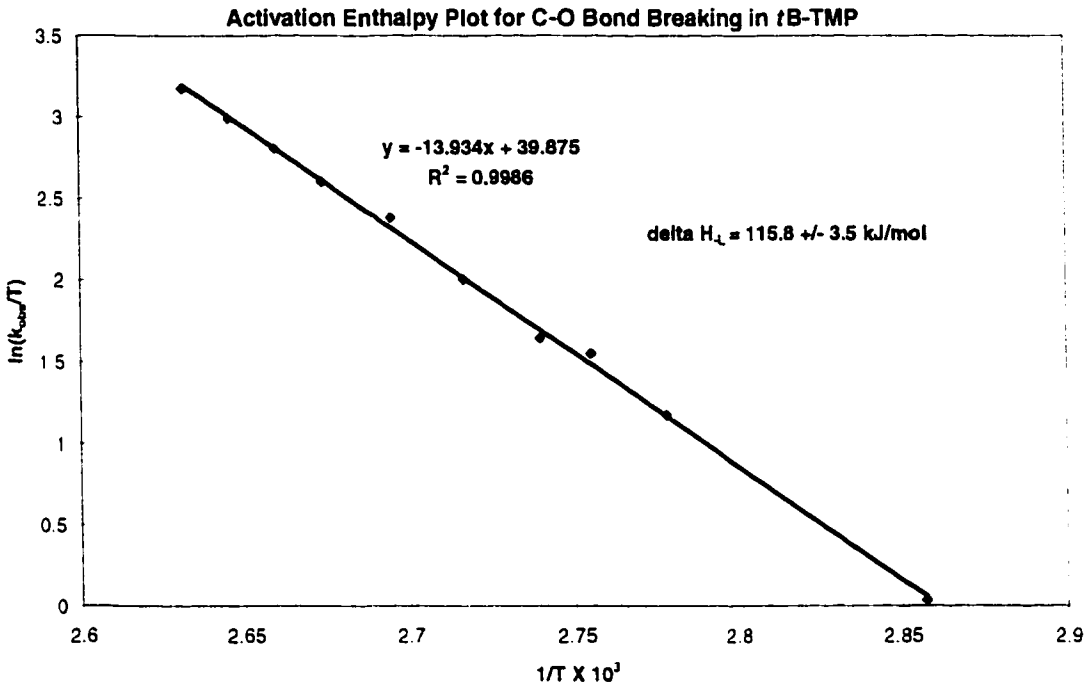

Figure 20: The activation enthalpy plot for the carbon-oxygen bond breaking reaction in *t*B-TMP.

in Figure 20 was used to calculate the enthalpy of activation ($\Delta H_{k\text{-}L}^{\ddagger}$). The best-fit line was determined using the rates k_{obs} for the nitroxide rate formation, $\ln(k_{obs} / T)$ vs 1/T. The slope of the line was used to calculate the enthalpy of activation for carbon-oxygen bond cleavage in *t*B-TMP. This procedure for determining the enthalpy of activation for homolytic cleavage of the C-O bond was performed on all 10 of the different nitroxide adducts listed in Table 3. The enthalpy of activation values for breaking the C-O bond in each adduct is summarized in Table 5, along with the error in the calculations and a comparison of calculated BDEs from AM1 and PM3 semi-empirical MO methods. A few

Table 5: A Comparison of the Calculated Bond Dissociation Enthalpy Values with Experimental Enthalpy of Activation Values for Different Nitroxide Adducts.

Model Compounds	Expt. ($\Delta H_{k\text{-}L}^{\neq}$) (kJ/mol)	Expt.($\Delta H_{k\text{-}L}^{\neq}$) (kcal/mol)	Cal. AM1 BDE (kcal/mol)	Cal. PM3 BDE (kcal/mol)
BST[2]	130 ± 4	31.1 ± 0.9	24.6	27.3
tButoxy-ST[13]	138.8 ± 18			
BSP[2]	113 ± 4	27.0 ± 0.9	30.9	26.6
MB-3CP[14]		27.8		
B-TMP	138.8 ± 7.5	33.2 ± 1.8	30.4	34.8
MB-TMP	131.2 ± 7.2	31.3 ± 1.7	22.4	27.6
tA-TMP	62.7 ± 6.8	15.0 ± 1.6	13.3	21.6
tB-TMP	115.8 ± 3.5	27.7 ± 0.8	13.9	22
EiB-TMP	119.2 ± 3.4	28.5 ± 0.8	14.2	20
CH-TMP	142.9 ± 11.8	34.2 ± 2.8	24.6	27.8
MiP-TMP	125.3 ± 5.4	29.9 ± 1.3	23.2	28.1
MiP-4BenTMP	132.1 ± 6.7	31.6 ± 1.6	22.9	26.7
MB-TMI	132.6 ± 7.0	31.7 ± 1.7	23.6	25.8
MB-TEI	127.9 ± 2.7	30.5 ± 0.6	N/A	N/A

literature enthalpy of activation values for C-O bond cleavage of similar nitroxide adducts measured by others are also included in Table 5 for comparison.

The error limit was calculated as the 95% confidence interval using the following equation.

$$CI_{0.95} = b \pm t_{0.025,n-2} \frac{b}{r} \sqrt{\frac{1}{n-2}} \sqrt{\left(1-r^2\right)}$$

The variables are defined where b is the slope of the line obtained by plotting $\ln(k_{obs}/T)$ vs $1/T \times 10^3$, n is the number of data points in the curve, $t_{0.025}$ is the 95% confidence

[13] Bon, S. A. F.; Chambard, G.; Bergman, F. A. C.; Snellen, E. H. H.; Klumperman, B.; German, A. L. *Polym. Prepr. (Am. Chem. Soc. Div. Polym. Chem.)* **1997**, *38(1)*, 748.

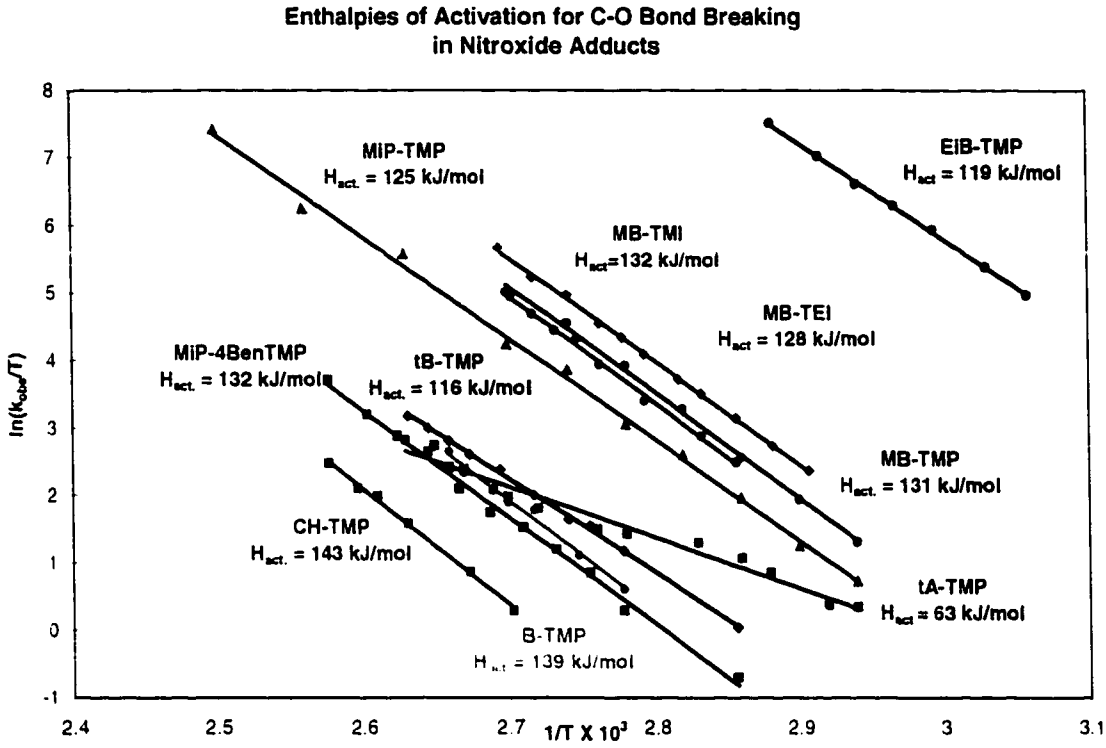

Figure 21: Summary plot of activation enthalpy curves for homolytic cleavage of the C-O bond all 10 nitroxide adducts.

value found in the *t*-tables in Statistics for Experimenters[15] and v is the number of degrees of freedom defined as v = n-2. The activation enthalpy curves for each nitroxide adduct are summarized in Figure 21.

The stablility of the C-O bond in the series of model nitroxide adducts, RO-TMP, shows some interesting trends. As mentioned before, the aryloxy and alkoxy-2,2,6,6-

---

[14] Li, I.; Howell, B. A.; Priddy, D. B. *Polym. Prepr. (Am. Chem. Soc. Div. Polym. Chem.)* **1996**, *37(2)*, 511.

[15] Box, G. E. P., Hunter, W. G., Hunter, J. S. Statistics for Experimenters; An Introduction to Design, Data Analysis, and Model Building, J. Wiley, & Sons, Toronto, 1978, pg. 631.

tetramethylpiperidine series of adducts comprise R groups that represent the propagating polymer chain end of styrenics, acrylate or methacrylate polymers or benzylic, aliphatic tertiary or secondary initiating carbon radicals bonded to TEMPO. The enthalpy of activation ($\Delta H_{k\text{-}L}^{\neq}$) and the necessary bond energy for breaking the C-O bond is dependent on the structure of R and the nitroxide. In the series of adducts, MB-TMP, MiP-TMP and EiB-TMP which mimic the vinyl monomers styrene, acrylate and methacrylate respectively, the enthalpy of activation decreases from 131.2 ± 7.2, 125.3 ± 5.4 to 119.2 ± 3.4 kJ/mol, respectively. This indicates that the C-O bond strength between the propagating polymer chain end and TEMPO is the weakest for a methacrylate chain end and increases in strength for an acrylate and styrenic chain end. Part of this difference may be due to steric crowding of the bulkier tertiary radical center of the methacrylate propagating carbon radical versus a secondary carbon center of the acrylate monomer or a secondary benzylic radical of styrene. In addition, the electron withdrawing ability of the ester functional group decreases the C-O bond strength by 5.9 kJ/mol as compared to the phenyl functional group in MB-TMP. The semi-empirical molecular orbital calculations performed using AM1 and PM3 MO methods predict that the C-O bond strength in EiB-TMP (BDE_{AM1} = 14.2 kcal/mol, BDE_{PM3} = 20.0 kcal/mol) should be weaker than MB-TMP (BDE_{AM1} = 22.4 kcal/mol, BDE_{PM3} = 27.6 kcal/mol). This is the order that was determined by the ESR study. On the other hand, when two adducts are closer in C-O bond strength as for example MiP-TMP ($\Delta H_{k\text{-}L}^{\neq}$ =125.3 ± 5.4 kJ/mol) and MB-TMP ($\Delta H_{k\text{-}L}^{\neq}$ =131.2 ± 7.2 kJ/mol), MO calculations are inaccurate.

Both AM1 and PM3 predict that MiP-TMP (BDE_{AM1} = 23.2 kcal/mol, BDE_{PM3} = 28.1 kcal/mol) would have a stronger C-O bond than MB-TMP, whereas, experimental data (see Table 5) demonstrates that MiP-TMP has a weaker C-O bond than MB-TMP. Semi-empirical MO calculations are not parameterized precisely enough to describe the N-O bond and as a consequence, these methods can not be used to calculate bond dissociation enthalpies in nitroxide adducts. This conclusion was discussed in greater detail in Chapter 3.

In the series of TEMPO adducts where R represents different initiating radicals, the enthalpy of activation was also measured by ESR spectroscopy. For the series of adducts; benzyloxy-TMP, cycloheptoxy-TMP, *tert*-butoxy-TMP and *tert*-amyloxy-TMP, the enthalpies of activation are 138.8 ± 7.5, 142.9 ± 11.8, 115.8 ± 3.5 and 62.7 ± 6.8 kJ/mol, respectively. A primary benzylic carbon in B-TMP bonded to TEMPO has a weaker C-O bond than a cyclic secondary carbon of CH-TMP due to electron delocalization of the unpaired electron into the phenyl ring making the benzylic radical more stable than the secondary aliphatic carbon radical. Replacing a primary benzylic carbon or secondary aliphatic carbon with a tertiary carbon decreased the enthalpy of activation significantly. This illustrates the effect of increasing steric crowding at the propagating carbon center, which weakened the C-O bond. The addition of a CH_2 unit in the *tert*-amyl group relative to the *tert*-butyl group significantly decreases the energy required to break the C-O bond by 53.1 kJ/mol. This large decrease in the C-ON bond strength is somewhat unexpected especially when a substitution of four methyls by four

ethyl groups decreases the C-ON bond strength by only 4.7 kJ/mol. This drop of 53.1 kJ/mol may also indicate that the tA-TMP adduct is not thermally stable at room temperature. Semi-empirical MO calculations were not able to predict this trend in decreasing C-O bond strength.

In addition to the acrylate-TEMPO adduct, MiP-TMP, ($\Delta H_{k\text{-}L}^{\neq}$ = 125.3 kJ/mol) the acrylate-4-benzoate-TEMPO adduct, MiP-4-BenTMP, ($\Delta H_{k\text{-}L}^{\neq}$ = 132.1 kJ/mol) was evaluate by ESR spectroscopy to determine the energy required to break the C-O bond. Adding an ester substituent to the 4-position of the piperidine ring in TEMPO increased the C-O bond strength by 6.8 kJ/mol. This increase in the C-O bond strength is attributed to a through space charge transfer interaction of the ester functional group with the nitrogen of the piperidine ring previously reported by Wagner *et al.*[16] in 4-benzoylpiperdines. The data is in agreement with an increase in the hyperfine coupling

Table 6: Measured Hyperfine Coupling Constants to Nitrogen and Spin Purity of Various Nitroxyl Radicals

Nitroxide Radical	Spin Purity (%)	Hyperfine Coupling Constant a_N (Gauss)
4-benzoyloxy-TEMPO	94	15.36 ± 0.06
4-acetoxy-TEMPO	90	15.24 ± 0.07
TEMPO	100	15.14 ± 0.06
4-OH-TEMPO	100	14.93 ± 0.1
4-oxo-TEMPO	90	14.13 ± 0.08
1,1,3,3-tetramethy-isoindolin-2-yloxyl	94	13.98 ± 0.05
1,1,3,3-tetraethyl-isoindolin-2-yloxyl	90	13.74 ± 0.04

constant for 4-benzoyloxy-TEMPO (a_N = 15.36 Gauss) as compared to TEMPO (a_N = 15.14 Gauss) as illustrated in Table 6. A larger a_N value indicates an increased contribution of the ionic canonical form B of the nitroxide where the unpaired electron

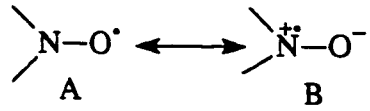

A B

density is more associated with nitrogen than oxygen producing a stronger C-O bond with more ionic character. To weaken the C-O bond, the preferred nitroxide radical should have a lower a_N value favouring canonical form A where the unpaired electron density is more associated with the oxygen atom than nitrogen.

Both the tetramethyl- and the tetraethylisoindoline nitroxides had lower hyperfine coupling constants than TEMPO, a_N = 13.98 Gauss and a_N = 13.74 Gauss, respectively. The α–methylbenzyl nitroxide adducts, MB-TMI and MB-TEI, were also evaluated in the ESR study and the enthalpy of activation for breaking the C-O bond was also obtained. A direct comparison can be made between MB-TMP, MB-TMI and MB-TEI. Here, the R group is the same and any changes in the C-O bond strength will be due to changes in the nitroxyl radical. As illustrated in Table 5, the enthalpy of activation for MB-TMP and MB-TMI are essential the same, 131.2 and 132.6 respectively. This suggests that changing from a flexible six membered piperidine ring system to a larger and more rigid planar isoindoline ring system did not make any difference in the strength of the C-O bond between the carbon radical and the nitroxide. This can be attributed to having the

---

[16] Wagner, P. J.; Scheve, B. J. *J. Am. Chem. Soc.* **1977**, *99(6)*, 1858.

same methyl substituents on the carbons alpha to the nitroxide in both nitroxides and that changes in the molecule further away from this center did not affect the strength of the bond of interest. However, when the substituents on the carbons alpha to the nitroxide are varied from four methyls to sterically bulkier ethyl substituents, a decrease in the enthalpy of activation was observed. The enthalpy of activation for MB-TMI was 132.6 kJ/mol as compared to 127.9 kJ/mol for MB-TEI. The weakening of the C-O bond by 4.7 kJ/mol is attributed solely to an increase in steric bulk on the carbons alpha to the nitroxyl functional group resulting in a significant decrease.

Previously reported enthalpies of activation for the C-O bond have also been included in Table 5 for completeness. The enthalpies of activation reported by Veregin *et al.*[2] for BST (130 ± 4 kJ/mol) agree well with the value obtained in this study for MB-TMP (131.2 ± 7.2 kJ/mol). The numbers should be identical within experimental error since the R group is the same and the nitroxyl radical is TEMPO. Bon *et al.*[13] also measured the enthalpy of activation for breaking the same C-O bond in a similar molecule, *tert*-butoxy-styrene-TEMPO, *t*BST, but they reported a value of 138.8 ± 18 kJ/mol which is high but within the 95% confidence limit of their measurement. The process used to determine the rate of homolytic dissociation in the alkoxyamine was by a nitroxide exchange experiment. Specific details of the experiment were not given but this technique does not seem as accurate as the ESR approach used in this work.

Veregin *et al.*[2] reported the enthalpy of activation (113 ± 4 kJ/mol) for breaking the C-O bond in benzoyloxy-styrene-3-carboxyl-PROXYL, BSP. Li *et al.*[14] also

determine the C-O bond strength in ethylbenzyl-3-carboxyl-PROXYL, CPEPY, by a different route to be 27.8 kcal/mol. This compares favorably with the BSP[2] value of 27.0 kcal/mol. The decrease in the enthalpy of activation for BSP has been attributed to changing the nitroxyl radical from TEMPO to the smaller PROXYL nitroxide. More recently though, this conclusion has been questioned. In fact, the more labile C-O bond may be attributed to the acid functional group on the nitroxide radical and not due to changing the nitroxide.

Chapter 5

Kinetic and Mechanistic Study of Thermal Decomposition of MB-TMP Monitored by NMR and ESR Spectroscopy

5.1 Introduction and Rationale

The stable free radical polymerization process was first applied to styrene monomer and this work demonstrated a controlled "living" polymerization. When this new polymerization process was applied to other monomers, such as acrylates and methyacrylates, the extension of the SFRP process was not as successful. Typically, the early attempts to polymerize *n*-butyl acrylate using BPO or AIBN as initiators, with a molar excess of TEMPO as the nitroxyl radical, produced living polymers with maximum Mn = 16,000 - 20,000 and polydispersities between 1.5 and 2.0. At this point the polymerization stopped. Upon heating the reaction mixture further, no additional polymerization occurred. After numerous changes in reagent amounts and varying reaction conditions, the SFRP process could not produce Mn values above 20,000. One possible explanation for this was that the polymer chains were terminated by some mechanism liberating nitroxyl radicals and thus halting the "living" polymerization process.

Early work by Solomon *et al.*[1,2] on nitroxides trapping carbon-centered radicals formed by initiator decomposition and subsequent addition to monomer, showed that hydrogen abstraction by the nitroxide from MA and MMA occurred. In some cases, the formation of the *N*-hydroxylamine was detected. It was then proposed by Moffat that a similar hydrogen abstraction from the β–carbon of the propagating chain end by another molecule of nitroxide could result in a terminal vinyl group. This reaction would terminate the chain, prevent further chain growth and produce the *N*-hydroxylamine. Upon exposure to air, the hydroxylamine is then oxidized to the nitroxyl radical. This chapter focuses on determining if such a mechanism exists using the model initiator / reversible terminating adduct MB-TMP. This adduct is an ideal compound to study possible termination reactions since it mimics the propagating polystyrene chain end.

Other groups working in the SFRP area have suggested that TEMPO is involved in hydrogen abstraction, but the experimental proof for the formation of the corresponding *N*-hydroxylamine is not conclusive. Connolly and Scaiano[3] heated TEMPO in the presence of toluene, ethylbenzene or cumene for 12 hours and observed the formation of adducts produced by initial hydrogen radical abstraction from the benzylic position. The resulting carbon-centered benzylic radicals were trapped by

---

[1] Griffiths, P. G.; Rizzardo, E.; Solomon, D. H. *Tet. Lett.* **1982**, *23*, 1309. Rizzardo, E.; Solomon, D. H. *Polym. Bull.* **1979**, *1*, 529.
[2] Griffiths, P. G.; Rizzardo, E.; Solomon, D. H. *J. Macromol. Sci. Chem.* **1982**, *A17*, 45. Rizzardo, E.; Serelis, A. K.; Solomon, D. H. *Aust. J. Chem.* **1982**, *35*, 2013. Cuthbertson, M. J.; Moad, G.; Rizzardo, E.; Solomon, D. H. *Polym. Bull.* **1982**, *6*, 647. Busfield, W. K.; Jenkins, I. D.; Rizzardo, E.; Solomon, D. H. *J. Chem. Soc. Perkin Trans.* **1991**, *1*, 1351.
[3] Connolly, T. J.; Scaiano, J. C. *Tet. Lett.* **1997**, *38(7)* 1133.

TEMPO. They implied that during a SFR polymerization, subsequent hydrogen radical abstraction from the benzylic carbon in a polystyrene chain could occur. If this reaction did occur, then the resulting benzylic centers would be branching points for additional SFR polymerization. Conclusive experimental evidence for branching in polystyrene chains has not been found.

Yoshida and Okada[4] studied the nitroxide radical transformation of a low molecular weight polystyrene (Mn = 2170, MWD = 1.15) in benzene at 130°C. The starting polystyrene prepared by SFRP was capped with 4-hydroxy-TEMPO. After 24 hours they demonstrated 80% nitroxide chain end substitution of the 4-hydroxy-TEMPO with 4-methoxy-TEMPO. When they pushed the reaction further, the degree of substitution decreased with time. This was attributed to hydrogen radical abstraction from the β-carbon by 4-methoxy-TEMPO to produce a terminal vinyl group and the resulting *N*-hydroxylamine of 4-methoxy-TEMPO. The signals discerned at 5.9-6.2 ppm were attributed to one of the vinyl protons. NMR evidence for the hydroxylamine was not reported. The important conclusion from this work is, that to produce a terminal vinyl group at the end of a polystyrene chain, very long reaction times (>24 hours) are required. These conditions are not normal SFR polymerization conditions.

Li, Howell and Priddy[5], [6] reported a proposed mechanism for the decomposition of MB-TMP involving hydrogen radical abstraction by TEMPO to produce the

---

[4] Yoshida, E.; Okada, Y. *Bull. Chem.Soc. Jpn.* **1997**, *70*, 275.
[5] Li, I.; Howell, B. A.; Koster, R.; Priddy, D. B. *Polym. Prepr. J. Am. (Chem. Soc. Div. Polym. Chem.)* **1996**, *37(2)*, 517.

corresponding *N*-hydroxylamine and styrene as the major reaction products. Additional minor reactions were proposed involving the coupling of two 1-phenylethyl radicals to produce 2,3-diphenylbutane and smaller amounts of ethylbenzene prepared by reacting the 1-phenylethyl radical with a hydrogen radical source such as *N*-hydroxylamine. To produce 2,3-dipenylbutane, the concentration of 1-phenylethyl radicals must be significant for this dimer to form. The temperature at which this study was conducted was 140°C. At this temperature, the rate constant for homolytic cleavage of the C-ON bond in MB-TMP is higher thus enabling such larger concentrations of 1-phenylethyl radicals which led to the formation of the dimer, 2,3-diphenylbutane. Using HPLC and ^{1}H NMR they monitored the thermal decomposition kinetics of MB-TMP in 1,2,4-trichlorobenzene, DMSO-d_6 and toluene. Based on these results they concluded that the nitroxide capped polystyrene chain end undergoes a similar decomposition reaction and is likely a major source of polydispersity broadening.

This chapter reports our kinetic study on the thermal decomposition kinetics of MB-TMP at elevated temperatures using high temperature ^{1}H NMR and ESR spectroscopy to identify and quantify the various reaction products. This study in which an alternate mechanism is proposed does not completely agree with the results or the proposed mechanism by Li *et al.*[5], [6] for MB-TMP decomposition.

---

[6] Li, I.; Howell, B. A.; Matyjaszewski, K.; Shigemoto, T.; Smith, P. B.; Priddy, D. B. *Macromolecules* **1995**, *28*, 6692.

5.2 Experimental Section

All adduct solutions were prepared in the same manner in an Innovative Technology Inc. dry box model System 1DC. The dry box was equipped with moisture and O_2 detectors and a freezer compartment. The atmosphere in the dry box was anhydrous argon. Described herein is the procedure used to prepare one of the MB-TMP samples for both the ^{1}H NMR and ESR measurements.

The nitroxide adduct MB-TMP was recrystallized from methylene chloride and dried under vacuum to remove residual solvent and water. The sample was placed in the dry box free of moisture and oxygen and all sample preparation was performed in the dry box. Into a 50 mL beaker was dissolved 32 mg of MB-TMP in 1 mL of *ortho*-xylene-d_{10}. Into an 8" thin walled NMR tube, constricted 1" from the top of the tube, was added 650 μL of this solution using a syringe, and then the tube was attached to a Wilmad Taperlok NMR valve. Similarly, for the ESR sample, 110 mg of the above solution of MB-TMP in *ortho*-xylene-d_{10} was added into a NMR tube and the tube was attached to a Wilmad Taperlok NMR valve. The sealed samples were removed from the dry box and attached to a vacuum line. Using the freeze-pump-thaw (FPT) technique, each sample was degassed 4-5 times to remove molecular oxygen and then sealed under vacuum.

Since the ESR and the ^{1}H NMR experiments were performed on the same adduct solution, the temperature of the ESR cavity and of the NMR sample probe were adjusted to the same temperature, within ± 0.5 K. The internal temperature of the ESR cavity was calibrated using a solution of *ortho*-xylene-d_{10} in a NMR tube containing a thermocouple

placed in the solvent. The Bruker variable temperature ER4111 controller on the ESR spectrometer was adjusted until the desired temperature of the cavity was reached.

To calibrate the temperature of the NMR probe, a sample of ethylene glycol was placed in the probe. Using the calibration equation below, which relates the chemical shift differences $\Delta\delta$ (ppm)[7,8] between the two ethylene glycol peaks to the temperature of the cavity, the probe temperature was adjusted.

$$T\ (K)\ (\text{ethylene glycol}) = 466.5 - 102.00\ \Delta\delta$$

Using the Bruker variable temperature controller, the temperature was adjusted until it was within ± 0.5 K of the temperature used for the complimentary ESR experiment. The ^{1}H NMR spectra were referenced internally to the residual methyl protons in the solvent *ortho*-xylene-d_{10} which appeared at 2.25 ppm.

5.3 Results and Discussion

5.3.1 Monitoring TEMPO Release in Thermal Decomposition of Nitroxide-Adducts by ESR Spectroscopy

The increase in the TEMPO concentration at elevated temperatures during the thermal decomposition of adducts MB-TMP and MiP-TMP was measured as a function of time by ESR spectroscopy. The initial concentrations of MB-TMP in either toluene-d_8 or *ortho*-xylene-d_{10} were 0.113 M, 0.111 M and 0.123 M. The initial concentration of MiP-TMP in *ortho*-xylene-d_{10} was 9.57×10^{-2} M. The initial concentrations of MB-TMP

Table 7: Release of TEMPO as a Function of Time for Nitroxide Adducts MB-TMP and MiP-TMP.

$[Adduct]_0$	Temp.(°C)	Solvent	$[TEMPO]_0$	Rate 1 ($M^{-1}s^{-1}$)	Rate 2 ($M^{-1}s^{-1}$)
$[MB\text{-}TMP]_0 = 1.126 \times 10^{-1}$ M	103	toluene-d_8	2.0×10^{-5} M	2.64×10^{-2}	4.94×10^{-4}
$[MB\text{-}TMP]_0 = 1.11 \times 10^{-1}$ M	125	*o*-xylene-d_{10}	4.43×10^{-5} M	1.21×10^{-2}	1.38×10^{-3}
$[MB\text{-}TMP]_0 = 1.23 \times 10^{-1}$ M	132	*o*-xylene-d_{10}	3.14×10^{-6} M	4.43×10^{-2}	3.02×10^{-4}
$[MiP\text{-}TMP]_0 = 9.57 \times 10^{-2}$ M	100	*o*-xylene-d_{10}	1.59×10^{-6} M	5.22×10^{-2}	7.79×10^{-4}

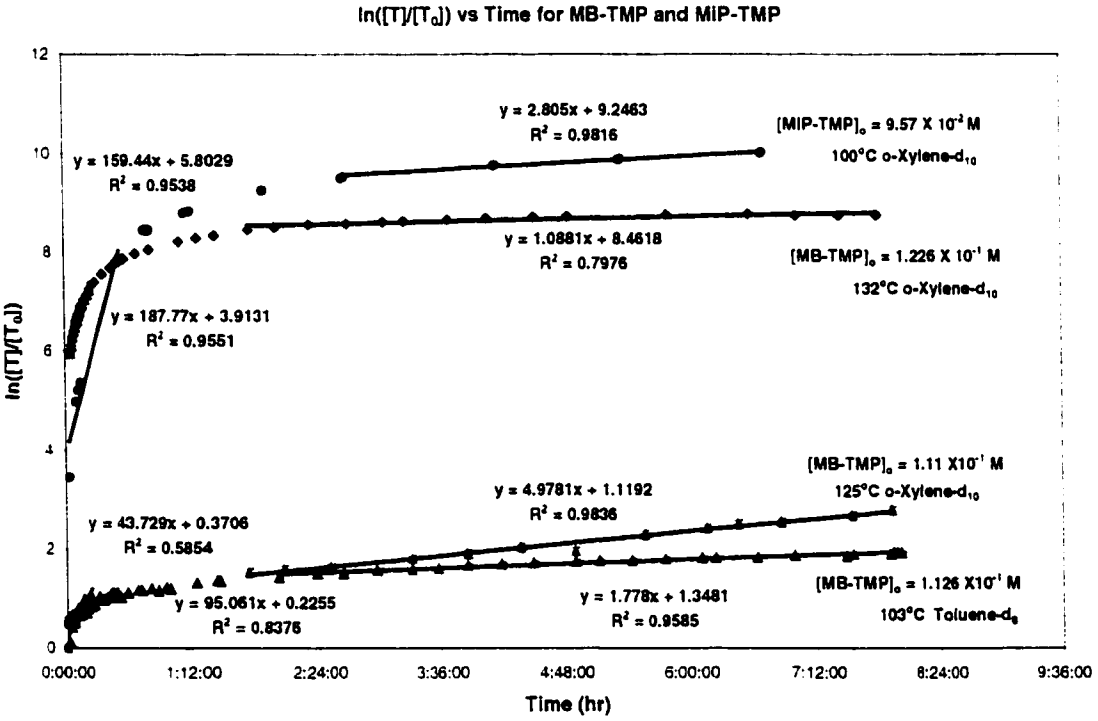

Figure 22: Plot of $\ln([T]/[T_0])$ vs time for nitroxide adducts MB-TMP at 103°C, 125°C and 132°C and MiP-TMP at 100°C obtained by ESR spectroscopy.

[7] Raiford, D. S.; Fisk, C. L.; Becker, E. D. *Anal. Chem.* **1979**, *51*, 2050.
[8] Ammann, C.; Meier, P.; Merbach, A. E. *J. Magn. Res.* **1982**, *46*, 319.

were kept reasonably constant and low enough so that, as the ESR experiment progressed, the free electron signal was not saturated, but high enough so that the intensity of the ^1H signals would enable a short data acquisition time (NS = 16). Prior to heating the samples, the concentrations of free TEMPO were determined and the values are reported in Table 7. Even though the adducts were very pure and great attempts were made to minimize the amount of free nitroxide present, there was always a low level of nitroxide in solution (10^{-6} to 10^{-5} M) in each sample that was easily detected by ESR spectroscopy. Many researchers[9], that use nitroxide adducts, such as MB-TMP, as the initiator and source of capping nitroxide for SFR polymerization, quote a 1:1 stoichiometric ratio of initiating radicals to nitroxide. In fact, this is not completely accurate as reported by Veregin *et al.*[10] There is always an excess of nitroxide present in solution which is difficult to detect except by ESR.

Contained in Figure 22 is an ESR kinetic plot of the $\ln([T]/[T_0])$ vs time showing the increase in TEMPO concentration as the thermal decomposition of the adduct proceeds. Data points were collected for 8 hours. MB-TMP was evaluated at three different temperatures (103°C, 125°C and 132°C) and, as expected, the rate of production of free TEMPO is the greatest for the highest temperature. Each curve has two portions to it. In the steepest portion of the curve, the rate constant for releasing TEMPO represents the liberation of free TEMPO required to establish the equilibrium with the

---

[9] Malmström, E.; Miller, R. D.; Hawker, C. J. *Tetrahedron* **1997**, *53(45)*, 15225.
[10] Veregin, R. P. N.; Kazmaier, P. M.; Odell, P. G.; Georges, M. K. *Chem. Lett.* **1997**, *5*, 467.

dormant adduct. The rate constant values are presented in Table 7 denoted as Rate 1. All values are approximately 10^{-2} $M^{-1}s^{-1}$. This is quite slow in comparison to the trapping of carbon-centered radicals by the nitroxide, which is close to a diffusion-controlled reaction with a rate constant k_L that approximately equals 10^9 $M^{-1}s^{-1}$. In *ortho*-xylene-d_{10}, MB-TMP at 125°C released TEMPO at a rate of 1.12 x10^{-2} s^{-1} and at 132°C in the same solvent, the release of TEMPO occurred at a rate of 4.43 x 10^{-2} s^{-1}, approximately 4 times faster. Using the same solvent, *ortho*-xylene-d_{10}, MiP-TMP at only 100°C released TEMPO radicals at a slightly faster rate than MB-TMP evaluated at a higher temperature (132°C). The rate of release of free TEMPO in MiP-TMP was 5.22 x 10^{-2} s^{-1}. This faster release of TEMPO in adduct MiP-TMP is consistent with the lower activation enthalpy for homolytic cleavage of the C-O bond to release TEMPO in adduct MiP-TMP ($\Delta H_{k\text{-}L}^{\ddagger}$ = 125.3 ± 5.4 kJ/mol) as compared to MB-TMP ($\Delta H_{k\text{-}L}^{\ddagger}$ = 131.2 ± 7.2 kJ/mol). The initial steep portion in all 4 data sets (Figure 22) begins to level off after 30-60 minutes.

In the second portion of each curve in Figure 22, the increase in TEMPO has slowed down with rates on the order of 10^{-4} to 10^{-3} s^{-1}. At this point in the reaction, not only is the carbon-centered radical of 1-phenylethyl trapped by the nitroxide, but other products are formed in significant quantities and these products continue to grow as the decomposition of the adduct is pushed to completion. At 125°C, 64 hours are required to completely decompose MB-TMP. The rate of trapping of the 1-phenylethyl radical by TEMPO is so efficient at close to a diffusion-controlled rate, and it is this fast rate of capture that is responsible for such a long decomposition time. This efficient rate of

capture of the 1-phenylethyl radical by TEMPO can be compared to when MB-TMP is used to initiate the SFRP of styrene. After 5 minutes at 135°C all of the adduct is consumed to initiate the polymerization of polymer chains which are rapidly captured by the nitroxide.

5.3.2 Product Study of Thermal Decomposition of MB-TMP by High Temperature ^1H NMR Spectroscopy

Complementary to the kinetic ESR experiment at 125°C which followed the rate of increase in TEMPO concentration over 8 hours, was the ^{1}H NMR experiment at 125°C to monitor the formation of the byproducts from the decomposition of MB-TMP. The sample of MB-TMP in *ortho*-xylene-d_{10} used for the NMR experiment was prepared as describe in the experimental section of this chapter and the concentration was equal to that used in the ESR experiment. The integrated area of the methine proton resonance at δ 5.03 for MB-TMP was determined relative to the residual methyl protons (2.25 ppm) of *ortho*-xylene-d_{10}. The vinyl methine proton of styrene at 6.75 ppm was integrated and monitored as a function of reaction time. Both the alcohol proton at δ 3.91 and the12 methyl protons (1.30 ppm) of *N*-hydroxylamine were followed. The two *ortho*-aromatic protons at δ 7.90 and the 3 methyl protons resonating at 2.37 ppm in acetophenone were monitored. The methine proton at 4.76 ppm of *sec*-phenethyl alcohol was followed, but accurate integration for this signal was difficult to obtain due to an unknown singlet resonating at the same position. All integrated areas were normalized to the methyl

quintet of the solvent set at 100. Integrated peak areas were divided by the number of protons and normalized to one proton. Illustrated in Figure 23, for the first 8 hours of the reaction, is the increase in the formation of various byproducts and the decrease in MB-TMP. Also added to the plot is the TEMPO concentration data taken from the ESR experiment for the first 8 hours. Unexpectedly, the concentration of TEMPO over that time changed from 4.4×10^{-5} M to 7.2×10^{-4} M which is a minor increase in comparison to the other changes in the system. Throughout this reaction the free nitroxide

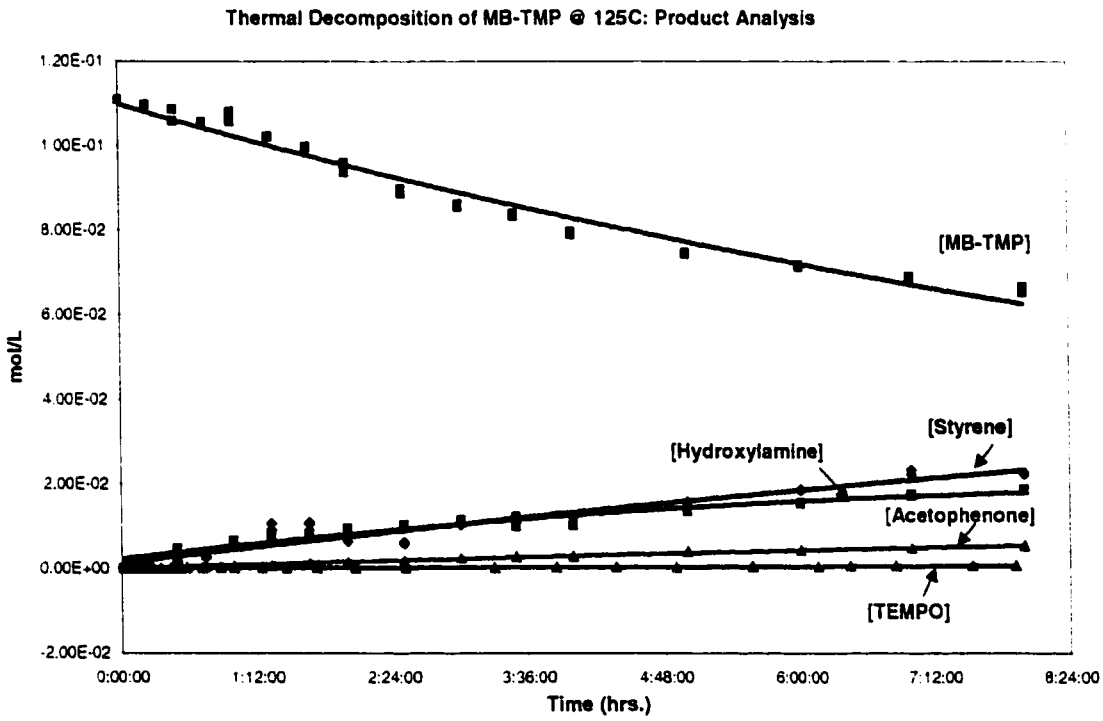

Figure 23: Product formation (mol/L) as a function of time during the thermal decomposition of MB-TMP at 125°C.

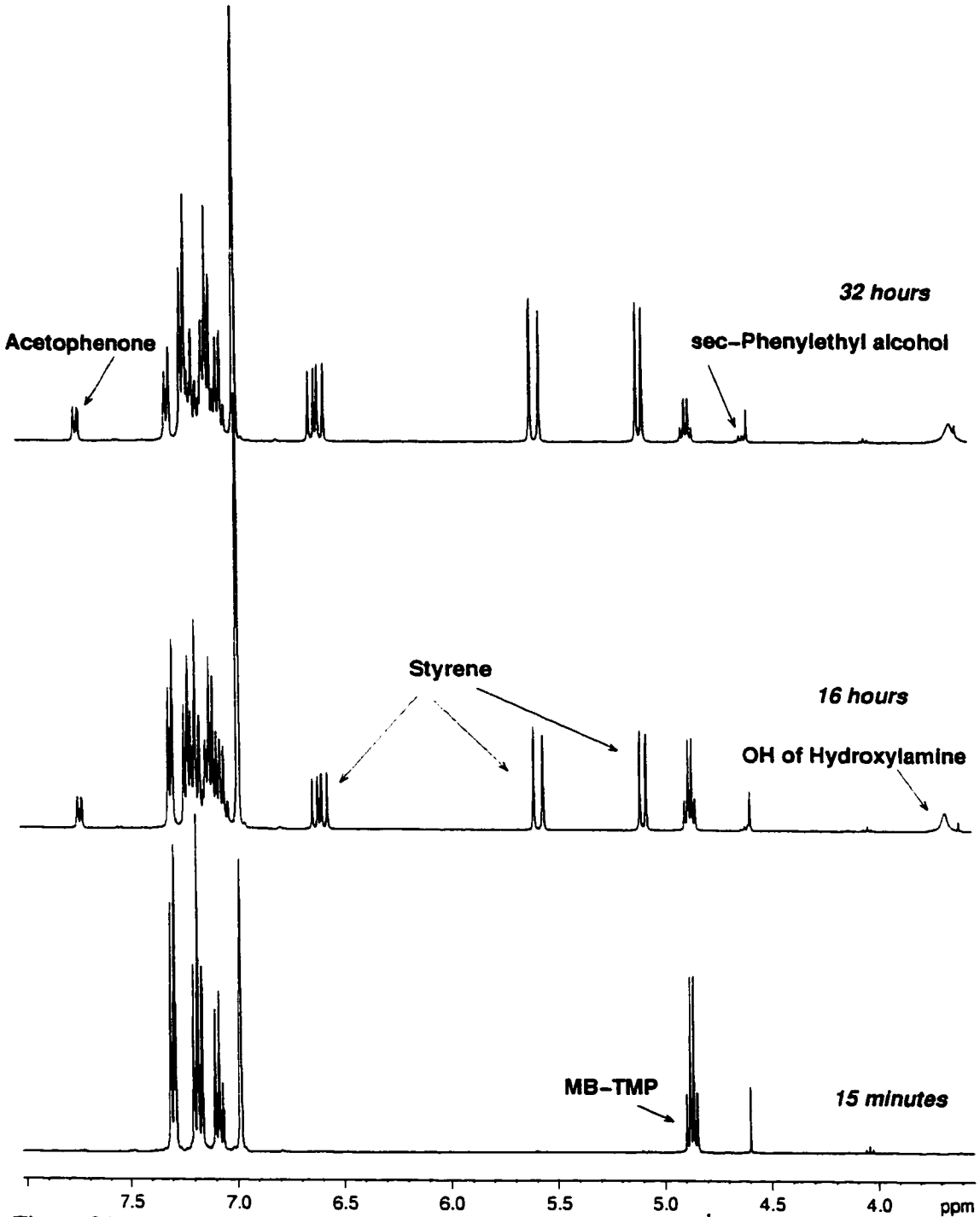

Figure 24: A series of three high temperature (125°C) 400 MHz ^{1}H NMR spectra at 15 minutes, 16 and 32 hours reaction time illustrating the decomposition of MB-TMP and formation of styrene, the *N*-hydroxylamine and acetophenone covering 3.5 to 8.0 ppm.

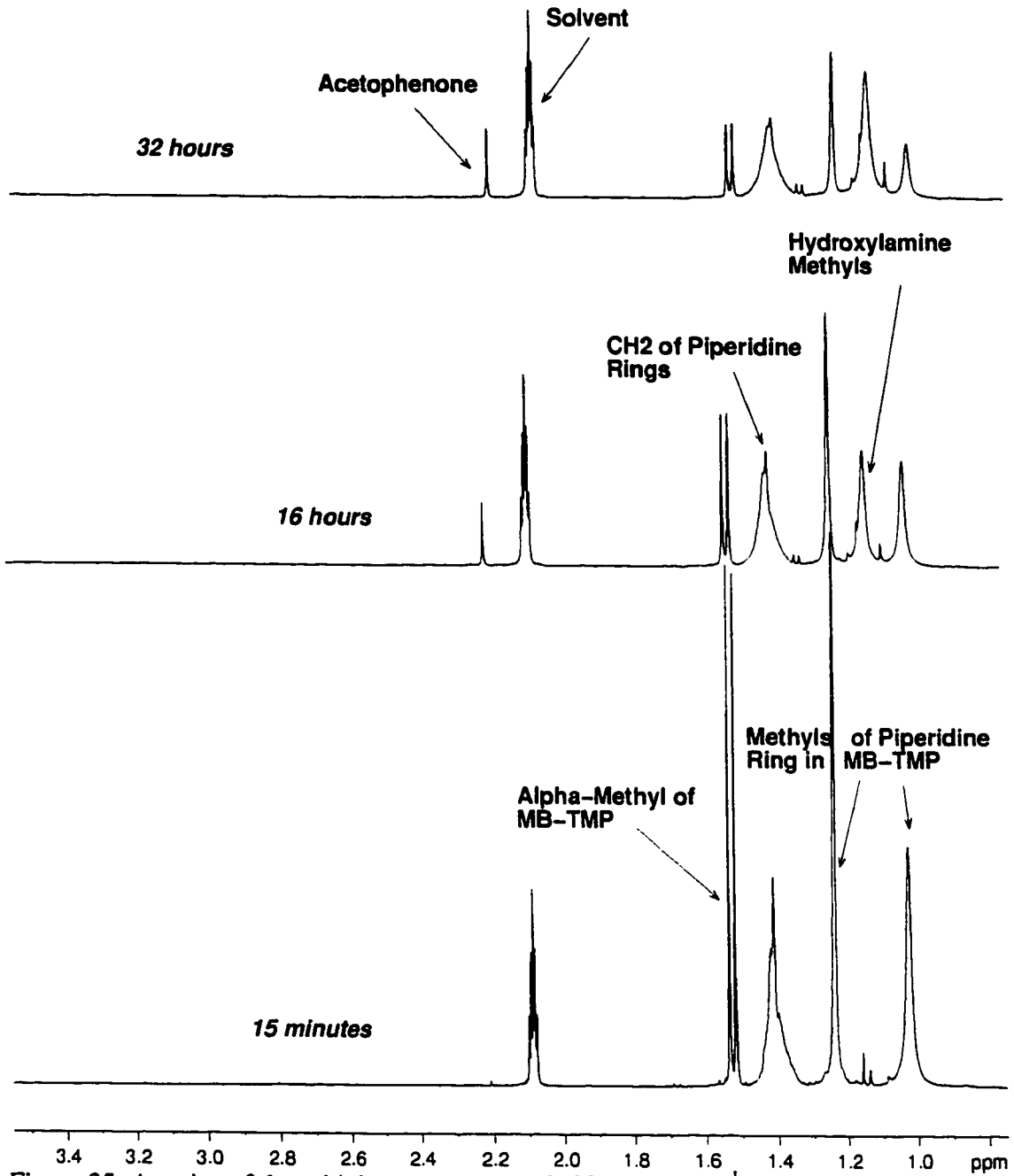

Figure 25: A series of three high temperature (125°C) 400 MHz ^{1}H NMR spectra at 15 minutes, 16 and 32 hours reaction time illustrating the decomposition of MB-TMP and formation of styrene, the *N*-hydroxylamine and acetophenone, covering 0.5 to 3.5 ppm.

concentration increased by a factor of 16. The byproducts of the thermal decomposition of MB-TMP consist of styrene, acetophenone, the *N*-hydroxylamine derivative of TEMPO and a very small amount of *sec*-phenethyl alcohol which was not included in Figure 23 because the concentrations were too small.

Figures 24 and 25 are high temperature 400 MHz ^{1}H NMR spectra at 125°C taken at different times throughout the experiment. Figure 24 contains the region from 3.5 ppm to 8.0 ppm at 15 minutes, 16 hours and 32 hours. The peaks of interest include the *ortho*-aromatic protons of acetophenone resonating at 7.90 ppm, which did not increase in intensity going from 16 hours to 32 hours. The characteristic vinyl methine proton of styrene appears as a doublet of doublets at 6.77 ppm, along with the two vinyl methylene protons at δ 5.74 and δ 5.25. All three signals grow significantly over the course of the reaction. The quartet at δ 5.03 of the methine proton of MB-TMP decreases in intensity, and by 32 hours into the reaction, MB-TMP is only a minor component in the system. At 4.76 ppm is the weak multiplet of the methine proton of *sec*-phenethyl alcohol with a sharp singlet resonating at the same position. The characteristic broad singlet at δ 3.91 is due to the alcohol proton of the *N*-hydroxylamine derivative of TEMPO.

The region covered in Figure 25 at 15 minutes, 16 hours and 32 hours is from 0.5 to 3.5 ppm. Downfield of the methyl resonance (2.25 ppm) of *ortho*-xylene-d_{10} are the methyl protons of acetophenone at 2.37 ppm. Contained in the aliphatic region between 1.19 to 1.70 ppm is the doublet at 1.69 ppm due to the methyl group on the asymmetric center of MB-TMP. The ring methylene protons of both TEMPO and the *N*-

hydroxylamine of TEMPO are found in the broad peak at 1.57 ppm. The four methyl groups of the piperidine portion of MB-TMP are found at 1.40 and 1.19 ppm and as the reaction proceeds, these two peaks decrease in intensity as the ring methyls of the *N*-hydroxylamine of TEMPO increase at 1.30 ppm.

Based on the ESR and ^{1}H NMR experimental data a somewhat different mechanism from that of Li *et al.*[5], [6] for the thermal decomposition of MB-TMP was proposed. The mechanism of Li *et al.* is shown in Figure 26. Their study identified ethylbenzene and 2,3-diphenylbutane as secondary products of the reaction. These compounds probably formed due to the high reaction temperature of 140°C producing a

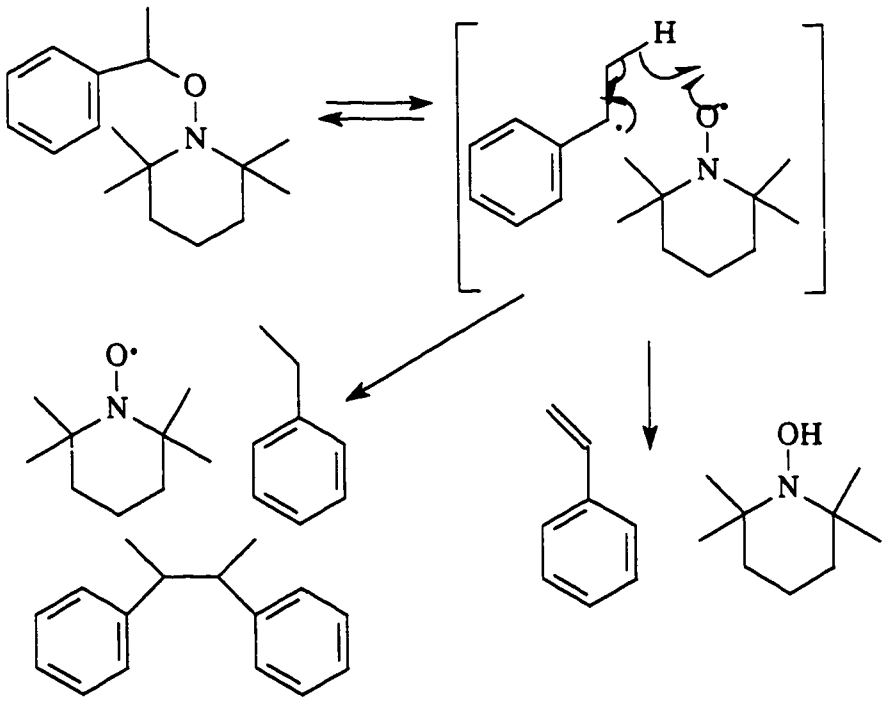

Figure 26: The mechanism for thermal decomposition of MB-TMP proposed by Li *et al.*[5],[6]

greater concentration of 1-phenyethyl radicals which dimerized to give 2,3-diphenylbutane or reacted with a hydrogen radical source to produce ethylbenzene.

The mechanism proposed based on the high temperature ^{1}H NMR experiments of this study is shown in Figure 27 which accounts for all of the major byproducts identified in the reaction. Upon homolytic cleavage of the C-O bond in MB-TMP, the TEMPO radical and the carbon-centered 1-phenylethyl radical are produced. In the absence of O_2 the nitroxide radical abstracts a hydrogen radical from the β-carbon of 1-phenylethyl radical to form the *N*-hydroxylamine derivative of TEMPO and styrene. This reaction is

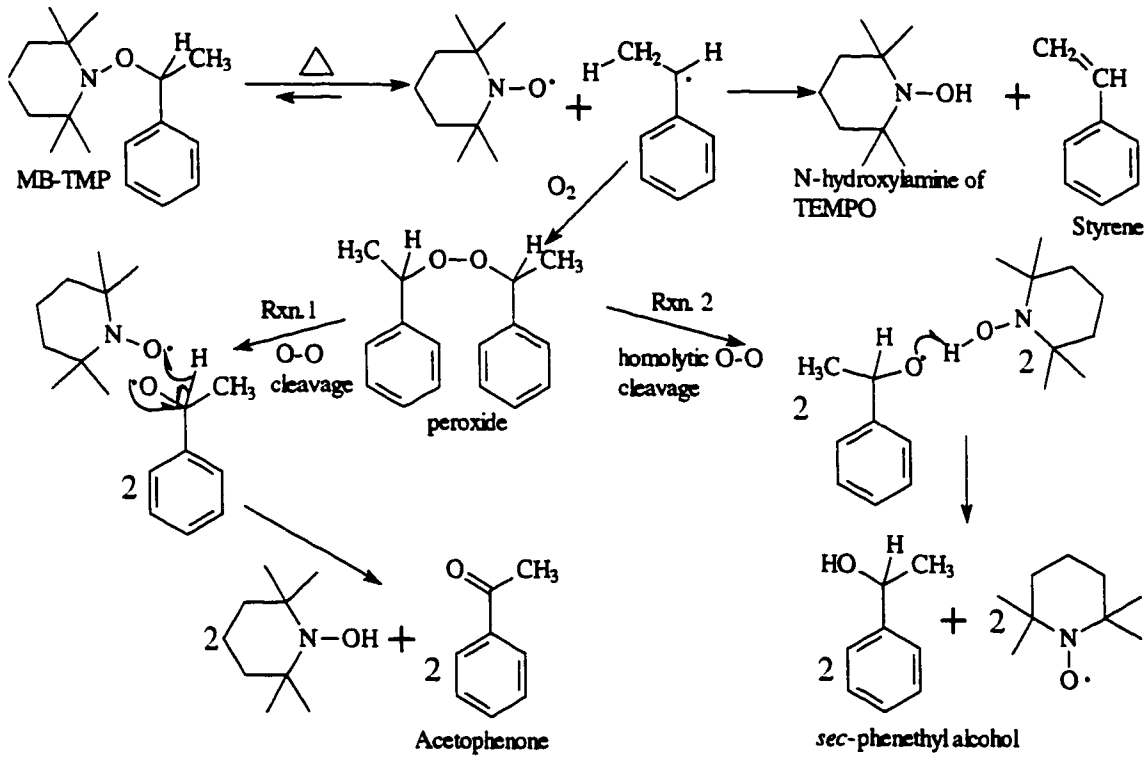

Figure 27: Mechanism for the thermal decomposition of MB-TMP in *ortho*-xylene-d_{10} producing styrene, *N*-hydroxylamine of TEMPO, acetophenone and *sec*-phenylethyl alcohol.

very fast and within 15 minutes at 125°C the vinyl protons of styrene are just visible by ^{1}H NMR. Even though the samples were thoroughly degassed to remove O_2 by the freeze-pump-thaw technique, in fact, the samples were not oxygen free. The deuterated aromatic solvent retained oxygen. In the presence of oxygen, the biradical O_2 reacts with the carbon-centered 1-phenylethyl radical and is subsequently trapped by another 1-phenylethyl radical to form the peroxide intermediate. The peroxide is very short-lived and decomposes into an oxygen-centered radical, which produces acetophenone and the *N*-hydroxylamine by hydrogen abstraction from the benzylic position of the benzyloxy radical by TEMPO. The proposed peroxide intermediate was not detected in our experiments but it is hypothesized that at 125°C this component is very unstable. Also competing with the acetophenone production is the formation of the least concentrated component, *sec*-phenethyl alcohol. By monitoring the increase in intensity of the methine proton, it can be seen that this product is not produced in significant quantities until there is an appreciable amount of hydroxylamine present. The same oxygen-centered radical that is involved in producing acetophenone also reacts with the hydroxylamine abstracting the reactive hydroxyl hydrogen radical to generate TEMPO and *sec*-phenethyl alcohol.

Prior to initiating the thermal decomposition of adduct MB-TMP, the ^{1}H NMR spectrum of the *N*-hydroxylamine derivative of 4-benzoate-TEMPO was measured and further characterized as reported in Chapter 4. The position of the hydroxyl resonance at

4.25 ppm in the ^{1}H NMR spectrum for the hydroxylamine of 4-benzoate-TEMPO was confirmed through mass spectroscopy. The corresponding resonance of the hydroxyl proton for the *N*-hydroxylamine derivative of TEMPO (H-TEMPO) in *ortho*-xylene-d_{10} was observed at 3.91 ppm. The identification of the *N*-hydroxylamine of 4-benzoate-TEMPO gave us confidence in assigning the broad singlet at δ 3.91 to H-TEMPO which is difficult to isolate since it is readily oxidized to TEMPO in air.

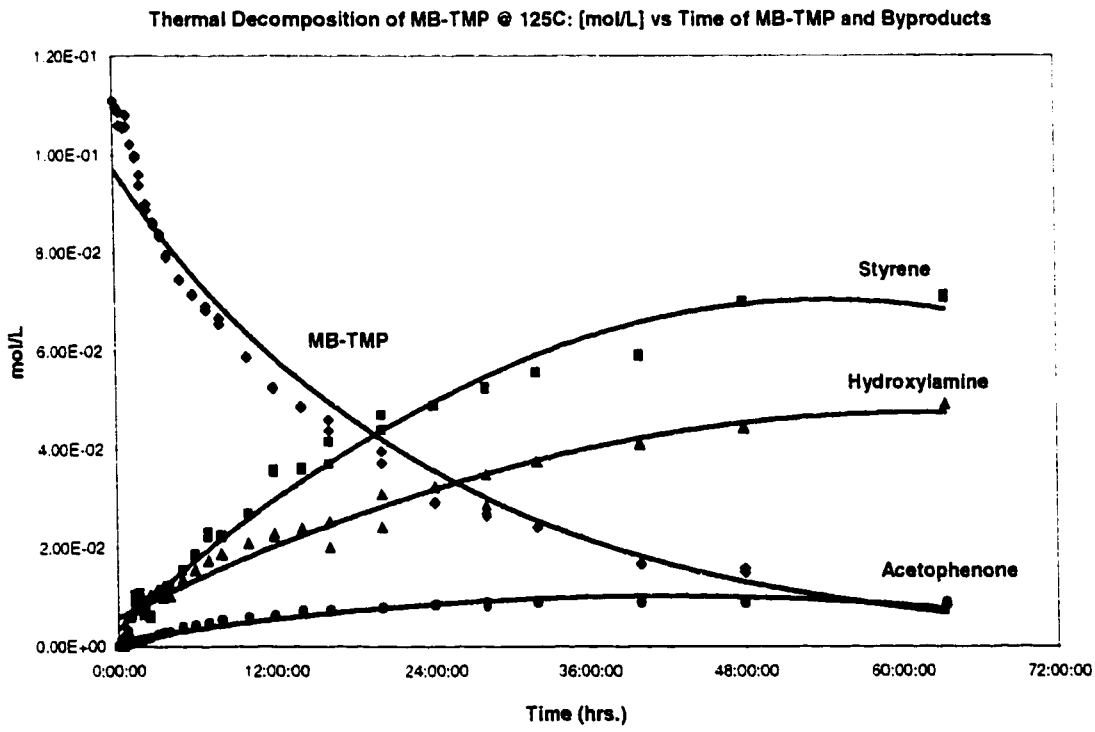

Figure 28: A plot of mol/L of MB-TMP, styrene, the *N*-hydroxylamine derivative of TEMPO and acetophenone production as a function of time at 125°C.

The decomposition of MB-TMP monitored by ^{1}H NMR was continued for 64 hours until it had completely dissociated. Shown in Figure 28 is the complete set of molar concentrations for each product formed and the decay of MB-TMP as a function of time.

Prior to the use of nitroxide radicals in the SFRP process, nitroxide radicals were employed as scavengers of carbon-centered radical. Bolsman *et al.*[11] reported on the catalytic scavenging of radicals in autoxidizing hydrocarbons by secondary amines and some derivatives (hydroxylamines and nitroxides) and on the mechanism of the catalytic scavenging process.[12] The paper by Bolsman *et al.*[11] on the mechanism of the catalytic inhibition of autoxidation of hydrocarbons at 130°C by nitroxides strongly suggests that the involvement of oxygen by an autoxidation step in the proposed mechanism for the thermal decomposition of MB-TMP is reasonable. To further support this proposed mechanism is a study by Grattan[13] who reported the thermal decomposition of a similar nitroxide adduct 1-(2′-cyano-2′-propoxy)-4-oxo-2,2,6,6-tetramethylpiperidine, **65**.

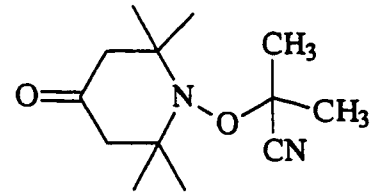

1-(2'-cyano-2'-propoxy)-4-oxo TEMPO

65

[11] Bolsman, T. A. B. M.; Blok, A. P.; Frijns, J. H. G. *Recl. Trav. Chim. Pays-Bas* **1978**, *97*, 313.
[12] Bolsman, T. A. B. M.; Blok, A. P.; Frijns, J. H. G. *J. Roy. Net. Chem. Soc.* **1978**, *97*, 313.
[13] Grattan, D. W.; Carlsson, D. J.; Howard, J. A.; Wiles, D. M. *Can. J. Chem.* **1979**, *57*, 2834.

In O_2-free solvents the decomposition of **65** according to Grattan *et al.*[13] can be rationalized by the mechanism shown in Scheme 18 where, upon C-O homolytic bond cleavage, the resulting nitroxide abstracts a β-hydrogen atom from the cyano-*iso*-propyl radical to produce the hydroxylamine and methacrylonitrile.

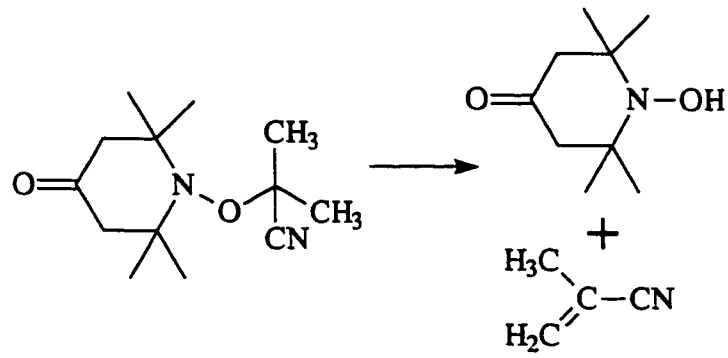

Scheme 18: Thermal decomposition of 1-(2′-cyano-2′-propoxy)-4-oxo-TEMPO, **65**.

In the presence of O_2, a different mechanism was reported where the radical scavenger O_2 reacts with the cyano-*iso*-propyl radical. The cyano-*iso*-propyl radical produced from the thermal decomposition of adduct **65**, then abstracts a hydrogen radical from the solvent to generate the corresponding 2-hydroxy-2-cyano-propane, $CH_3C(OH)(CN)CH_3$.

To further test the mechanism as outlined in Figure 27, and the inhibition by O_2, two additional experiments were performed. In the dry box, two identical samples were prepared containing MB-TMP in *ortho*-xylene-d_{10} $[MB\text{-}TMP]_o = 8.43 \times 10^{-2}$ M. A solution of 650 μL was added into one NMR tube and the sample was attached to a Wilmad Taperlok NMR value to seal the tube, Sample 1. The same volume of sample

was added into a second tube but this sample was capped with a regular plastic NMR cap, Sample 2. Both samples were removed from the dry box and Sample 1 was attached to a vacuum line to degas the solution of oxygen. Ten freeze-pump-thaw cycles were used. This was twice the number of FPT cycles used in the other experiments which did not completely remove O_2. The plastic cap of Sample 2 was removed and the MB-TMP solution was purposely exposed to atmospheric moisture and oxygen. By comparing the ^1H NMR spectra of these two samples after heating at 125°C, we set out to determine to what extent autoxidation affects the thermal decomposition of MB-TMP and verify the proposed mechanism. The samples were placed in an oil bath set to 125°C and, after 2 hours, the samples were quenched in an ice water bath (15 minutes). The ^1H NMR spectra were obtained at room temperature on the 300 MHz spectrometer. This cycle was continued until approximately 8 hours of heating was performed. Illustrated in Figure 29 is the normalized NMR proton peak area for each byproduct of the reaction plotted as a function of time. The rate of decomposition of MB-TMP is faster when exposed to atmospheric air and O_2 as compared to the FPT sample. The most dramatic difference is the amount of acetophenone produced. In the air + O_2 sample (Sample 2), three times the amount of acetophenone is generated after 8 hours 45 minutes of heating as compared to the controlled FPT sample. The rate of formation of styrene is similar in both samples. Quantifying the amount of *N*-hydroxylamine produced is more difficult when the spectra are acquired at room temperature. The piperidine ring methylene protons of both MB-TMP and the hydroxylamine form a very broad peak which prevents baseline resolution

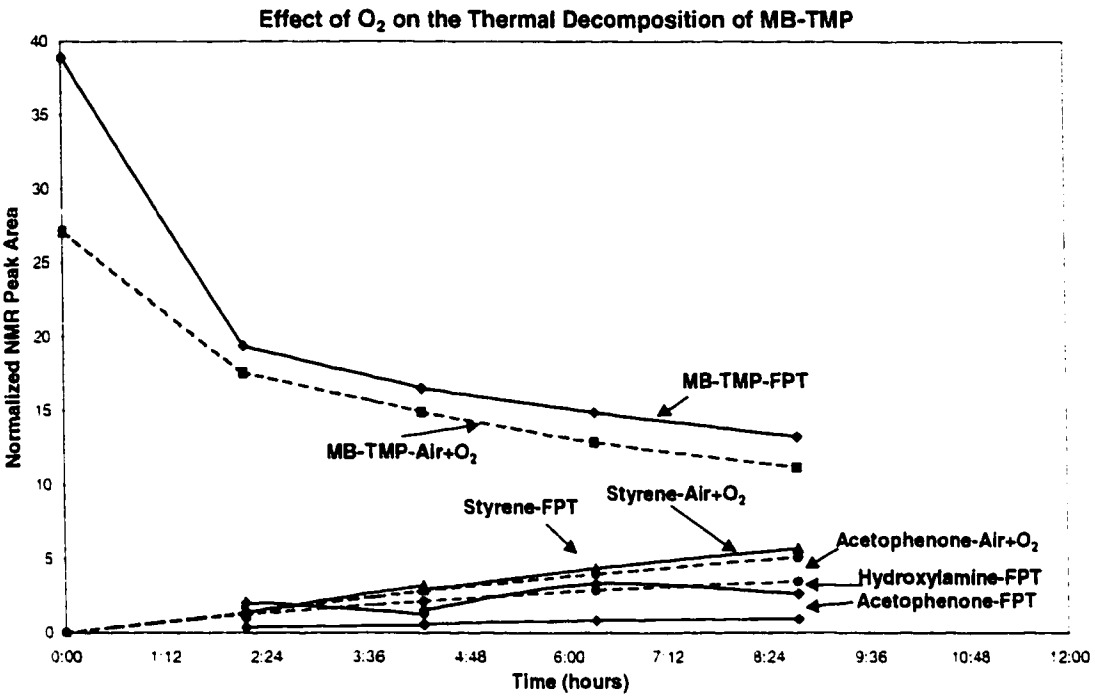

Figure 29: A plot of normalized ^{1}H NMR (300 MHz) resonance peak area as a function of time illustrating the effect of O_2 on the products from the thermal decomposition of MB-TMP at 125°C.

of the key methyl protons used to integrate the hydroxylamine. This is evident in the ^{1}H NMR spectra of Figure 30 where the spectrum of the starting FPT sample was compared to the spectrum obtained at room temperature after 4 hours 15 minutes of heating. The sharp singlet at 1.35 ppm was assigned to the four methyls of the *N*-hydroxylamine derivative of TEMPO. Even though 10 FPT cycles were performed on Sample 1, acetophenone was still produced, as evident by the peaks at 7.9 ppm. This means oxygen was still retained by the solvent.

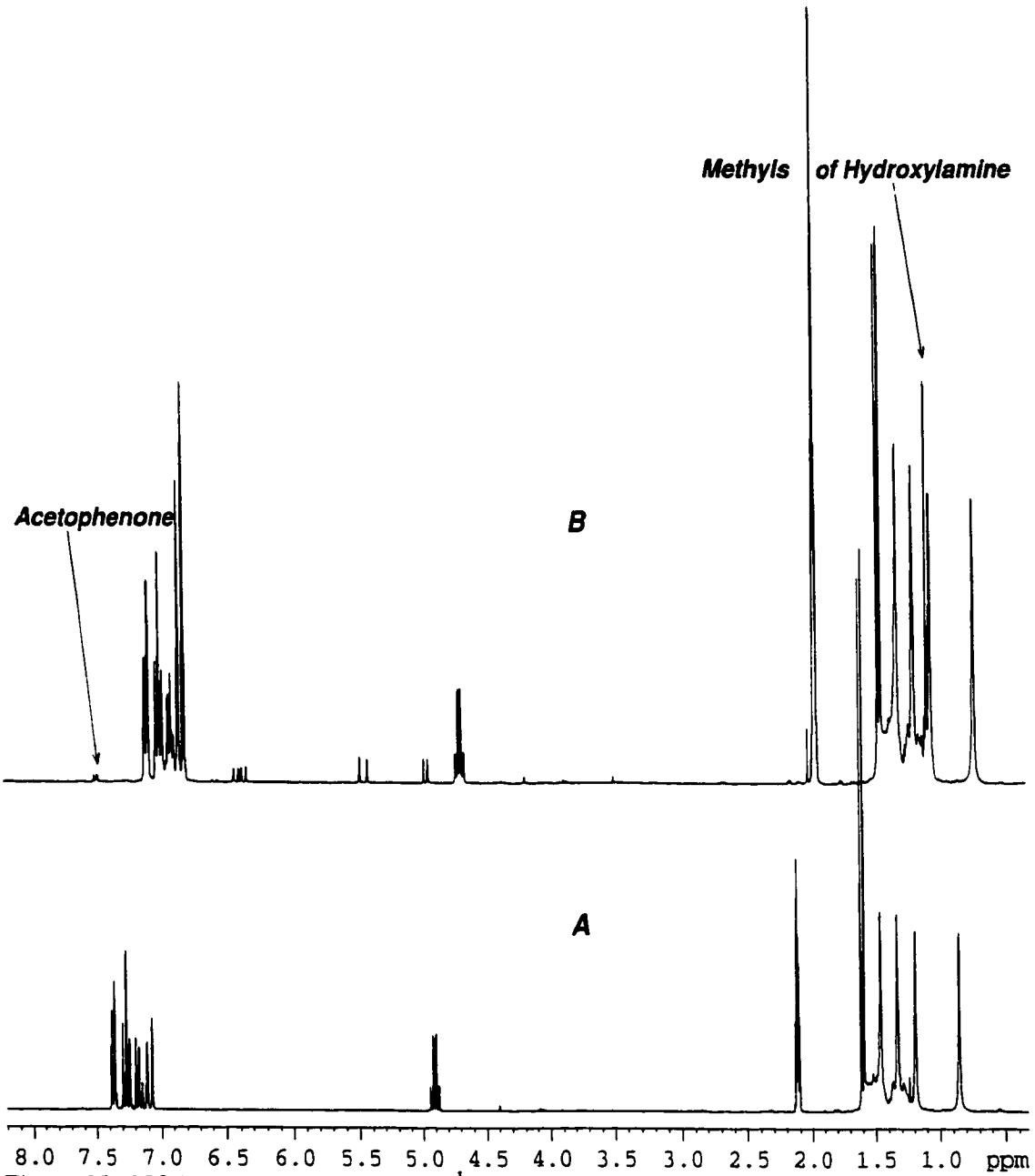

Figure 30: 300 MHz room temperature ^{1}H NMR spectra of a:) Sample 1 (FPT) at time zero and b:) Sample 1 after heating at 125°C for 4 hours 15 minutes.

How does the proposed mechanism for the thermal decomposition of MB-TMP in the presence and absence of oxygen, relate to the possible termination of polystyrene chains prepared via the stable free radical polymerization process? As originally suggested, the abstraction of hydrogen from the propagating chain end by the nitroxide can produce a terminal vinyl group. As demonstrated by Yoshida *et al.*[4] in their nitroxide chain end transformation experiment, long reaction times (24 hours) at 130°C are required to show any evidence of terminal vinyl protons. In addition to terminal vinyl groups, oxygen in the polymerization system could rapidly produce a phenyl ketone chain end which would appear as a single carbonyl resonance in the ^{13}C NMR spectrum. The autoxidation reaction inhibiting the SFR polymerization would occur at the beginning of the polymerization. Provided the polymerization is under an inert atmosphere of N_2 or Ar, the probability of this reaction is reduced. As long as the concentration of free nitroxide is kept low then vinyl chain ends should be absent or minimized. The overall contribution of chain end termination in a SFRP of styrene by the mechanisms described above is probably no more than 5%, but this has yet to be proven.

Chapter 6

Stable Free Radical Polymerization of Styrene Initiated with Nitroxide Adducts

6.1 Introduction

A polymerization thesis would not be complete without a chapter containing some polymerization data. This chapter focuses on evaluating two nitroxide adducts, *N*-(1´-methylbenzyloxy)-2,2,6,6-tetramethylpiperidine, MB-TMP and *N*-(benzyloxy)-2,2,6,6-tetramethylpiperidine, B-TMP as initiator reversible terminating agents for the stable free radical polymerization of styrene. Upon homolytic cleavage of the C-O bond in the two adducts, the resulting carbon centered radical fragment initiates the SFR polymerization followed by rapid capture by the reversible terminating agent. In addition, a direct comparison is made between MB-TMP and the unimer BST and the effect excess nitroxide has on the polymerization. The efficiency of these adducts are evaluated in terms of molecular weight and polydispersity control and conversion of monomer to polymer.

During the course of this work, other research groups, such as those of Solomon[1], Hawker[2], Li, Howell and Priddy[3], and Matyaszewski[4], also prepared nitroxide adducts and used them to synthesize various homopolymers, as well as random and block copolymers by the stable free radical polymerization process. Their work was described in detail in section 1.6 of the thesis introduction.

6.2 Experimental Section

6.2.1 Purification of Styrene Monomer

To purify styrene monomer, 400 mL of commercial styrene was stirred with NaH for 3-4 hours to react with water present in with the monomer. Using vacuum distillation, the middle fraction of monomer was collected and then stored in the fridge until needed.

---

[1] Solomon, D. H.; Rizzardo, E.; Cacioli, P. U. S. Pat. **4,581,429**, April 8, 1986. Rizzardo, E. *Chem. Aust.* **1987**, *54*, 32. Moad, G.; Rizzardo, E. *Pac. Polym. Prepr.* **1993**, *3*, 651.

[2] Hawker, C. J. *J. Am. Chem. Soc.* **1994**, *116*, 11185. Hawker, C. J.; Hedrick, J. L. *Macromolecules* **1995**, *28*, 2993. Hawker, C. J. *TRIP* **1996**, *4(6)*, 183. Barclay, G. G.; Orellana, A.; Hawker, C. J.; Elce, E. Dao, J. *Polym. Mater. Sci. Eng.* **1996**, *74*, 311. Hawker, C. J.; Barclay, G. G.; Orellana, A.; Dao, J.; Devonport, W. *Macromolecules* **1996**, *29(16)*, 5245. Grubbs, R. B.; Hawker, C. J.; Dao, J.; Fréchet, J. M. J. *Angew. Chem. Int. Ed. Engl.* **1997**, *36(3)*, 270. Hawker, C. J.; Mecerreyes, D.; Elce, E.; Dao, J.; Hedrick, J. L.; Barakat, I.; Dubois, P. Jérôme, R.; Volksen,W. *Macromol. Chem. Phys.* **1997**, *198*, 155. Mecerreyes, D.; Dubois, P.; Jérôme, R.;Hedrick, J. L.; Hawker, C. J.; Beinat, S.; Schappacher, M.; Deffieux, A. *Polym. Mat. Sci. Eng.* **1997**, *77*, 189.

[3] Li, I.;Howell, B. A.; Matyjaszewski, K.; Shigemoto, T.; Smith, P. B.; Priddy, D. B. *Macromolecules* **1995**, *28*, 6692. Howell, B. A.; Priddy, D. B.; Li, I. Q.; Smith, P. B.; Kastl, P. E. *Polymer Bulletin* **1996**, *37*, 451. Li, I. Q.; Howell, B. A.; Koster, R. A.; Priddy, D. B. *Macromolecules* **1996**, *29*, 8554. Howell, B. A.; Pan, B.; Priddy, D. B. *Polym. Mater. Sci. Eng.* **1997**, *76*, 387.

6.2.2 Polymerization Procedure

Into a 100 mL three necked round bottom flask equipped with an argon purge inlet, a mechanical stirring shaft and a water condenser, was added distilled styrene monomer and the appropriate amount of nitroxide adduct. The polymerization flask was immersed in an oil bath preheated to the desired temperature varying from 120°C to 150°C. The polymerization proceeded for approximately 6 hours after which the polymeric solution was cooled and isolated. Throughout the polymerization reaction, samples were removed to monitor the polymer molecular weight by Gel Permeation Chromatography (GPC) and monomer conversion to polymer by Gas Chromatography (GC).

6.3 Results and Discussion

6.3.1 Stable Free Radical Polymerization Using Nitroxide Adducts

The approach taken to study the initiation of the SFRP process was to prepare a series of 2,2,6,6-tetramethylpiperidin-1-alkoxy and 2,2,6,6-tetramethylpiperdin-1-aryloxy compounds (RO-TMP) and to evaluate the ability of these nitroxide adducts to perform as initiator reversible trapping agents in the SFRP of styrene. Initially, Georges *et al.*[5]

---

[4] Greszta, D.; Matyjaszewski, K. *J. Polym. Sci. A: Polym. Chem.* **1997**, *35*, 1857.
[5] Georges, M. K.; Veregin, R. P. N.; Kazmaier, P. M.; Hamer, G. K. *Macromolecules* **1993**, *26*, 2987. Veregin, R. P. N.; Georges, M. K.; Kazmaier, P. M.; Hamer, G. K.; *Macromolecules* **1993**, *26*, 5316. Georges, M. K.; Veregin, R. P. N.; Kazmaier, P. M.; Hamer, G. K. *Trends Polym. Sci.* **1994**, *2*, 66.

used conventional free radical initiators, BPO and AIBN with a stable nitroxyl radical, to initiate the stable free radical polymerization. It was determined that more than one molar equivalent of nitroxide was necessary to provide efficient reversible capping of the propagating chain end during the polymerization to enable narrow polydispersities. As the concentration of excess nitroxide decreased, the rate of polymerization increased, but if the concentration of nitroxide was too low, the polydispersity broadened. By preparing model initiator reversible terminating agents such as MB-TMP and B-TMP which in solution have a low concentration of excess nitroxide (10^{-7} to 10^{-5} M), we were interested in determining if these molecules would initiate a SFR polymerization and also enable narrow molecular weight distributions. The structure of MB-TMP, **32**, is very similar to the unimer BST, **33**, which has been isolated and identified as an intermediate from the BPO initiated stable free radical polymerization of styrene. BST[6] is produced when the initiating benzoyloxy radical from BPO attacks a styrene monomer molecule and subsequently is trapped by TEMPO. The benzoyloxy functional group of BST is replaced by hydrogen in MB-TMP and the initiating ability of MB-TMP was compared to BST. The initiating ability of the nitroxide adducts are dependent on the rate of homolytic C-ON bond cleavage. In both BST and MB-TMP, the oxygen atom of TEMPO is bonded to a substituted benzylic carbon, whereas, in B-TMP this carbon is a primary benzylic center. Evaluating the initiating ability of MB-TMP and B-TMP

---

[6] Veregin, R. P. N.; Georges, M. K.; Hamer, G. K.; Kazmaier, P. M. *Macromolecules* **1995**, *28*, 4391.

compares the rate of homolytic C-ON bond cleavage of these two benzylic carbons which controls the initiation of an SFR polymerization.

6.3.2 Polymerization of Styrene Using B-TMP

The nitroxide adduct B-TMP was evaluated as an initiator reversible terminating agent to polymerize styrene via the SFRP process. Illustrated in Figure 31, are three separate polymerization reactions performed at various temperatures (120°C (solid curve), 130°C (dotted curve) and 143°C (dot dash curve)). The corresponding polymerization data is presented in Table 8. Into each reaction was added B-TMP and benzoic acid to prevent or diminish the spontaneous self-initiation of styrene. It appears that after 4 hours at 120°C in the presence of benzoic acid, self-initiation to polymerize styrene did not occur. Molecular weight analysis indicated that only 1 or 2 monomer units were added, Mn = 450 and MWD = 1.63. These results suggested that the C-O bond between the benzyl initiating radical portion and TEMPO in B-TMP did not break at 120°C. To increase the probability of C-O bond cleavage in B-TMP, the polymerization was repeated at 130°C. This time, thermal initiation of polystyrene occurred via the Mayo mechanism[7] (Scheme 15, section 1.6) with minimal or no homolytic cleavage of the C-O bond. This is illustrated by curve b) of Figure 31 where very high molecular weight polymer was observed after 3 minutes into the reaction. The presence of benzoic acid did not inhibit the self-initiation of styrene at 130°C thus,

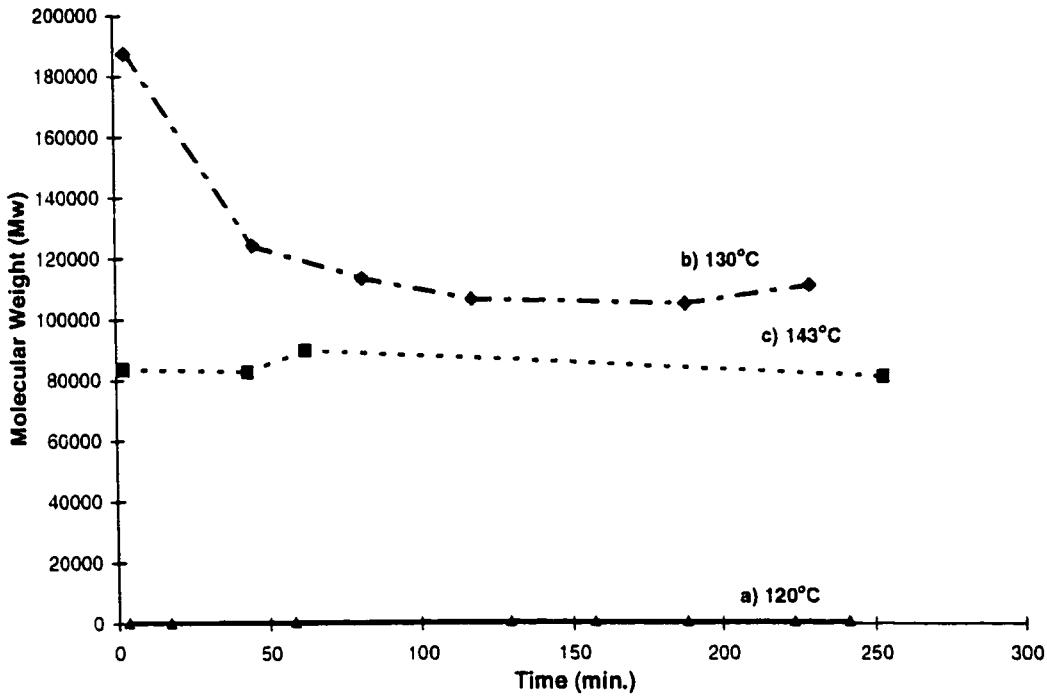

Figure 31: Dependence of weight-average molecular weight Mw as a function of polymerization time for the bulk polymerization of styrene in the presence of B-TMP and benzoic acid (BA) at a) 120°C, $[B\text{-}TMP]_0 = 2.1 \times 10^{-2}$ M, $[BA]_0 = 8.0 \times 10^{-2}$ M, b) 130°C, $[B\text{-}TMP]_0 = 1.1 \times 10^{-2}$ M, $[BA]_0 = 8.0 \times 10^{-2}$ M and c) at 143°C, $[B\text{-}TMP]_0 = 1.1 \times 10^{-2}$ M, $[BA]_0 = 8.0 \times 10^{-2}$ M.

Table 8: Characterization Data for Styrene Bulk Polymerization with Nitroxide Adduct B-TMP and Benzoic Acid

$[B\text{-}TMP]_0$ (mol/L)	$[Benzoic\ Acid]_0$ (mol/L)	Polym. Temp. (°C)	Polym. Time (hrs.)	Conversion[a] (%)	Mn	MWD
0.021	0.08	120	4	8.2	450	1.49
0.011	0.08	130	4.25	57.3	43900	2.12
0.011	0.08	143	4	76.2	28800	2.82

[a] Evaluated by GC using acetone as an internal reference.

[7] Mayo, F. R. *J. Am. Chem. Soc.* **1968**, *90*, 1289.

resulting in a typical conventional free radical polymerization. A third reaction (curve c) was performed at 143°C also containing benzoic acid. Similar to the polymerization at 130°C, styrene was polymerized by a conventional free radical mechanism with self-initiation by the Mayo[7] mechanism. At 143°C more polymer chains were initiated resulting in a lower Mn and higher monomer conversion to polymer (see Table 8). From this set of experiments, it was concluded that the rate of homolytic cleavage of the C-O bond in B-TMP was too slow to control the initiation of styrene polymerization by a SFRP mechanism. Instead, self or autoinitiation of styrene dominated resulting in a conventional free radical polymerization. From the ESR study (Chapter 4) it was determined that the C-O bond in B-TMP is labile but the rate of homolytic cleavage to produce the primary benzylic carbon radical is slower due to a higher enthalpy of activation of 138.3 kJ/mol. This value is significantly higher than the enthalpy of activation measured for MB-TMP (131.2 kJ/mol) and BST[8] (130 kJ/mol) which, as shown in the following section does initiate SFRP of styrene. Nitroxide adducts containing primary benzylic carbon bonded to TEMPO do not contain a weak enough C-O bond to initiate styrenic stable free radical polymerization without autoinitiation of styrene dominating the reaction. Hawker[2] and Li[3] concluded that a primary benzylic carbon bonded to a nitroxyl radical does not form a labile C-O bond under styrene SFR polymerization conditions. When the primary benzylic carbon radical of B-TMP is

---

[8] Veregin, R. P. N.; Georges, M. K.; Hamer, G. K.; Kazmaier, P. M. *Macromolecules* **1995**, *28*, 4391.

replaced with a substituted benzylic carbon as in MB-TMP, the C-O bond is more labile. Increasing steric bulk on the carbon of the initiating radical fragment is responsible for lowering the C-O bond strength.

6.3.3 Polymerization of Styrene Using MB-TMP

The stable free radical polymerization of styrene using MB-TMP as the initiator and nitroxide source was evaluated at various temperatures using different concentrations of MB-TMP. Figure 32 shows the peak molecular weight, Mp, as a function of polymerization time (solid curves) and polydispersity (dashed curves) at different polymerization temperatures; 132°C, 135°C, 140°C and 150°C. As each reaction proceeded, Mp increased in a linear fashion as a function of polymerization time. Depending on the reaction conditions, polymerization temperature and initial concentration of MB-TMP, final peak molecular weights ranged from 20,000 to 80,000 and MWD values less than 1.5 were obtained. In the four reactions, the initial concentration of MB-TMP in styrene decreased from $[MB\text{-}TMP]_o = 1.5 \times 10^{-2}$ M at 132°C to $[MB\text{-}TMP]_o = 1.0 \times 10^{-2}$ M at 150°C which also contributed to the observed increase in the rate of polymerization.

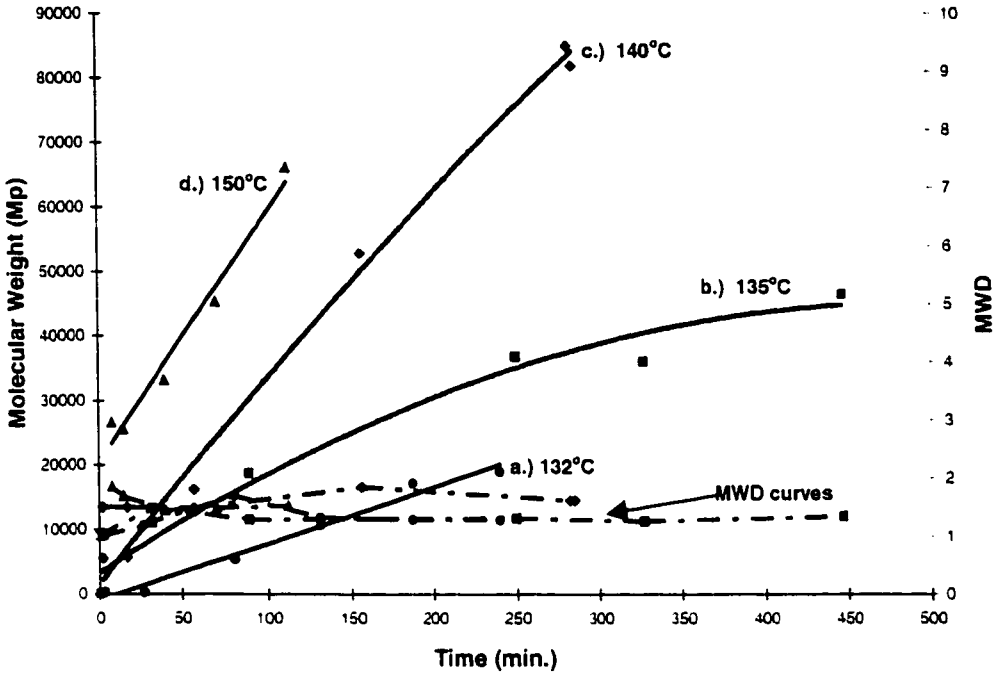

Figure 32: Peak molecular weight Mp. (solid lines) and molecular weight distribution MWD. (dashed lines) as a function of polymerization time for the bulk SFRP of styrene at different reaction temperatures and initial concentrations of MB-TMP. a) 132°C $[MB\text{-}TMP]_0 = 1.5x10^{-2}$ M. b) 135°C $[MB\text{-}TMP]_0 = 1.5x10^{-2}$ M. c) 140°C $[MB\text{-}TMP]_0 = 9.5 \times 10^{-3}$ M. d.) 150°C $[MB\text{-}TMP]_0 = 1.0x10^{-2}$ M.

The initiating ability of the MB-TMP and the unimer BST were evaluated and compared in the SFRP process at 138°C. Illustrated in Figure 33 are the Mn curves as a function of percent monomer conversion to polymer for four different reactions. Curves a) and b) both show linear increases in Mn as a function of monomer conversion. The

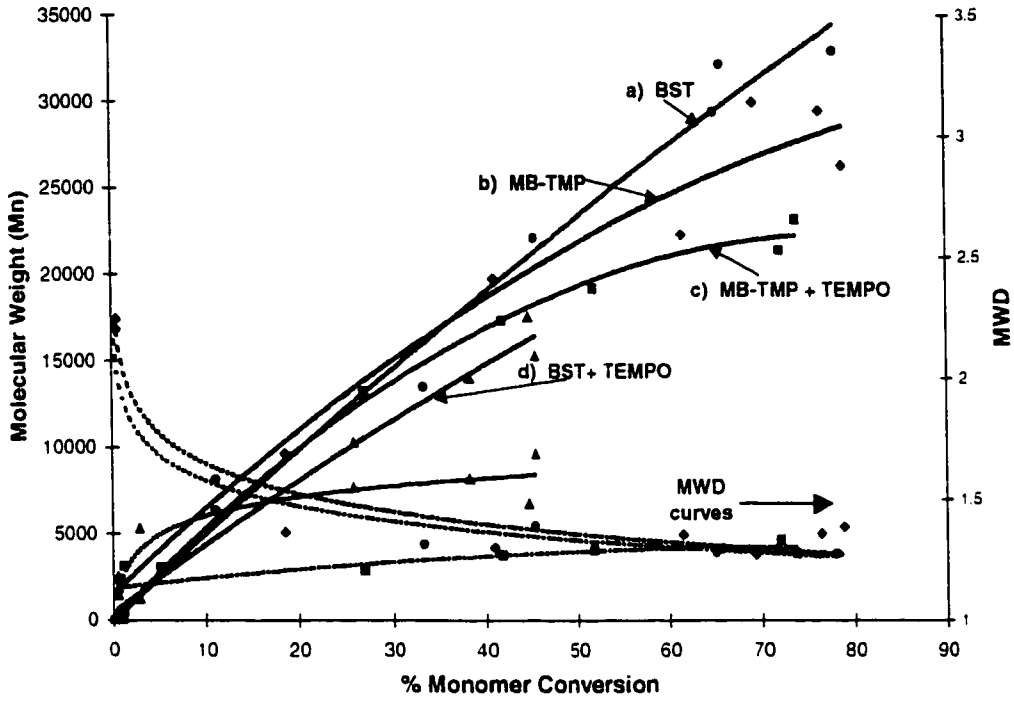

Figure 33: Polymer number-average molecular weight Mn, (solid lines) and polydispersity MWD, (dashed lines) as a function of monomer conversion for the SFRP of styrene with MB-TMP compared to BST with and without added TEMPO, at 138°C. a) $[BST]_0 = 1.4x10^{-2}$ M, no added TEMPO, b) $[MB\text{-}TMP]_0 = 1.5x10^{-2}$ M, no added TEMPO, c) $[MB\text{-}TMP]_0 = 1.5x10^{-2}$ M, $[TEMPO]_0 = 2.6x10^{-3}$ M, d) $[BST]_0 = 1.5x10^{-2}$ M, $[TEMPO]_0 = 3.2x10^{-3}$M.

corresponding polydispersity curves are also shown in Figure 33 as dashed lines. Polydispersities greater than 2 during the initiation stage of the polymerization decrease to typical MWD values of 1.2 to 1.3. The contribution of some autoinitiation of polystyrene chains in combination with a statistical distribution of monomer units per chain produced MWD >2 during the first 5-10 minutes of the reaction. The statistical

distribution becomes less significant as the chains propagate and the polydispersity values decreased. Also, the thermal initiated polystyrene chains were capped by the nitroxide radical and continue to propagate in a living manner.

To control a stable free radical polymerization and produce polymers with low MWD values, an equilibrium exists between the dormant capped chains and the propagating chains with free nitroxide radicals. To reach this equilibrium, some of the initially formed polymer chains terminate, which may only be one or two chains, to generate free TEMPO. Once this equilibrium is reached, chain propagating continues in a controlled manner producing low polydispersity polymer.

Also included in Figure 33, are two additional reactions where an excess of free TEMPO was added. As measured by ESR spectroscopy (Chapter 4), there is always free nitroxide in solution with MB-TMP and BST, but the concentration levels are very small (10^{-7} to 10^{-5} M). In reaction c), a 0.17 mole excess of TEMPO was added. Mn increased in a linear manner as a function of monomer conversion. The polydispersity remained very narrow throughout the entire reaction at 1.2 even during the initiation stage. The same behaviour was also demonstrated by curve d) for BST with a 0.22 mole excess of TEMPO. The GPC chromatograms for this reaction are shown in Figure 34, illustrating a shift in the molecular weight peak from $t_1 = 9$ minutes to $t_6 = 416$ minutes. The presence of excess nitroxide enabled a narrow MWD during the initiation and oligomer formation stage of the SFR polymerization. This data suggests that MB-TMP initiated the polymer chains without any significant contribution of autoinitiation of polystyrene.

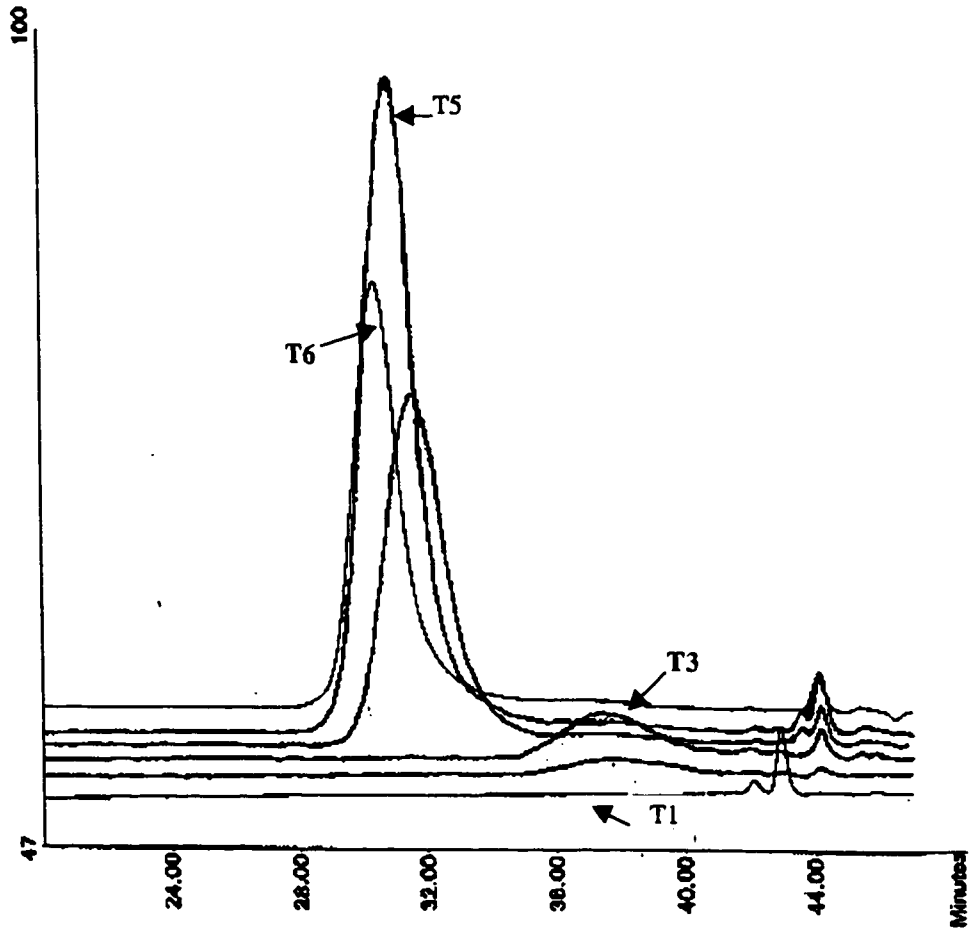

Figure 34: A series of GPC chromatograms taken from the SFRP of styrene initiated with BST and excess TEMPO, $[BST]_o = 1.5x10^{-2}$ M, $[TEMPO]_o = 3.2x10^{-3}$ M.

Figure 35 shows the conversion versus time data (solid lines) and the logarithmic conversion, $\ln([M]_o/[M]_t)$ versus time data (dashed lines) for the same four reactions

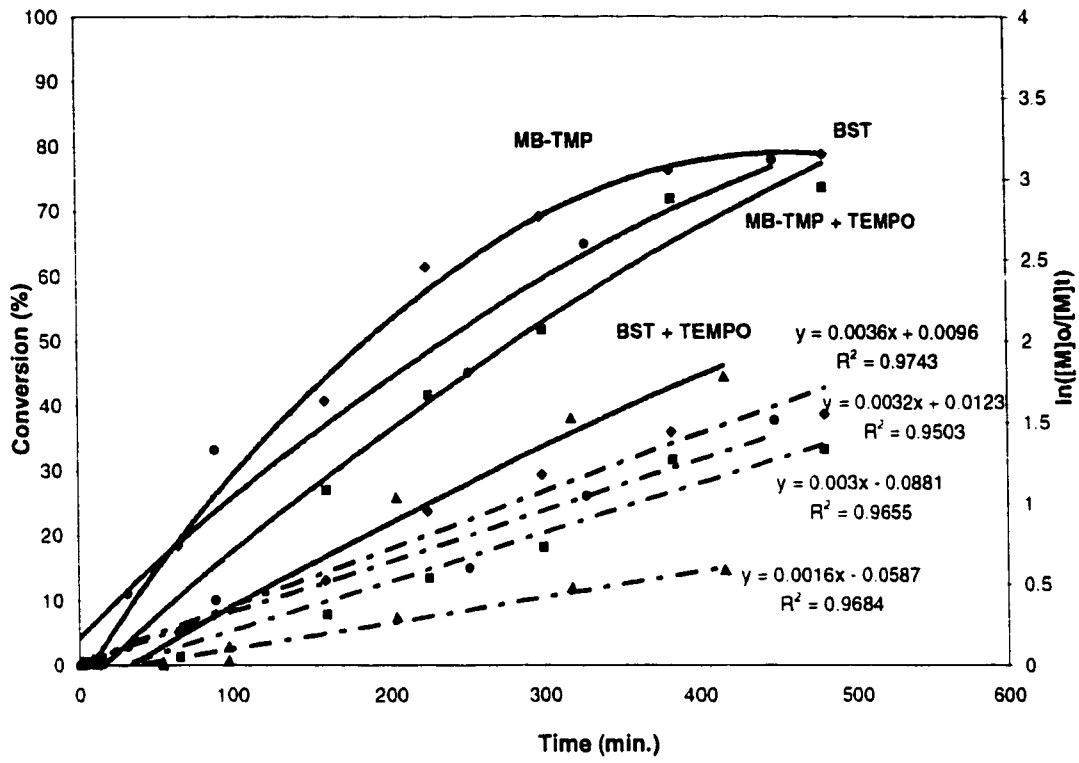

Figure 35: Conversion and $\ln([M]_0/[M]_t)$ plots vs. time for the bulk SFRP of styrene at 138°C initiated with MB-TMP and BST with and without added TEMPO for the same four reactions presented in Figure 33.

at 138°C presented in Figure 33. The monomer conversion approached 80 % after 7 hours for the bulk polymerization of styrene using MB-TMP as initiator and nitroxide source. This illustrates a faster rate of polymerization at 138°C than the first reported SFRP of bulk styrene[9] that required 69 hours at 123°C. $[M]_0$ and $[M]_t$ denotes the initial monomer concentration and the monomer concentration at time *t*, respectively. The first-order rate plots (dashed lines) are linear, indicating that the polymerization is internally

first order with respect to monomer and that the concentration of propagating species remains constant. The two reactions with added excess TEMPO (MB-TMP + 0.17 mol TEMPO, ■ and BST + 0.22 mol. TEMPO, ▲) decreases the apparent rate constants k_{obs}, of propagation and thus slowed down the reaction. The apparent rate constants for propagation for the kinetic curves of Figure 35 are presented in Table 9. The observed rate constants k_{obs} are comparable to the previously reported [10]rate constants (k_{obs} = 4.9×10^{-5} s^{-1}) for a SFRP of styrene initiated with BPO and an initial ratio of TEMPO to BPO of 1.5.

Table 9: Apparent Rate Constant Data from the Kinetic Plots Comparing Bulk SFRP of Styrene Initiated with MB-TMP and BST.

Adduct	Added TEMPO (mol)	Slope of Kinetic Curves	R^2	Appr. Rate, k_{app}, (sec^{-1})
MB-TMP	0	0.0036	0.9743	6.0×10^{-5}
BST	0	0.0032	0.9503	5.33×10^{-5}
MB-TMP	0.17	0.003	0.9655	5.0×10^{-5}
BST	0.22	0.0016	0.9484	2.7×10^{-5}

The initiating efficiency of MB-TMP and BST are the same within experimental error. The same number-average molecular weight (Mn = 29,000) was obtained at the same monomer conversion (66 %) point for the bulk stable free radical polymerization of styrene. The addition of excess nitroxide slows down the propagation rate.

---

[9] Georges, M. K.; Veregin, R. P. N., Kazmaier, P. M.; Hamer, G. K. *Macromolecules* **1993**, *26*, 2987.

[10] Veregin, R. P. N.; Georges, M. K.; Hamer, G. K.; Kazmaier, P. M. *Macromolecules* **1995**, *28*, 4391.

Chapter 7

Conclusions and Future Work

Model nitroxide adducts have proven to be very useful in developing the chemistry and enhancing the fundamental understanding of the stable free radical polymerization process. These nitroxide adducts mimic the propagating chain end of the SFR polymerization and provided a method to study the C-O bond on a small molecule scale instead of working directly with polymers. This approach simplified the chemistry and enabled a direct correlation of the data to the SFRP process.

This thesis described the synthesis, characterization and evaluation of model initiator / reversible terminating agents, to enhance the fundamental understanding of the stable free radical polymerization process. One portion of this research, involved AM1 and PM3 semi-empirical molecular orbital calculations on a model SFR reaction. The aim of this work was to identify new nitroxyl radicals with a labile C-O bond, but it became apparent that semi-empirical MO calculations were not accurate enough to differentiate between various nitroxyl radicals. To calibrate the MO calculations and determine where the deficiencies in the methods were, the single crystal X-ray structure of MB-TMP was

obtained. Future work in the area of semi-empirical MO calculations will not be possible until the theoretical chemists improve the accuracy and precision of this technique.

A series of alkoxy and aryloxy-tetramethylpiperidine compounds, RO-TMP were prepared by the reaction of tri-*n*-butyl tin hydride with various alkyl or aryl halides and TEMPO. Using the same synthetic route, the 1-phenylethyl carbon radical fragment was trapped by 1,1,3,3-tetramethyl- and 1,1,3,3-tetraethylisoindoline nitroxide to form MB-TMI and MB-TEI. All compounds were isolated, purified and characterized by ^{1}H and ^{13}C NMR spectroscopy. Using ESR spectroscopy, the enthalpy of activation to homolytically cleave the C-O bond in ten of the nitroxide adducts was measured. In the adduct series, MB-TMP, MiP-TMP and EiB-TMP which mimic the styrene, acrylate and methacrylate monomers respectively, the enthalpy of activation decreased from 131.2 ± 7.2, 125.3 ± 5.4 to 119.2 ± 3.4 kJ/mol, respectively. This indicated that the C-O bond strength between the propagating polymer chain end and TEMPO was the weakest for a methacrylate monomer with increasing C-O bond strength for acrylate and styrene monomers. Steric bulk of the tertiary methacrylate radical carbon contributed to a weaker and more labile C-O bond. In the series of initiating carbon radicals bonded to TEMPO, it was demonstrated that increasing the steric crowding about the carbon radical decreased the enthalpy of activation to break the C-O bond. Also, when steric bulk was increased on the alpha carbons to the nitroxyl functional group in the tetraethylisoindoline nitroxide, the

C-O bond in 1-phenylethyl-tetraethylisoindoline adduct, MB-TEI was 4.7 kJ/mol weaker than in MB-TMI.

The thermal decomposition of nitroxide adduct MB-TMP was measured as a function of time at 125°C by ESR and ^{1}H NMR spectroscopy. As a result of this kinetic study, an alternative mechanism to that of Li *et al.* was proposed for possible polymer chain termination when the excess nitroxide in the polymerization system builds up. All major products from the thermal decomposition of MB-TMP were identified and the effect of oxygen in the polymerization via an autoxidation mechanism was observed. This study has identified that hydrogen radical abstraction by a significant excess of TEMPO can produce a terminal vinyl group at the end of a polystyrene chain. In the presence of oxygen and excess TEMPO, a phenyl ketone functional group can also be produced to terminate a polystyrene chain end. The presence of such functional groups SFRP polymers will be investigated in the future.

This high temperature ^{1}H NMR and ESR study will be extended to MiP-TMP which will provide additional information on possible termination reactions in the acrylate polymerization.

Two nitroxide adducts, MB-TMP and B-TMP and the unimer BST were evaluated as initiators and only source of nitroxyl radical in the bulk polymerization of styrene by the stable free radical polymerization process. The C-O bond in B-TMP did not cleave at a fast enough rate to enable a controlled SFR polymerization. Instead, polystyrene chains

were self-initiated by the Mayo mechanism resulting in a conventional free radical polymerization process. The initiating efficiency of MB-TMP was found to be equivalent to BST and a controlled 'living' stable free radical polymerization with narrow polydispersities was demonstrated. The alpha-methyl group on the benzylic carbon in MB-TMP was responsible for increasing the steric bulk around the C-O bond and making the bond more labile. The addition of excess nitroxide to the polymerization decreased the rate constant of propagation and lowered the molecular weight distribution during the initiation period of polymerization.

Appendix I

Table 1: Crystal data and structure refinement for MB-TMP, **32** at 27°C.

Identification code	km1
Empirical formula	C17 H27 N O
Formula weight	261.40
Temperature	300(2) K
Wavelength	0.71073 A
Crystal system	monoclinic
Space group	P2(1)/n
Unit cell dimensions	a = 13.7809(4) A alpha = 90 deg. b = 7.8345(2) A beta =91.5420(10) deg. c = 15.1637(3) A gamma = 90 deg.
Volume, Z	1636.58(7) A^3, 4
Density (calculated)	1.061 Mg/m^3
Absorption coefficient	0.065 mm^-1
F(000)	576
Crystal size	.38 x .25 x .18 mm
Theta range for data collection	1.97 to 26.20 deg.
Limiting indices	-16<=h<=17, -9<=k<=9, -18<=l<=18
Reflections collected	12957
Independent reflections	3221 [R(int) = 0.0462]
Refinement method	Full-matrix least-squares on F^2
Data / restraints / parameters	3221 / 0 / 173

Goodness-of-fit on F^2	0.967
Final R indices [I>2sigma(I)]	R1 = 0.0550, wR2 = 0.1602
R indices (all data)	R1 = 0.0975, wR2 = 0.2014
Extinction coefficient	0.018(4)
Largest diff. peak and hole	0.171 and -0.129 e.A^-3

Table 2. Atomic coordinates (x 10^4) and equivalent isotropic displacement parameters (A^2 x 10^3) for **32** at 27°C. U(eq) is defined as one third of the trace of the orthogonalized Uij tensor.

	x	y	z	U(eq)
O(3)	2275(1)	3464(2)	5687(1)	49(1)
N(4)	2401(1)	2599(2)	4838(1)	47(1)
C(12)	3061(1)	1083(3)	5015(1)	51(1)
C(13)	3313(2)	316(3)	4114(2)	66(1)
C(19)	3722(2)	1589(4)	3471(2)	80(1)
C(17)	2996(2)	3038(4)	3340(2)	73(1)
C(11)	2750(2)	3949(3)	4205(1)	56(1)
C(15)	3987(2)	1469(3)	5573(2)	68(1)
C(14)	2476(2)	-260(3)	5514(2)	69(1)
C(16)	3620(2)	5037(3)	4543(2)	70(1)
C(18)	1895(2)	5168(3)	4016(2)	78(1)
C(6)	90(2)	1225(3)	6058(2)	58(1)
C(8)	-268(2)	-187(3)	6512(2)	72(1)
C(9)	141(2)	-618(4)	7328(2)	80(1)
C(10)	888(2)	343(4)	7687(2)	83(1)
C(7)	1240(2)	1743(3)	7240(2)	67(1)
C(5)	850(1)	2198(3)	6407(1)	50(1)
C(2)	1250(2)	3692(3)	5898(2)	54(1)
C(1)	1218(2)	5359(3)	6420(2)	85(1)

Table 3. Bond lengths [A] and angles [deg] for **32** at 27°C.

O(3)-C(2)	1.468(2)
O(3)-N(4)	1.470(2)
N(4)-C(12)	1.515(3)
N(4)-C(11)	1.515(3)
C(12)-C(14)	1.537(3)
C(12)-C(13)	1.540(3)
C(12)-C(15)	1.542(3)
C(13)-C(19)	1.515(4)
C(19)-C(17)	1.523(4)
C(17)-C(11)	1.539(3)
C(11)-C(16)	1.548(3)
C(11)-C(18)	1.538(3)
C(6)-C(5)	1.388(3)
C(6)-C(8)	1.400(3)
C(8)-C(9)	1.388(4)
C(9)-C(10)	1.376(4)
C(10)-C(7)	1.383(4)
C(7)-C(5)	1.406(3)
C(5)-C(2)	1.514(3)
C(2)-C(1)	1.528(3)
C(2)-O(3)-N(4)	112.58(14)
O(3)-N(4)-C(12)	106.88(14)
O(3)-N(4)-C(11)	106.28(14)
C(12)-N(4)-C(11)	117.4(2)
N(4)-C(12)-C(14)	107.7(2)
N(4)-C(12)-C(13)	107.3(2)
C(14)-C(12)-C(13)	107.6(2)
N(4)-C(12)-C(15)	115.3(2)
C(14)-C(12)-C(15)	107.5(2)
C(13)-C(12)-C(15)	111.1(2)
C(12)-C(13)-C(19)	114.3(2)
C(17)-C(19)-C(13)	108.7(2)
C(19)-C(17)-C(11)	113.2(2)
N(4)-C(11)-C(17)	107.3(2)
N(4)-C(11)-C(16)	115.5(2)
C(17)-C(11)-C(16)	110.5(2)
N(4)-C(11)-C(18)	107.3(2)
C(17)-C(11)-C(18)	108.3(2)
C(16)-C(11)-C(18)	107.6(2)
C(5)-C(6)-C(8)	121.3(2)

C(9)-C(8)-C(6)	119.3(2)
C(10)-C(9)-C(8)	120.1(3)
C(9)-C(10)-C(7)	120.6(3)
C(10)-C(7)-C(5)	120.7(2)
C(6)-C(5)-C(7)	118.0(2)
C(6)-C(5)-C(2)	120.8(2)
C(7)-C(5)-C(2)	121.3(2)
O(3)-C(2)-C(1)	105.0(2)
O(3)-C(2)-C(5)	112.5(2)
C(1)-C(2)-C(5)	112.4(2)

Table 4. Anisotropic displacement parameters (A^2 x 10^3) for **32** at 27°C.
The anisotropic displacement factor exponent takes the form:
-2 pi^2 [h^2 a*^2 U11 + ... + 2 h k a* b* U12]

	U11	U22	U33	U23	U13	U12
O(3)	41(1)	51(1)	53(1)	-6(1)	1(1)	2(1)
N(4)	45(1)	47(1)	48(1)	-2(1)	-3(1)	2(1)
C(12)	46(1)	47(1)	60(1)	-4(1)	-1(1)	4(1)
C(13)	58(1)	65(2)	75(2)	-20(1)	5(1)	-2(1)
C(19)	71(2)	104(2)	65(2)	-23(2)	17(1)	-9(2)
C(17)	74(2)	94(2)	52(1)	1(1)	3(1)	-16(2)
C(11)	53(1)	60(1)	54(1)	8(1)	-2(1)	-7(1)
C(15)	55(1)	69(2)	78(2)	-9(1)	-14(1)	14(1)
C(14)	69(2)	49(1)	88(2)	9(1)	13(1)	9(1)
C(16)	68(2)	61(1)	80(2)	4(1)	4(1)	-16(1)
C(18)	77(2)	75(2)	83(2)	32(1)	-7(1)	5(1)
C(6)	48(1)	65(1)	62(1)	0(1)	2(1)	2(1)
C(8)	56(1)	68(2)	93(2)	-1(1)	15(1)	-6(1)
C(9)	86(2)	73(2)	83(2)	16(2)	35(2)	3(2)
C(10)	104(2)	90(2)	54(2)	11(1)	1	
C(7)	71(2)	74(2)	55(1)	-1(1)	-2(1)	-1(1)
C(5)	44(1)	55(1)	52(1)	-5(1)	7(1)	9(1)
C(2)	42(1)	52(1)	67(1)	1(1)	4(1)	7(1)
C(1)	74(2)	58(2)	123(2)	-16(2)	29(2)	8(1)

Table 5. Hydrogen coordinates (x 10^4) and isotropic displacement parameters (A^2 x 10^3) for **32** at 27°C.

	x	y	z	U(eq)
H(31)	2731(2)	-188(3)	3851(2)	79
H(30)	3782(2)	-593(3)	4209(2)	79
H(25)	4335(2)	2034(4)	3701(2)	96
H(26)	3837(2)	1035(4)	2911(2)	96
H(23)	2404(2)	2585(4)	3072(2)	88
H(24)	3260(2)	3865(4)	2935(2)	88
H(37)	4366(2)	2314(3)	5280(2)	102
H(35)	4361(2)	442(3)	5646(2)	102
H(36)	3809(2)	1890(3)	6141(2)	102
H(34)	2308(2)	184(3)	6080(2)	103
H(32)	2859(2)	-1274(3)	5593(2)	103
H(33)	1894(2)	-530(3)	5181(2)	103
H(20)	3458(2)	5584(3)	5086(2)	105
H(22)	3768(2)	5889(3)	4112(2)	105
H(21)	4175(2)	4315(3)	4641(2)	105
H(27)	1735(2)	5756(3)	4548(2)	118
H(28)	1343(2)	4525(3)	3805(2)	118
H(29)	2073(2)	5983(3)	3576(2)	118
H(42)	-186(2)	1517(3)	5513(2)	70
H(43)	-776(2)	-830(3)	6269(2)	87
H(44)	-90(2)	-1558(4)	7633(2)	96
H(45)	1159(2)	49(4)	8234(2)	99
H(46)	1739(2)	2389(3)	7494(2)	80
H(38)	869(2)	3829(3)	5347(2)	65
H(41)	1481(2)	6266(3)	6074(2)	127
H(39)	1594(2)	5238(3)	6958(2)	127
H(40)	557(2)	5619(3)	6555(2)	127

Table 6. Crystal data and structure refinement for MB-TMP **32** at -63°C.

Identification code	km1lt
Empirical formula	C17 H27 N O
Formula weight	261.40
Temperature	210(2) K
Wavelength	0.71073 A
Crystal system	monoclinic
Space group	P2(1)/n
Unit cell dimensions	a = 13.5584(2) A alpha = 90 deg. b = 7.72710(10) A beta =91.6260(10) deg. c = 14.9489(2) A gamma = 90 deg.
Volume, Z	1565.52(4) A^3, 4
Density (calculated)	1.109 Mg/m^3
Absorption coefficient	0.068 mm^-1
F(000)	576
Crystal size	.3 x .3 x .2 mm
Theta range for data collection	2.00 to 26.42 deg.
Limiting indices	-16<=h<=16, -9<=k<=9, -18<=l<=18
Reflections collected	13148
Independent reflections	3032 [R(int) = 0.0261]
Refinement method	Full-matrix least-squares on F^2
Data / restraints / parameters	3032 / 0 / 281
Goodness-of-fit on F^2	1.005
Final R indices [I>2sigma(I)]	R1 = 0.0363, wR2 = 0.0912

R indices (all data)	R1 = 0.0443, wR2 = 0.0969
Extinction coefficient	0.008(2)
Largest diff. peak and hole	0.185 and -0.138 e.A^-3

Table 7. Atomic coordinates (x 10^4) and equivalent isotropic displacement parameters (A^2 x 10^3) for **32** at –63°C. U(eq) is defined as one third of the trace of the orthogonalized Uij tensor.

	x	y	z	U(eq)
O(3)	2282(1)	3478(1)	5697(1)	32(1)
N(4)	2403(1)	2609(1)	4842(1)	31(1)
C(12)	3064(1)	1080(1)	5014(1)	33(1)
C(13)	3307(1)	300(2)	4103(1)	43(1)
C(19)	3720(1)	1587(2)	3452(1)	51(1)
C(17)	2989(1)	3046(2)	3326(1)	48(1)
C(11)	2753(1)	3966(2)	4204(1)	37(1)
C(15)	4007(1)	1459(2)	5569(1)	44(1)
C(14)	2476(1)	-270(2)	5522(1)	44(1)
C(16)	3640(1)	5046(2)	4536(1)	44(1)
C(18)	1893(1)	5207(2)	4023(1)	50(1)
C(6)	78(1)	1227(2)	6050(1)	38(1)
C(8)	-284(1)	-205(2)	6499(1)	47(1)
C(9)	119(1)	-652(2)	7324(1)	52(1)
C(10)	876(1)	319(2)	7700(1)	54(1)
C(7)	1232(1)	1747(2)	7254(1)	45(1)
C(5)	843(1)	2205(2)	6416(1)	33(1)
C(2)	1252(1)	3717(2)	5908(1)	36(1)
C(1)	1223(1)	5384(2)	6444(1)	54(1)

Table 8. Bond lengths [A] and angles [deg] for **32** at –63°C.

O(3)-C(2)	1.4531(13)
O(3)-N(4)	1.4574(11)
N(4)-C(12)	1.5010(14)
N(4)-C(11)	1.5024(14)
C(12)-C(14)	1.528(2)
C(12)-C(15)	1.532(2)
C(12)-C(13)	1.534(2)
C(13)-C(19)	1.510(2)
C(19)-C(17)	1.510(2)
C(17)-C(11)	1.534(2)
C(11)-C(18)	1.527(2)
C(11)-C(16)	1.535(2)
C(6)-C(5)	1.384(2)
C(6)-C(8)	1.391(2)
C(8)-C(9)	1.378(2)
C(9)-C(10)	1.377(2)
C(10)-C(7)	1.383(2)
C(7)-C(5)	1.392(2)
C(5)-C(2)	1.507(2)
C(2)-C(1)	1.518(2)
C(2)-O(3)-N(4)	112.45(8)
O(3)-N(4)-C(12)	107.08(8)
O(3)-N(4)-C(11)	106.27(8)
C(12)-N(4)-C(11)	117.40(8)
N(4)-C(12)-C(14)	107.78(9)
N(4)-C(12)-C(15)	115.31(9)
C(14)-C(12)-C(15)	107.49(11)
N(4)-C(12)-C(13)	107.41(9)
C(14)-C(12)-C(13)	107.52(10)
C(15)-C(12)-C(13)	111.04(10)
C(19)-C(13)-C(12)	113.97(11)
C(17)-C(19)-C(13)	108.53(11)
C(19)-C(17)-C(11)	113.04(11)
N(4)-C(11)-C(18)	107.31(9)
N(4)-C(11)-C(16)	115.65(10)
C(18)-C(11)-C(16)	107.64(11)
N(4)-C(11)-C(17)	107.26(10)
C(18)-C(11)-C(17)	108.36(11)
C(16)-C(11)-C(17)	110.39(10)
C(5)-C(6)-C(8)	120.99(12)
C(9)-C(8)-C(6)	119.65(13)

C(10)-C(9)-C(8)	120.02(13)
C(9)-C(10)-C(7)	120.29(14)
C(10)-C(7)-C(5)	120.53(13)
C(6)-C(5)-C(7)	118.51(12)
C(6)-C(5)-C(2)	120.45(10)
C(7)-C(5)-C(2)	121.04(11)
O(3)-C(2)-C(5)	112.33(9)
O(3)-C(2)-C(1)	105.19(10)
C(5)-C(2)-C(1)	112.11(10)

Table 9. Anisotropic displacement parameters (A^2 x 10^3) for **32** at –63°C. The anisotropic displacement factor exponent takes the form:
-2 pi^2 [h^2 a*^2 U11 + ... + 2 h k a* b* U12]

	U11	U22	U33	U23	U13	U12
O(3)	27(1)	34(1)	34(1)	-4(1)	1(1)	1(1)
N(4)	29(1)	32(1)	31(1)	-2(1)	0(1)	0(1)
C(12)	29(1)	32(1)	40(1)	-4(1)	-1(1)	2(1)
C(13)	36(1)	44(1)	49(1)	-14(1)	3(1)	0(1)
C(19)	45(1)	67(1)	41(1)	-14(1)	9(1)	-4(1)
C(17)	48(1)	62(1)	34(1)	2(1)	2(1)	-10(1)
C(11)	35(1)	40(1)	36(1)	6(1)	-2(1)	-5(1)
C(15)	34(1)	46(1)	50(1)	-6(1)	-8(1)	9(1)
C(14)	44(1)	32(1)	57(1)	3(1)	8(1)	6(1)
C(16)	43(1)	42(1)	48(1)	3(1)	2(1)	-11(1)
C(18)	49(1)	50(1)	51(1)	18(1)	-5(1)	1(1)
C(6)	30(1)	43(1)	42(1)	-2(1)	3(1)	3(1)
C(8)	36(1)	45(1)	60(1)	-3(1)	1	
C(9)	56(1)	46(1)	54(1)	9(1)	24(1)	4(1)
C(10)	69(1)	58(1)	35(1)	5(1)	8(1)	8(1)
C(7)	47(1)	50(1)	37(1)	-4(1)	-1(1)	0(1)
C(5)	29(1)	37(1)	34(1)	-3(1)	5(1)	6(1)
C(2)	26(1)	36(1)	44(1)	1(1)	2(1)	4(1)
C(1)	47(1)	38(1)	79(1)	-1		

Table 10. Hydrogen coordinates (x 10^4) and isotropic displacement parameters (A^2 x 10^3) for **32** at –63°C.

	x	y	z	U(eq)
H(1)	-186(10)	1546(17)	5452(10)	47(4)
H(2)	864(9)	3843(16)	5334(8)	34(3)
H(3)	2350(11)	2612(19)	3066(9)	51(4)
H(4)	1281(12)	4567(19)	3820(10)	53(4)
H(5)	2689(11)	-201(18)	3833(9)	48(4)
H(6)	4269(13)	4415(21)	4542(10)	63(4)
H(7)	3778(11)	-671(20)	4207(9)	51(4)
H(8)	1767(11)	2410(20)	7533(10)	54(4)
H(9)	3548(11)	5504(19)	5134(10)	52(4)
H(10)	3216(11)	3938(20)	2904(10)	56(4)
H(11)	4365(11)	2032(19)	3684(10)	52(4)
H(12)	2869(11)	-1382(20)	5528(10)	57(4)
H(13)	4517(11)	2110(20)	5216(10)	56(4)
H(14)	2372(11)	96(19)	6128(11)	55(4)
H(15)	4316(11)	381(21)	5753(10)	57(4)
H(16)	1835(12)	-461(19)	5206(10)	57(4)
H(17)	1754(11)	5911(21)	4568(11)	58(4)
H(18)	-805(11)	-898(20)	6212(10)	57(4)
H(19)	-131(12)	-1656(22)	7620(11)	67(5)
H(20)	2077(12)	6025(22)	3553(11)	66(5)
H(21)	3713(12)	6049(22)	4142(11)	63(4)
H(22)	553(13)	5603(21)	6641(11)	69(5)
H(23)	3861(12)	999(21)	2877(11)	63(4)
H(24)	3853(11)	2094(20)	6109(10)	54(4)
H(25)	1673(13)	5261(22)	6988(12)	71(5)
H(26)	1175(12)	6(21)	8266(12)	65(5)
H(27)	1421(14)	6356(25)	6098(12)	78(5)